

**AD-A267 686**

IDENTIFICATION PAGE

FORM APPROVED  
OMB No. 0704-0186

1. AGENCY USE ONLY (Leave blank)

2. REPORT DATE

December 1992

3. REPORT TYPE AND DATES COVERED

THESIS/ ~~DISSERTATION~~

4. TITLE AND SUBTITLE

Turbine Blade Tip Film Cooling Measurements

5. FUNDING NUMBERS

6. AUTHOR(S)

1st Lt Dean A. Ward

7. PERFORMING ORGANIZATION NAME(S) AND ADDRESS(ES)

AFIT Student Attending: Arizona State University

8. PERFORMING ORGANIZATION  
REPORT NUMBER

AFIT/CI/CIA-93-011

9. SPONSORING/MONITORING AGENCY NAME(S) AND ADDRESS(ES)

AFIT/CI  
Wright-Patterson AFB OH 45433-658310. SPONSORING/MONITORING  
AGENCY REPORT NUMBER

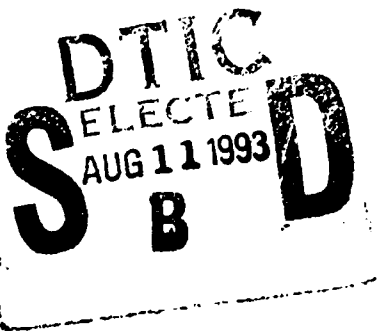
11. SUPPLEMENTARY NOTES

12a. DISTRIBUTION/AVAILABILITY STATEMENT

Approved for Public Release IAW 190-1  
Distribution Unlimited  
MICHAEL M. BRICKER, SMSgt, USAF  
Chief Administration

12b. DISTRIBUTION CODE

13. ABSTRACT (Maximum 200 words)



## Accession For

NTIS GRA&I ☒DTIC TAB ☐Unannounced ☐Justification ☐

By \_\_\_\_\_

Distribution/

Availability Codes

Dist

Avail and/or  
Special

A-1

**93-18506**

14. SUBJECT TERMS

DTIC QUALITY INSPECTED 3

15. NUMBER OF PAGES

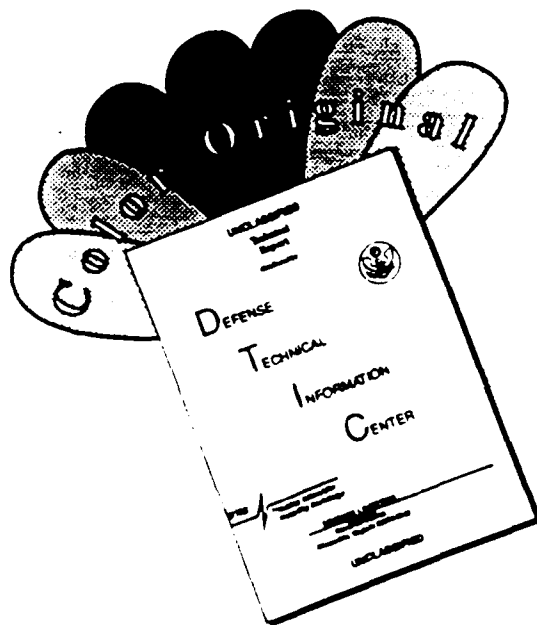
166

16. PRICE CODE

17. SECURITY CLASSIFICATION  
OF REPORT18. SECURITY CLASSIFICATION  
OF THIS PAGE19. SECURITY CLASSIFICATION  
OF ABSTRACT

20. LIMITATION OF ABSTRACT

# DISCLAIMER NOTICE



THIS DOCUMENT IS BEST QUALITY AVAILABLE. THE COPY FURNISHED TO DTIC CONTAINED A SIGNIFICANT NUMBER OF COLOR PAGES WHICH DO NOT REPRODUCE LEGIBLY ON BLACK AND WHITE MICROFICHE.

**TURBINE BLADE TIP FILM COOLING MEASUREMENTS**

**by**

**Dean Andrew Ward**

**A Thesis Presented in Partial Fulfillment  
of the Requirements for the Degree  
Master of Science**

**ARIZONA STATE UNIVERSITY**

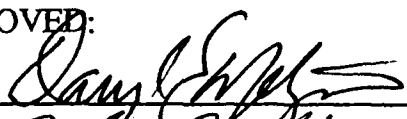


**December 1992**

TURBINE BLADE TIP FILM COOLING MEASUREMENTS

by  
Dean Andrew Ward

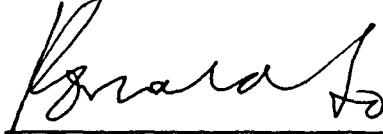
has been approved  
December 1992

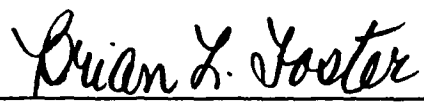
APPROVED:

, Chairperson  
  


Supervisory Committee

ACCEPTED:

  
Department Chairperson

  
Dean, Graduate College

## ABSTRACT

In the design of gas turbine engines, the need to accurately know the heat transfer characteristics of the turbine blade tip is of extreme importance. The pressure differential between the pressure and suction side of the blade induces a strong secondary flow of hot combustion gases through the clearance gap between the turbine blade tip and shroud. This leakage flow is detrimental to the tip of the blade. In order to minimize this leakage flow, designers need to accurately know the heat transfer characteristics of the blade and blade tip so that dimensional changes may be accurately predicted. If dimensional changes are accurately known, the clearance gap and thus the secondary flow may be minimized and the overall thermal efficiency of the gas turbine engine increased. In addition, increased blade life is often achieved by cooling of the blade and blade tip. Unfortunately this cooling has a detrimental affect on cycle efficiency and must be used accurately and sparingly. Results are presented for the measurements of heat transfer coefficients and effectiveness for three test configurations, modeling blade tips with and without cavities and with and without film cooling. The blade tip cavity provides a resistance to the secondary flow. The results indicate a weak dependence of heat transfer coefficient on the blowing ratio, but a strong dependence of effectiveness on the blowing ratio. Also, the deeper the test cavity, the lower the heat transfer of the test surface (blade tip). Additionally it was found that pressure side

injection within the tip cavity yielded more uniform heat transfer contour in the cavity due to increased mixing than did the suction side injection.

"When you are getting kicked from the rear, it means you are out in front."

Fulton Sheen

## ACKNOWLEDGEMENTS

I wish to thank my wife, Jana, for her constant support and encouragement. I appreciate the United State Air Force's confidence in my abilities, and giving me the opportunity to chase my dreams. I am also grateful to Professor Darryl Metzger for the opportunity to participate in his research effort. Finally I wish to thank Yong Kim, Neal Barlow, and Yu Yufeng for answering my constant questioning.



## TABLE OF CONTENTS

	Page
LIST OF TABLES .....	ix
LIST OF FIGURES .....	x
NOMENCLATURE.....	xx
CHAPTER	
1 INTRODUCTION .....	1
2 EXPERIMENTAL APPARATUS AND PROCEDURE.....	5
2.1 Test Section.....	5
2.2 Test Surface .....	6
2.3 Air Supply .....	6
2.4 Instrumentation.....	7
2.5 Experimental Procedure.....	8
2.6 Data Reduction.....	10
2.7 Calibration .....	11
2.8 Test Matrix.....	12
3 RESULTS AND DISCUSSION .....	19
3.1 Baseline Tests.....	19
3.2 3/8" Cavity with Injection.....	21
3.3 1.0" Cavity with Injection.....	22
4 SUMMARY.....	112
4.1 Conclusions from Results.....	112
4.2 Recommendations for Study.....	113

	Page
REFERENCES .....	1 1 4
APPENDIX	
A DATA REDUCTION THEORY.....	1 1 6
B SPANWISE VARIATION DATA.....	1 2 1
C REPEATABILITY DATA .....	1 5 4

## LIST OF TABLES

Table	Page
1 Test Matrix, baseline and $\frac{3}{8}$ " cavity .....	14
2 Test Matrix, 1.0" cavity.....	15

## LIST OF FIGURES

Figure	Page
1 Clearance gap flow.....	4
2 Test facility.....	16
3 Test setup.....	17
4 Cavity models.....	18
5 Heat transfer coeff., streamwise variation, flat plate, 3/16" clearance gap.....	24
6 Heat transfer coeff., streamwise variation, flat plate, 5/16" clearance gap.....	25
7 Heat transfer coeff., streamwise variation, 3/8" cavity, 3/16" clearance gap.....	26
8 Heat transfer coeff., streamwise variation, 3/8" cavity, 5/16" clearance gap.....	27
9 Heat transfer coeff., streamwise variation, 1.0" cavity, 3/16" clearance gap.....	28
10 Heat transfer coeff., streamwise variation, 1.0" cavity, 5/16" clearance gap.....	29
11 Heat transfer coeff., streamwise variation, suction side injection, 3/8" cavity, 3/16" clearance gap.....	30
12 Effectiveness, streamwise variation, suction side injection, 3/8" cavity, 3/16" clearance gap.....	31
13 Heat transfer coeff., streamwise variation, suction side injection, 3/8" cavity, 3/16" clearance gap, #1.....	32
14 Effectiveness, streamwise variation, suction side injection, 3/8" cavity, 3/16" clearance gap.....	33

Figure	Page
15 Heat transfer coeff., streamwise variation, suction side injection, $\frac{3}{8}$ " cavity, $\frac{3}{16}$ " clearance gap, #2.....	34
16 Effectiveness, streamwise variation, suction side injection, $\frac{3}{8}$ " cavity, $\frac{3}{16}$ " clearance gap, #2.....	35
17 Heat transfer coeff., streamwise variation, suction side injection, $\frac{3}{8}$ " cavity, $\frac{5}{16}$ " clearance gap, #1.....	36
18 Effectiveness, streamwise variation, suction side injection, $\frac{3}{8}$ " cavity, $\frac{5}{16}$ " clearance gap, #1.....	37
19 Heat transfer coeff., streamwise variation, suction side injection, $\frac{3}{8}$ " cavity, $\frac{5}{16}$ " clearance gap, #2.....	38
20 Effectiveness, streamwise variation, suction side injection, $\frac{3}{8}$ " cavity, $\frac{5}{16}$ " clearance gap, #2.....	39
21 Heat transfer coeff., streamwise variation, suction side injection, $\frac{3}{8}$ " cavity, $\frac{5}{16}$ " clearance gap.....	40
22 Effectiveness, streamwise variation, suction side injection, $\frac{3}{8}$ " cavity, $\frac{5}{16}$ " clearance gap.....	41
23 Heat transfer coeff., streamwise variation, pressure side injection, $\frac{3}{8}$ " cavity, $\frac{3}{16}$ " clearance gap.....	42
24 Effectiveness, streamwise variation, pressure side injection, $\frac{3}{8}$ " cavity, $\frac{3}{16}$ " clearance gap.....	43
25 Heat transfer coeff., streamwise variation, pressure side injection, $\frac{3}{8}$ " cavity, $\frac{3}{16}$ " clearance gap.....	44
26 Effectiveness, streamwise variation, pressure side injection, $\frac{3}{8}$ " cavity, $\frac{3}{16}$ " clearance gap.....	45
27 Heat transfer coeff., streamwise variation, pressure side injection, $\frac{3}{8}$ " cavity, $\frac{5}{16}$ " clearance gap.....	46
28 Effectiveness, streamwise variation, pressure side injection, $\frac{3}{8}$ " cavity, $\frac{5}{16}$ " clearance gap.....	47

Figure	Page
29 Heat transfer coeff., streamwise variation, pressure side injection, $\frac{3}{8}$ " cavity, $\frac{5}{16}$ " clearance gap.....	48
30 Effectiveness, streamwise variation, pressure side injection, $\frac{3}{8}$ " cavity, $\frac{5}{16}$ " clearance gap.....	49
31 Heat transfer coeff., streamwise variation, suction side injection, 1.0" cavity, $\frac{3}{16}$ " clearance gap, #1.....	50
32 Effectiveness, streamwise variation, suction side injection, 1.0" cavity, $\frac{3}{16}$ " clearance gap, #1.....	51
33 Heat transfer coeff., streamwise variation, suction side injection, 1.0" cavity, $\frac{3}{16}$ " clearance gap, #2.....	52
34 Effectiveness, streamwise variation, suction side injection, 1.0" cavity, $\frac{3}{16}$ " clearance gap, #2.....	53
35 Heat transfer coeff., streamwise variation, suction side injection, 1.0" cavity, $\frac{3}{16}$ " clearance gap.....	54
36 Effectiveness, streamwise variation, suction side injection, 1.0" cavity, $\frac{3}{16}$ " clearance gap.....	55
37 Heat transfer coeff., streamwise variation, suction side injection, 1.0" cavity, $\frac{5}{16}$ " clearance gap.....	56
38 Effectiveness, streamwise variation, suction side injection, 1.0" cavity, $\frac{5}{16}$ " clearance gap.....	57
39 Heat transfer coeff., streamwise variation, suction side injection, 1.0" cavity, $\frac{5}{16}$ " clearance gap, #1.....	58
40 Effectiveness, streamwise variation, suction side injection, 1.0" cavity, $\frac{5}{16}$ " clearance gap, #1.....	59
41 Heat transfer coeff., streamwise variation, suction side injection, 1.0" cavity, $\frac{5}{16}$ " clearance gap, #2.....	60
42 Effectiveness, streamwise variation, suction side injection, 1.0" cavity, $\frac{5}{16}$ " clearance gap, #2.....	61

Figure	Page
43 Heat transfer coeff., streamwise variation, pressure side injection, 1.0" cavity, $\frac{3}{16}$ " clearance gap .....	62
44 Effectiveness, streamwise variation, pressure side injection, 1.0" cavity, $\frac{3}{16}$ " clearance gap .....	63
45 Heat transfer coeff., streamwise variation, pressure side injection, 1.0" cavity, $\frac{3}{16}$ " clearance gap, #1 .....	64
46 Effectiveness, streamwise variation, pressure side injection, 1.0" cavity, $\frac{3}{16}$ " clearance gap, #1 .....	65
47 Heat transfer coeff., streamwise variation, pressure side injection, 1.0" cavity, $\frac{3}{16}$ " clearance gap, #2 .....	66
48 Effectiveness, streamwise variation, pressure side injection, 1.0" cavity, $\frac{3}{16}$ " clearance gap, #2 .....	67
49 Heat transfer coeff., streamwise variation, pressure side injection, 1.0" cavity, $\frac{5}{16}$ " clearance gap .....	68
50 Effectiveness, streamwise variation, pressure side injection, 1.0" cavity, $\frac{5}{16}$ " clearance gap .....	69
51 Heat transfer coeff., streamwise variation, pressure side injection, 1.0" cavity, $\frac{5}{16}$ " clearance gap, #1 .....	70
52 Effectiveness, streamwise variation, pressure side injection, 1.0" cavity, $\frac{5}{16}$ " clearance gap, #1 .....	71
53 Heat transfer coeff., streamwise variation, pressure side injection, 1.0" cavity, $\frac{5}{16}$ " clearance gap, #2 .....	72
54 Effectiveness, streamwise variation, pressure side injection, 1.0" cavity, $\frac{5}{16}$ " clearance gap, #2 .....	73
55 Flat plate, $\frac{3}{16}$ " clearance gap, $Re = 30,000$ .....	74
56 Flat plate, $\frac{5}{16}$ " clearance gap, $Re = 30,000$ .....	75

Figure	Page
57 $3/8$ " cavity, $3/16$ " clearance gap, no injection, Re = 30,000.....	76
58 $3/8$ " cavity, $5/16$ " clearance gap, no injection, Re = 30,000.....	77
59 1.0" cavity, $3/16$ " clearance gap, no injection, Re = 30,000.....	78
60 1.0" cavity, $5/16$ " clearance gap, no injection, Re = 30,000.....	79
61 $3/8$ " cavity, $3/16$ " clearance gap, suction side injection, Re = 30,000; M=0.1.....	80
62 $3/8$ " cavity, $3/16$ " clearance gap, suction side injection, Re = 30,000; M=0.1.....	81
63 $3/8$ " cavity, $3/16$ " clearance gap, suction side injection, Re = 30,000; M=0.5.....	82
64 $3/8$ " cavity, $3/16$ " clearance gap, suction side injection, Re = 30,000; M=0.5.....	83
65 $3/8$ " cavity, $5/16$ " clearance gap, suction side injection, Re = 30,000; M=0.1.....	84
66 $3/8$ " cavity, $5/16$ " clearance gap, suction side injection, Re = 30,000; M=0.1.....	85
67 $3/8$ " cavity, $5/16$ " clearance gap, suction side injection, Re = 30,000; M=0.5.....	86
68 $3/8$ " cavity, $5/16$ " clearance gap, suction side injection, Re = 30,000; M=0.5.....	87
69 $3/8$ " cavity, $3/16$ " clearance gap, pressure side injection, Re = 30,000; M=0.1.....	88
70 $3/8$ " cavity, $3/16$ " clearance gap, pressure side injection, Re = 30,000; M=0.1.....	89



Figure	Page
71 $\frac{3}{8}$ " cavity, $\frac{3}{16}$ " clearance gap, pressure side injection, Re = 30,000; M=0.5.....	90
72 $\frac{3}{8}$ " cavity, $\frac{3}{16}$ " clearance gap, pressure side injection, Re = 30,000; M=0.5.....	91
73 $\frac{3}{8}$ " cavity, $\frac{5}{16}$ " clearance gap, pressure side injection, Re = 30,000; M=0.1.....	92
74 $\frac{3}{8}$ " cavity, $\frac{5}{16}$ " clearance gap, pressure side injection, Re = 30,000; M=0.1.....	93
75 $\frac{3}{8}$ " cavity, $\frac{5}{16}$ " clearance gap, pressure side injection, Re = 30,000; M=0.5.....	94
76 $\frac{3}{8}$ " cavity, $\frac{5}{16}$ " clearance gap, pressure side injection, Re = 30,000; M=0.5.....	95
77 1.0" cavity, $\frac{3}{16}$ " clearance gap, suction side injection, Re = 30,000; M=0.1.....	96
78 1.0" cavity, $\frac{3}{16}$ " clearance gap, suction side injection, Re = 30,000; M=0.1.....	97
79 1.0" cavity, $\frac{3}{16}$ " clearance gap, suction side injection, Re = 30,000; M=0.5.....	98
80 1.0" cavity, $\frac{3}{16}$ " clearance gap, suction side injection, Re = 30,000; M=0.5.....	99
81 1.0" cavity, $\frac{5}{16}$ " clearance gap, suction side injection, Re = 30,000; M=0.1.....	100
82 1.0" cavity, $\frac{5}{16}$ " clearance gap, suction side injection, Re = 30,000; M=0.1.....	101
83 1.0" cavity, $\frac{5}{16}$ " clearance gap, suction side injection, Re = 30,000; M=0.5.....	102
84 1.0" cavity, $\frac{5}{16}$ " clearance gap, suction side injection, Re = 30,000; M=0.5.....	103

Figure	Page
85 1.0" cavity, $\frac{3}{16}$ " clearance gap, pressure side injection, Re = 30,000; M=0.1.....	104
86 1.0" cavity, $\frac{3}{16}$ " clearance gap, pressure side injection, Re = 30,000; M=0.1.....	105
87 1.0" cavity, $\frac{3}{16}$ " clearance gap, pressure side injection, Re = 30,000; M=0.5.....	106
88 1.0" cavity, $\frac{3}{16}$ " clearance gap, pressure side injection, Re = 30,000; M=0.5.....	107
89 1.0" cavity, $\frac{5}{16}$ " clearance gap, pressure side injection, Re = 30,000; M=0.1.....	108
90 1.0" cavity, $\frac{5}{16}$ " clearance gap, pressure side injection, Re = 30,000; M=0.1.....	109
91 1.0" cavity, $\frac{5}{16}$ " clearance gap, pressure side injection, Re = 30,000; M=0.5.....	110
92 1.0" cavity, $\frac{5}{16}$ " clearance gap, pressure side injection, Re = 30,000; M=0.5.....	111
93 Heat transfer coeff., spanwise variation, suction side injection, $\frac{3}{8}$ " cavity, $\frac{3}{16}$ " clearance gap.....	117
94 Effectiveness, spanwise variation, suction side injection, $\frac{3}{8}$ " cavity, $\frac{3}{16}$ " clearance gap.....	118
95 Heat transfer coeff., spanwise variation, suction side injection, $\frac{3}{8}$ " cavity, $\frac{3}{16}$ " clearance gap, #1.....	119
96 Effectiveness, spanwise variation, suction side injection, $\frac{3}{8}$ " cavity, $\frac{3}{16}$ " clearance gap, #1.....	120
97 Heat transfer coeff., spanwise variation, suction side injection, $\frac{3}{8}$ " cavity, $\frac{5}{16}$ " clearance gap, #1.....	121
98 Effectiveness, spanwise variation, suction side injection, $\frac{3}{8}$ " cavity, $\frac{5}{16}$ " clearance gap, #1.....	122

Figure	Page
99 Heat transfer coeff., spanwise variation, suction side injection, $\frac{3}{8}$ " cavity, $\frac{5}{16}$ " clearance gap.....	123
100 Effectiveness, spanwise variation, suction side injection, $\frac{3}{8}$ " cavity, $\frac{5}{16}$ " clearance gap.....	124
101 Heat transfer coeff., spanwise variation, pressure side injection, $\frac{3}{8}$ " cavity, $\frac{3}{16}$ " clearance gap, #1.....	125
102 Effectiveness, spanwise variation, pressure side injection, $\frac{3}{8}$ " cavity, $\frac{3}{16}$ " clearance gap, #1.....	126
103 Heat transfer coeff., spanwise variation, pressure side injection, $\frac{3}{8}$ " cavity, $\frac{3}{16}$ " clearance gap.....	127
104 Effectiveness, spanwise variation, pressure side injection, $\frac{3}{8}$ " cavity, $\frac{3}{16}$ " clearance gap, #1.....	128
105 Heat transfer coeff., spanwise variation, pressure side injection, $\frac{3}{8}$ " cavity, $\frac{5}{16}$ " clearance gap.....	129
106 Effectiveness, spanwise variation, pressure side injection, $\frac{3}{8}$ " cavity, $\frac{5}{16}$ " clearance gap.....	130
107 Heat transfer coeff., spanwise variation, pressure side injection, $\frac{3}{8}$ " cavity, $\frac{5}{16}$ " clearance gap, #2.....	131
108 Effectiveness, spanwise variation, pressure side injection, $\frac{3}{8}$ " cavity, $\frac{5}{16}$ " clearance gap, #2.....	132
109 Heat transfer coeff., spanwise variation, suction side injection, 1.0" cavity, $\frac{3}{16}$ " clearance gap, #1.....	133
110 Effectiveness, spanwise variation, suction side injection, 1.0" cavity, $\frac{3}{16}$ " clearance gap, #1.....	134
111 Heat transfer coeff., spanwise variation, suction side injection, 1.0" cavity, $\frac{3}{16}$ " clearance gap.....	135
112 Effectiveness, spanwise variation, suction side injection, 1.0" cavity, $\frac{3}{16}$ " clearance gap.....	136

Figure	Page
113 Heat transfer coeff., spanwise variation, suction side injection, 1.0" cavity, $\frac{5}{16}$ " clearance gap.....	137
114 Effectiveness, spanwise variation, suction side injection, 1.0" cavity, $\frac{5}{16}$ " clearance gap.....	138
115 Heat transfer coeff., spanwise variation, suction side injection, 1.0" cavity, $\frac{5}{16}$ " clearance gap, #1.....	139
116 Effectiveness, spanwise variation, suction side injection, 1.0" cavity, $\frac{5}{16}$ " clearance gap, #1.....	140
117 Heat transfer coeff., spanwise variation, pressure side injection, 1.0" cavity, $\frac{3}{16}$ " clearance gap.....	141
118 Effectiveness, spanwise variation, pressure side injection, 1.0" cavity, $\frac{3}{16}$ " clearance gap.....	142
119 Heat transfer coeff., spanwise variation, pressure side injection, 1.0" cavity, $\frac{3}{16}$ " clearance gap, #1.....	143
120 Effectiveness, spanwise variation, pressure side injection, 1.0" cavity, $\frac{3}{16}$ " clearance gap, #1.....	144
121 Heat transfer coeff., spanwise variation, pressure side injection, 1.0" cavity, $\frac{5}{16}$ " clearance gap.....	145
122 Effectiveness, spanwise variation, pressure side injection, 1.0" cavity, $\frac{5}{16}$ " clearance gap.....	146
123 Heat transfer coeff., spanwise variation, pressure side injection, 1.0" cavity, $\frac{5}{16}$ " clearance gap.....	147
124 Effectiveness, spanwise variation, pressure side injection, 1.0" cavity, $\frac{5}{16}$ " clearance gap.....	148
125 Heat transfer coeff., streamwise variation, suction side injection, $\frac{3}{8}$ " cavity, $\frac{3}{16}$ " clearance gap repeatability.....	150

Figure	Page
126 Effectiveness, streamwise direction, suction side injection, $\frac{3}{8}$ " cavity, $\frac{3}{16}$ " clearance gap Repeatability.....	151
127 Heat transfer coeff., streamwise variation, suction side injection, $\frac{3}{8}$ " cavity, $\frac{5}{16}$ " clearance gap repeatability.....	152
128 Effectiveness, streamwise direction, suction side injection, $\frac{3}{8}$ " cavity, $\frac{5}{16}$ " clearance gap repeatability.....	153
129 Heat transfer coeff., streamwise variation, suction side injection, 1.0" cavity, $\frac{3}{16}$ " clearance gap repeatability.....	154
130 Effectiveness, streamwise direction, suction side injection, 1.0" cavity, $\frac{5}{16}$ " clearance gap repeatability.....	155
131 Heat transfer coeff., streamwise variation, suction side injection, 1.0" cavity, $\frac{5}{16}$ " clearance gap repeatability.....	156
132 Effectiveness, streamwise direction, suction side injection, 1.0" cavity, $\frac{5}{16}$ " clearance gap repeatability.....	157
133 Heat transfer coeff., streamwise variation, pressure side injection, 1.0" cavity, $\frac{3}{16}$ " clearance gap repeatability.....	158
134 Effectiveness, streamwise direction, pressure side injection, 1.0" cavity, $\frac{3}{16}$ " clearance gap repeatability.....	159

## NOMENCLATURE

$D_h$	hydraulic diameter
$h$	convection heat transfer coefficient
$k$	thermal conductivity
$M$	blowing ratio $(\rho V)_f/(\rho V)_m$
$q$	local surface heat transfer rate
$Re$	Reynolds number based on $D_h$
$T$	temperature
$V$	velocity
$x/d$	nondimensionalized length
$y/w$	nondimensionalized width
$\alpha$	thermal diffusivity
$\eta$	film cooling effectiveness
$\rho$	density
$\theta$	time
$\tau$	time

### Subscripts

$f$	film flow
$i$	initial
$m$	main flow
$r$	reference
$s$	surface

## CHAPTER 1

### INTRODUCTION

Increasing demands on engineers to develop gas turbine engines with higher performance and greater efficiencies has led to innovative ideas. In the turbine section, higher turbine inlet temperatures, lower clearance gap leakage flow, and creep resistant materials are a few ways to achieve these goals. This study examines the clearance gap region of the turbine blade. Axial turbine blade tips rotate in close proximity to a stationary peripheral outer seal or shroud. The pressure difference between the convex and concave blade sides drives a leakage flow through the clearance gap between the blade tip and shroud (Metzger and Reud, 1989) (Figure 1). Designers have attempted to eliminate this gap, but even with active clearance control, the gap always remains (Hennecke, 1984). Through this gap, the secondary flow carries hot combustion gases across the tip from the pressure side to the suction side of the blade. This in turn produces high heat transfer rates on the corresponding blade tip.

In order for designers to achieve higher temperatures and tighter clearance gaps, the heat transfer characteristics at the blade and blade tip must be known. To improve engine life at high turbine inlet temperatures, methods of minimizing the heat transfer rates are sought. Present tip designs most often use a flat tipped blade with the addition of an injected film cooling flow on to the surface when additional cooling is required. On more complex blade tip designs, the blade tip may be grooved to form a cavity on the tip

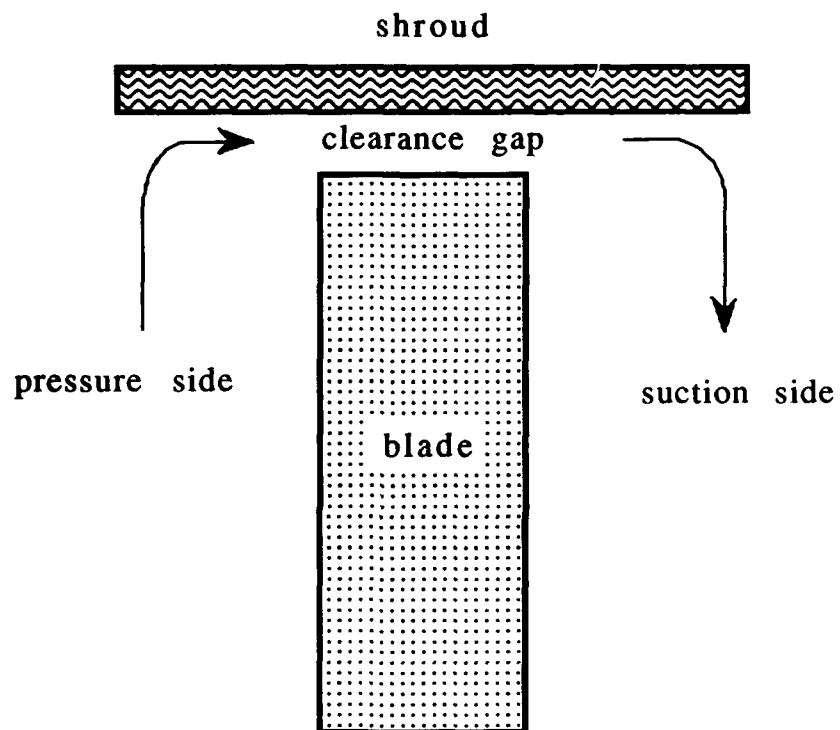
surface where film cooling may also be employed. Although several methods of reducing heat transfer rates at the tip have been developed, the flow patterns which can develop in a cavity tip currently are not generally known or predictable. Several researchers have made heat transfer measurements on plane tipped blades and shrouds (Dunn et al, 1984; Epstein et al, 1985). These studies were performed using short duration testing and documented the presence of a high heat transfer rate. Additional research has found that the clearance gap flow is attributable to a sink-like character whose magnitude is related primarily to the airfoil pressure loading distribution, while the relative motion of the blade tip to the shroud plays only a very minor role. As a result the heat transfer characteristics on the blade tip can be examined through stationary modeling (Mayel and Metzger, 1982; Metzger et al, 1990).

The steady state heat transfer conditions present on actual blade tips are modeled in the experiments by transient tests, where, in order to determine the heat transfer rates of the modeled blade tips, both time and temperature characteristics of the modeled surface must be known. This is accomplished by coating the test surface with a thin layer of encapsulated chiral nematic thermochromic liquid crystals (TLC). TLC have the property of displaying specific colors at unique temperatures. With these temperatures known, the test surface response is captured with a video camera during a transient test. This information is processed with a frame grabber on a work station to develop a time and



temperature correlation, on a very fine spatial scale, for the test surface.

The focus of this study is to model the heat transfer behavior on grooved turbine blade tips with film cooling. The laboratory models constructed for the study were fabricated at an enlarged scale compared to the size of the actual blade tips, but are geometrically similar to actual blade tip cross sections. Similarity in flowfields between the model and actual blade tip is established by testing Reynolds numbers, based on clearance channel height and mean velocity of the clearance flow, equal to those expected in actual hardware. Baseline tests were performed for plane tip models at two clearance channel heights without film injection, and test both with and without injection were performed on cavity models for combinations of two cavity depths, two clearance heights, two film hole locations, three flow Reynolds numbers, and two film injection rates.



Clearance Gap Flow  
Figure 1

## CHAPTER 2

### EXPERIMENTAL APPARATUS AND PROCEDURE

#### 2.1 Test Section

The test section is constructed from clear Plexiglas. Plexiglas is used because of its thermal conductivity ( $k$ ) and thermal diffusivity ( $\alpha$ ) are in preferred ranges for use with the data reduction technique. Also the visual transparency of Plexiglas allows for an unobstructed view of the test surface. The air flow enters a 2.5"x 4.0" rectangular settling chamber by means of an 1.5" ball diverter valve. The airflow passes through a series of porous material layers which straightens the flow and provides a uniform flow distribution to the rectangular duct. The rectangular chamber is 4.0" long with a pressure tap located on top to measure plenum pressure. A type K 30 gauge thermocouple placed 3.0" from the diverter valve in the middle of the entrance region, provides for measurement of main flow temperature. A second type K thermocouple placed in the second film tube, just prior to the Plexiglas test piece, provides the film flow temperature. At the end of the rectangular duct, the flow makes a 90 degree turn, and then accelerates into the clearance gap and over the test surface. The clearance gap size is varied through addition of different face plates. Clearance gaps of  $3/16$ " and  $5/16$ " are investigated. The test rig is securely mounted on a steel table to provide a stable platform.

## 2.2 Test Surface

The blade tip models are constructed of  $\frac{3}{8}$ " clear Plexiglas. Three surfaces are tested: Flat,  $\frac{3}{8}$ " cavity, and 1.0" cavity. O-ring material,  $\frac{1}{16}$ " diameter, seals the edges to prevent leakage. The two cavity models have four  $\frac{3}{16}$ " holes, located on the cavity floor, for injection of film cooling flow. Two locations on the surface are used,  $\frac{1}{4}$ " from the pressure edge of the cavity and  $\frac{1}{4}$ " from the suction side of the cavity (Figure 3). The back of the test surface is painted black to reduce internal reflections. The view surface is coated with a thin layer of black paint to provide a uniform surface as well as to minimize glare. The viewed surface is then sprayed with TLC. The thin TLC thickness of only approximately 30 microns ensures that the thermal conductance and capacitance effects of the TLC will be negligible.

## 2.3 Air Supply

Compressed air for both main and film flow is dried and filtered to ensure purity. Flow from the common storage is divided into two parts, each controlled via pressure regulators. Pressure readings from a 1.0" sharp edged orifice, installed per ASTM standards, are used to determine mass flow for the main flow. Pressure readings from a .32" sharp edge orifice, also installed per ASTM standards, are used similarly for the film flow. The respective flows are then heated to predetermined temperatures. The main flow is heated using a 2 KW tubular heater, and film flow is heated using a 400 W heater. Both heaters are connected to variacs to allow

for temperature adjustment. The main flow is connected to the rig by a 1.5" ball diverter valve, and the film flow is connected to the rig by a 1/4" ball diverter valve. Both flows are exhausted to the outdoors during preheating (Figure 2).

## 2.4 Instrumentation

Mass flow for the main flow is determined by recording pressure measurements at the orifice. The pressure of the main flow upstream of the orifice is measured with a manometer in inches of mercury within  $\pm .05$ " Hg. The  $\Delta P$  across the main flow orifice is measured with a manometer in inches of water within  $\pm .05$ " H<sub>2</sub>O. The pressure of the film flow upstream of the orifice is measured with a manometer in inches of mercury within  $\pm .05$ " Hg. The  $\Delta P$  across the film flow orifice is measured with a manometer in either inches of water within  $\pm .005$ " H<sub>2</sub>O or in inches of oil within .05" oil, depending on blowing ratio. Plenum pressure in the test rig is measured with a manometer in centimeters of oil within  $\pm .05$  cm oil. The ambient temperature is measured with a mercury thermometer to within  $\pm .05$  °F. The atmospheric pressure is measured with a mercury barometer within  $\pm .05$ " Hg. Temperature measurements of the main, film, and orifice flows are made with type K thermocouples. A data log unit (Fluke 2400 B Intelligent Computer Front End) records the transient temperatures. After a 0.2 degree temperature difference is detected, the Fluke samples the temperatures every .32 second. The Fluke has an internal cold reference junction for the thermocouples. The test surface is viewed

using a VHS camcorder which is connected live to a Sun workstation. The workstation uses a specially written C language program to direct the frame grabber board used for data acquisition (Kim et al, 1991).

## 2.5 Experimental Procedure

Testing involved three temperatures: the temperature of the test surface, main flow, and film flow. With the three temperature problem, an appropriate reference temperature ( $T_r$ ) is used in the calculation of the heat transfer coefficient and effectiveness (Vedula and Metzger, 1989). Effectiveness is defined as  $\eta = (T_m - T_r) / (T_m - T_f)$ . Because  $T_r$  can not be measured directly, two similar tests are run, one with a cold injected film flow, and one with a hot injected film flow. From these two tests an iterative solution is performed for the heat transfer coefficient and film cooling effectiveness (Appendix A).

The experimental procedure begins with preheating the main and film flows. For a cold test the main flow is heated approximately 20 degrees higher than the film flow. In a hot test the film flow is heated approximately 20 degrees higher than the main flow. The temperatures selected for the preheating are based on experimental experience. The flow must not be too hot or the test surface temperature changes too quickly, in less than 10 seconds, and uncertainty in the timing is high. Additionally, the entire color change of the test surface should be completed within 60 seconds to ensure validity of the 1-D assumption used in data reduction (Vedula and Metzger, 1989). While preheating the test rig, the video

capturing system is readied for use. The video camera is positioned on the test surface so the alignment for each test is the same. The temperature acquisition computer is turned on and the main and film flow chamber temperatures monitored. The preheating flow temperatures are also monitored just upstream of the ball diverter valves. The video capturing system uses a frame grabber board installed in a Sun workstation. A C language program gathers data from the frame grabber, and records the time required for each captured pixel to exceed a predetermined threshold for the color change of the TLC. The frame grabber captures a new frame about every 0.4 seconds. Prior to the test run, the background intensity of each pixel is checked to provide a base to which the threshold is added. The threshold value is determined by proper calibration of the TLC. This value must be high enough to eliminate noise, yet low enough to be obtained by the camera for each pixel. Before the background check, a small white object is placed in the corner of the test section. This serves as a starting mark. The computer program when started, will continually check the location of the white mark, waiting until it darkens (blown away, when the flow is directed to the test section) to start processing data. The marker results in only a small amount of uncertainty in absolute start time (less than .02 seconds). The initial temperature of the test chamber is recorded from the temperature acquisition computer, and the temperature gathering program is started. The temperature gathering program monitors both the main and film chamber flow temperatures until a 0.2 °F. change is detected. At this time the main and film flow

temperatures are recorded every .16 sec. After the air flow has been preheated and the flow pressures are set to the proper level, the temperature acquisition computer and Sun workstation are activated. The air stream valves are then switched to allow the streams to flow over the test surface. After 15 seconds the flow temperatures are elevated to ensure a quality color change. The pressure readings are recorded during the color change. After the color change is complete the video grabbing program is terminated, plenum pressure and orifice temperature are recorded. The test rig is allowed to cool between test runs for about 3 hours to ensure the re-establishment of a uniform initial test rig temperature necessary for a valid 1D heat conduction solution. A second hot test is performed and the time and temperature data from both experiments is further reduced on a computer main frame to find the heat transfer coefficient and effectiveness (Figure 3).

## 2.6 Data Reduction

The raw temperature data is reduced to a usable form by a FORTRAN program run on a PC. The temperature reduction program integrates the near step change in temperature numerically, and provides temperatures at a prescribed time interval. The usable temperature data is uploaded to the mainframe computer. The initial chamber temperatures are added to the file. A FORTRAN program, based on the logic in Appendix A, uses the temperature data, time data of the hot test, and the time data from the cold test. The program uses an iterative solution scheme to solve for the heat



transfer coefficient and effectiveness. The results are then processed on a Macintosh computer where graphs and color plots are created. The color plots were created using NCSA Datascope software with the interpolation option selected.

## 2.7 Calibration

Calibration of the TLC is an important step in the overall solution processes. The temperature for color change is used in the calculation of heat transfer coefficient and effectiveness. The TLC displays colors in response to temperature changes as a result of lattice reorientation of the crystal. When sprayed as a thin layer, the TLC is essentially clear and displays color with increasing temperature in sequence of red, green, blue, and back to clear. The process is reversible such that the calibration of temperature remains unchanged for a large number of cycles under laboratory conditions. While all TLC type coatings assume a finite time response for the lattice rotations, it has been shown that micro-encapsulated chiral nematic coatings on the order of  $10^{-3}$  cm thick require only a few milliseconds for this action (Ireland and Jones, 1987). This time lag is negligible in comparison with the thermal transients of the present study. The change of the color green is used in the present test because of its high intensity and low noise signal. The temperature at which the color green is achieved is determined with the use of a small piece of copper with a thermocouple embedded in the center. The copper surface is prepared in the same manner as the test surface. The copper piece is then inserted at the end of the

test surface. The background intensity of the test surface and copper piece are checked to ensure agreement. A test setup without film injection setup is used. The copper piece thermocouple is plugged into the temperature acquisition computer. The video capturing program is run in the same manner as an ordinary test. After the test is complete, the temperature file is displayed indicating time and temperature. The time data of the color change is displayed. The time to color change data is compared with the temperature data to find the temperature at color change. The video camera records an intensity value based on a color intensity scale of 0 to 255. The background value is recorded and a predetermined threshold is set. Several calibration tests yielded the same calibration temperature of 102.8 °F. within  $\pm 0.5$  °F for a threshold setting of 40 above the background intensity. All test surfaces were sprayed with the same batch of TLC, and the same calibration temperature was used for all calculations.

## 2.8 Test Matrix

The first set of tests performed are to provide a baseline datum. These tests are performed without film cooling. The three geometries used were flat plate,  $3/8$ " cavity, and 1.0" cavity. The tests without injection are performed at three different Reynolds numbers, based on hydraulic diameter of the clearance gap: 45,000, 30,000, and 15,000. The cavity test models used are the same models that are used in the injection tests except the injection holes are plugged with wood. The wooden plugs were sanded smooth so as

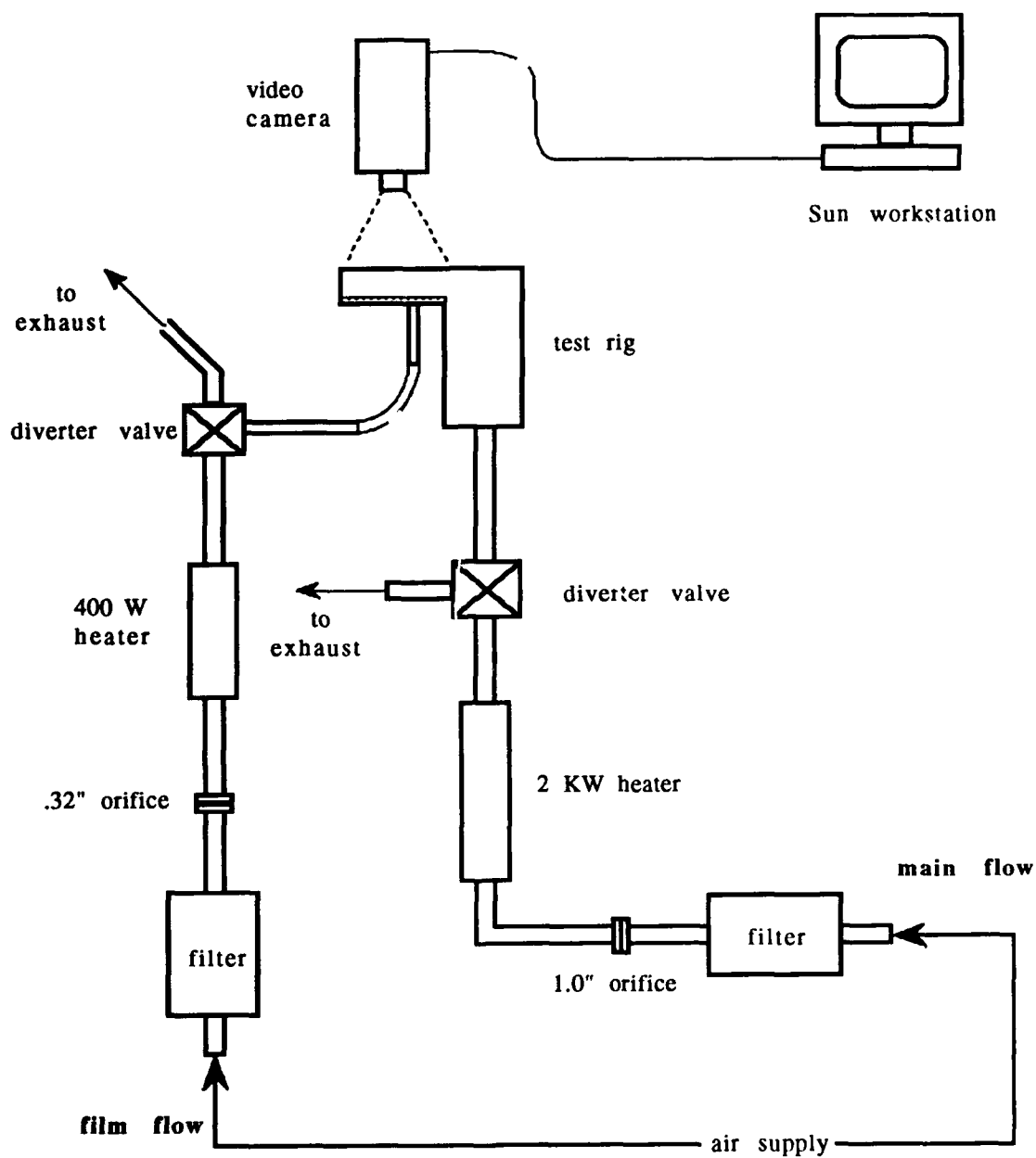
not to disturb the flow. The wood has a low thermal conductivity, therefore the plugs do not influence the heat transfer in the near-by Plexiglas. The main thrust of the present test program utilized the two cavity models. The two cavity depths are tested at a single Reynolds number of 30,000. Blowing ratios, based on mass flow, of 0.1 and 0.5 are used. The clearance gap is also changed to allow for different velocities over the test section; these gaps are  $3/16$ " and  $5/16$ ". The final variable is in the location of the injection holes. The holes are located  $1/4$ " from the edge of the cavity. Both pressure side and suction side locations are used. This test matrix mixed a variety of parameters thereby allowing the effects of single parameter variations to be known at selected combinations of the other parameters. Additional tests are performed to show repeatability, indicated by \* on the test matrix table.

Test surface	Re	Clearance gap	M	Location	
Flat Plate	45,000	3/16"	no injection		
	30,000				
	15,000				
	45,000	5/16"	no injection		
	30,000				
	15,000				
3/8" Cavity	45,000	*	3/16"	no injection	
	30,000				
	15,000				
	45,000	*	5/16"	no injection	
	30,000				
	15,000				
	30,000	*	3/16"	0.1	suction
			5/16"	0.1	pressure
				0.1	suction
				0.1	pressure
	30,000	*	3/16"	0.5	suction
			5/16"	0.5	pressure
				0.5	suction
				0.5	pressure

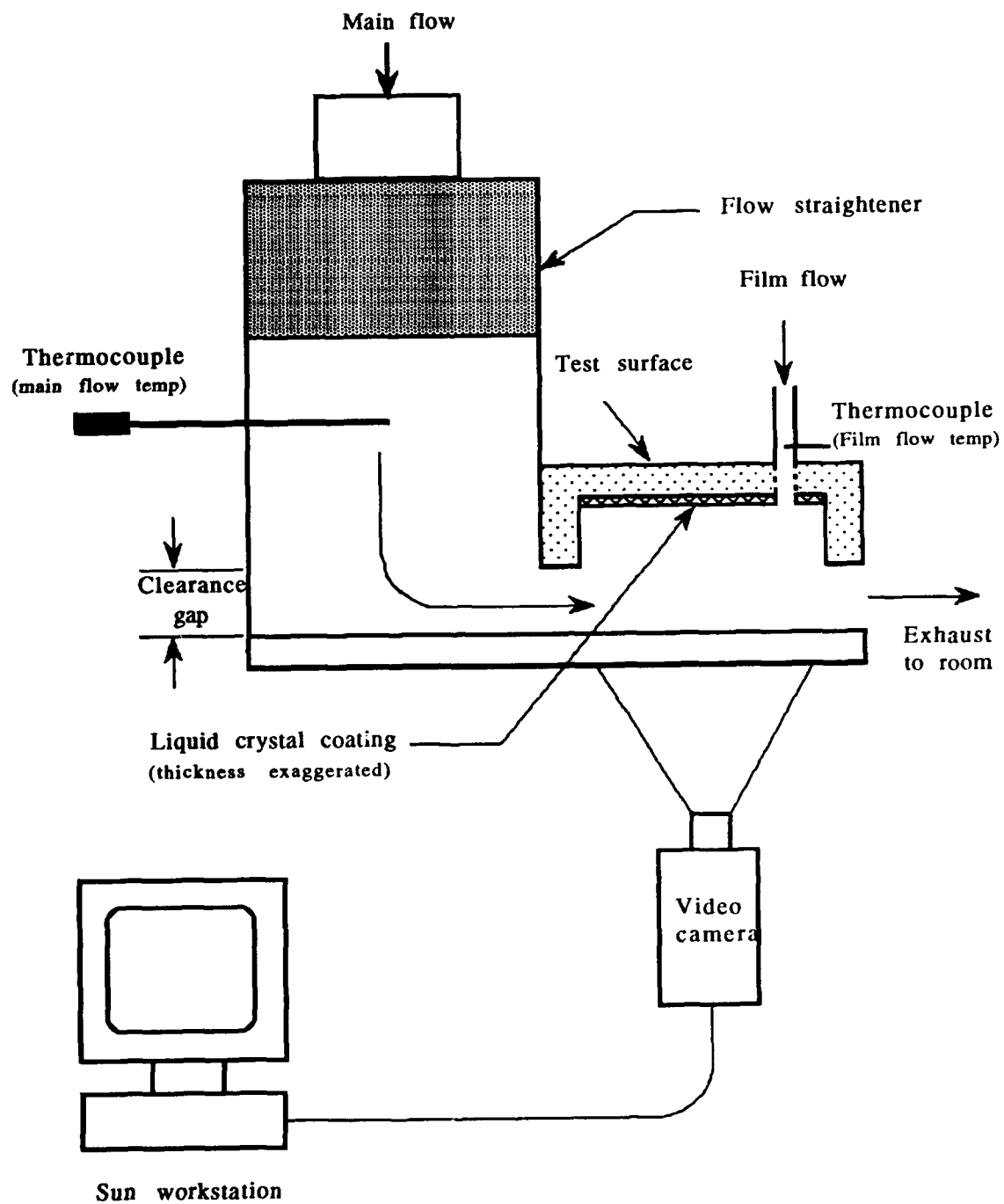
Test Matrix, baseline and  $3/8"$  cavity  
Table 1

Test surface	Re	Clearance gap	M	Location		
1.0" Cavity	45,000	3/16"	no injection			
	30,000				*	
	15,000					
	45,000	5/16"	no injection			
	30,000					
	15,000					
	30,000	*	3/16"		0.1	suction
			5/16"		0.1	pressure
					0.1	suction
					0.1	pressure
	30,000	*	3/16"		0.5	suction
			5/16"		0.5	pressure
					0.5	suction
					0.5	pressure

Test Matrix, 1.0" cavity  
Table 2



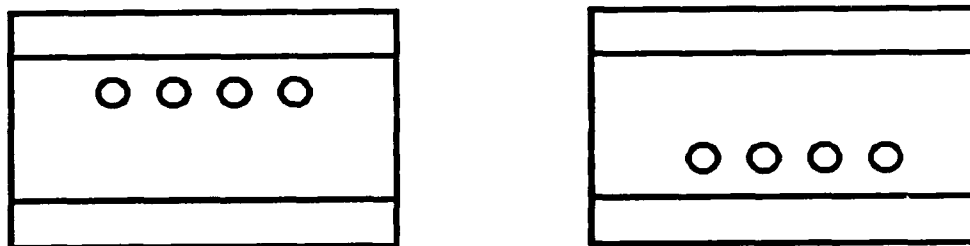
Test Facility  
Figure 2



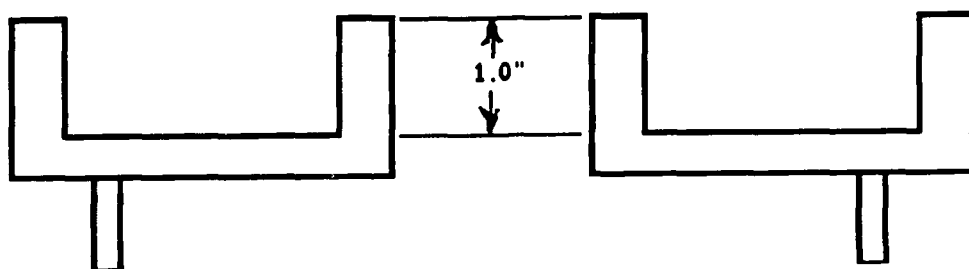
Test setup  
Figure 3

## Cavity models

## Top view

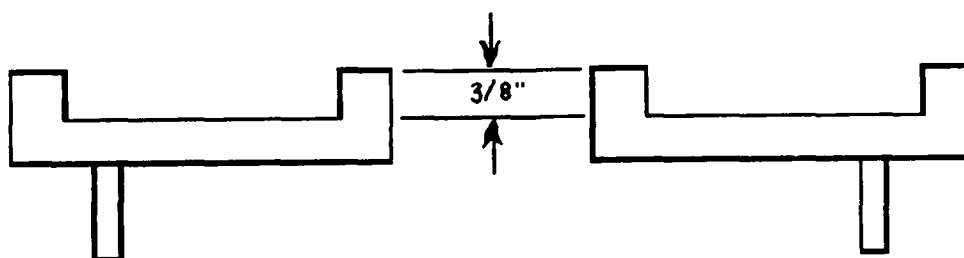


## Side view



Pressure side injection

Suction side injection



Pressure side injection

Suction side injection

Cavity models  
Figure 4



## CHAPTER 3

### RESULTS AND DISCUSSION

#### 3.1 Baseline Tests

In order to provide a base with which results can be compared, a series of tests are performed using the three basic geometries without film cooling injection. The three shapes are the flat plate,  $3/8$ " cavity, and the 1.0" cavity. The cavity models have injection holes located  $1/4$ " from the pressure edge; these holes are plugged and smoothed. Three Reynolds numbers are tested; 45,000, 30,000, and 15,000. In all cases, the Reynolds number is based on the hydraulic diameter of the clearance gap. In the case of the cavity models, the  $3/4$ " uncooled entrance length is thus the basis for the hydraulic diameter. This entrance length has the same clearance gap as for the flat plate, thereby resulting in the same hydraulic diameter for each geometry. Two clearance gaps are used,  $3/16$ " and  $5/16$ ". A narrower clearance gap results in a higher gap velocity for the same Reynolds number. One additional test is performed for each combination to ensure repeatability. No injection is performed in this series and effectiveness is not an applicable parameter.

Results are given for the streamwise variation of the spanwise averaged heat transfer coefficient from the pressure edge of the test surface to the suction edge. In the case of the cavity models, the streamwise average is from the suction edge of the plugged injection hole to the suction edge of the cavity. The average is taken  $1/4$ " from each edge to minimize the edge effects of the test rig. The heat

transfer coefficient is plotted versus the streamwise direction. The value of  $x/d$  corresponds to the nondimensionalized length of the test surface. The value  $d$  is set at .1, therefore the cavity surface at zero corresponds to an  $x/d$  value of 0. Likewise at the suction edge of the cavity surface, the  $x/d$  value of 20 corresponds to a length of 2.0". For the flat plate geometry the uncooled entrance length is  $3/8$ ", therefore the  $x/d$  value starts at -3.75. All three Reynolds numbers are plotted on the same graph, along with the additional test performed (Figures 5-10). Results for the spanwise average are taken from the pressure edge, center of the surface, and the suction edge,  $1/4$ " from each side. Again for the cavity models the pressure edge is replaced with the suction edge of the holes. Spanwise variations plots show the shape of the heat transfer coefficient front as it moves across the surface (Appendix B). These graphs are produced from raw data color plots found in Figures 55-60. Color plots of repeated tests data are not shown

The results show that for increasing Reynolds number the heat transfer coefficient increases as expected. The spanwise variation indicates a fairly uniform heat transfer contour, indicating a one-dimensional flow. The cavity model's results indicate that the flow travels across the surface, hits the back edge, circulating down and frontward against the main flow close to the surface, forming a classic recirculating region. As a result the cavity has the effect of smoothing out the heat transfer coefficient. The deeper the test cavity the lower the overall heat transfer. The possible reason for

this is that a lower percentage of the main flow is entrained into the recirculating flow.

### 3.2 $\frac{3}{8}$ " Cavity with Injection

The sequence of tests performed included the addition of film cooling flow injection. A single Reynolds number is used, 30,000. Two different clearance gaps of  $\frac{3}{16}$ " and  $\frac{5}{16}$ " are used. The blowing ratio is based on the specific mass flow of the film flow divided by the mass flow of the main flow. Two blowing ratios of  $M=0.1$  and  $M=0.5$  are used. Film cooling is provided by four  $\frac{3}{16}$ " holes placed in either of two locations;  $\frac{1}{4}$ " from the suction edge or  $\frac{1}{4}$ " from the pressure edge. The streamwise average is calculated for two locations. The average is taken from the edge of the suction side to the edge of the pressure side. One value is obtained by averaging the four values that correspond to the center line of the four holes, labeled center. The second value is an average centerline of the three locations between each hole, labeled between. The heat transfer coefficient and effectiveness are given for each of these combinations (Figures 11-30). Additional tests are presented to show repeatability. In Appendix B spanwise variation graphs are given for four row locations: suction edge, pressure edge, center surface, and center of holes. Color plots showing the complete test surface variations from which the graphs are produced are found in Figures 61-76.

In general, the results show that the effectiveness is highly dependent upon blowing ratio and injection location. The lower

blowing ratio has a more localized impact on effectiveness. This indicates that with the lower blowing ratio, the film cooling flow adheres to the surface better. With a blowing ratio of 0.5, the film flow apparently penetrates the circulating flow, producing a more uniform effectiveness. The overall effectiveness is higher for higher blowing ratios, and the suction side injection produces a higher overall effectiveness than the pressure side counterpart. The heat transfer coefficient shows a slight dependence on film cooling location, and the heat transfer coefficients tend to be higher with increasing blowing ratio. The smaller clearance gap ( $3/16$ " ) has higher flow velocities for the same test parameters than the  $5/16$ " clearance gap. This increase in velocities creates a higher overall effectiveness and heat transfer as compared to the larger clearance gap. Additional results showing repeatability are presented in Appendix C.

### 3.3 1.0" Cavity with Injection

The experiments conducted with the 1.0" cavity cover the same parameter ranges as those performed with the  $3/8$ " cavity. The exception is that different tests to determine repeatability are performed. The streamwise graphs are calculated in the same manner for the same injection locations (Figures 31-54). Color plots showing the results from which the graphs are extracted are found in Figures 77-92. Spanwise distributions are shown in the figures given in Appendix B.

The results indicate the same general trends with respect to the blowing ratio, injection location, and clearance gap as did those for the  $3/8$ " cavity. The main interest is the effects that the deeper cavity has on both the heat transfer coefficient and the effectiveness. In general, the deeper cavity results in lower overall heat transfer coefficient and more uniform effectiveness. Additional graphs presenting repeatability are found in Appendix C.

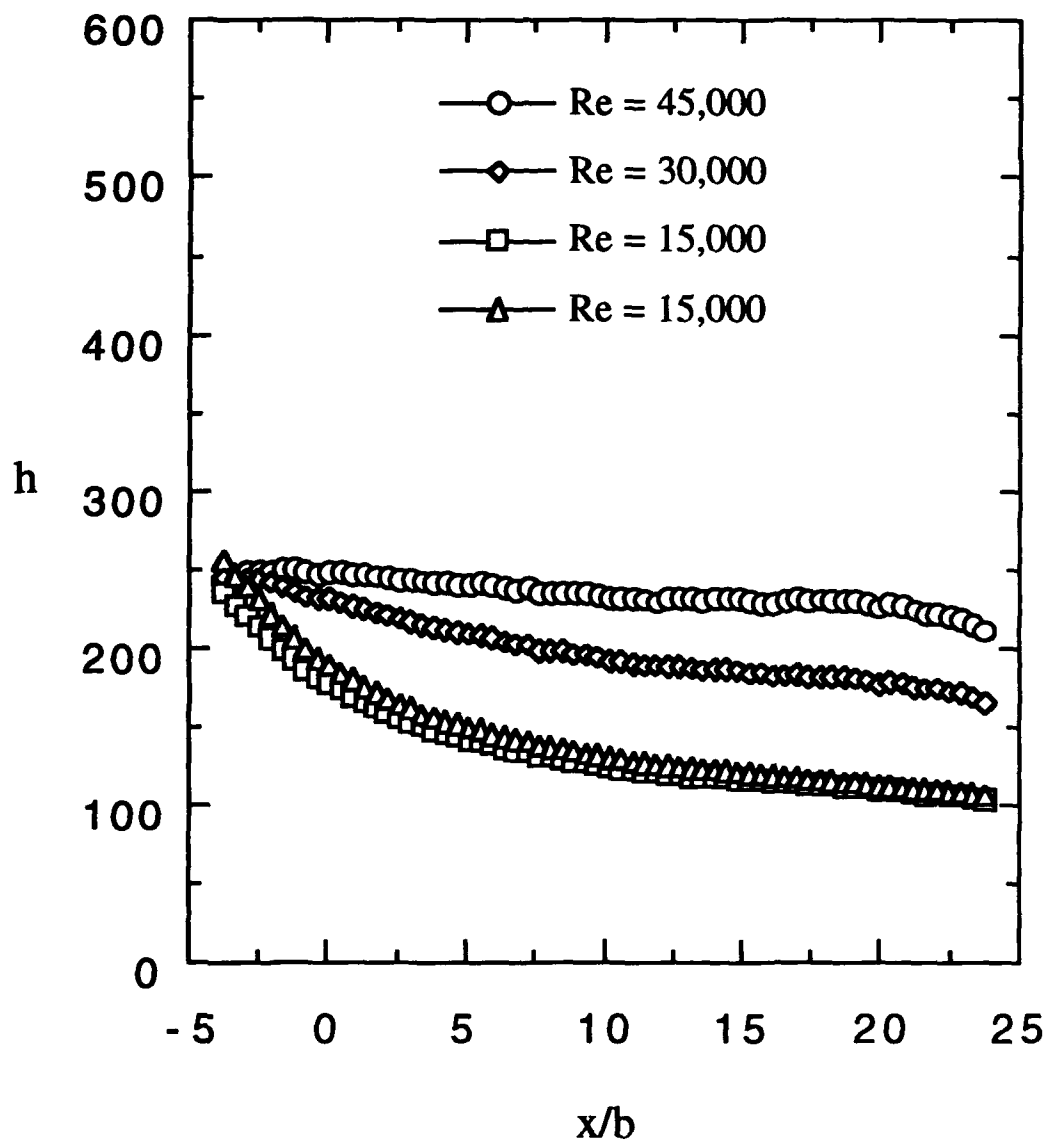


Fig. 5 Heat transfer coeff., streamwise variation,  
flat plate,  $3/16$ " clearance gap

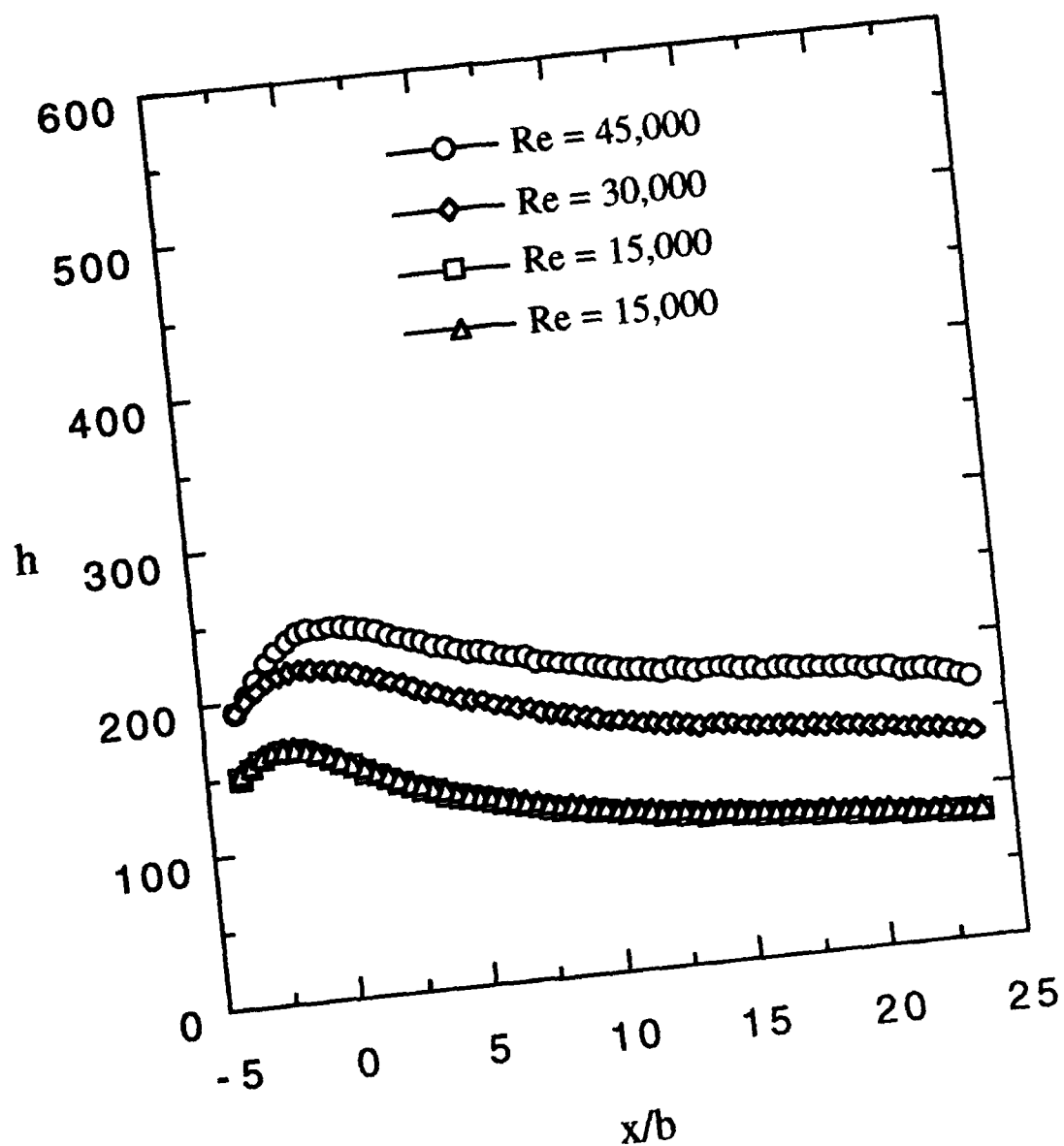


Fig. 6 Heat transfer coeff., streamwise variation,  
flat plate,  $5/16$ " clearance gap

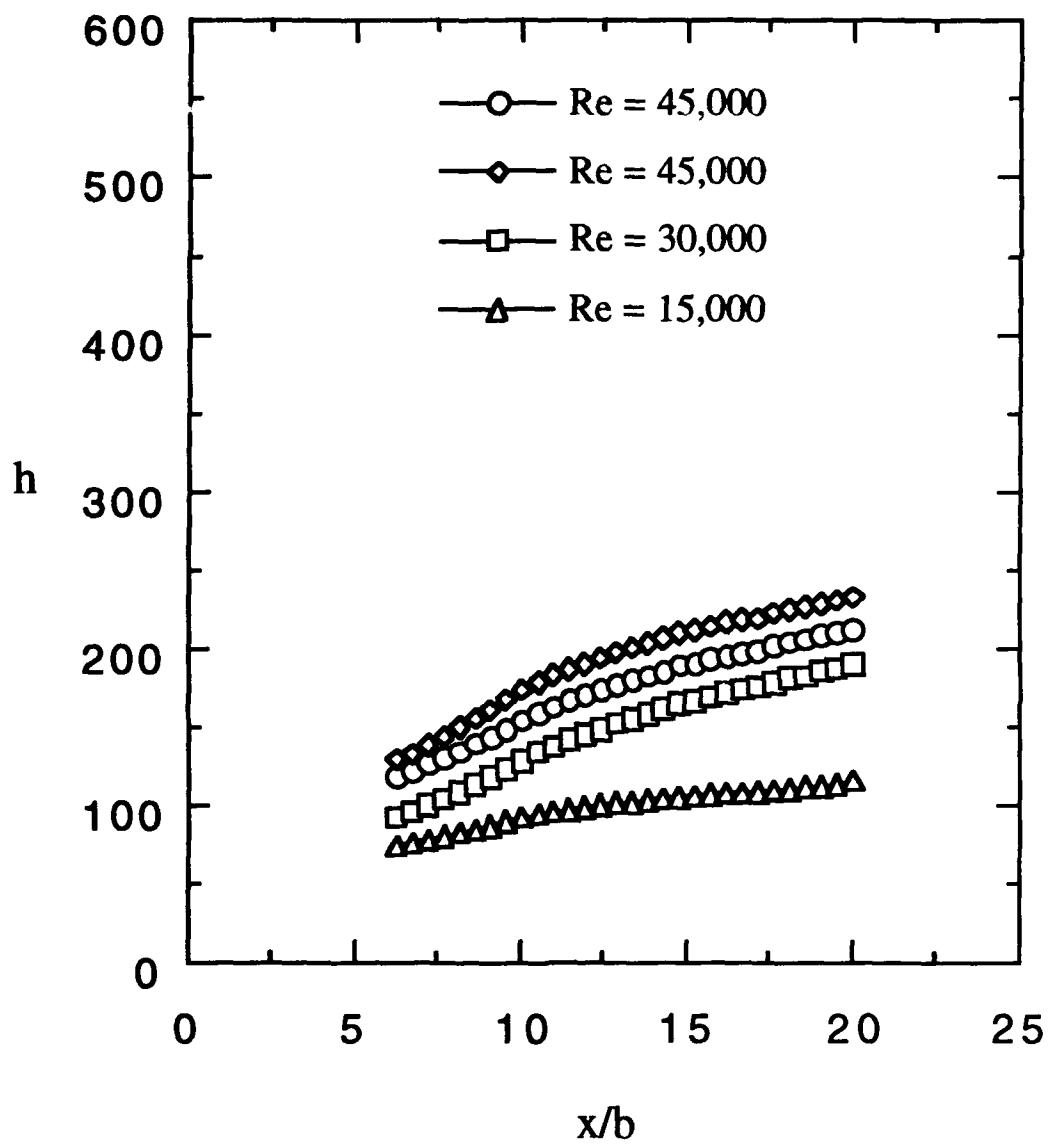


Fig. 7 Heat transfer coeff., streamwise variation,  
 $3/8$ " cavity,  $3/16$ " clearance gap



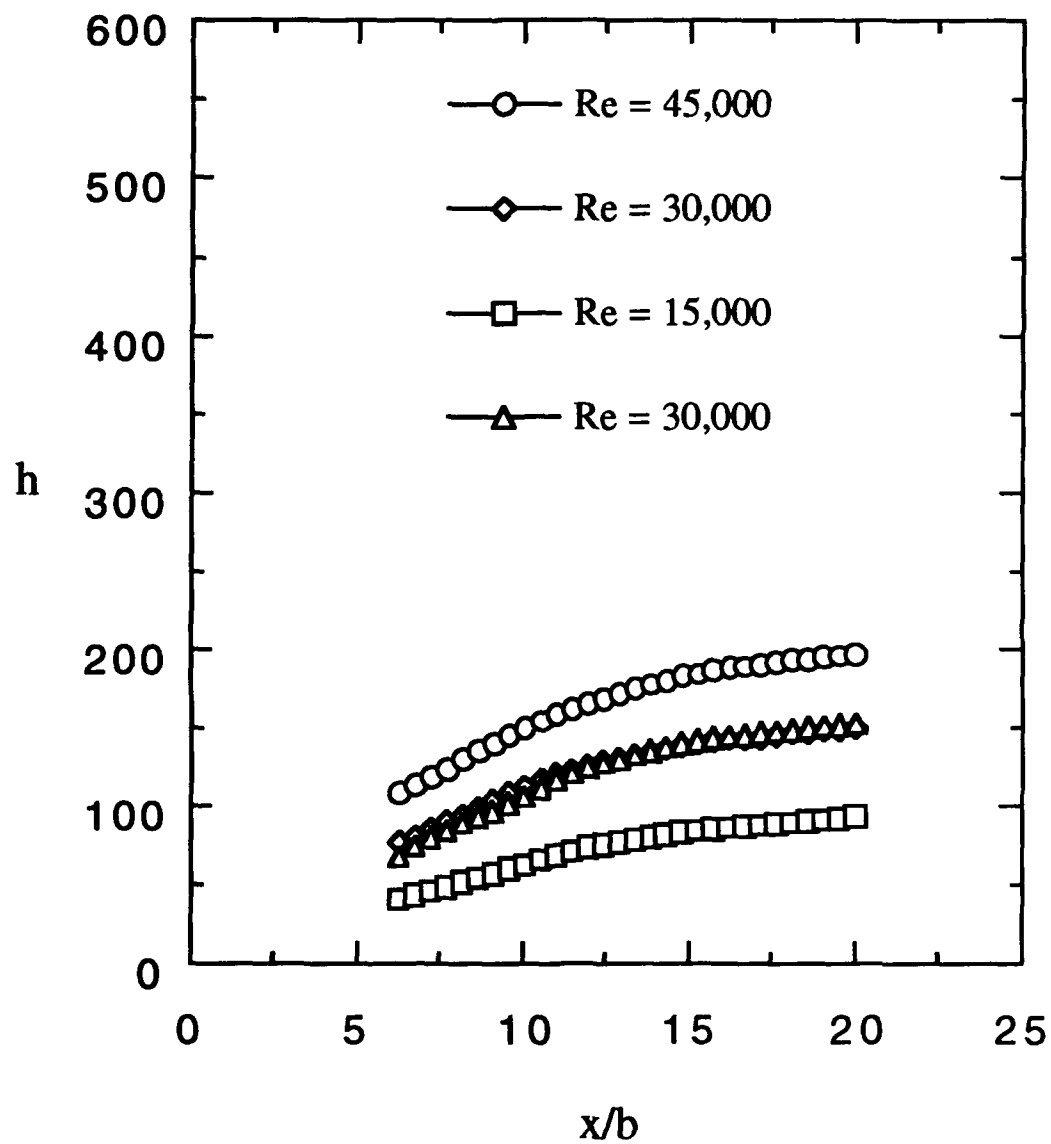


Fig. 8 Heat transfer coeff., streamwise variation,  
 $3/8$ " cavity,  $5/16$ " clearance gap

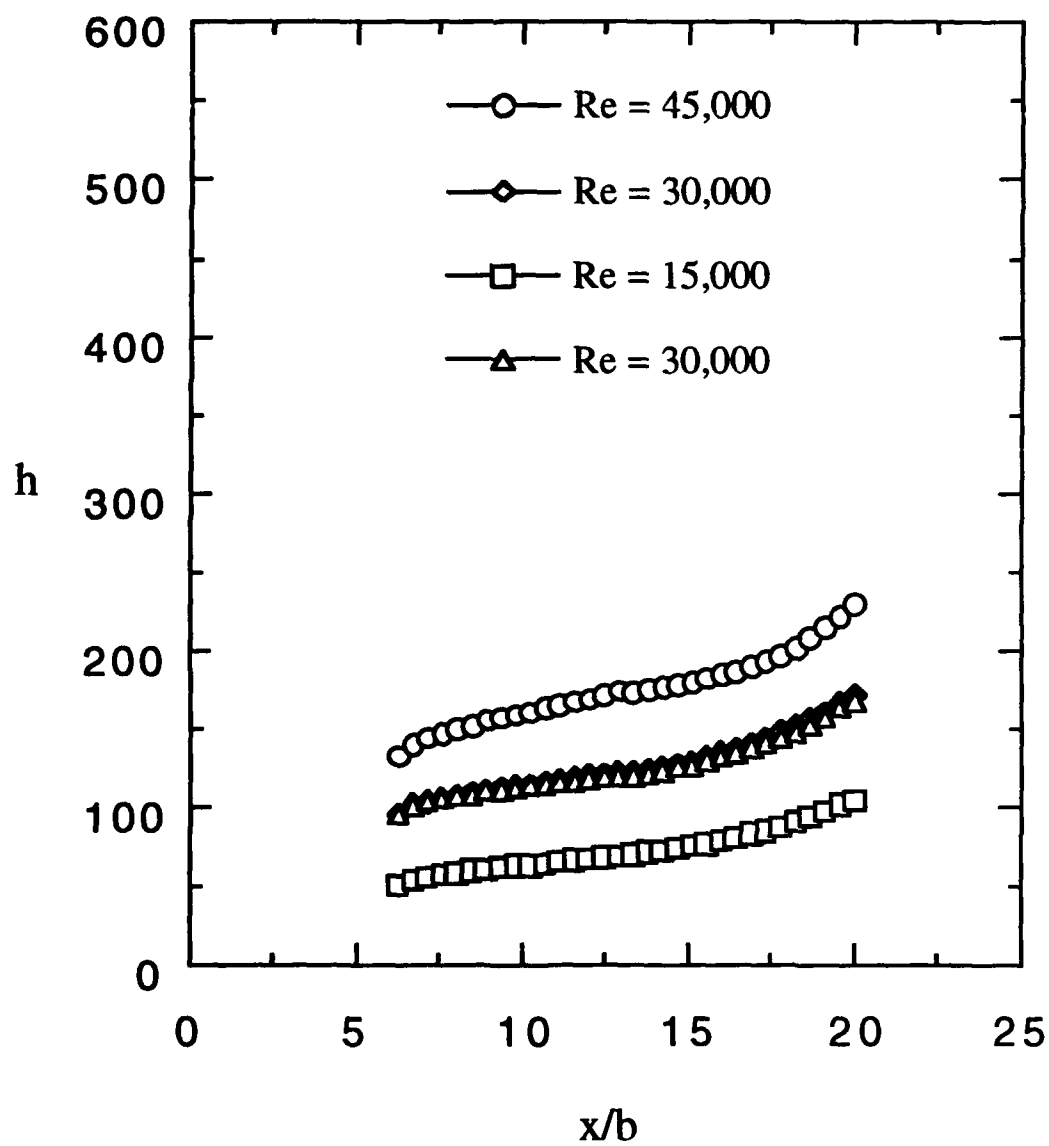


Fig. 9 Heat transfer coeff., streamwise variation,  
1.0" cavity,  $3/16$ " clearance gap

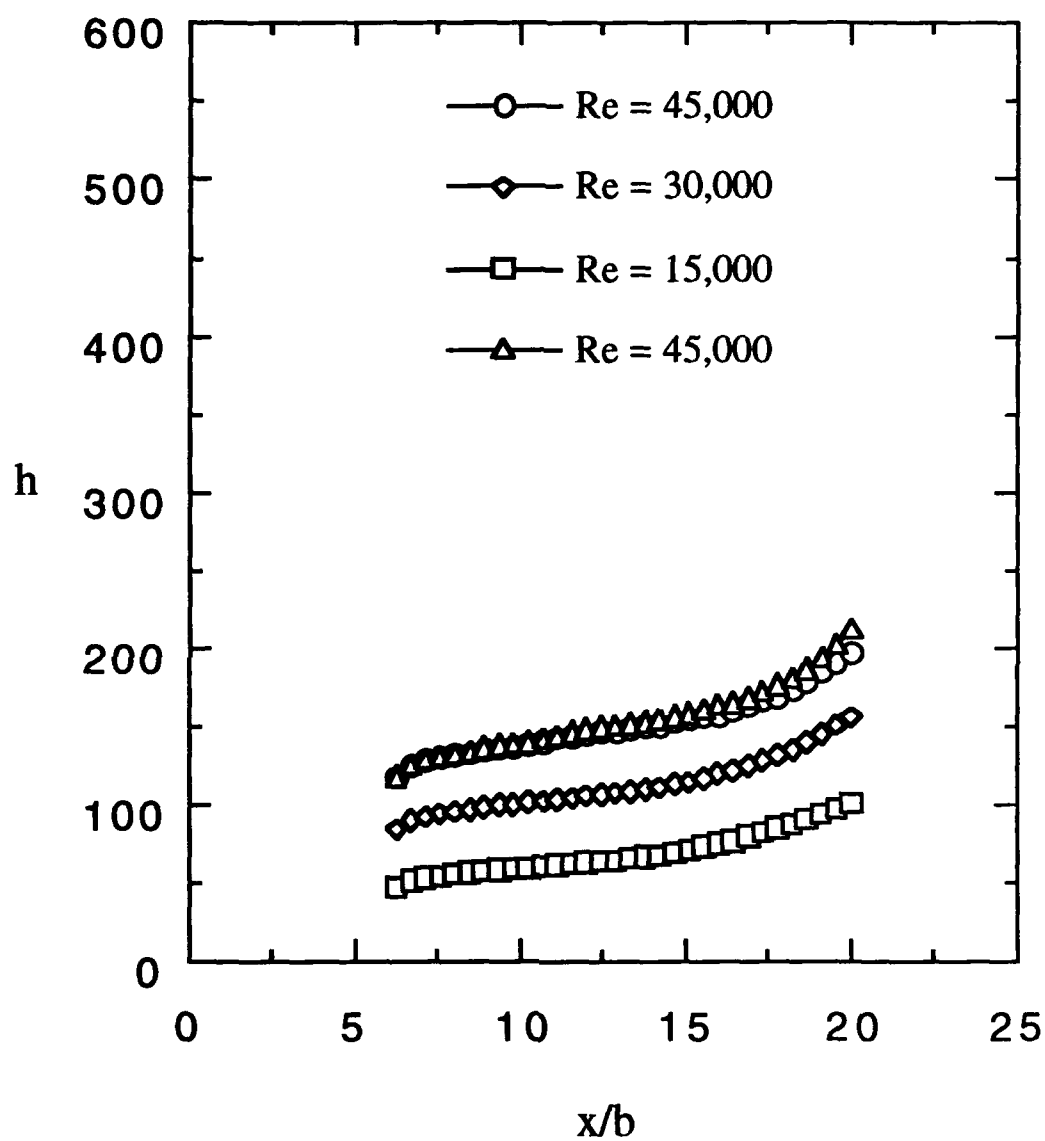


Fig. 10 Heat transfer coeff., streamwise variation,  
1.0" cavity,  $5/16$ " clearance gap

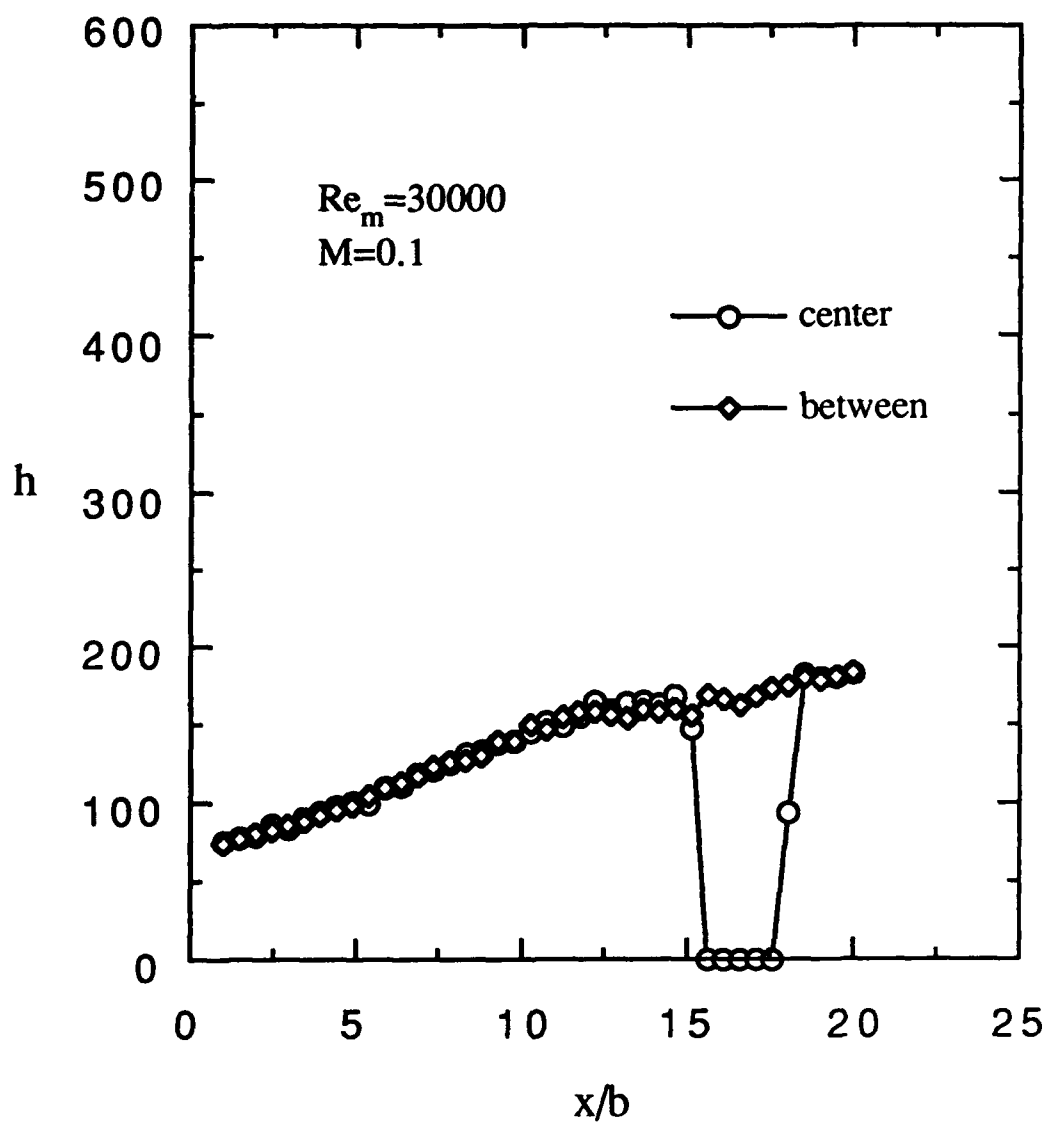


Fig. 11 Heat transfer coeff., streamwise variation,  
suction side injection,  
 $3/8$ " cavity,  $3/16$ " clearance gap

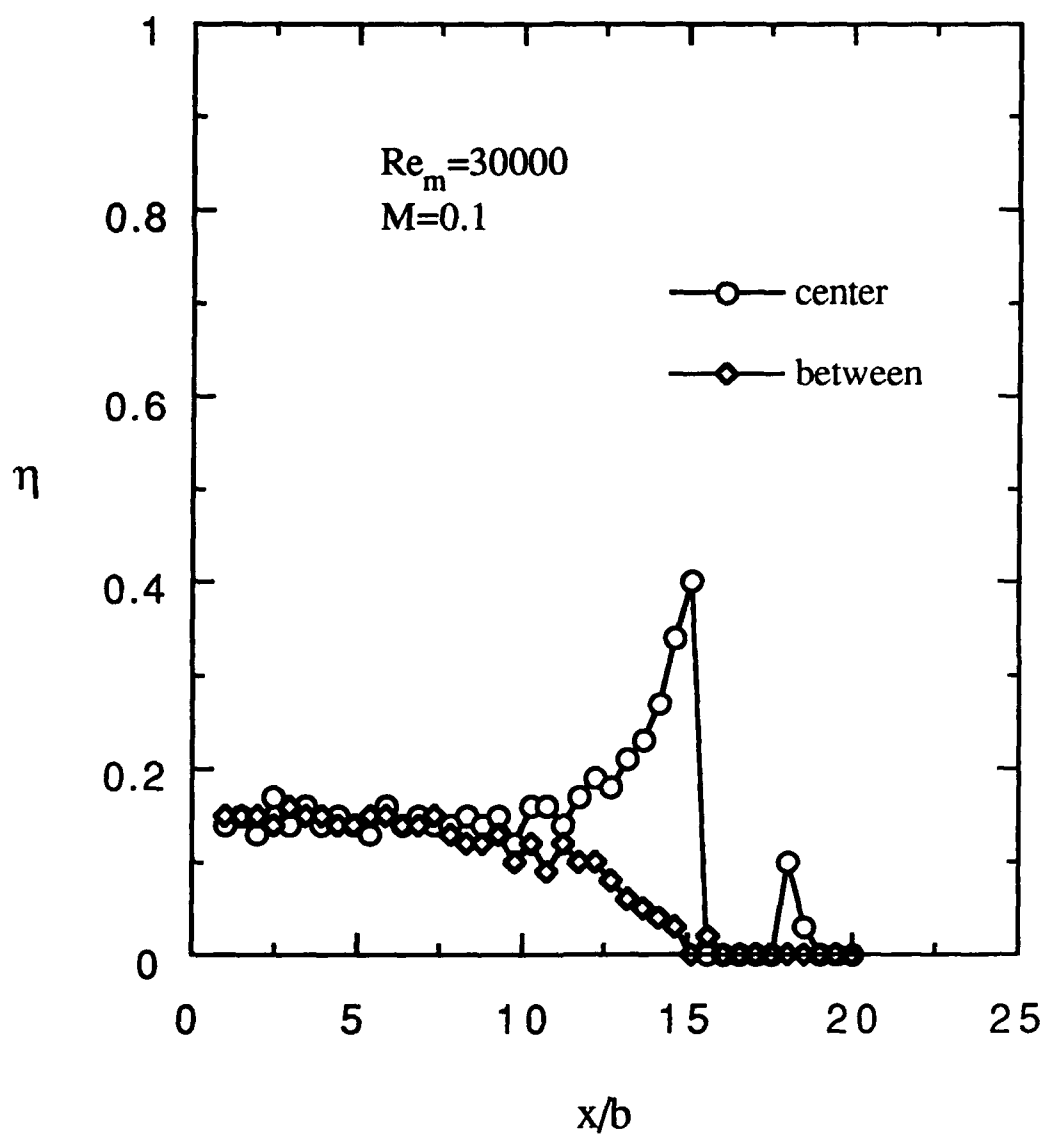


Fig. 12 Effectiveness, streamwise variation, suction side injection,  
 $3/8$ " cavity,  $3/16$ " clearance gap

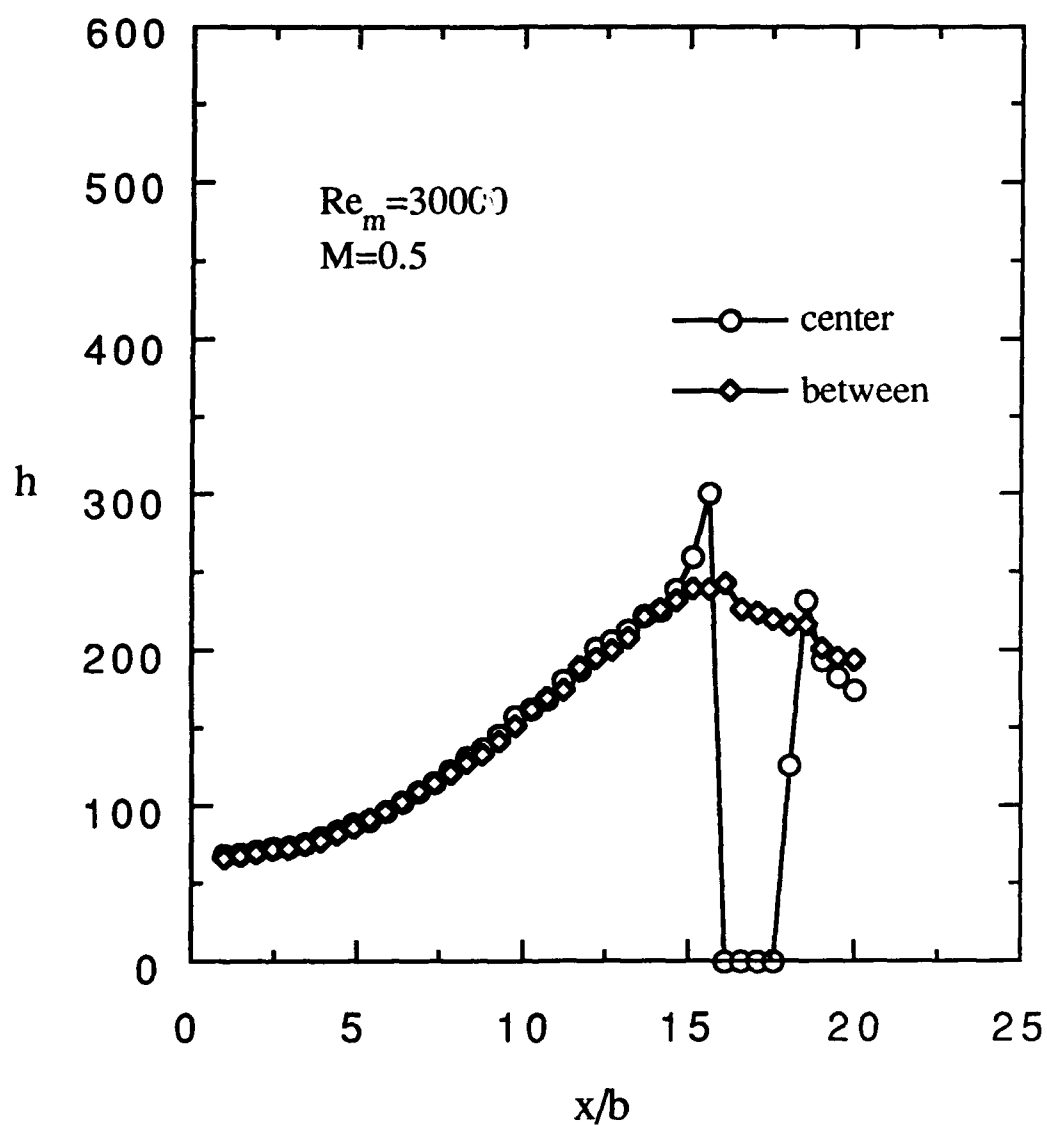


Fig. 13 Heat transfer coeff., streamwise variation,  
suction side injection,  
 $3/8$ " cavity,  $3/16$ " clearance gap, #1

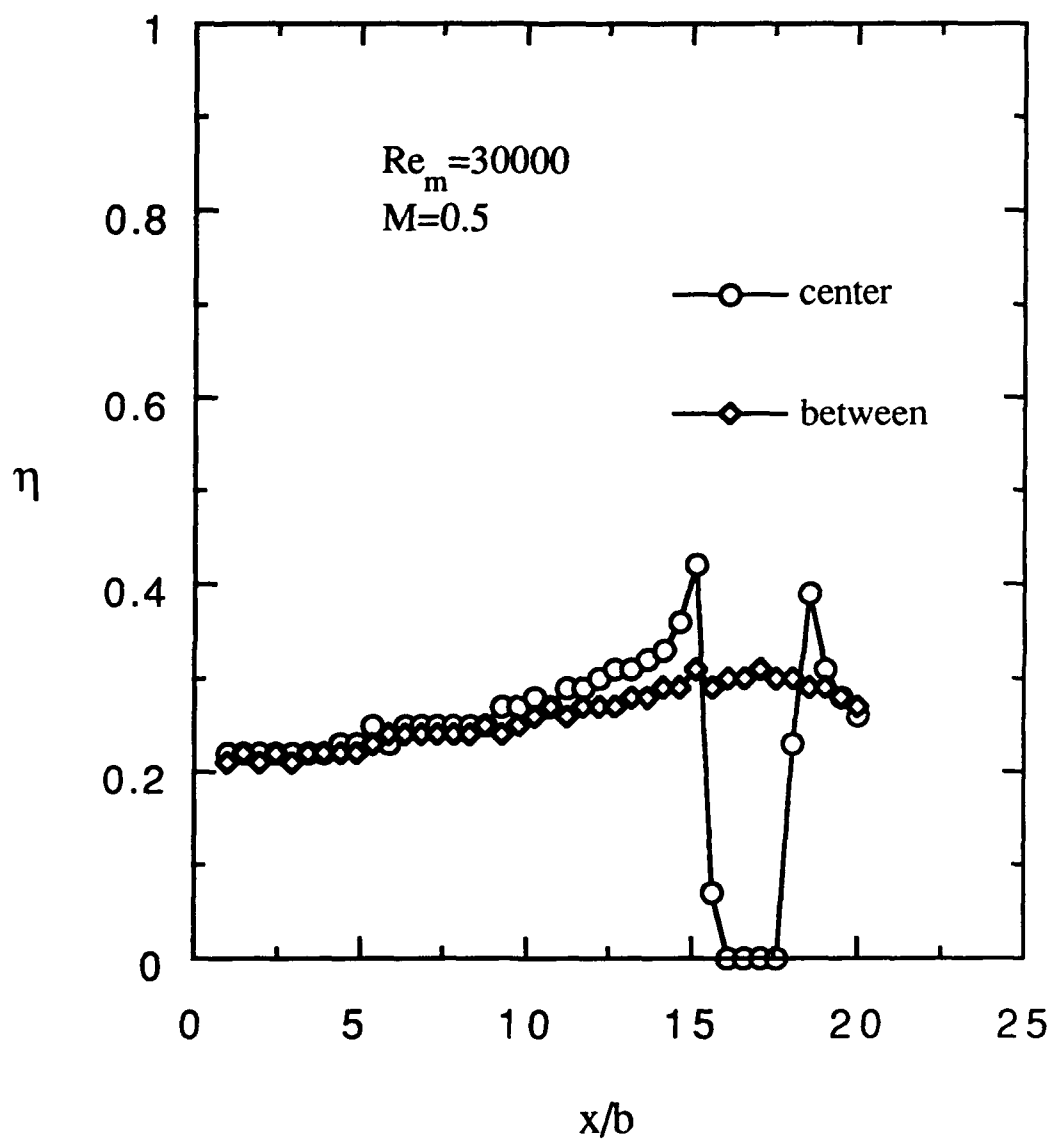


Fig. 14 Effectiveness, streamwise variation, suction side injection,  $3/8$ " cavity,  $3/16$ " clearance gap, #1

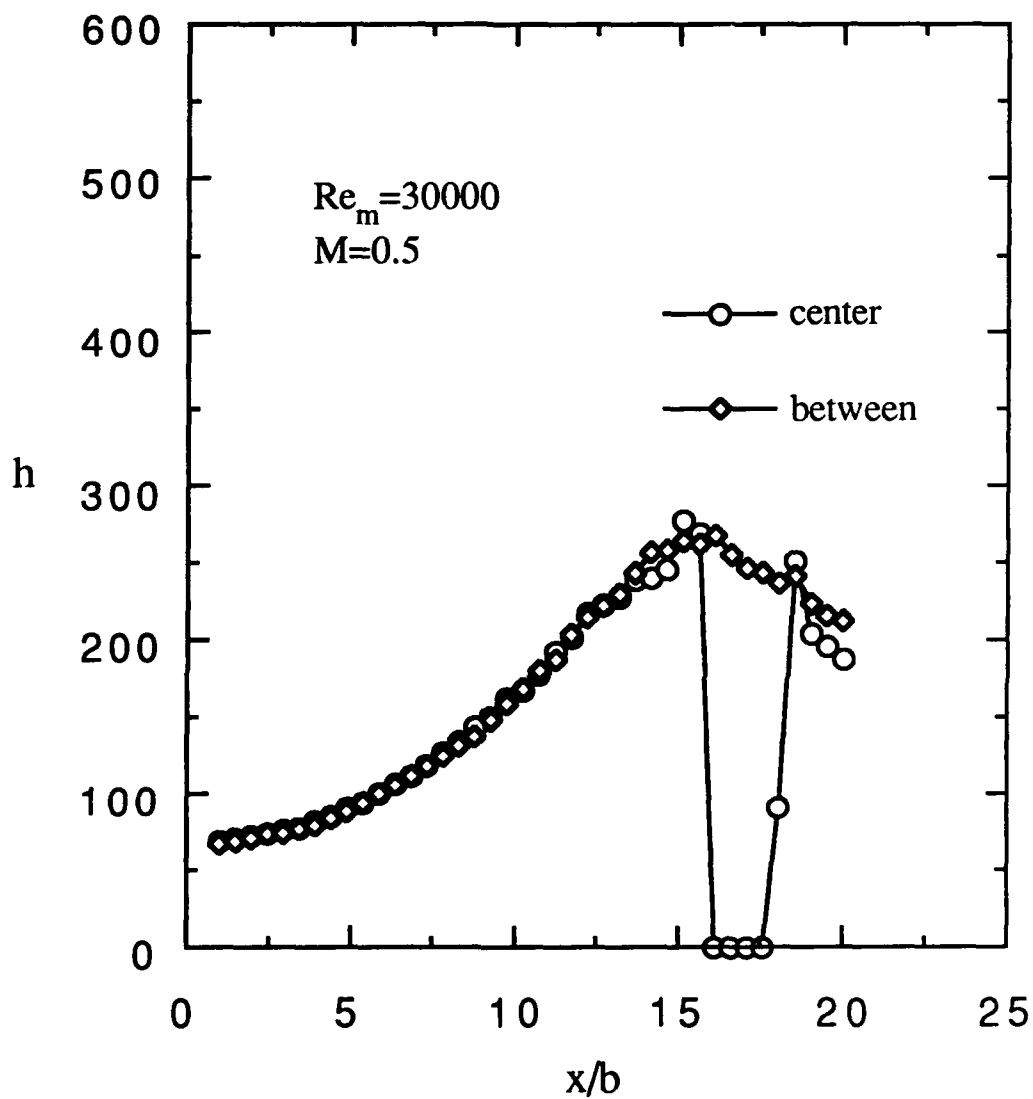


Fig. 15 Heat transfer coeff., streamwise variation,  
suction side injection,  
 $3/8$ " cavity,  $3/16$ " clearance gap, #2



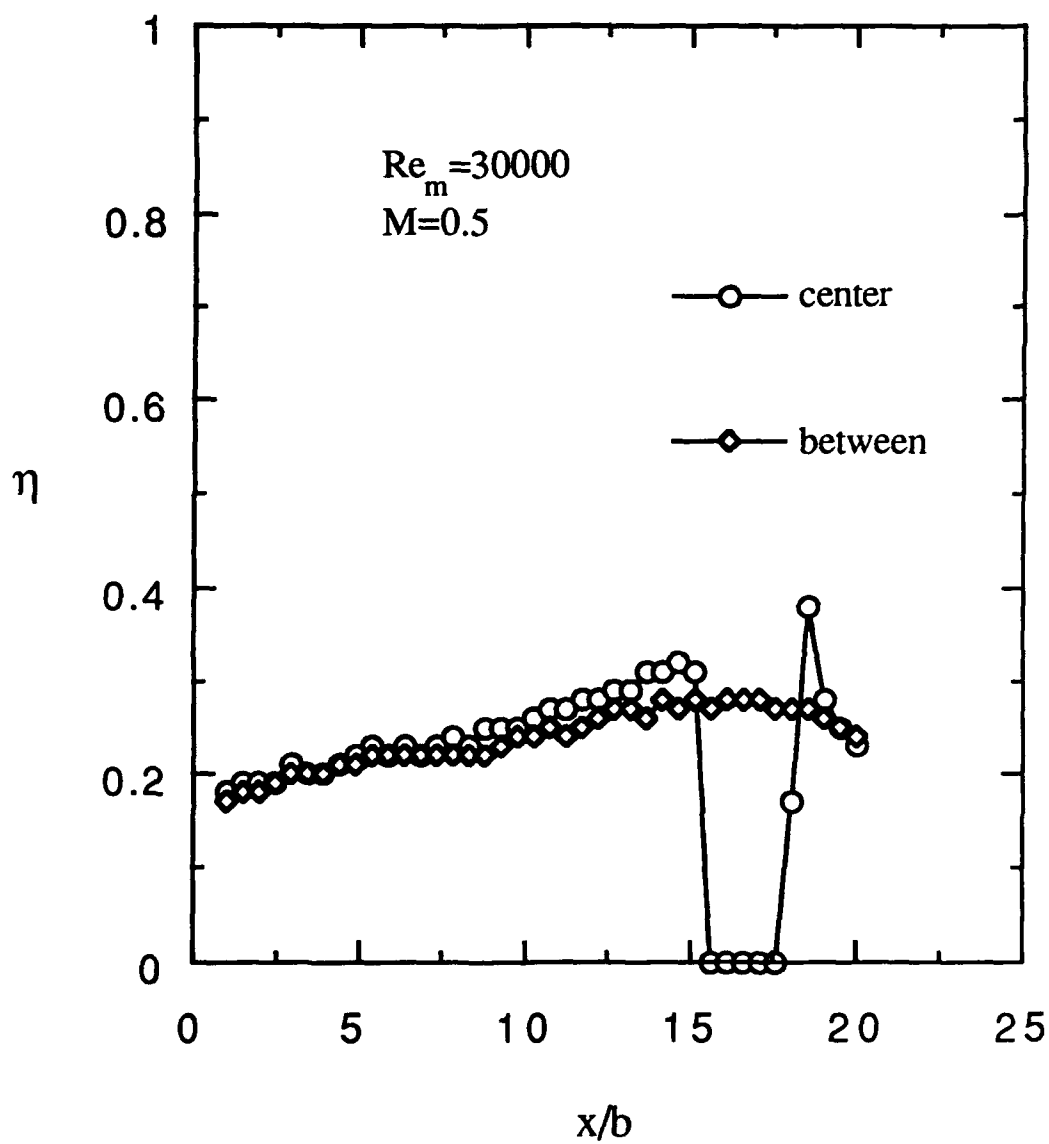


Fig. 16 Effectiveness, streamwise variation, suction side injection,  $3/8$ " cavity,  $3/16$ " clearance gap, #2

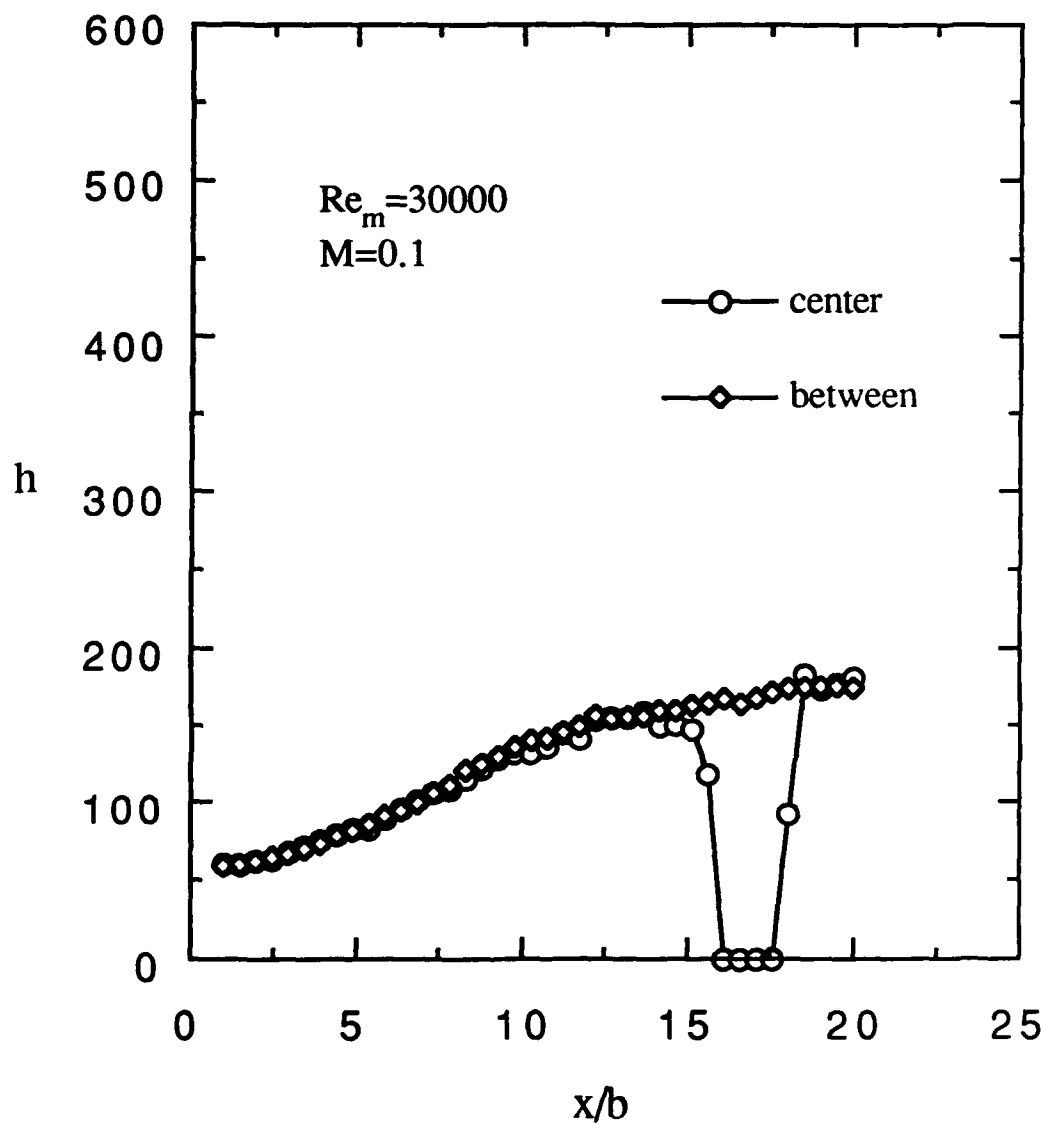


Fig. 17 Heat transfer coeff., streamwise variation,  
suction side injection,  
 $3/8$ " cavity,  $5/16$ " clearance gap, #1

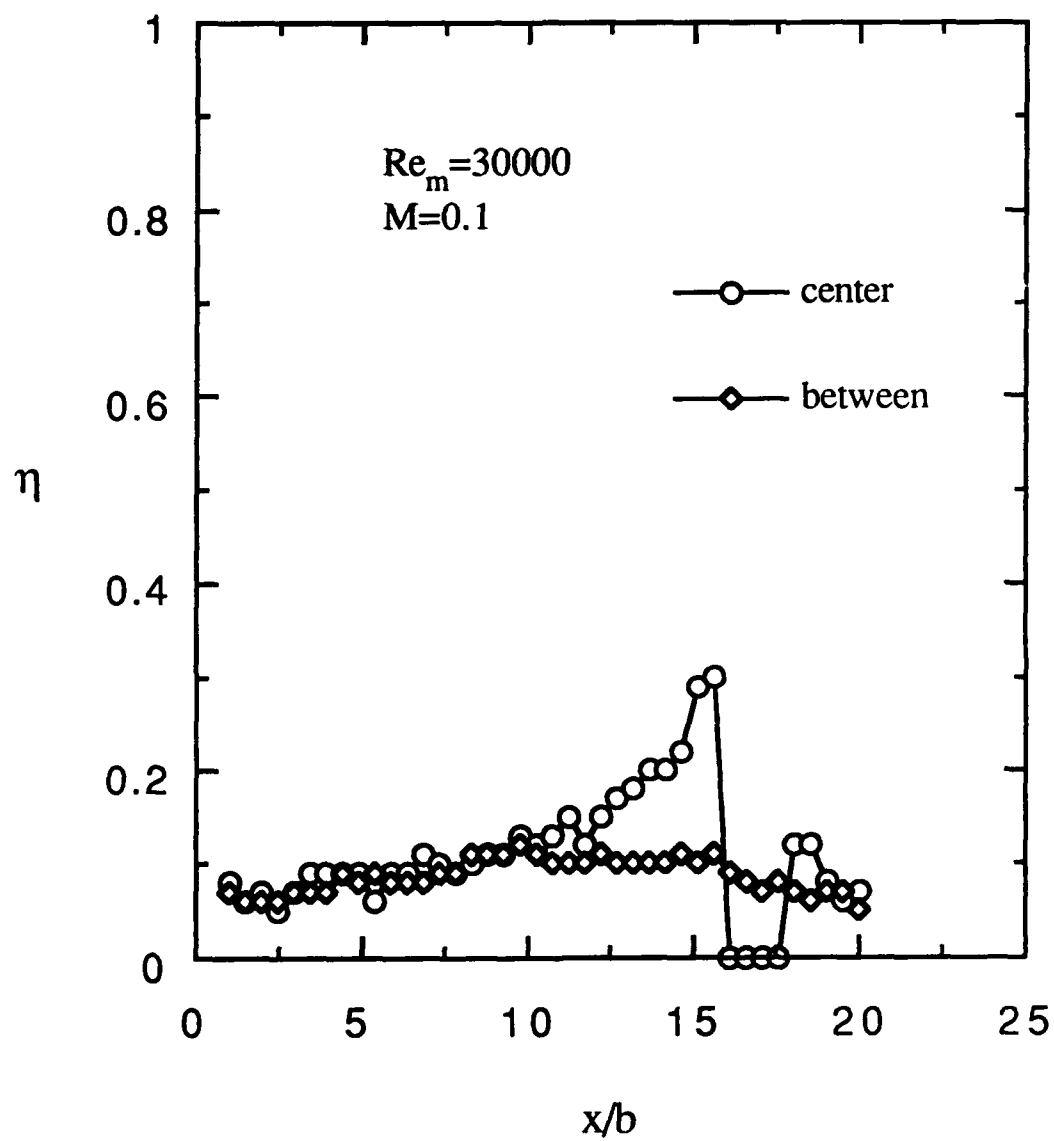


Fig. 18 Effectiveness, streamwise variation, suction side injection,  $3/8$ " cavity,  $5/16$ " clearance gap, #1

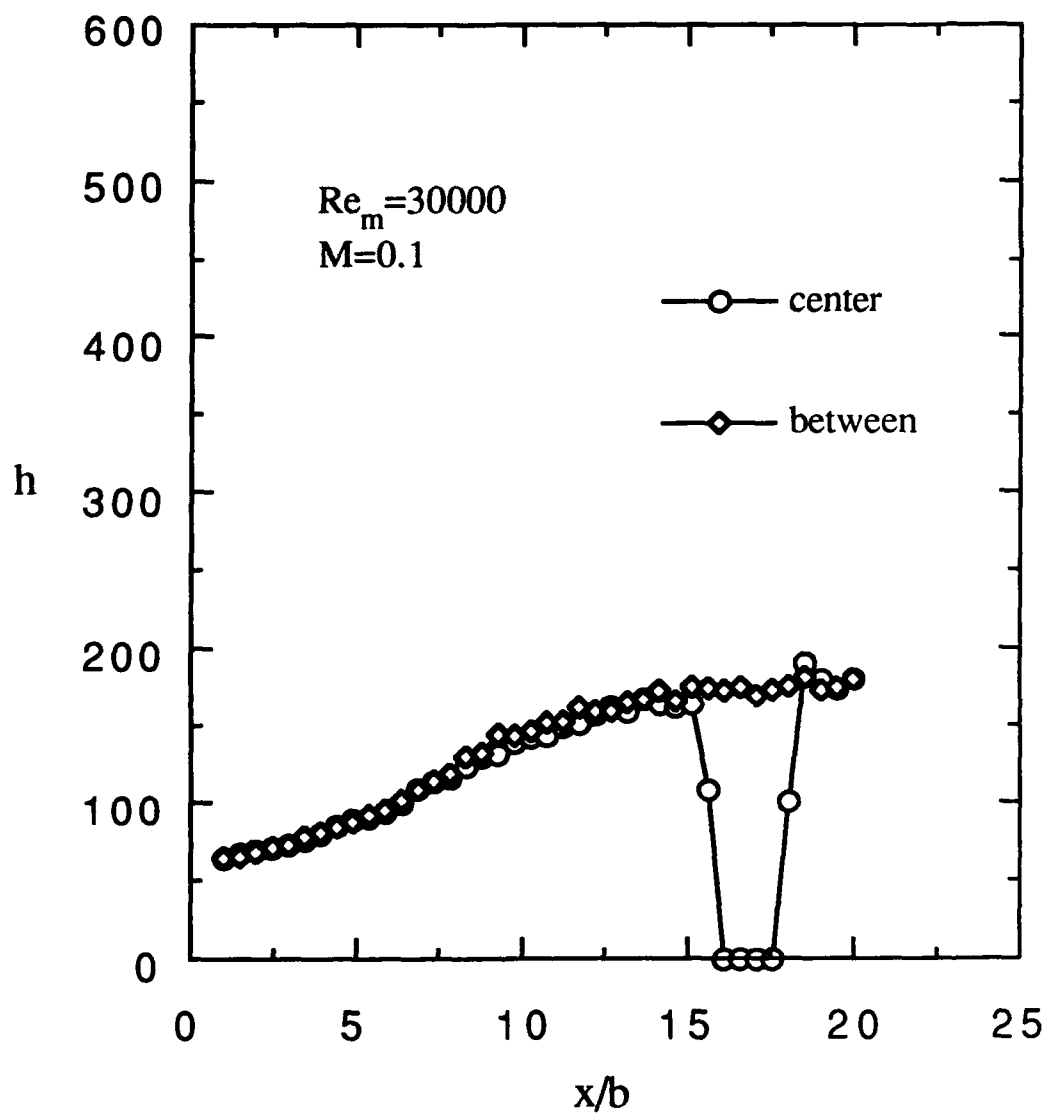


Fig. 19 Heat transfer coeff., streamwise variation,  
suction side injection,  
 $3/8$ " cavity,  $5/16$ " clearance gap, #2

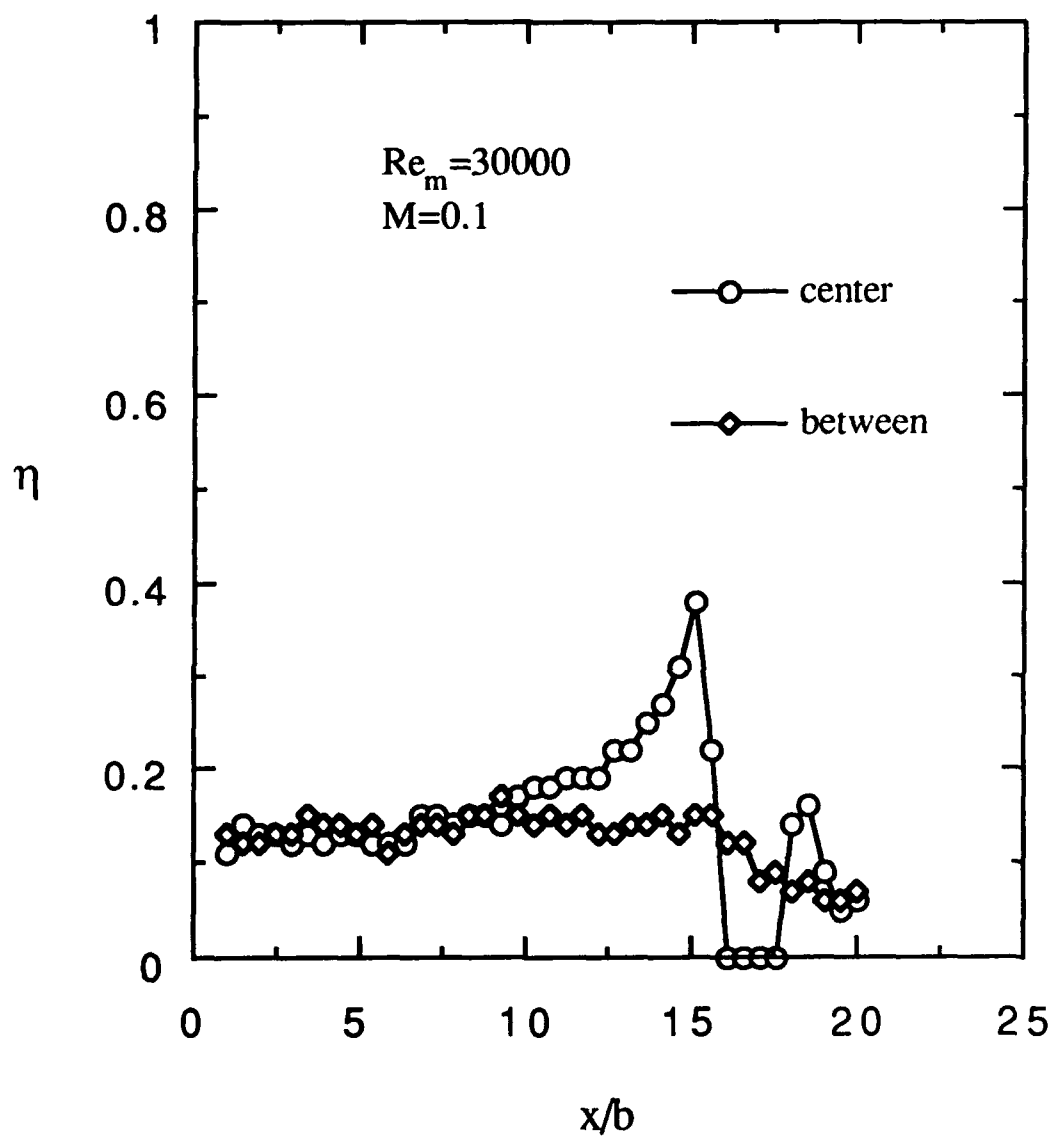


Fig. 20 Effectiveness, streamwise variation, suction side injection,  $3/8$ " cavity,  $5/16$ " clearance gap, #2

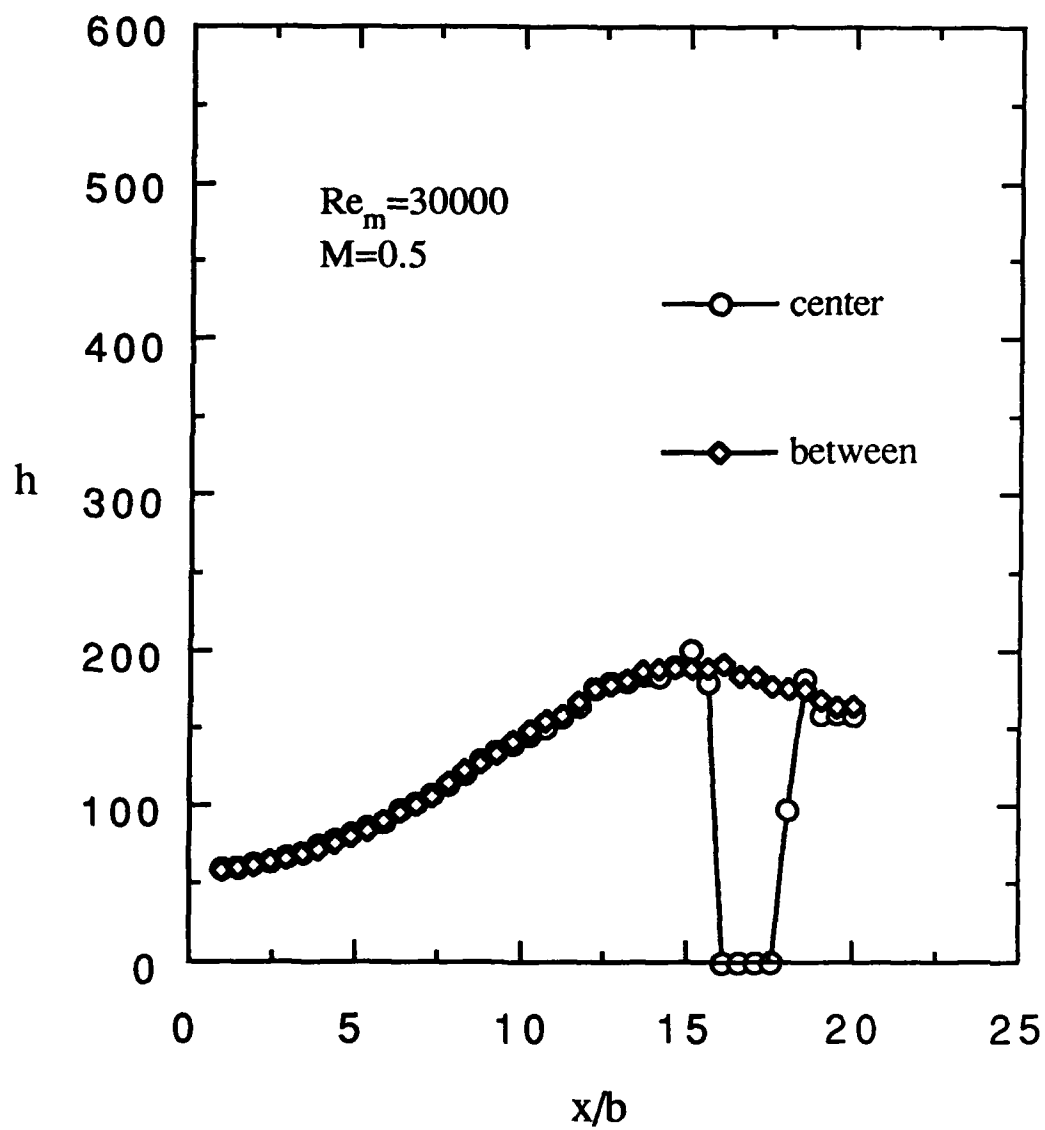


Fig. 21 Heat transfer coeff., streamwise variation,  
suction side injection,  
 $3/8$ " cavity,  $5/16$ " clearance gap

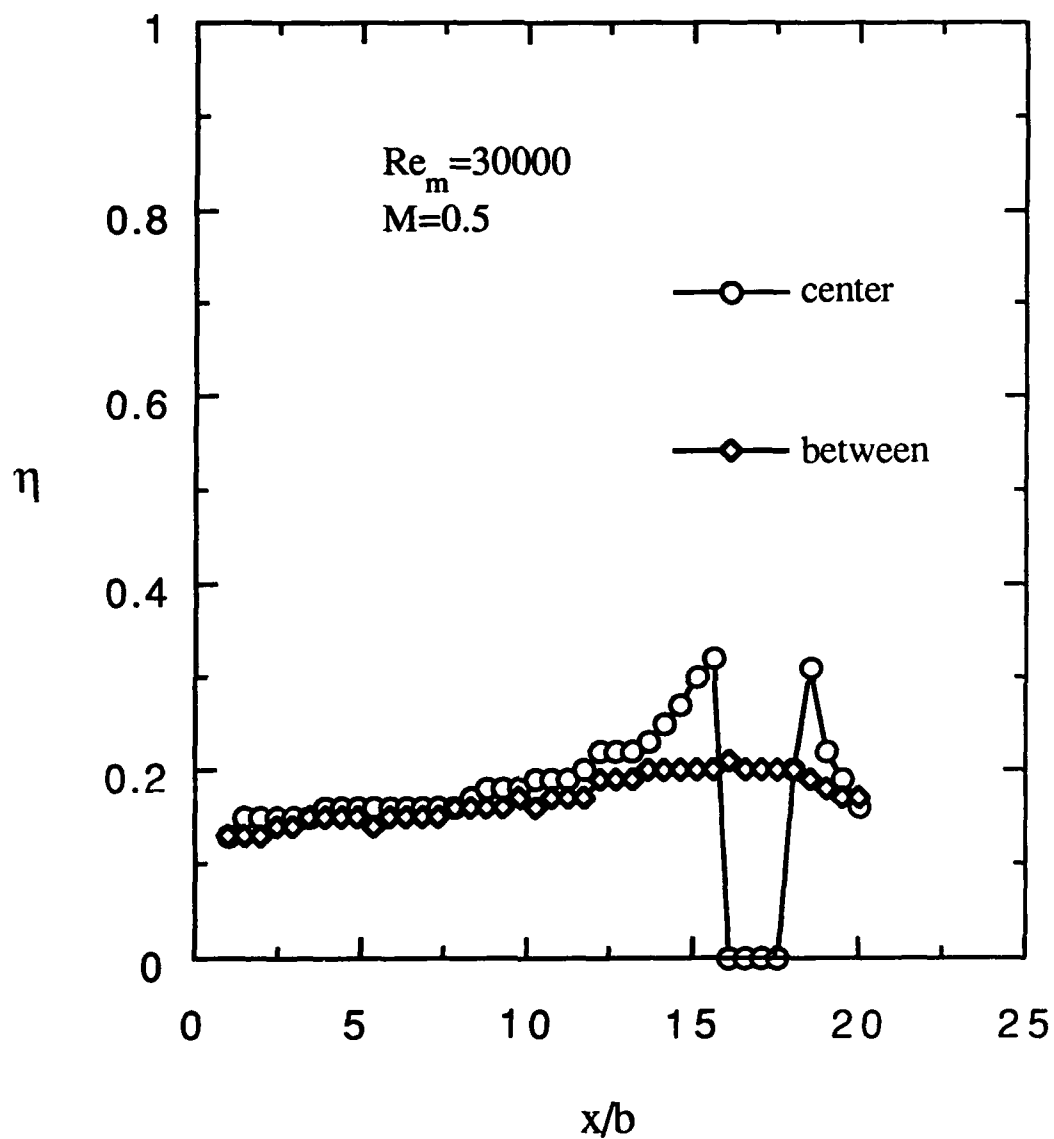


Fig. 22 Effectiveness, streamwise variation, suction side injection,  $3/8$ " cavity,  $5/16$ " clearance gap

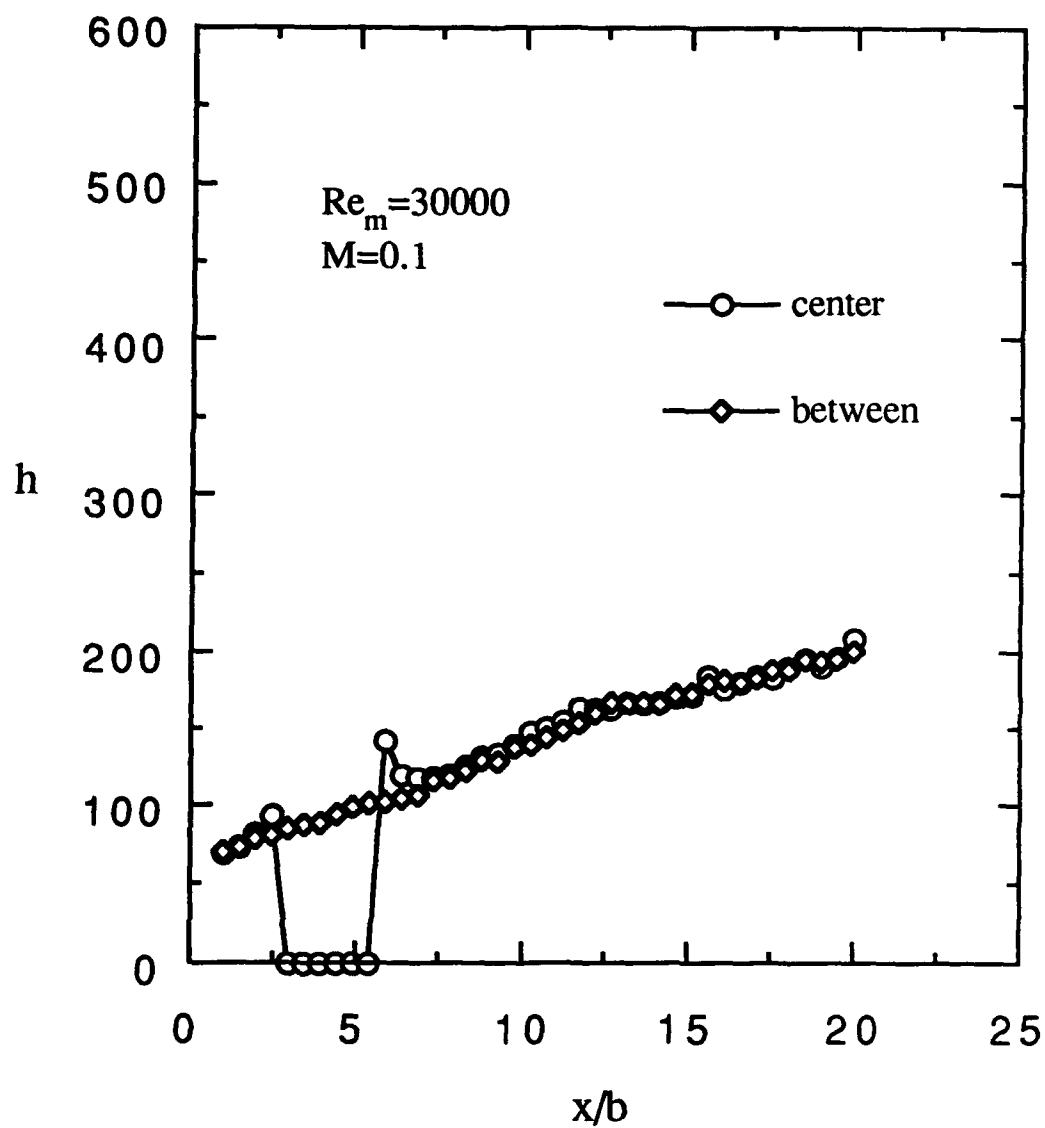


Fig. 23 Heat transfer coeff., streamwise variation,  
pressure side injection,  
3/8" cavity, 3/16" clearance gap



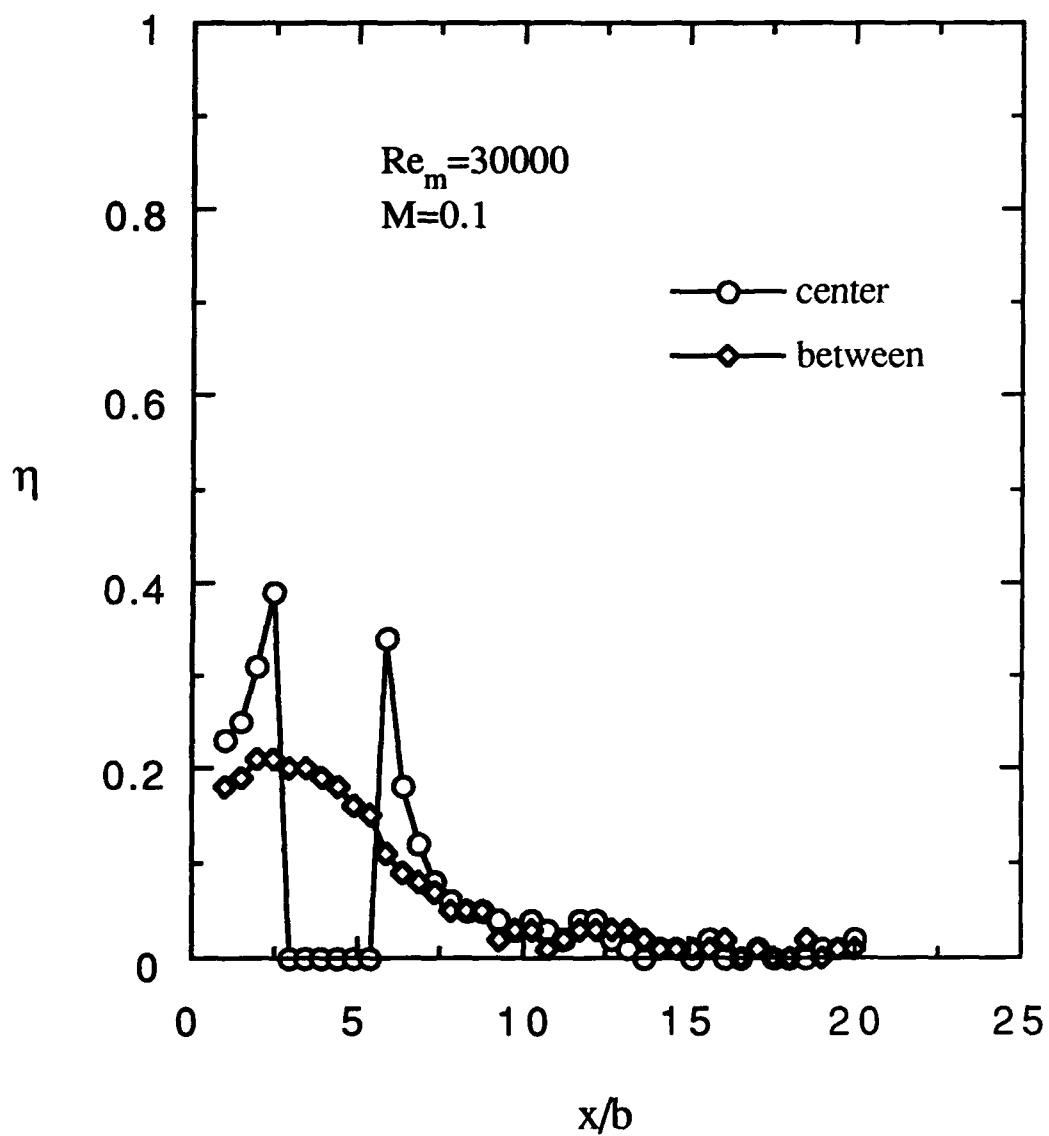


Fig. 24 Effectiveness, streamwise variation, pressure side injection,  $3/8$ " cavity,  $3/16$ " clearance gap

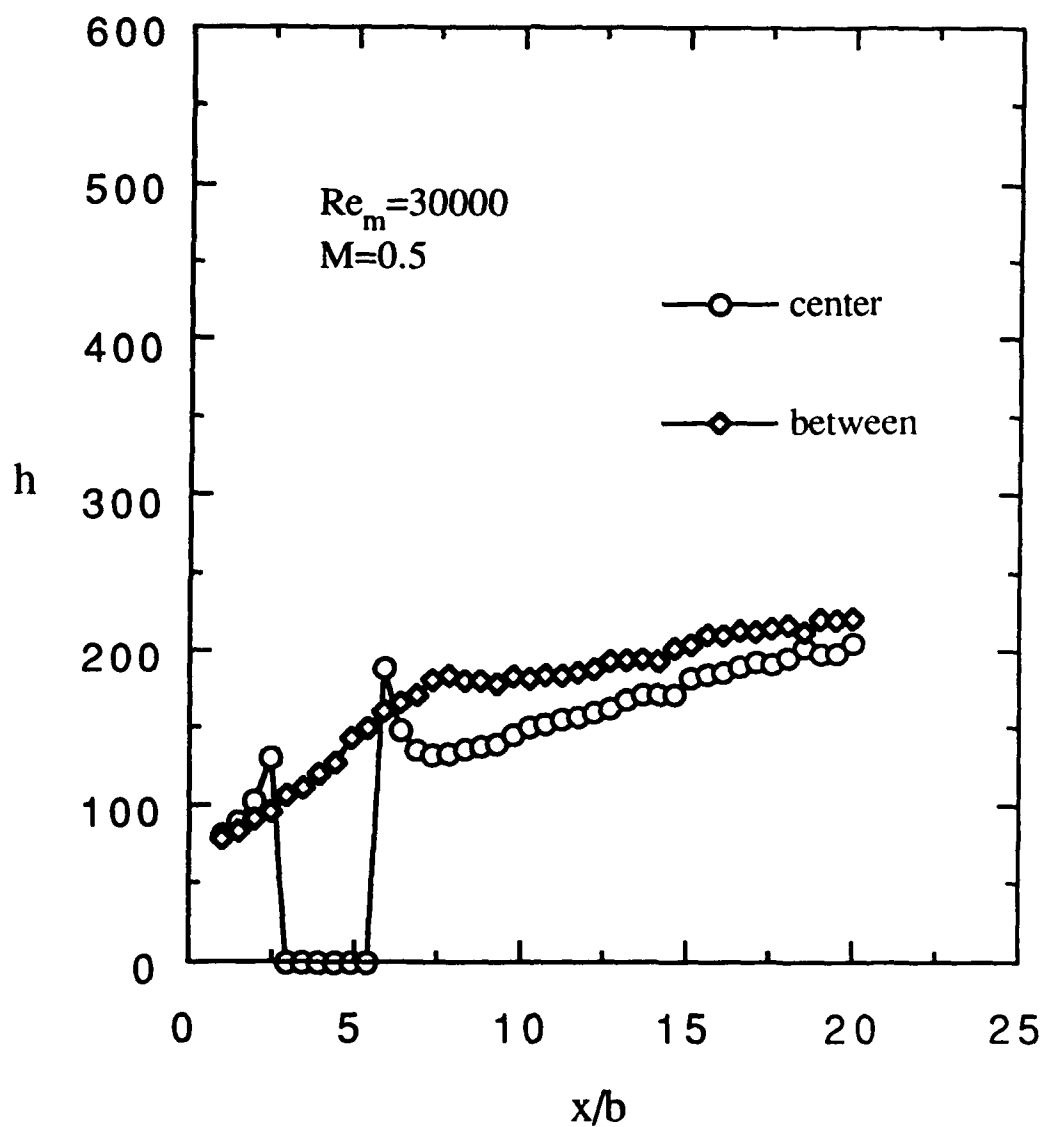


Fig. 25 Heat transfer coeff., streamwise variation,  
pressure side injection,  
 $3/8$ " cavity,  $3/16$ " clearance gap

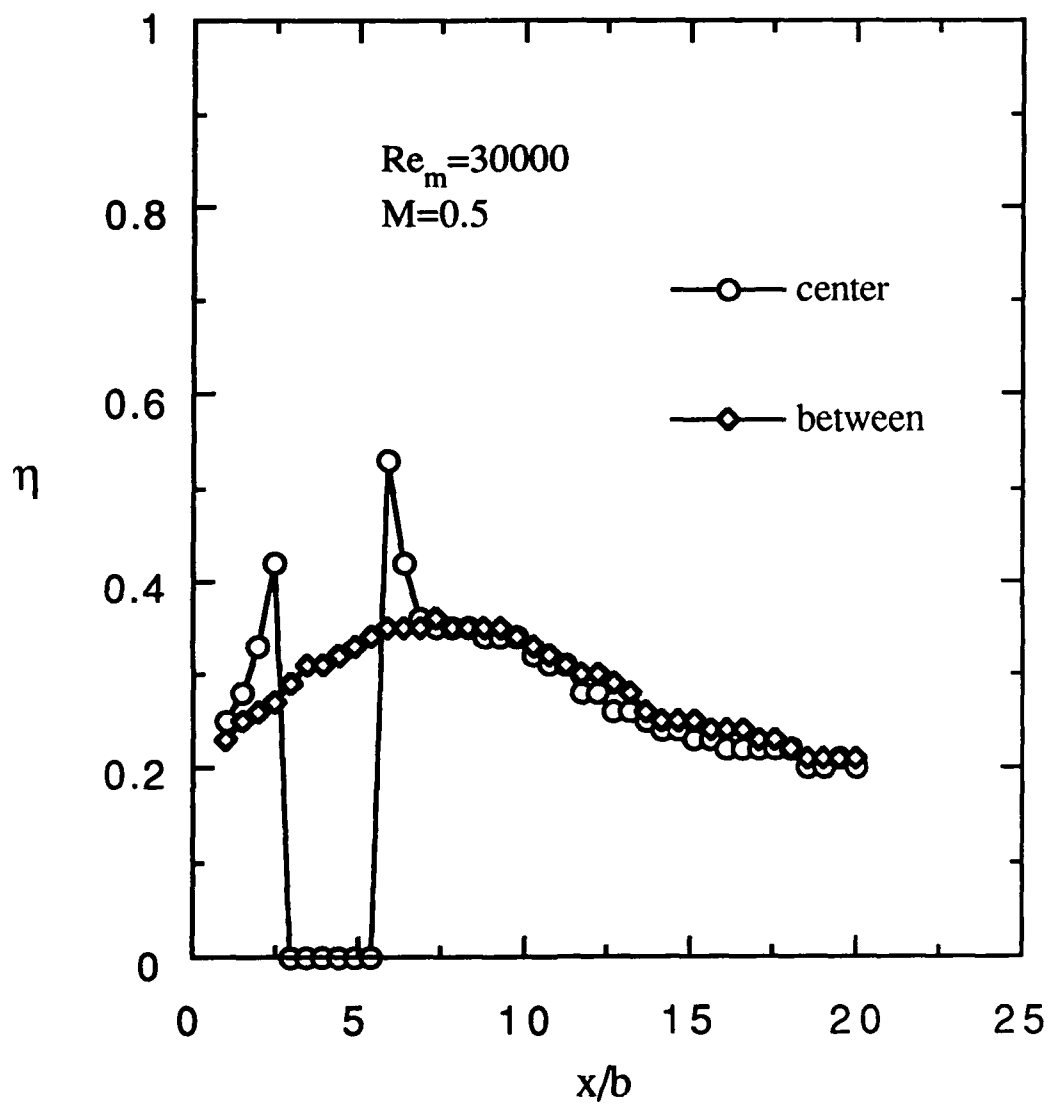


Fig. 26 Effectiveness, streamwise variation, pressure side injection,  $3/8$ " cavity,  $3/16$ " clearance gap

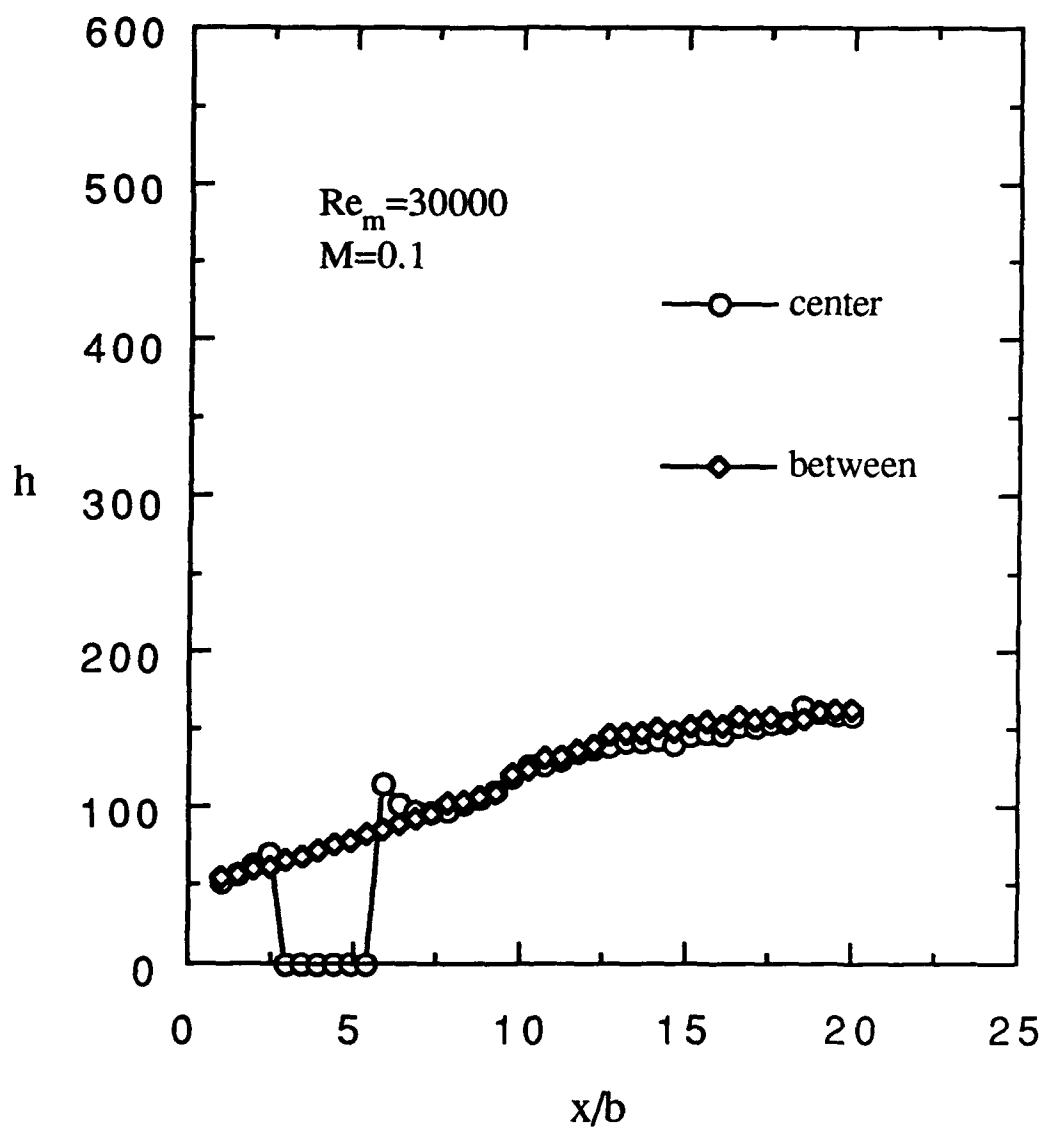


Fig. 27 Heat transfer coeff., streamwise variation,  
pressure side injection,  
3/8" cavity, 5/16" clearance gap

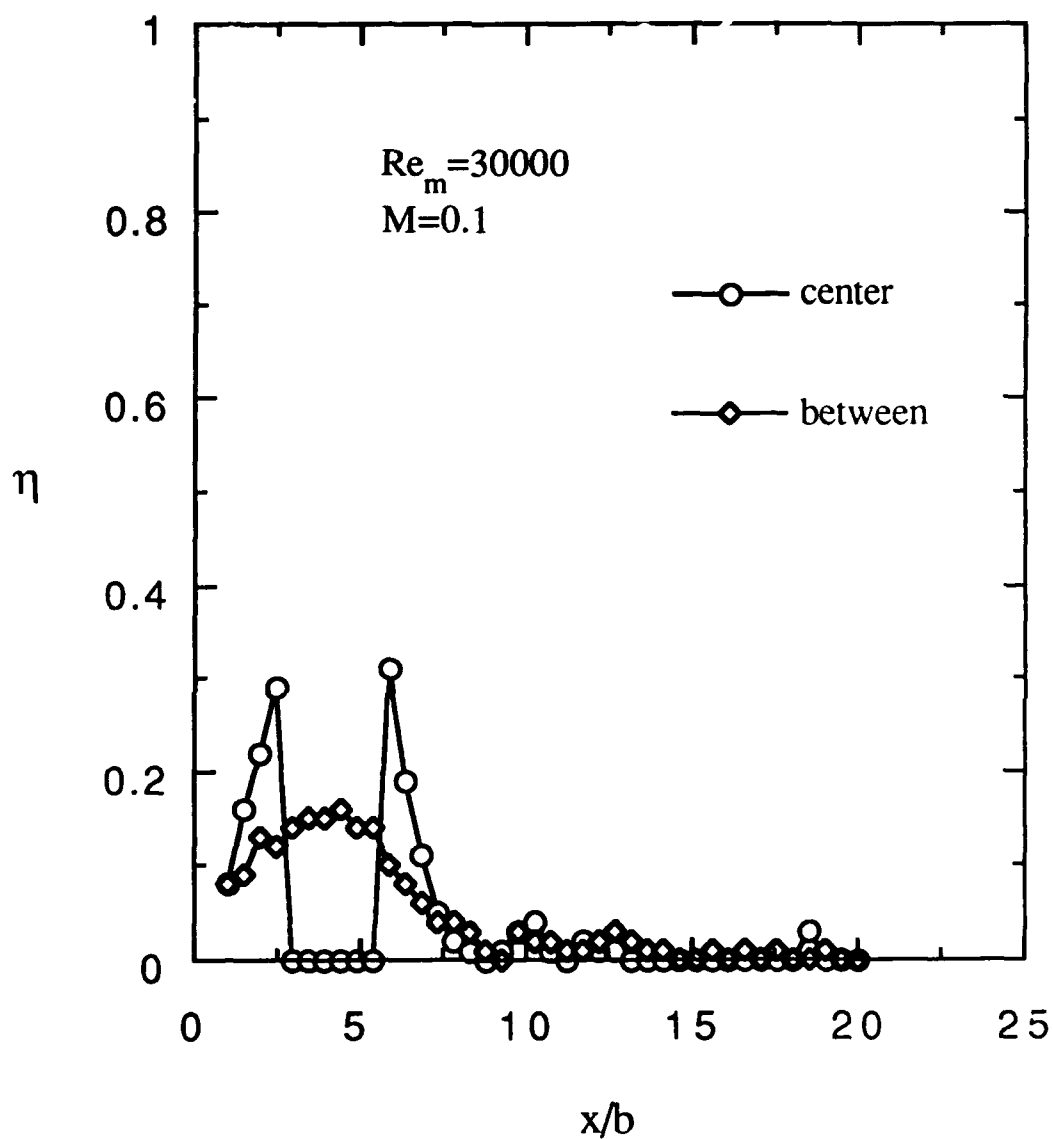


Fig. 28 Effectiveness, streamwise variation, pressure side injection,  
 $3/8$ " cavity,  $5/16$ " clearance gap

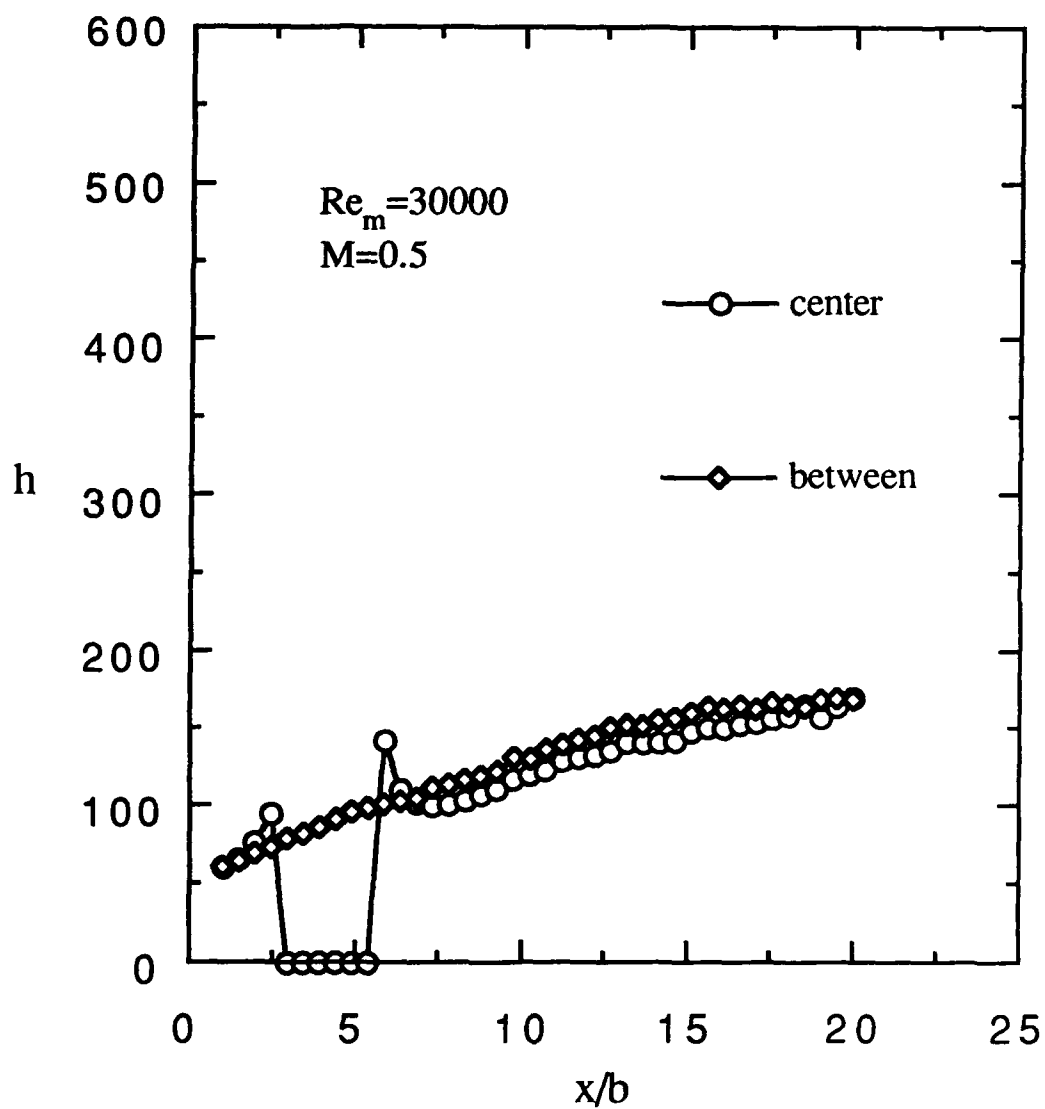


Fig. 29 Heat transfer coeff., streamwise variation,  
pressure side injection,  
 $3/8$ " cavity,  $5/16$ " clearance gap

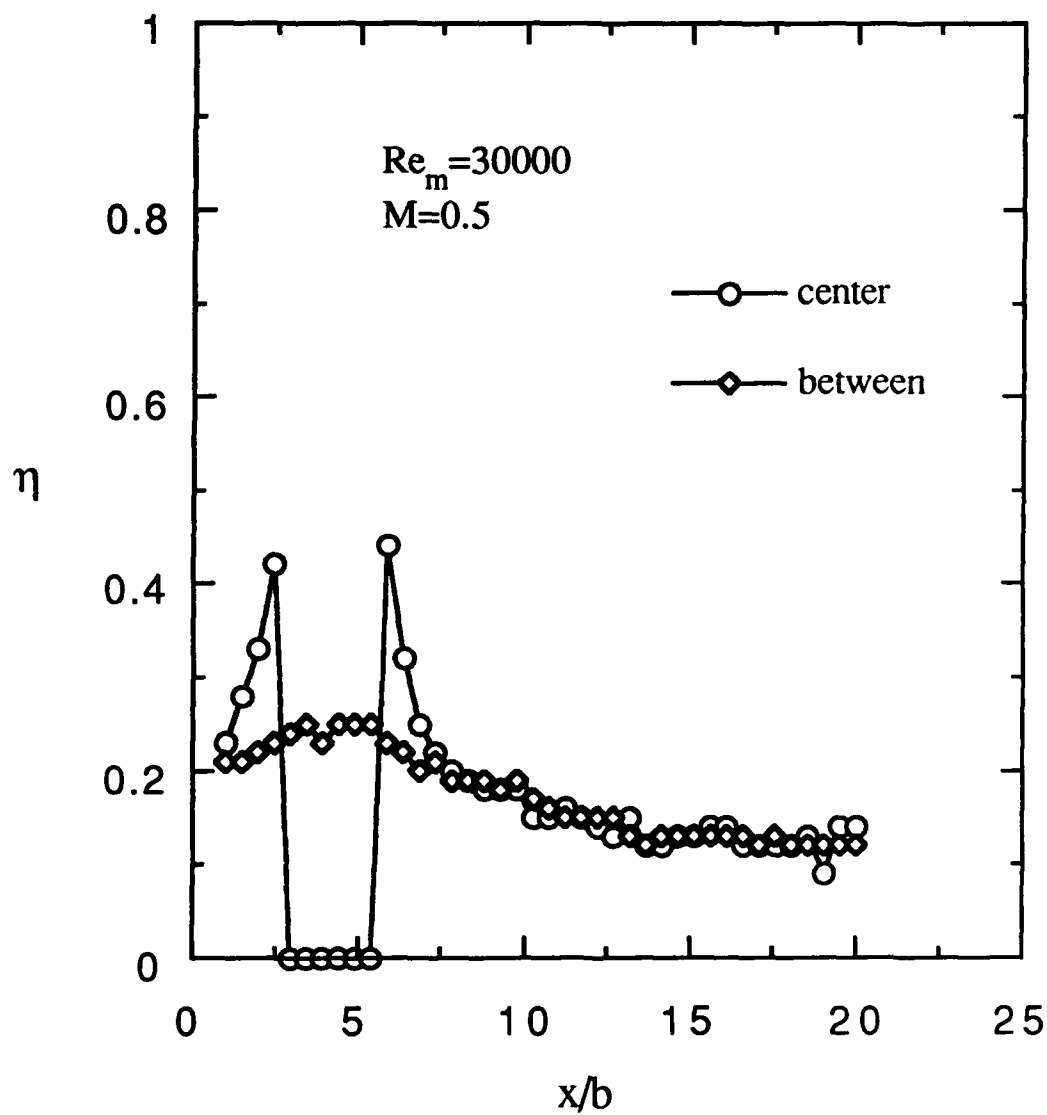


Fig. 30 Effectiveness, streamwise variation, pressure side injection,  $3/8$ " cavity,  $5/16$ " clearance gap

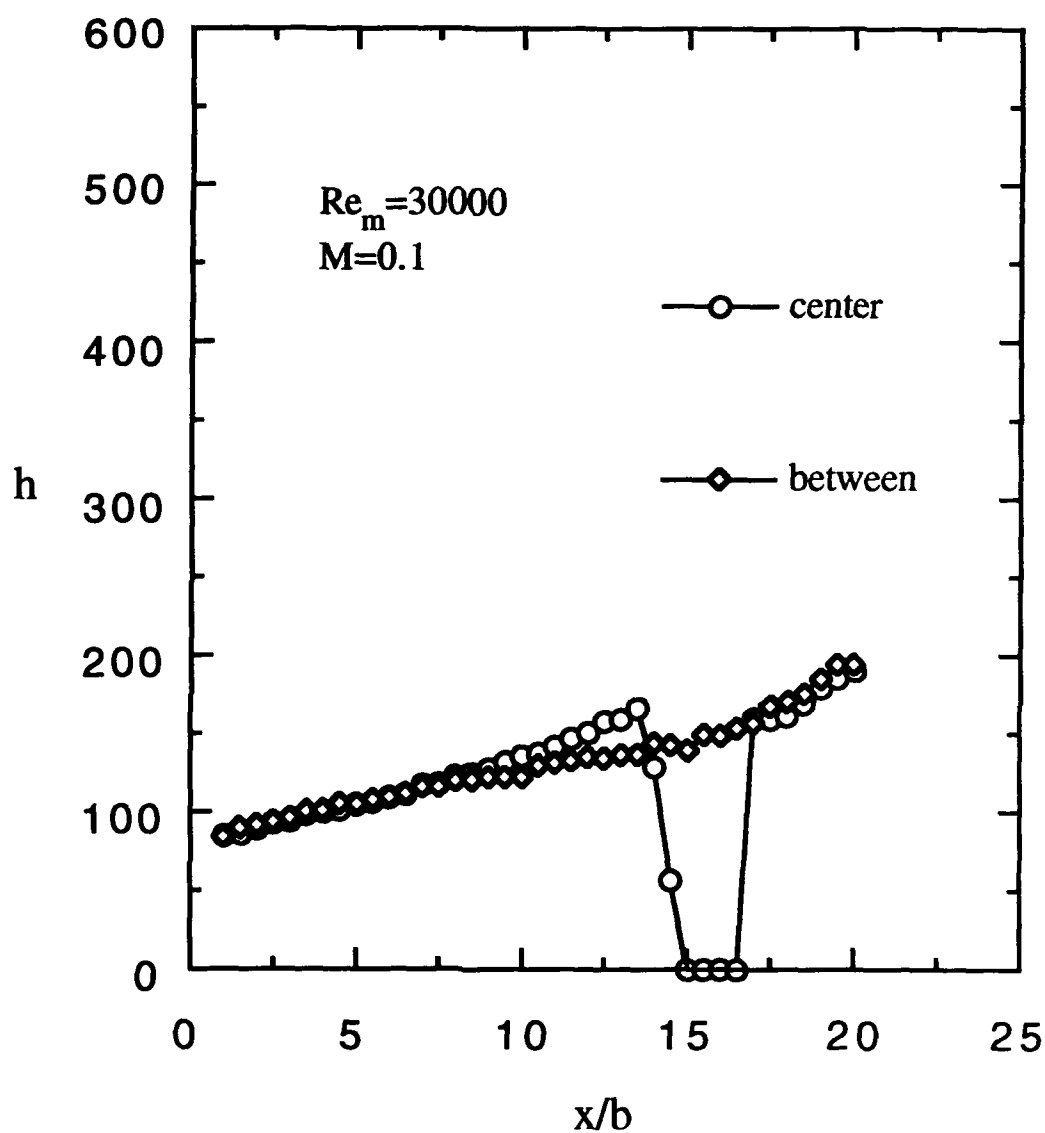


Fig. 31 Heat transfer coeff., streamwise variation,  
suction side injection,  
1.0" cavity,  $3/16$ " clearance gap, #1



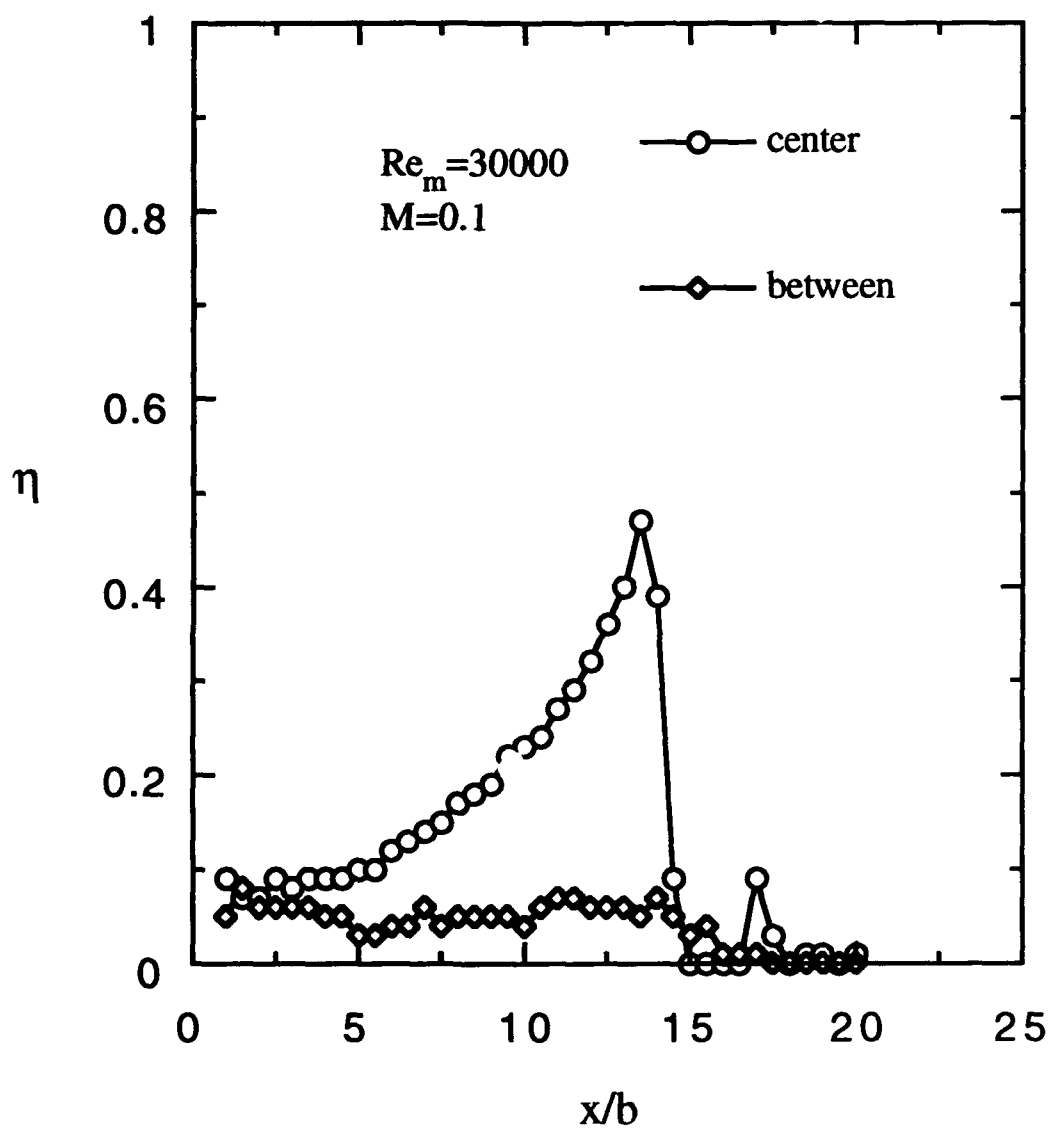


Fig. 32 Effectiveness, streamwise variation, suction side injection, 1.0" cavity,  $3/16$ " clearance gap, #1

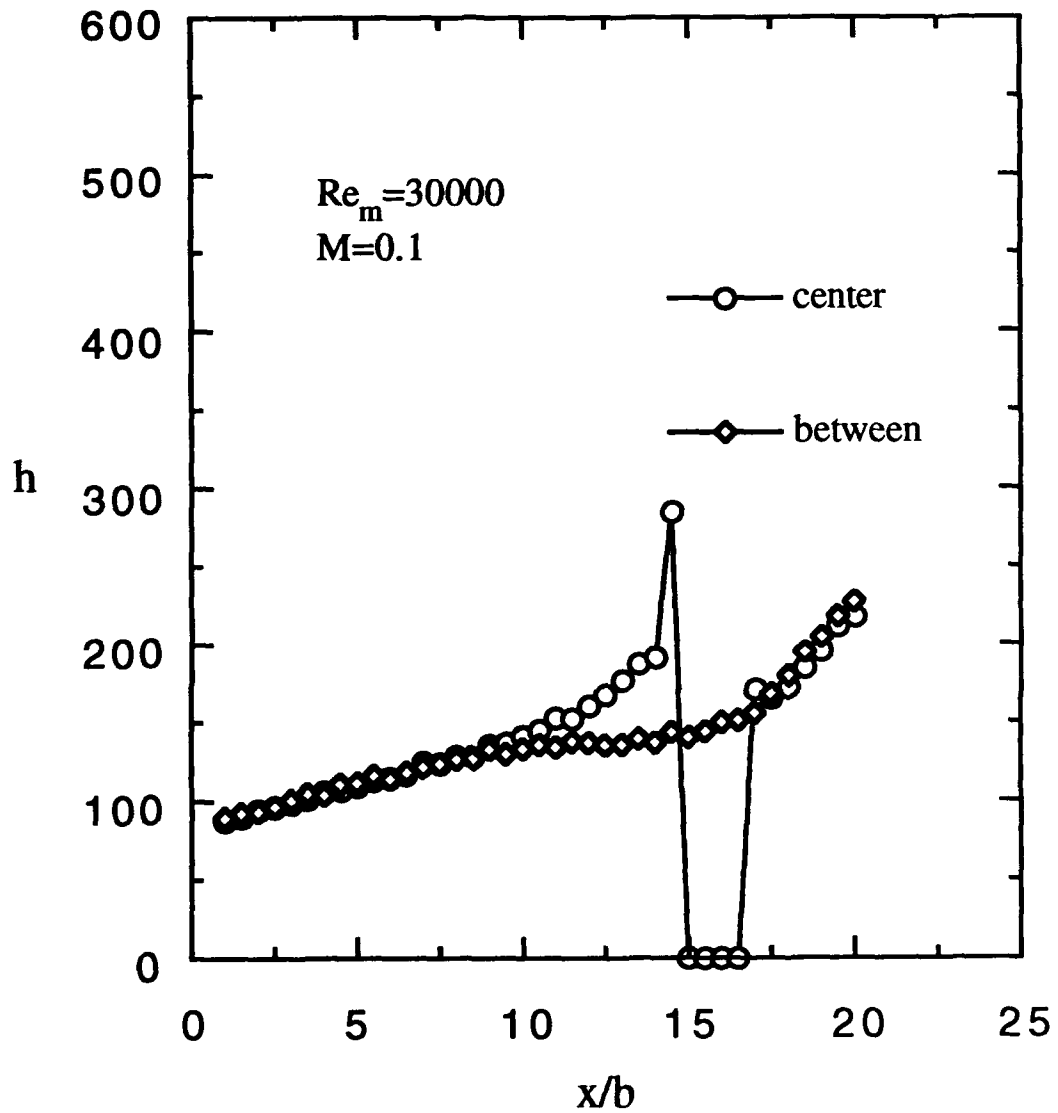


Fig. 33 Heat transfer coeff., streamwise variation,  
suction side injection,  
1.0" cavity,  $3/16$ " clearance gap, #2

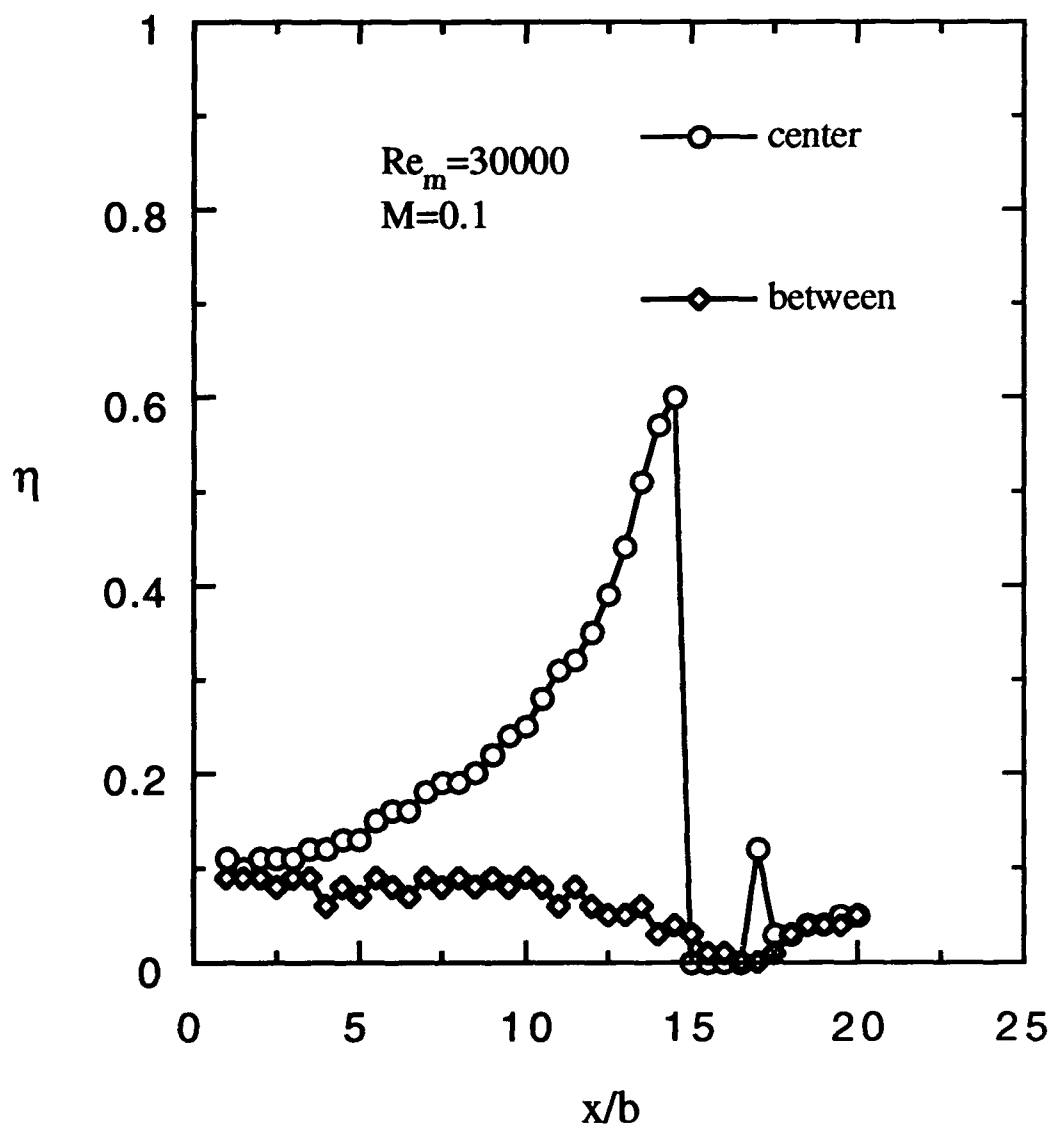


Fig. 34 Effectiveness, streamwise variation, suction side injection, 1.0" cavity,  $3/16$ " clearance gap, #2

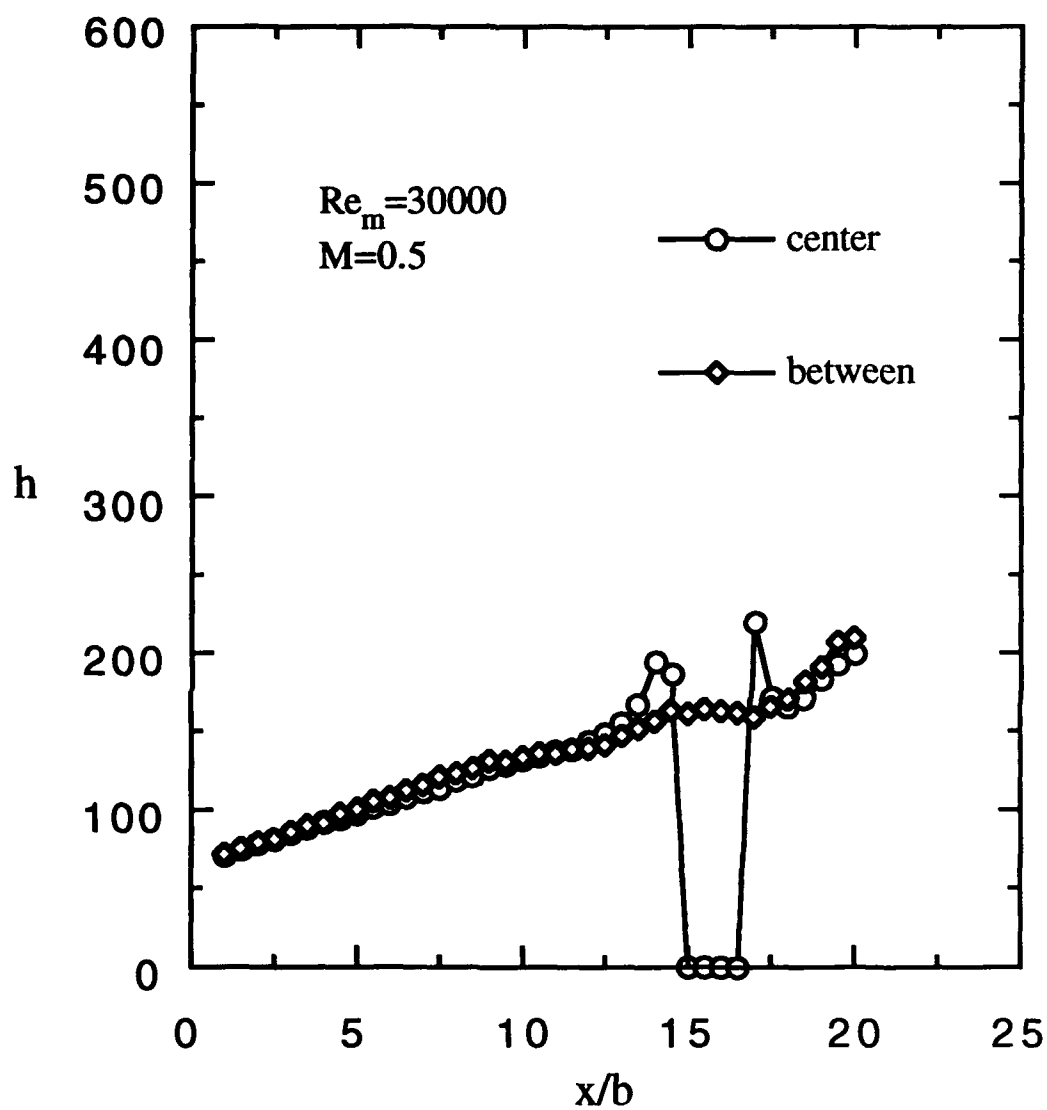


Fig. 35 Heat transfer coeff., streamwise variation,  
suction side injection,  
1.0" cavity,  $3/16$ " clearance gap

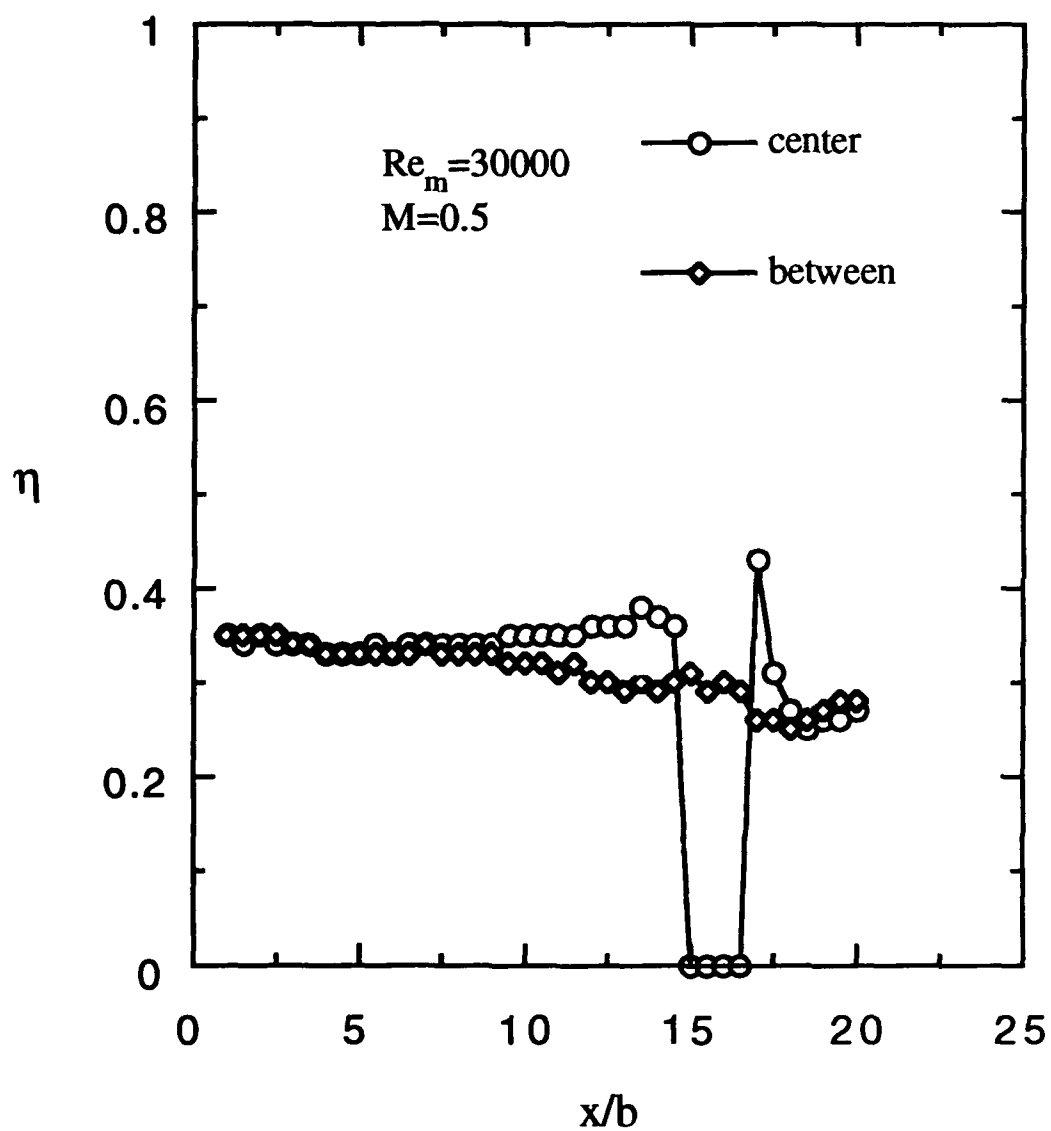


Fig. 36 Effectiveness, streamwise variation, suction side injection, 1.0" cavity,  $3/16$ " clearance gap

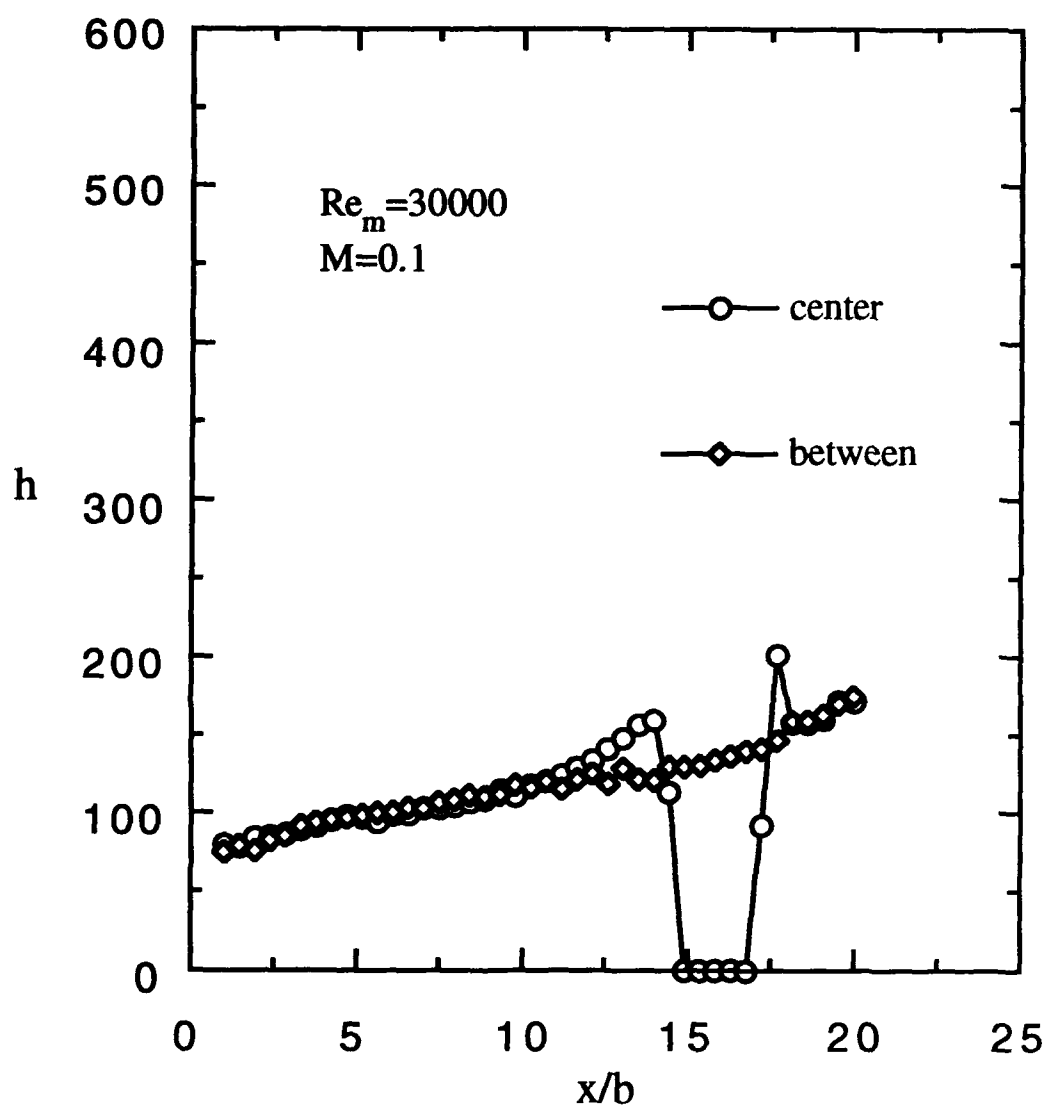


Fig. 37 Heat transfer coeff., streamwise variation,  
suction side injection,  
1.0" cavity,  $5/16$ " clearance gap

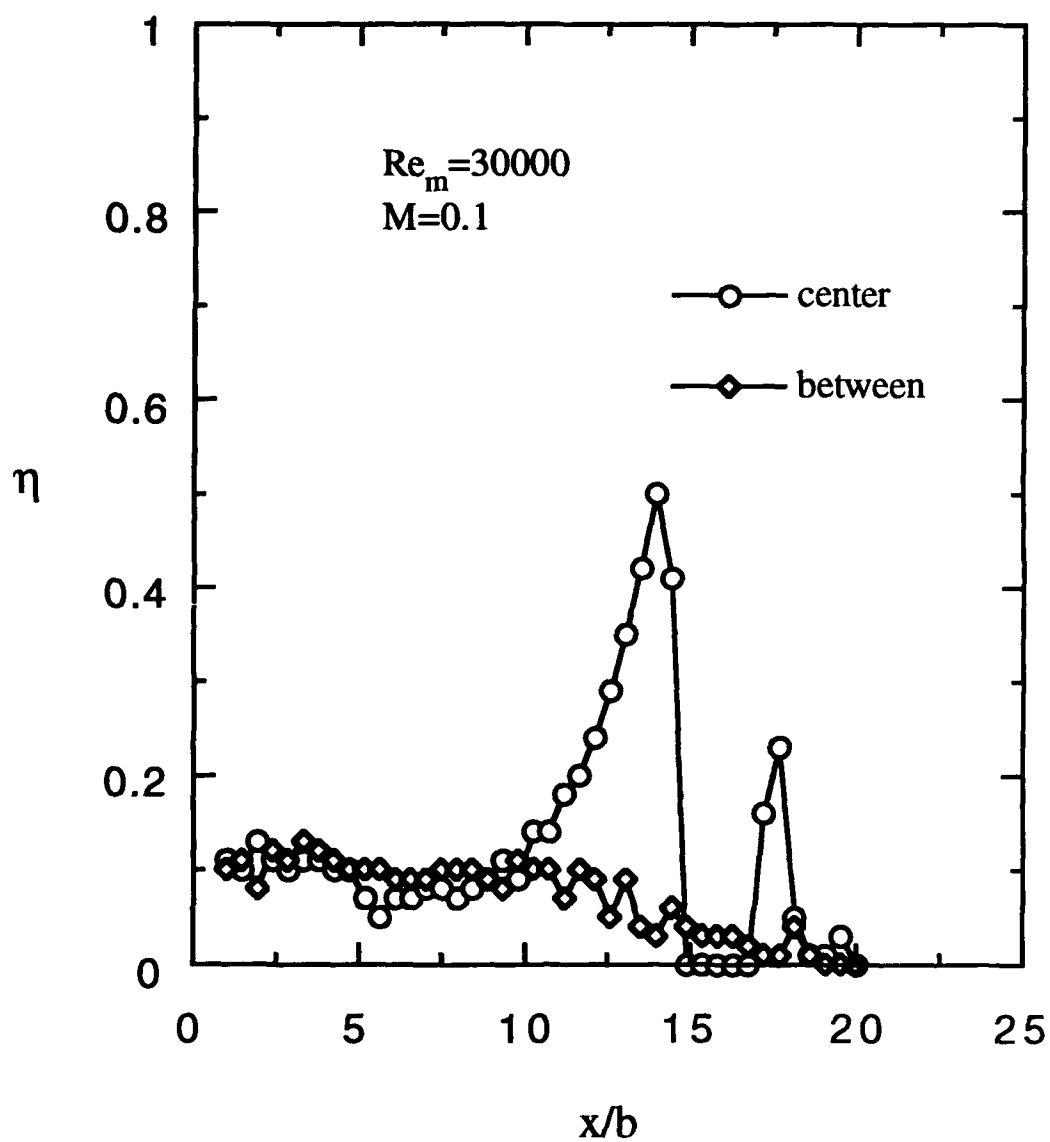


Fig. 38 Effectiveness, streamwise variation, suction side injection, 1.0" cavity,  $5/16$ " clearance gap

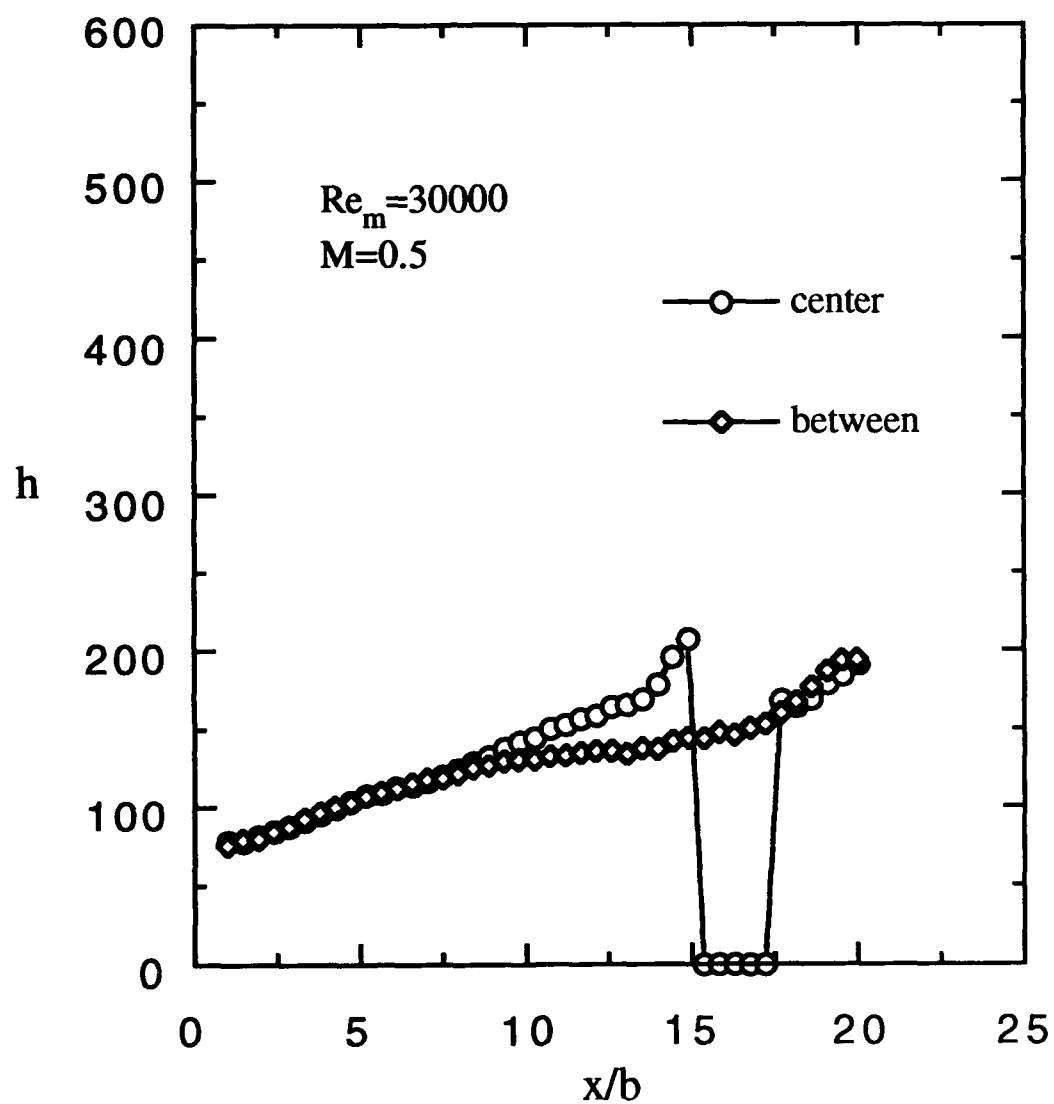


Fig. 39 Heat transfer coeff., streamwise variation,  
suction side injection,  
1.0" cavity,  $5/16$ " clearance gap, #1



TURBINE BLADE TIP FILM COOLING MEASUREMENTS

by  
Dean Andrew Ward

has been approved  
December 1992

APPROVED:

\_\_\_\_\_, Chairperson  
\_\_\_\_\_  
\_\_\_\_\_

Supervisory Committee

ACCEPTED:

\_\_\_\_\_  
Department Chairperson

\_\_\_\_\_  
Dean, Graduate College

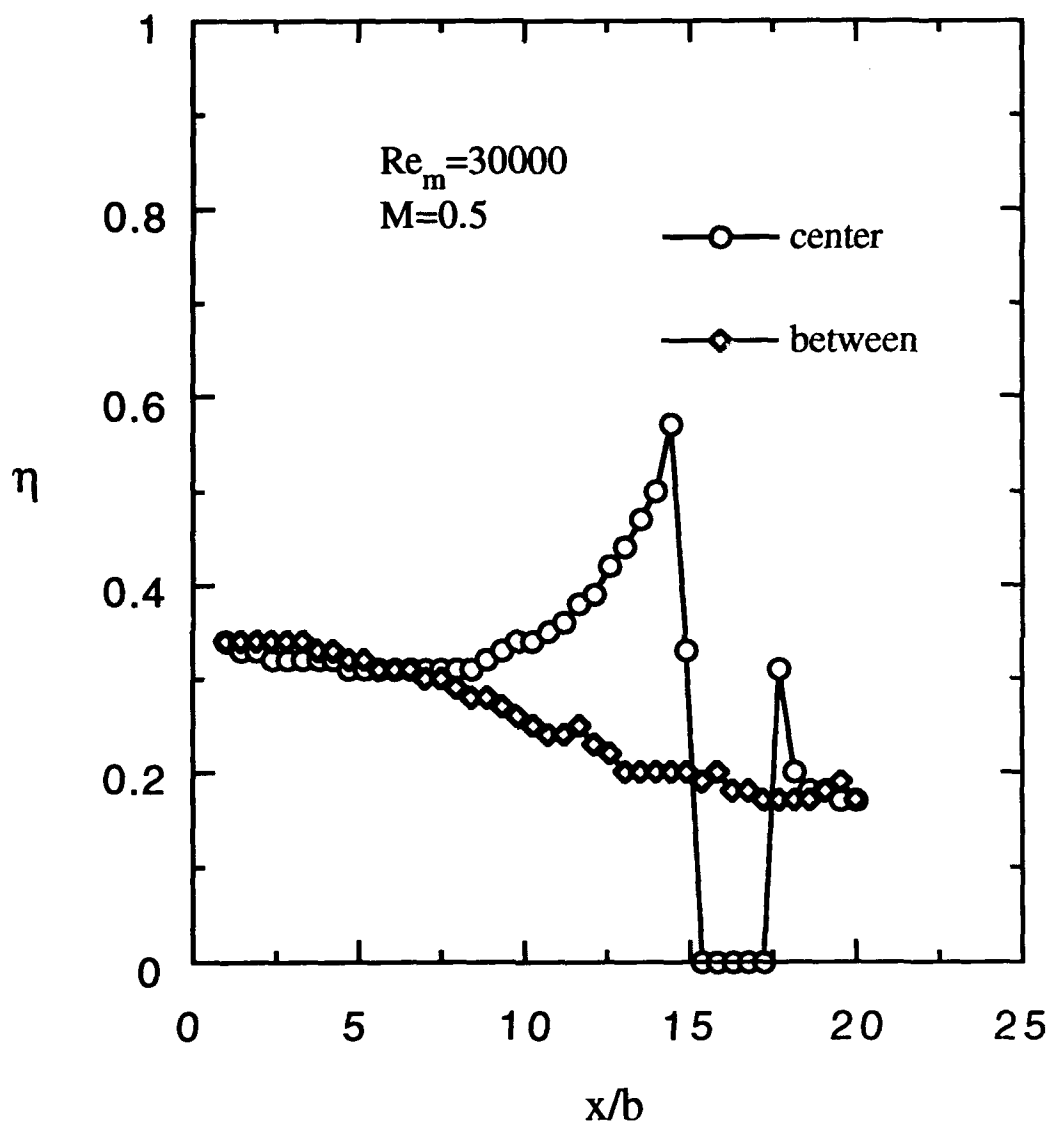


Fig. 39 Effectiveness, streamwise variation, suction side injection, 1.0" cavity,  $5/16$ " clearance gap, #1

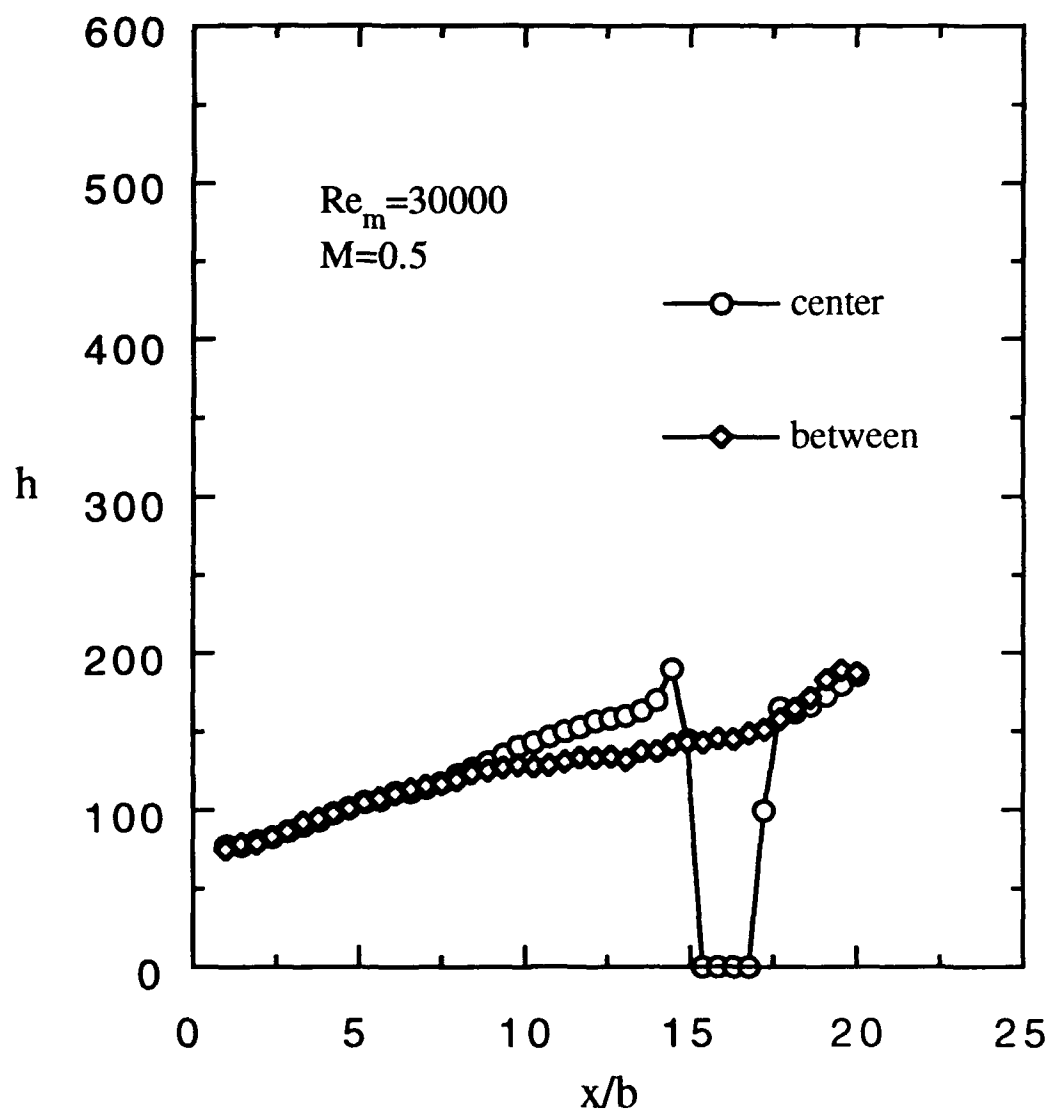


Fig. 41 Heat transfer coeff., streamwise variation,  
suction side injection,  
1.0" cavity,  $5/16$ " clearance gap, #2

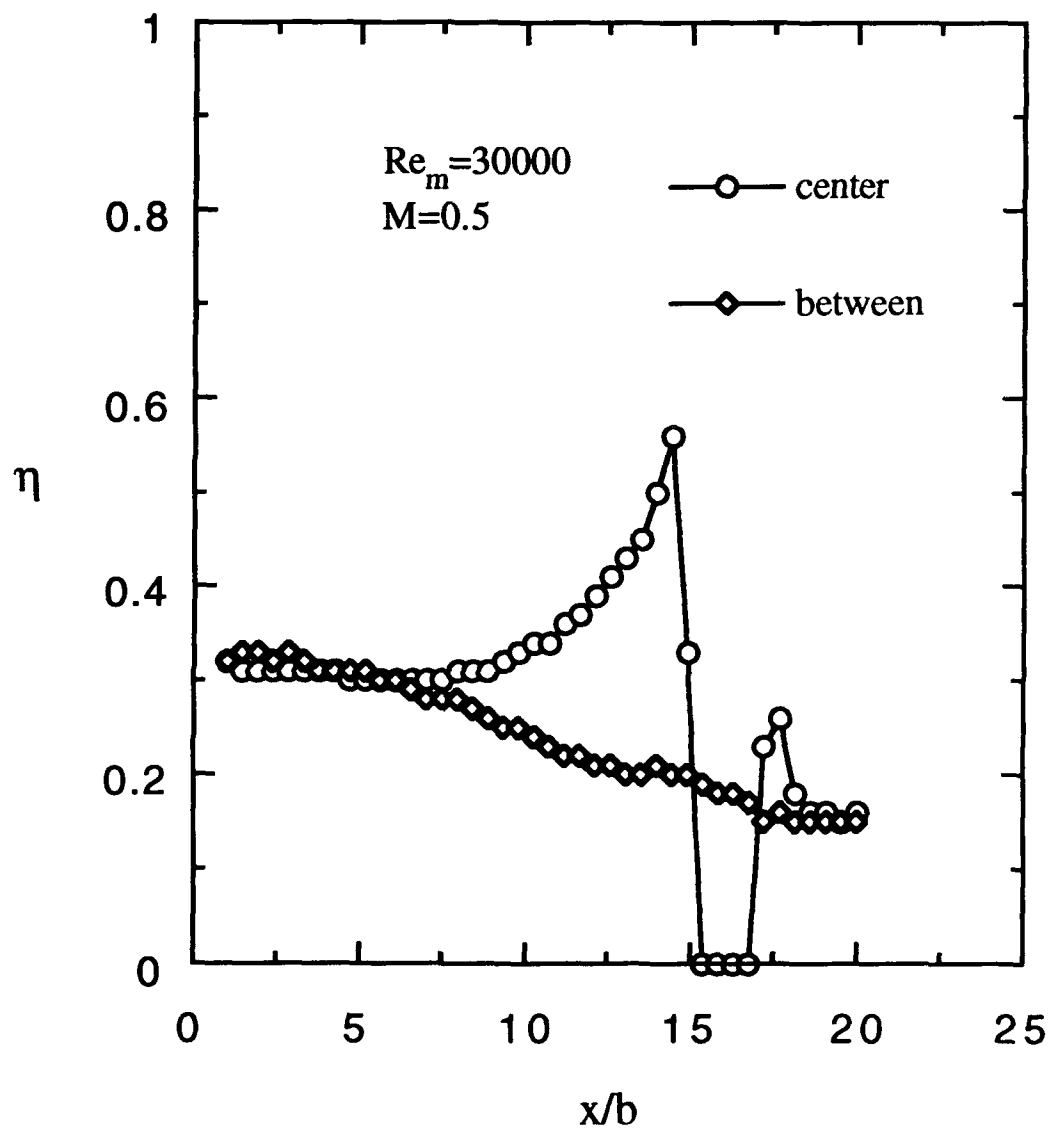


Fig. 42 Effectiveness, streamwise variation, suction side injection, 1.0" cavity,  $5/16$ " clearance gap, #2

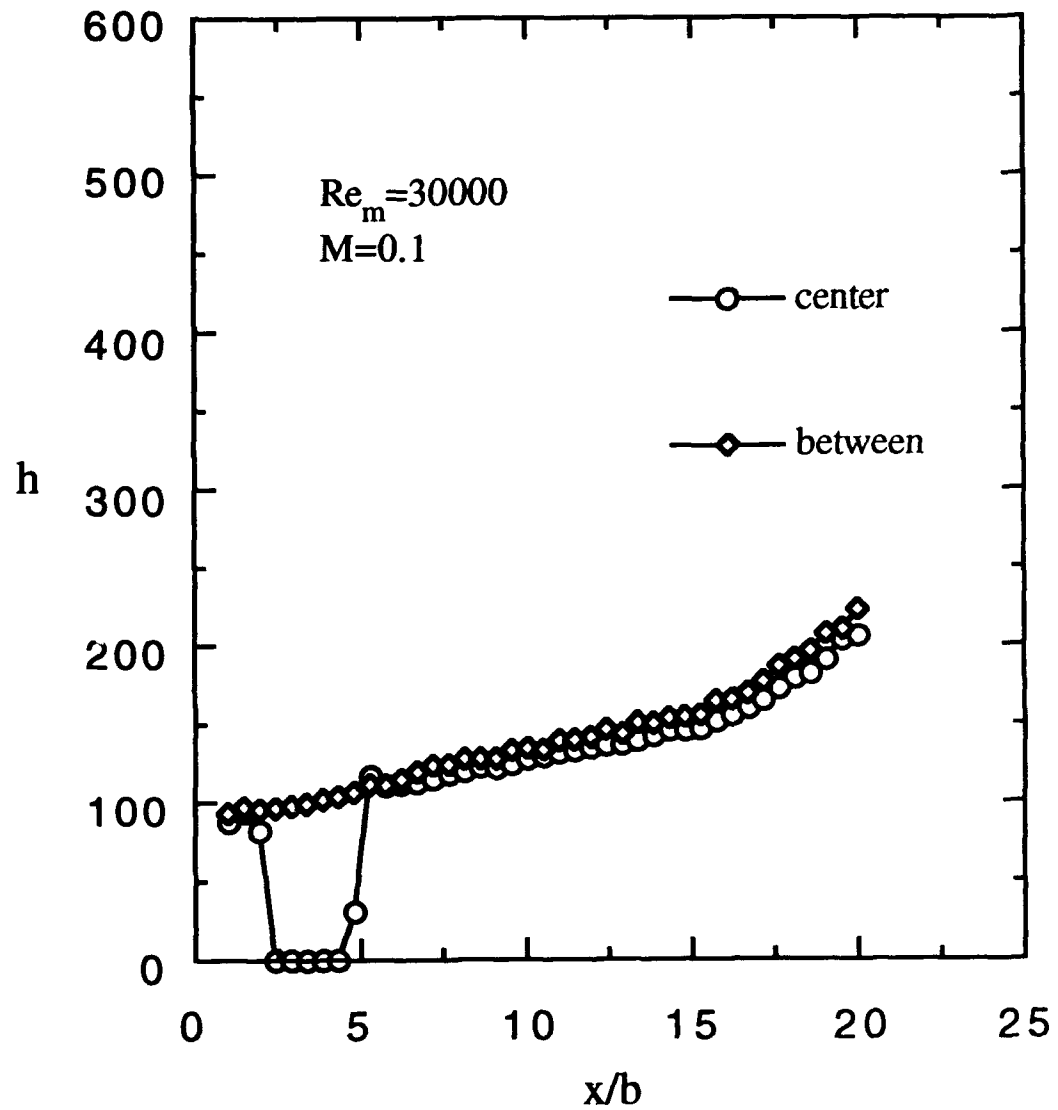


Fig. 43 Heat transfer coeff., streamwise variation,  
pressure side injection,  
1.0" cavity,  $3/16$ " clearance gap

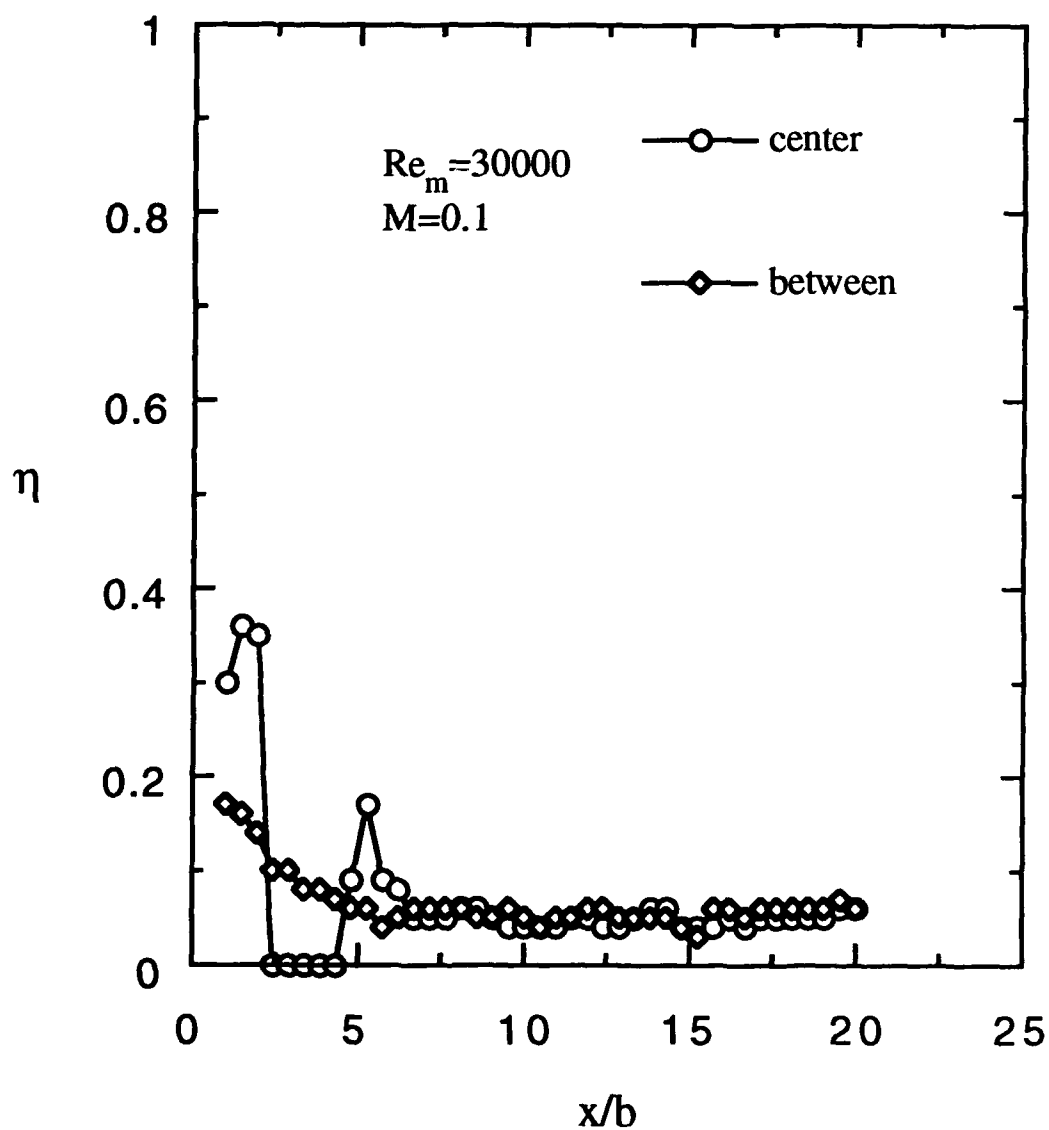


Fig. 44 Effectiveness, streamwise variation, pressure side injection, 1.0" cavity,  $3/16$ " clearance gap

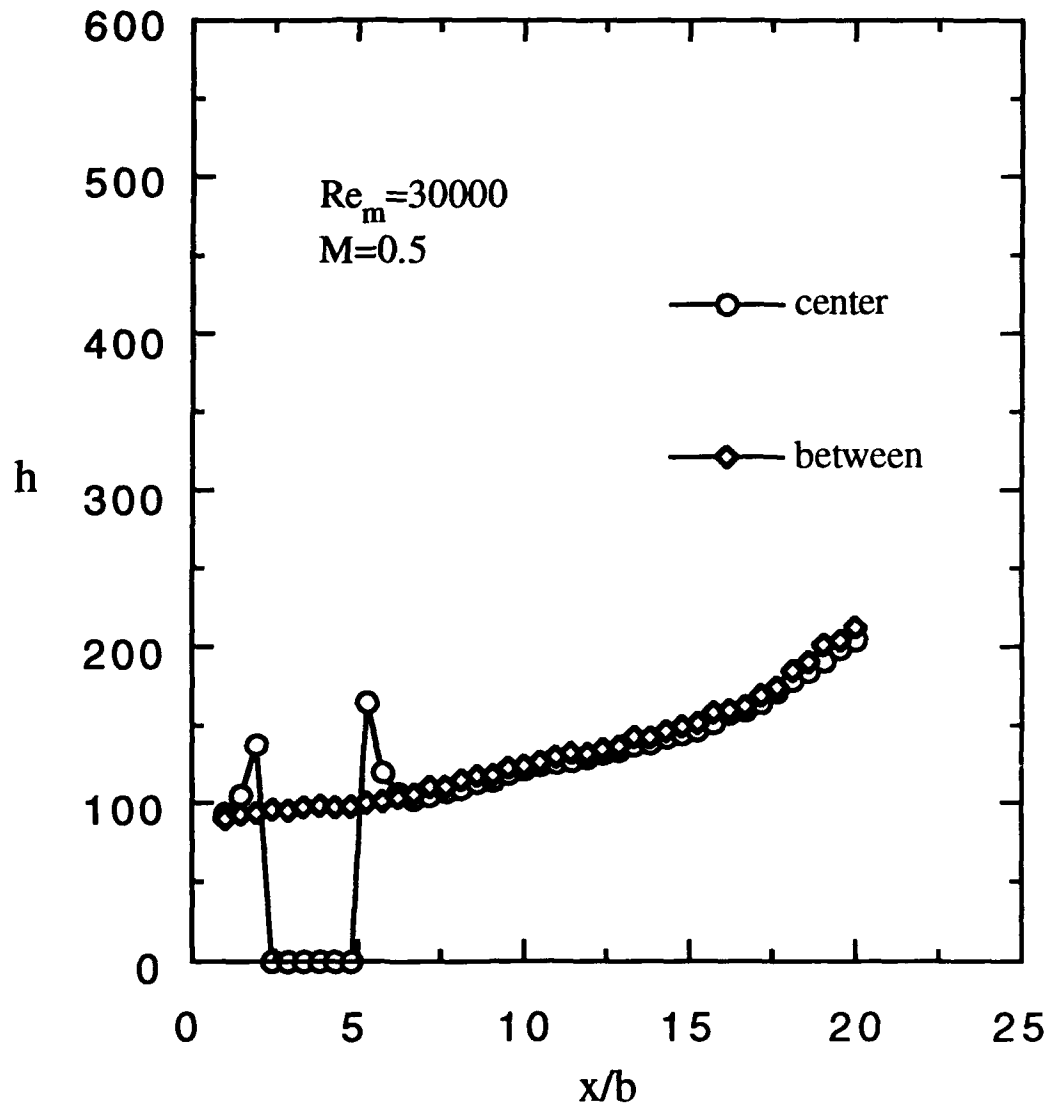


Fig. 45 Heat transfer coeff., streamwise variation,  
pressure side injection,  
1.0" cavity,  $3/16$ " clearance gap, #1

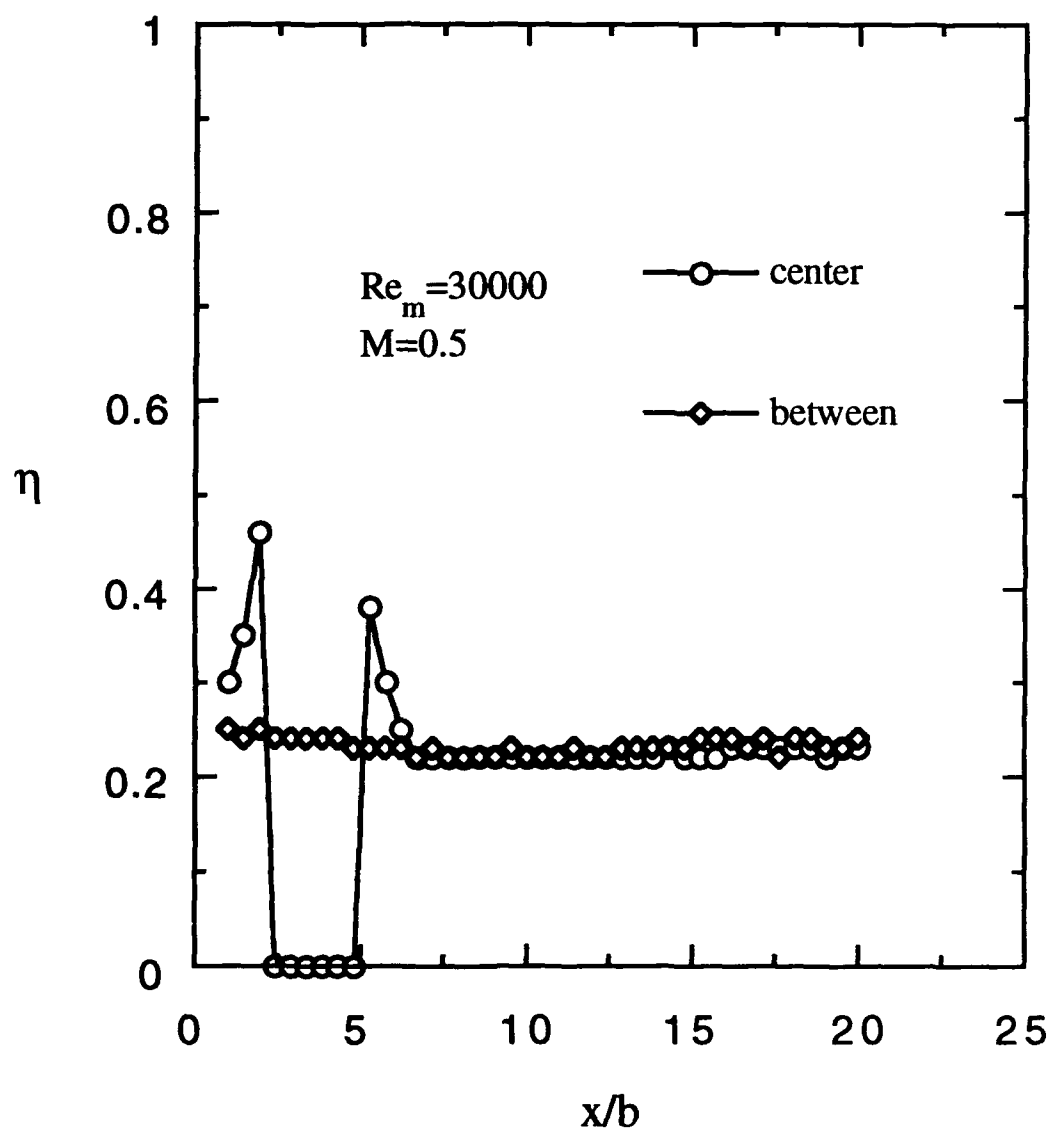


Fig. 46 Effectiveness, streamwise variation, pressure side injection, 1.0" cavity,  $3/16$ " clearance gap, #1



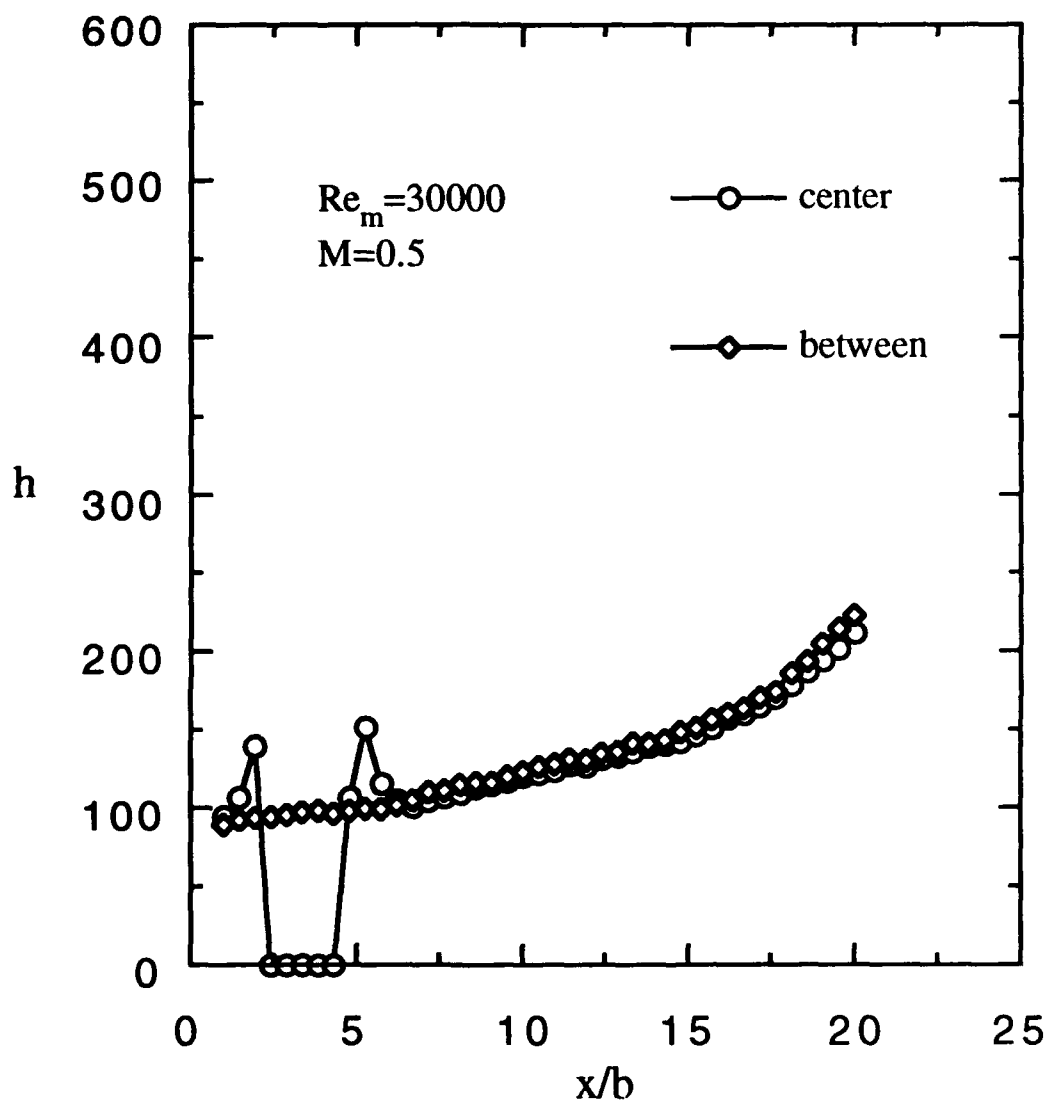


Fig. 47 Heat transfer coeff., streamwise variation,  
pressure side injection,  
1.0" cavity,  $3/16$ " clearance gap, #2

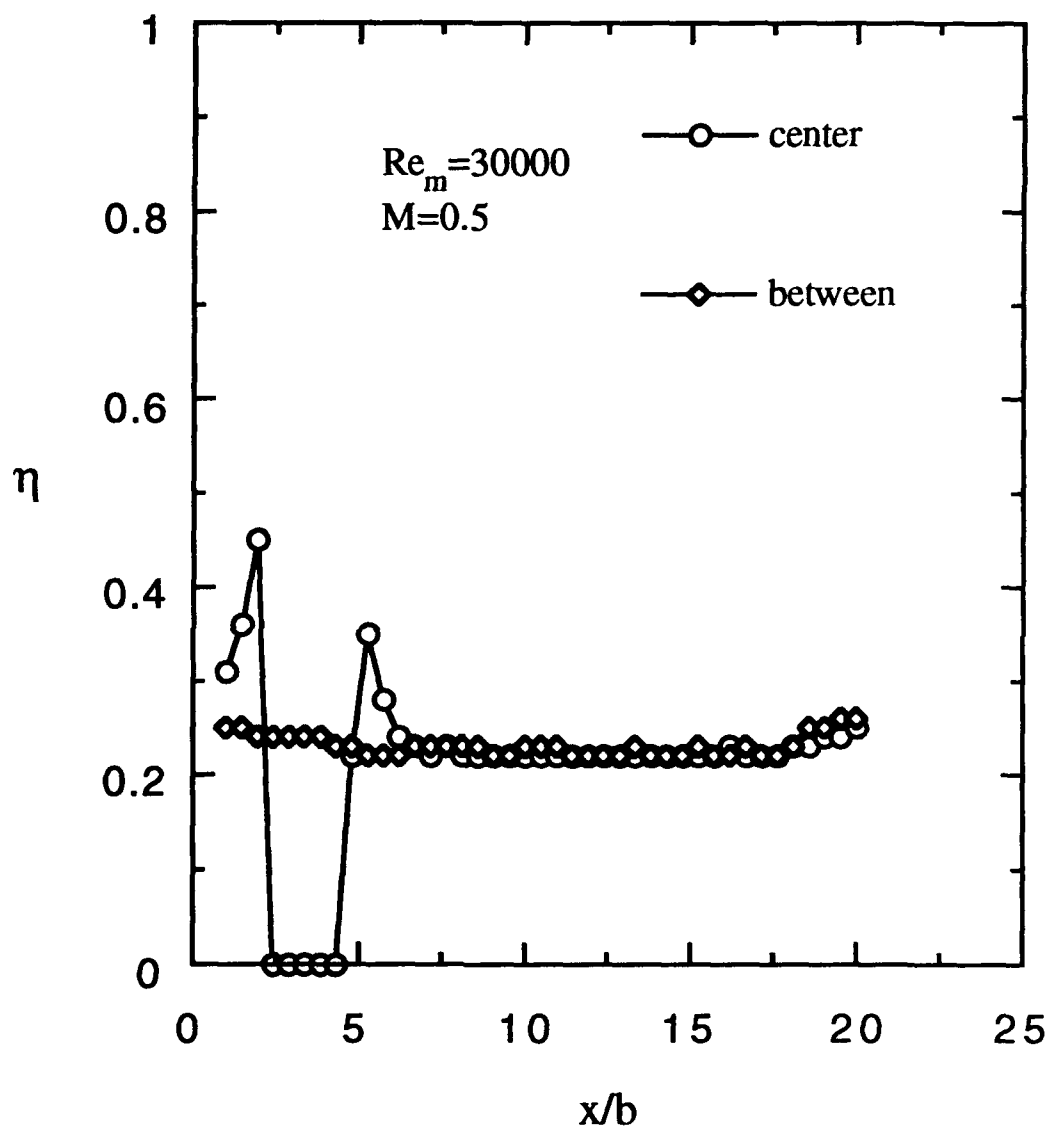


Fig. 48 Effectiveness, streamwise variation, pressure side injection, 1.0" cavity,  $3/16$ " clearance gap, #2

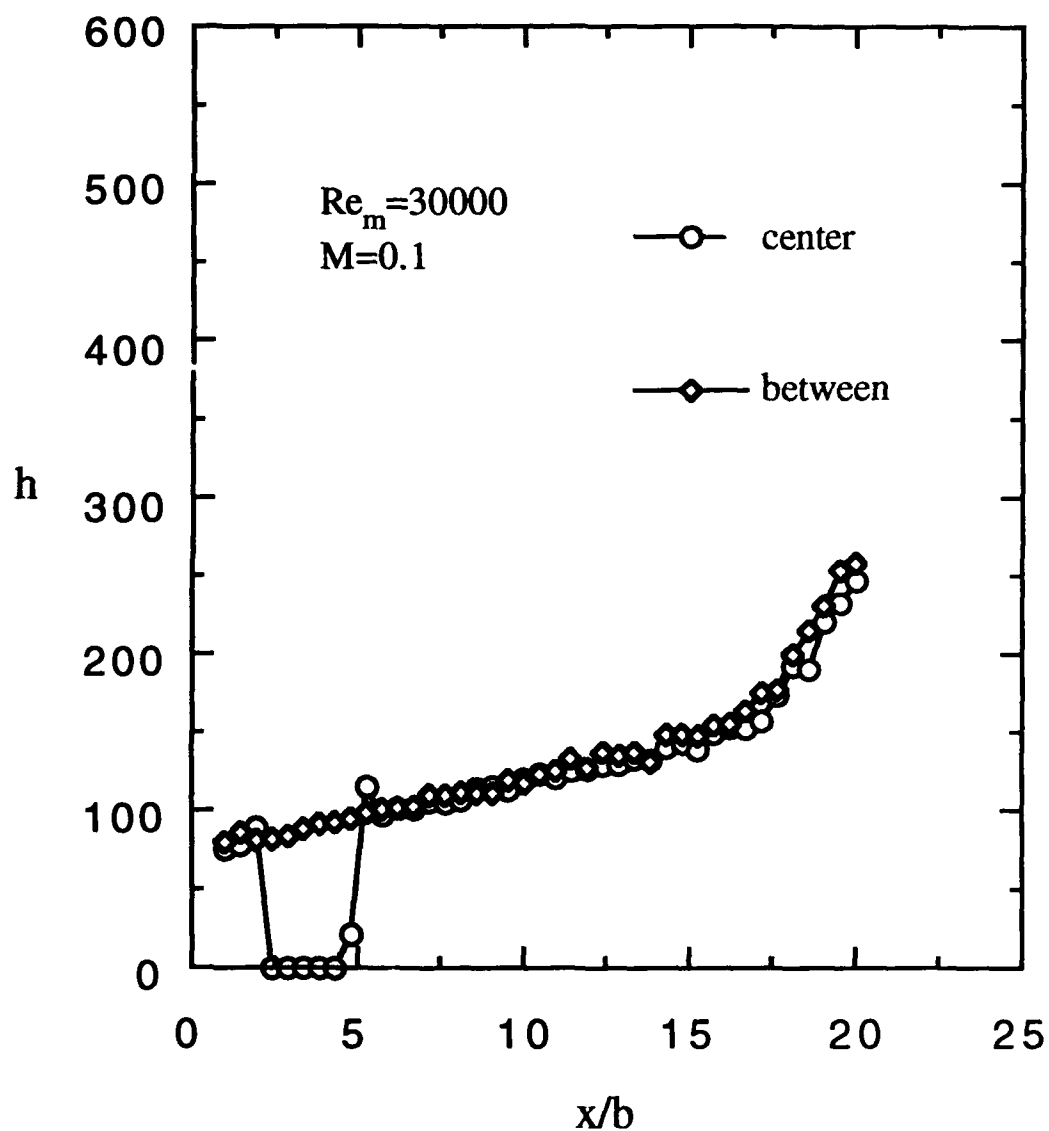


Fig. 49 Heat transfer coeff., streamwise variation,  
pressure side injection,  
1.0" cavity,  $5/16$ " clearance gap

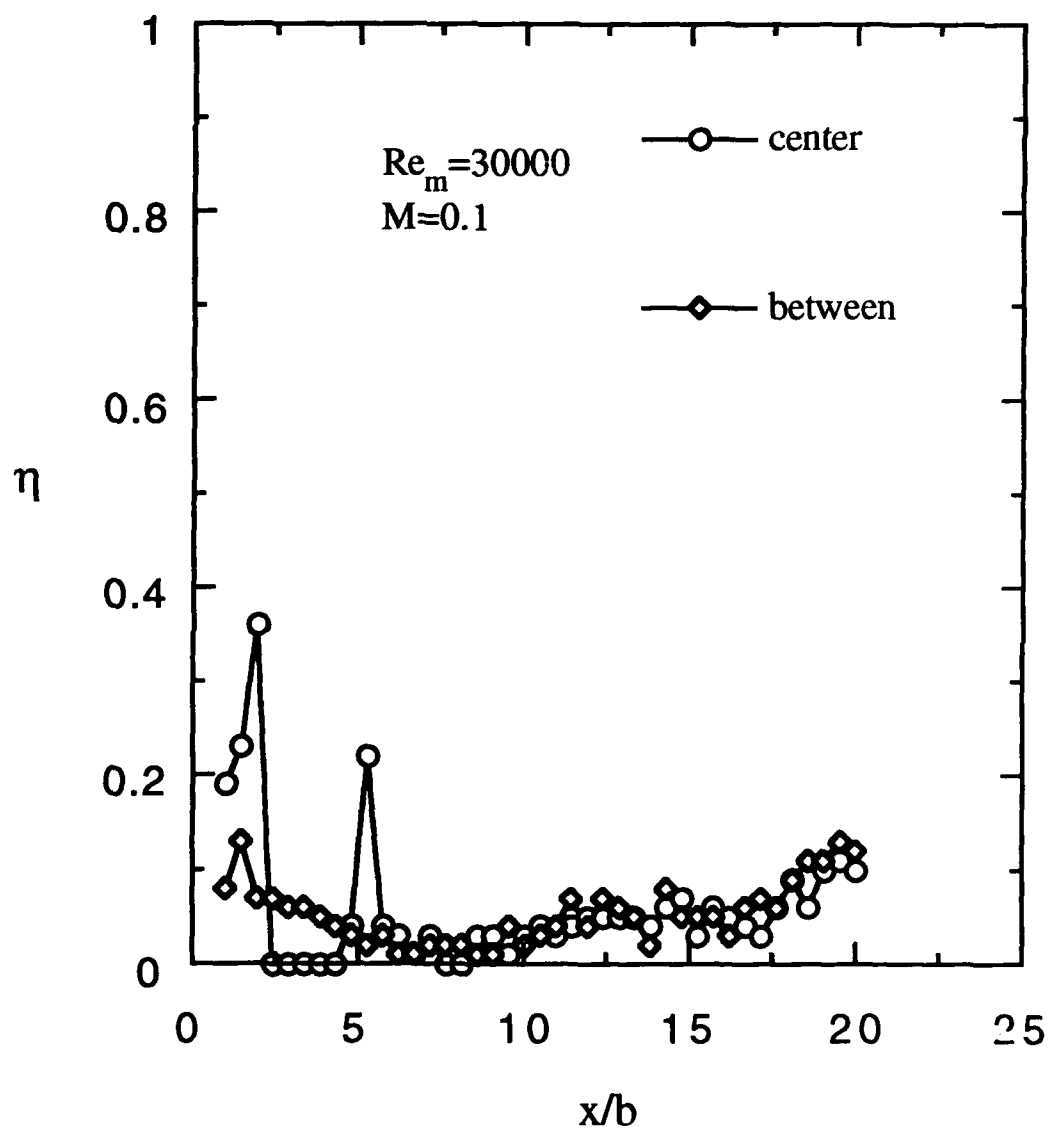


Fig. 50 Effectiveness, streamwise variation, pressure side injection, 1.0" cavity,  $5/16$ " clearance gap

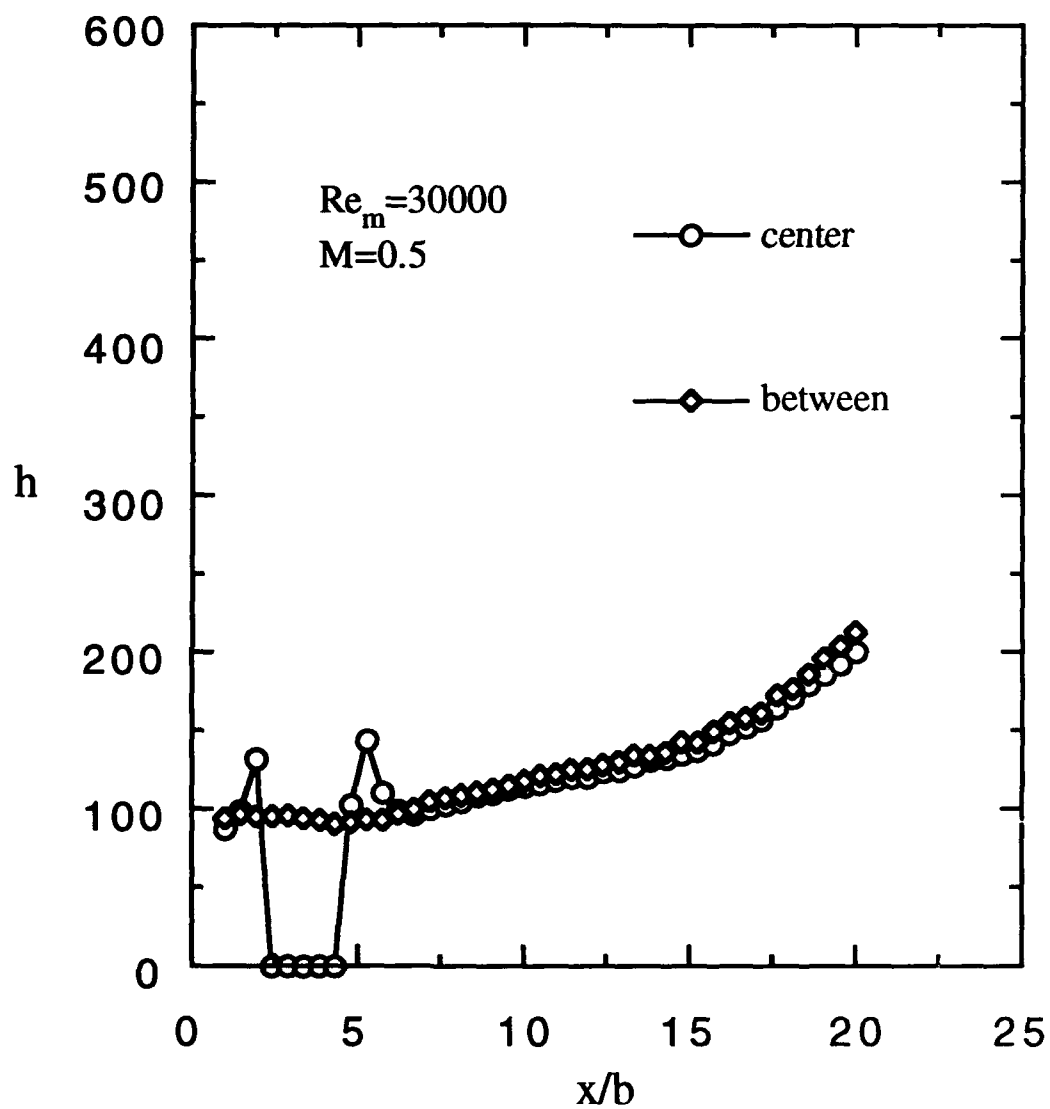


Fig. 51 Heat transfer coeff., streamwise variation,  
pressure side injection,  
1.0" cavity,  $5/16$ " clearance gap, #1

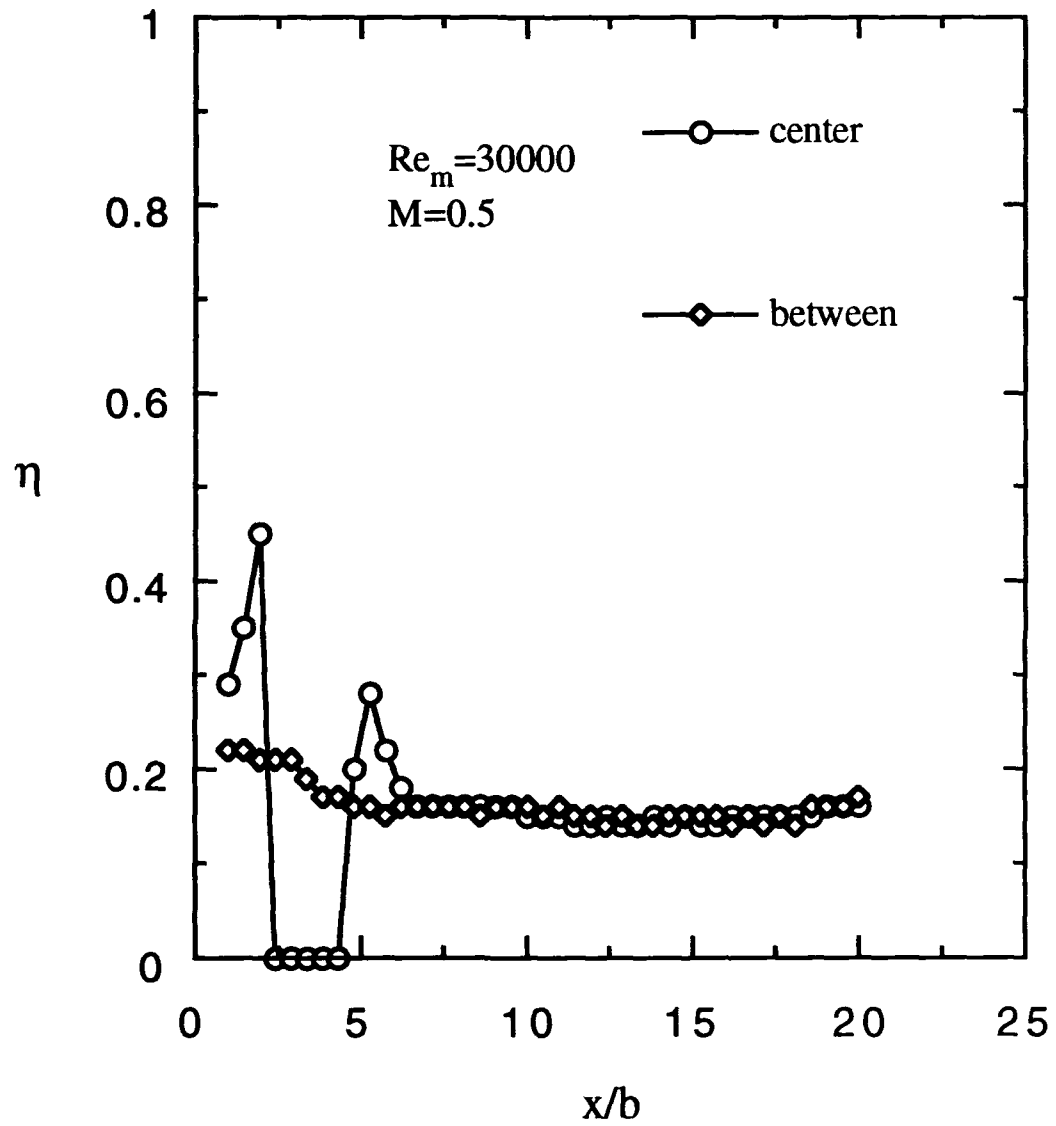


Fig. 52 Effectiveness, streamwise variation, pressure side injection, 1.0" cavity,  $5/16$ " clearance gap, #1

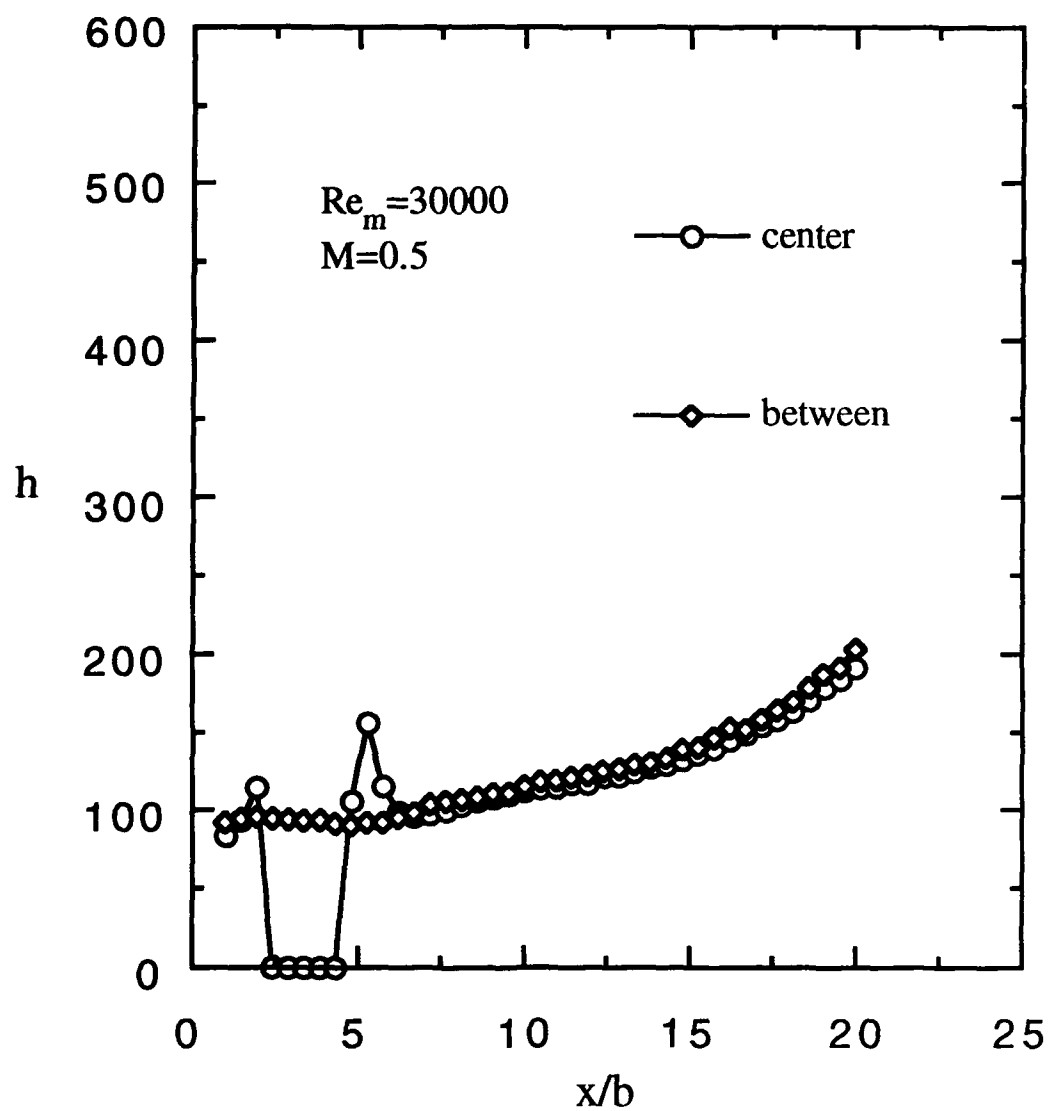


Fig. 53 Heat transfer coeff., streamwise variation,  
pressure side injection,  
1.0" cavity,  $5/16$ " clearance gap, #2

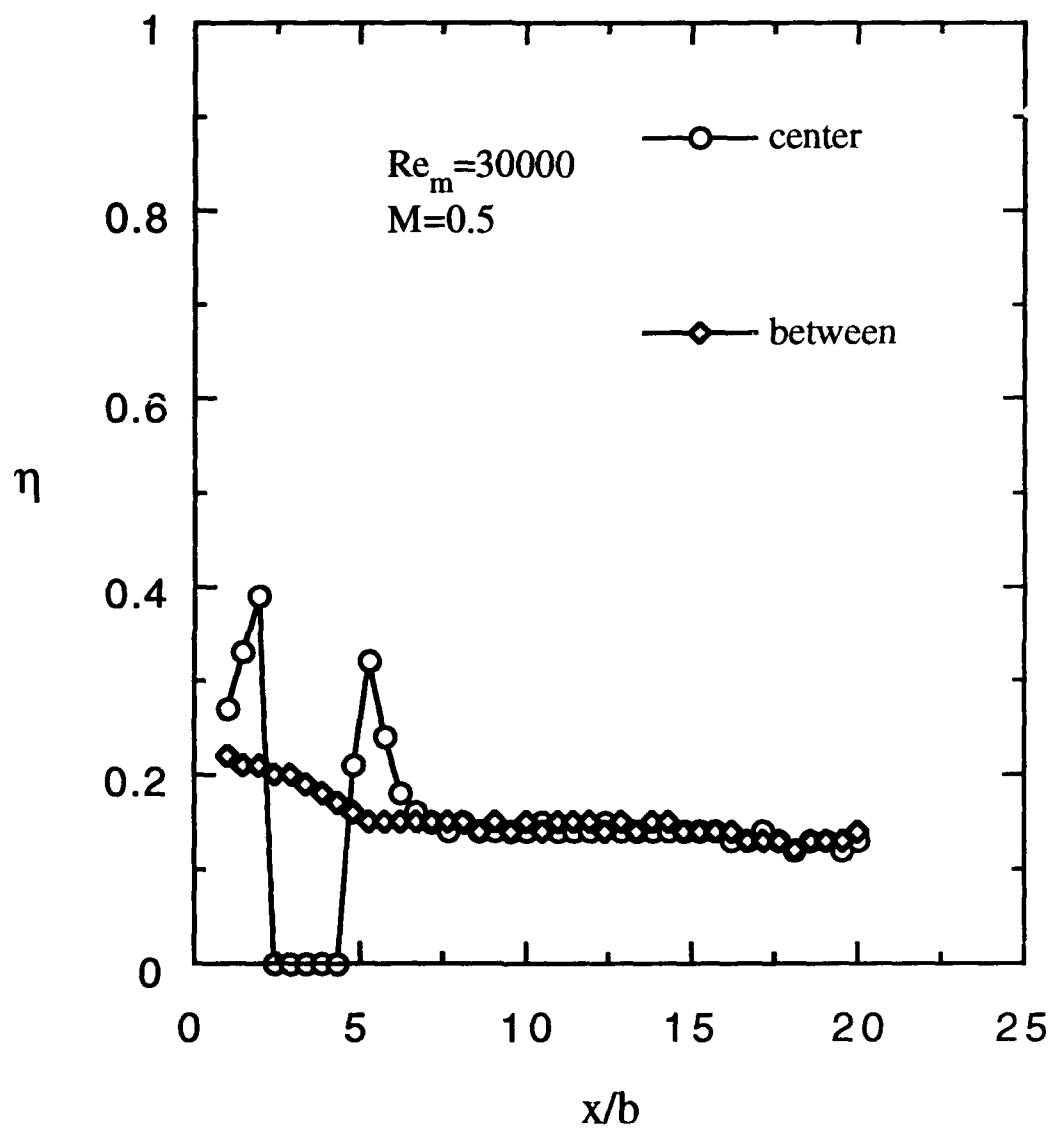


Fig. 54 Effectiveness, streamwise variation, pressure side injection, 1.0" cavity,  $5/16$ " clearance gap, #2





Fig. 55 Flat plate,  $3/16$ " clearance gap,  $Re = 30,000$

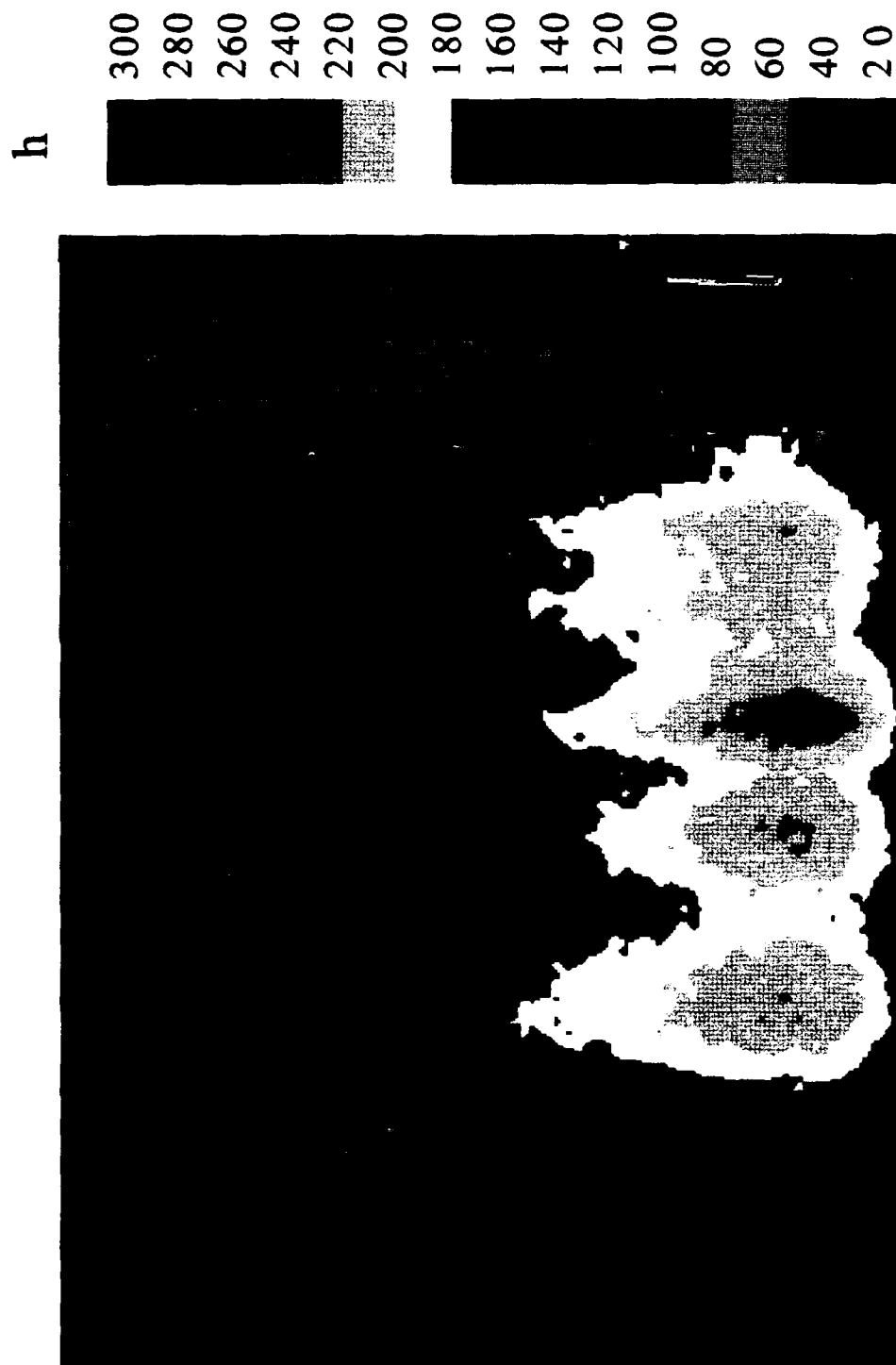


Fig. 56 Flat plate,  $5/16$ " clearance gap,  $Re = 30,000$

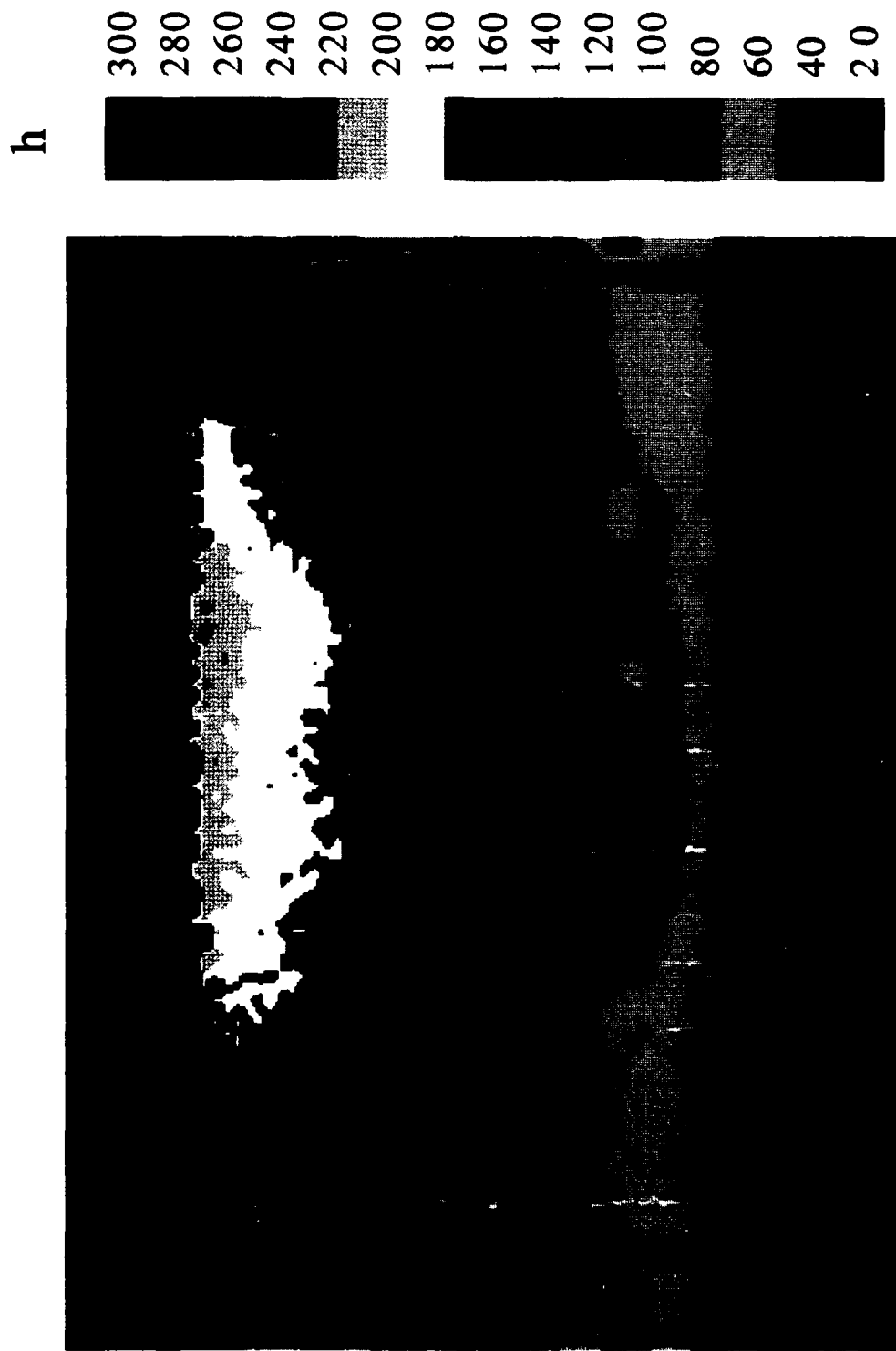


Fig. 57  $3/8$ " cavity,  $3/16$ " clearance gap, No Injection  
 $Re = 30,000$

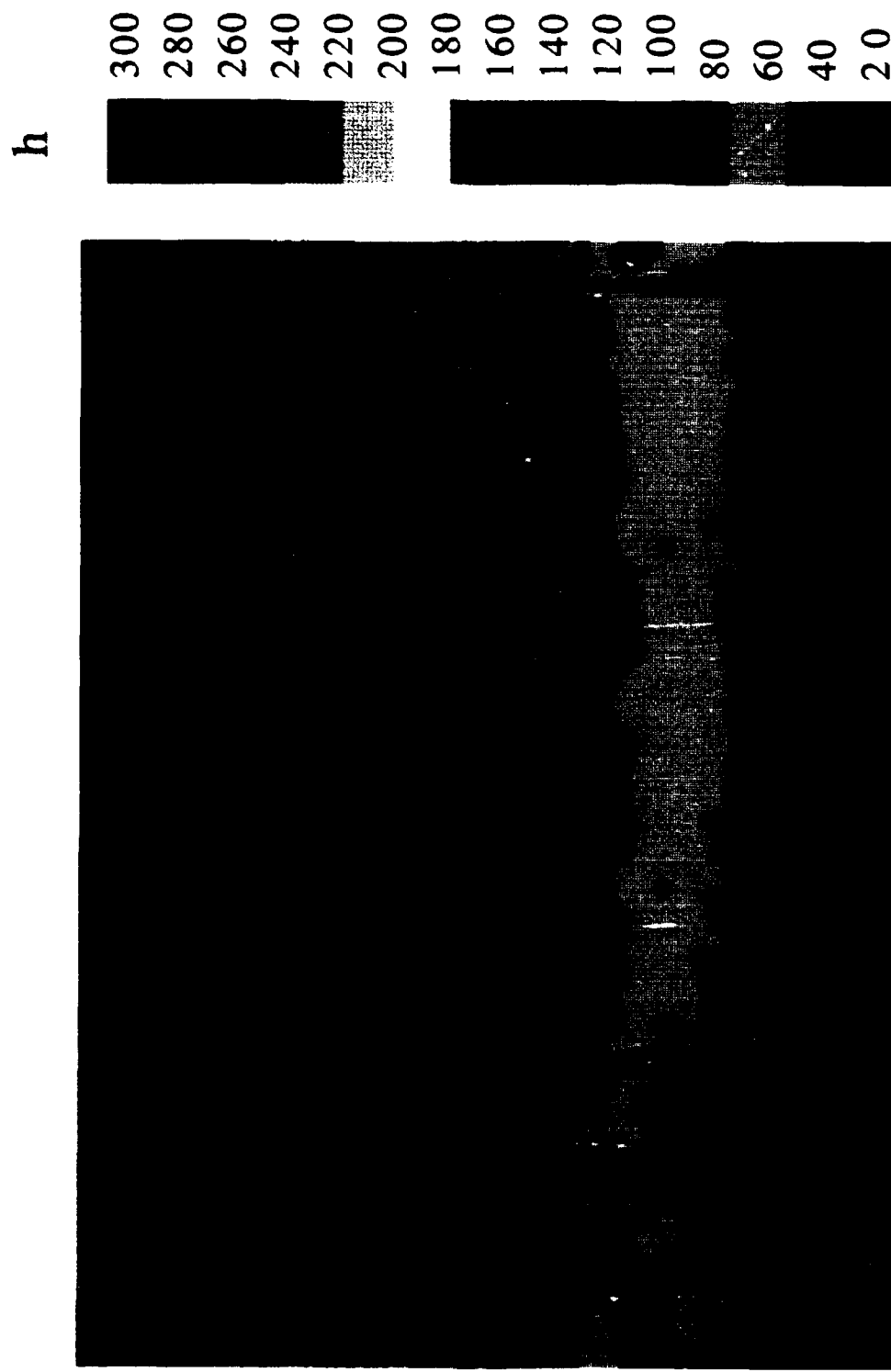


Fig. 58  $3/8$ " cavity,  $5/16$ " clearance gap, no injection,  
 $Re = 30,000$

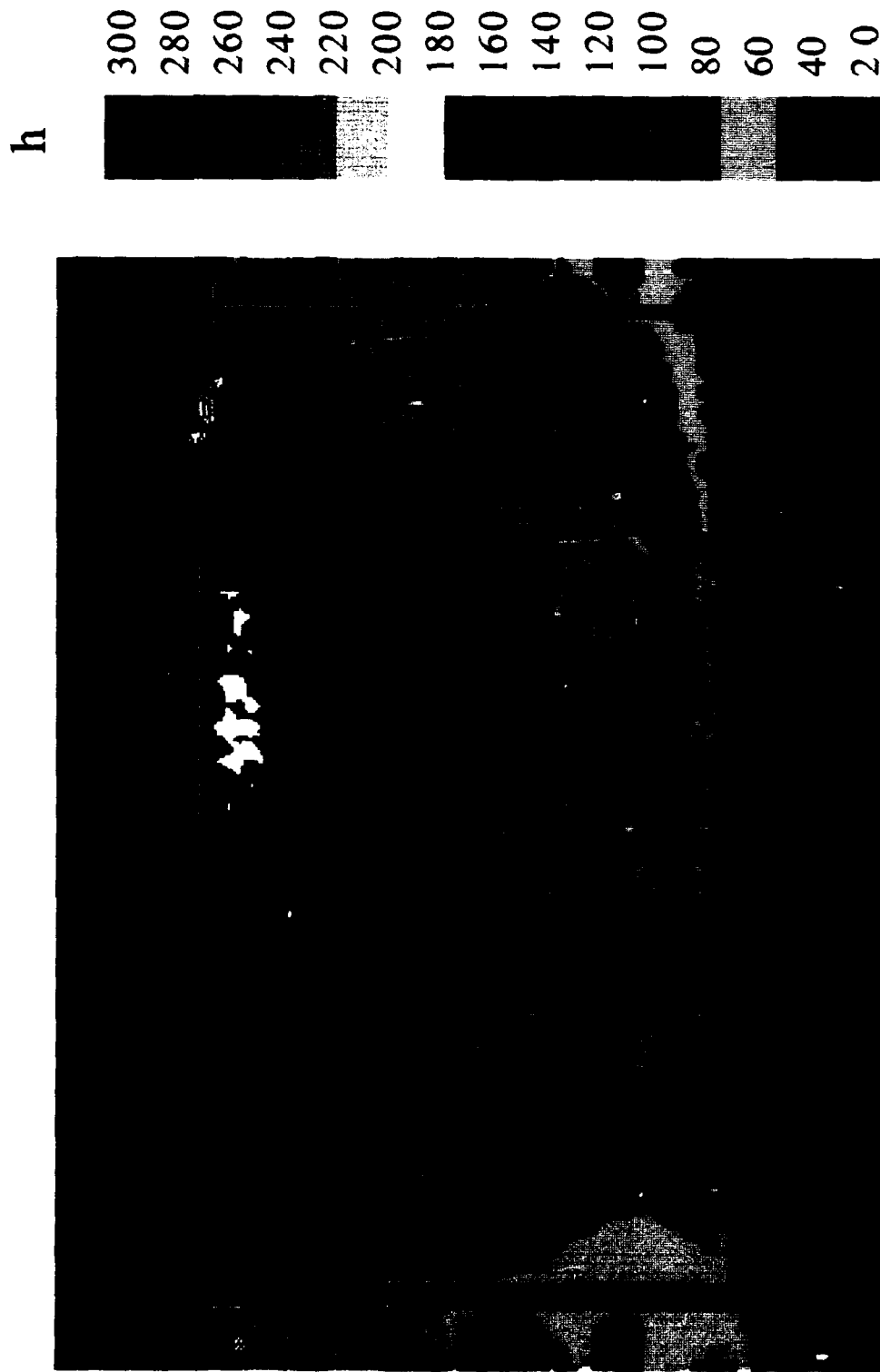


Fig. 59 1.0" cavity,  $\frac{3}{16}$ " clearance gap, no injection,  
 $Re = 30,000$

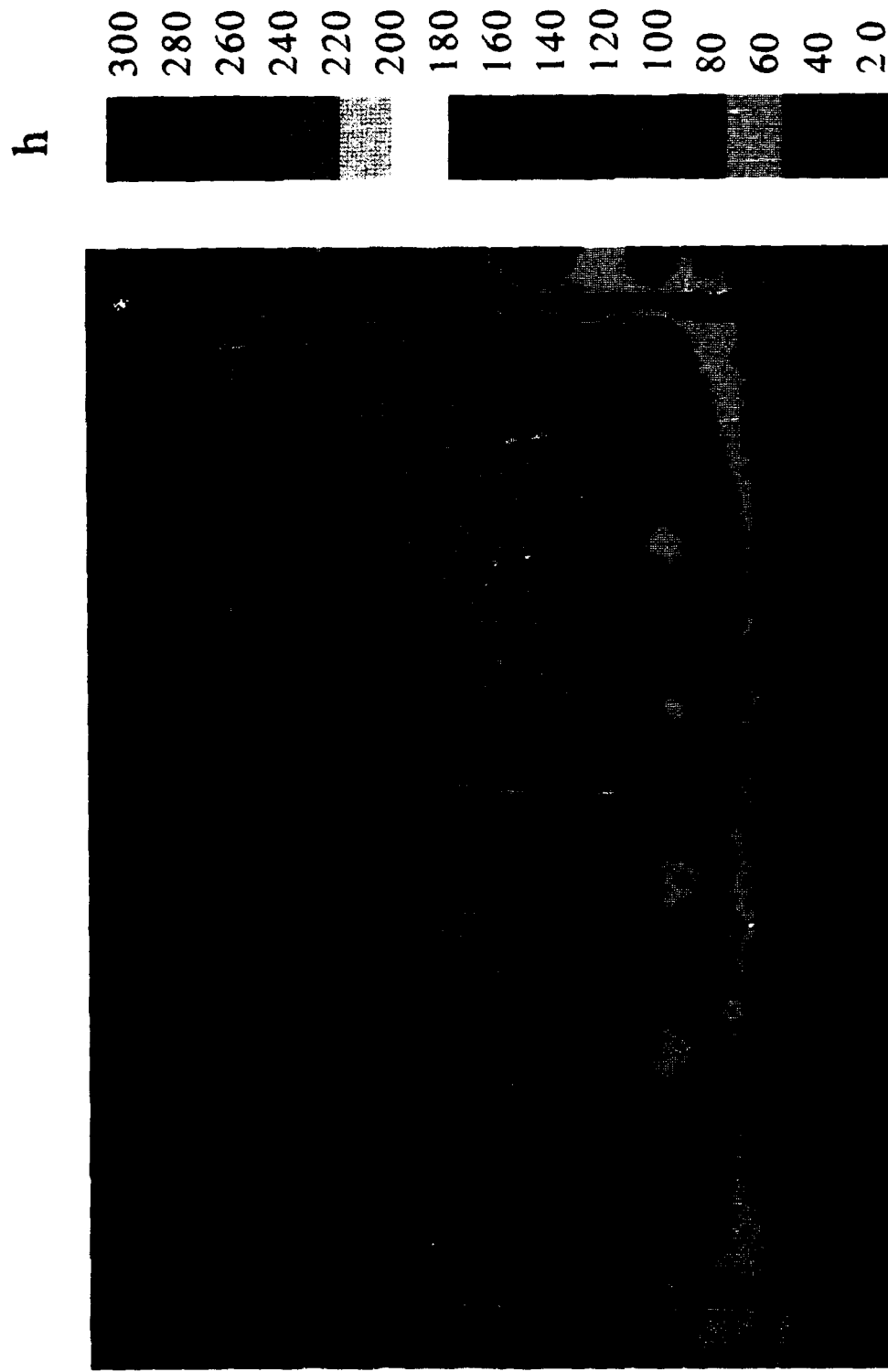


Fig. 60 1.0" cavity,  $5/16$ " clearance gap, no injection,  
Re = 30,000

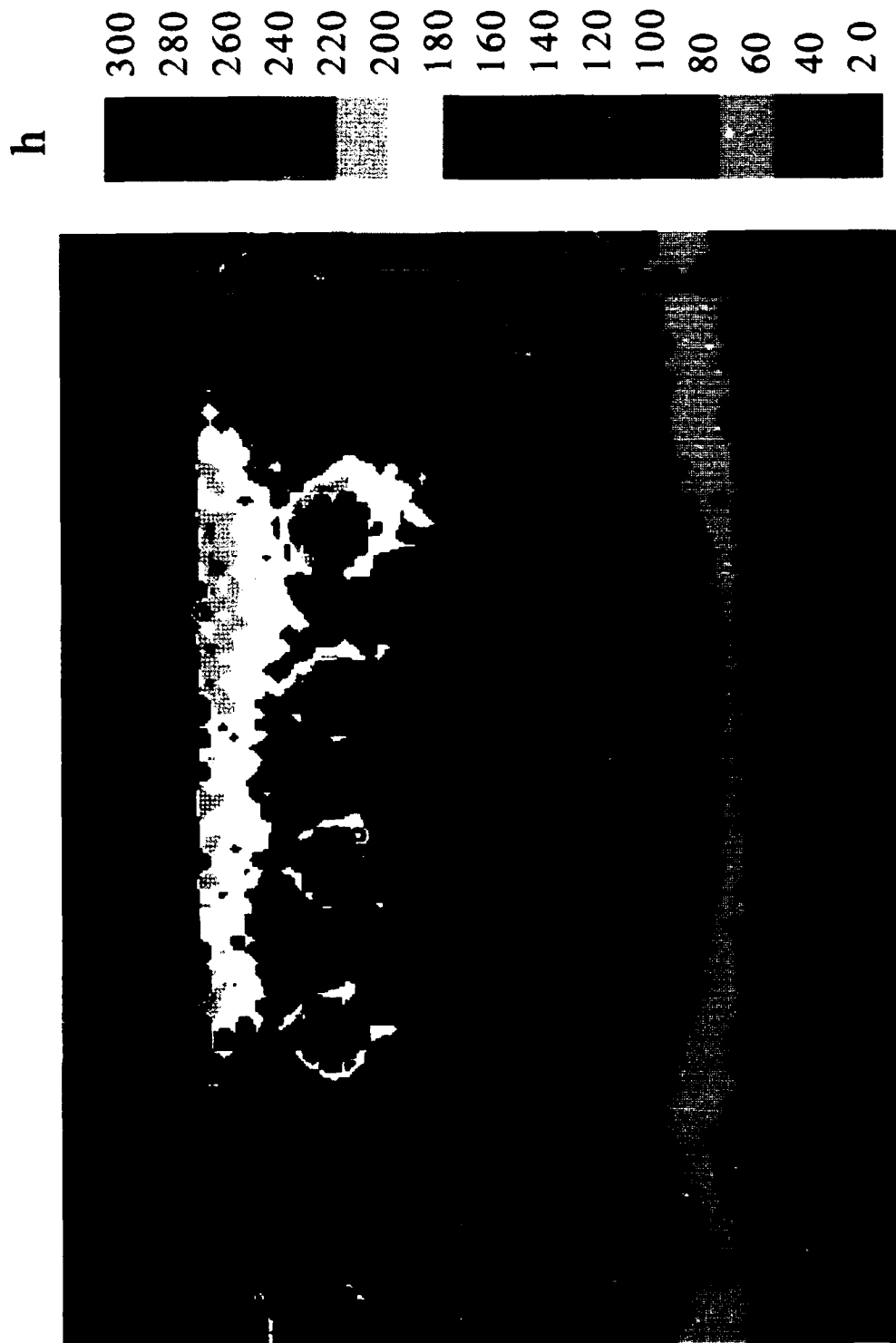


Fig. 61  $3/8$ " cavity,  $3/16$ " clearance gap, suction side injection,  
 $Re = 30,000$ ;  $M = 0.1$

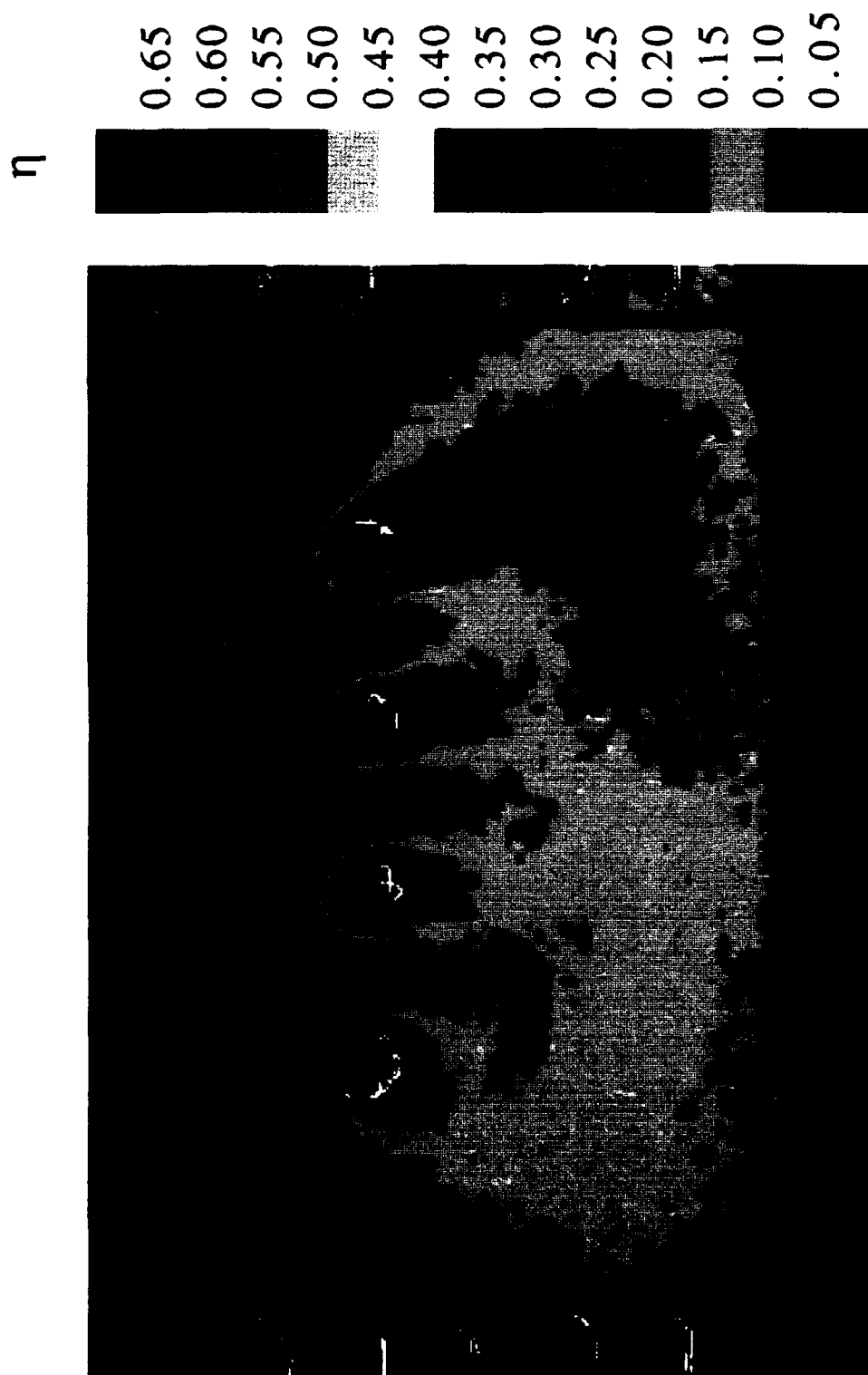


Fig. 62 3/8" cavity. 3/16" clearance gap, suction side injection,  
 $Re = 30,000$ ;  $M = 0.1$



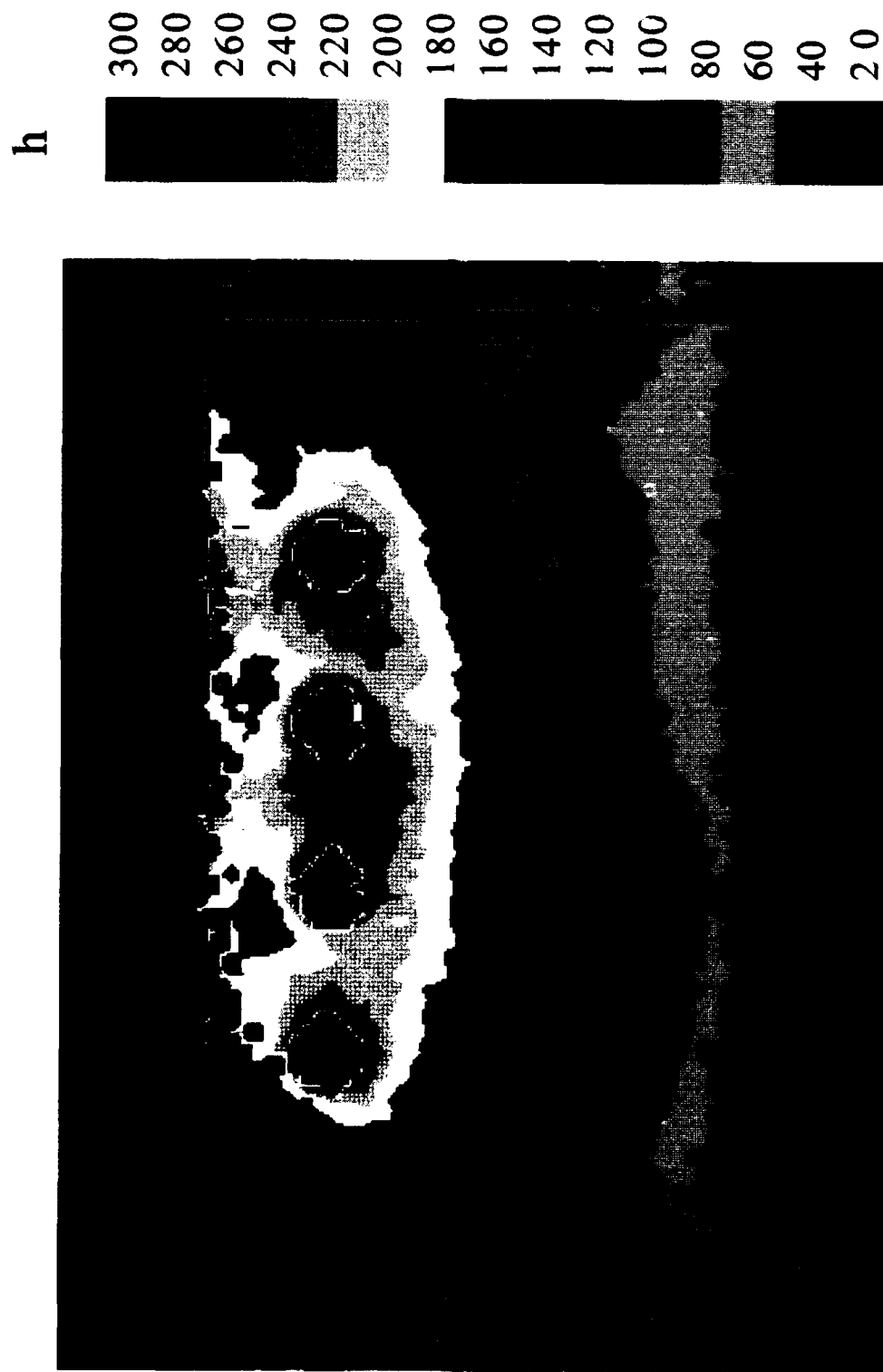


Fig. 63  $3/8$ " cavity,  $3/16$ " clearance gap, suction side injection,  
 $Re = 30,000$ ;  $M = 0.5$

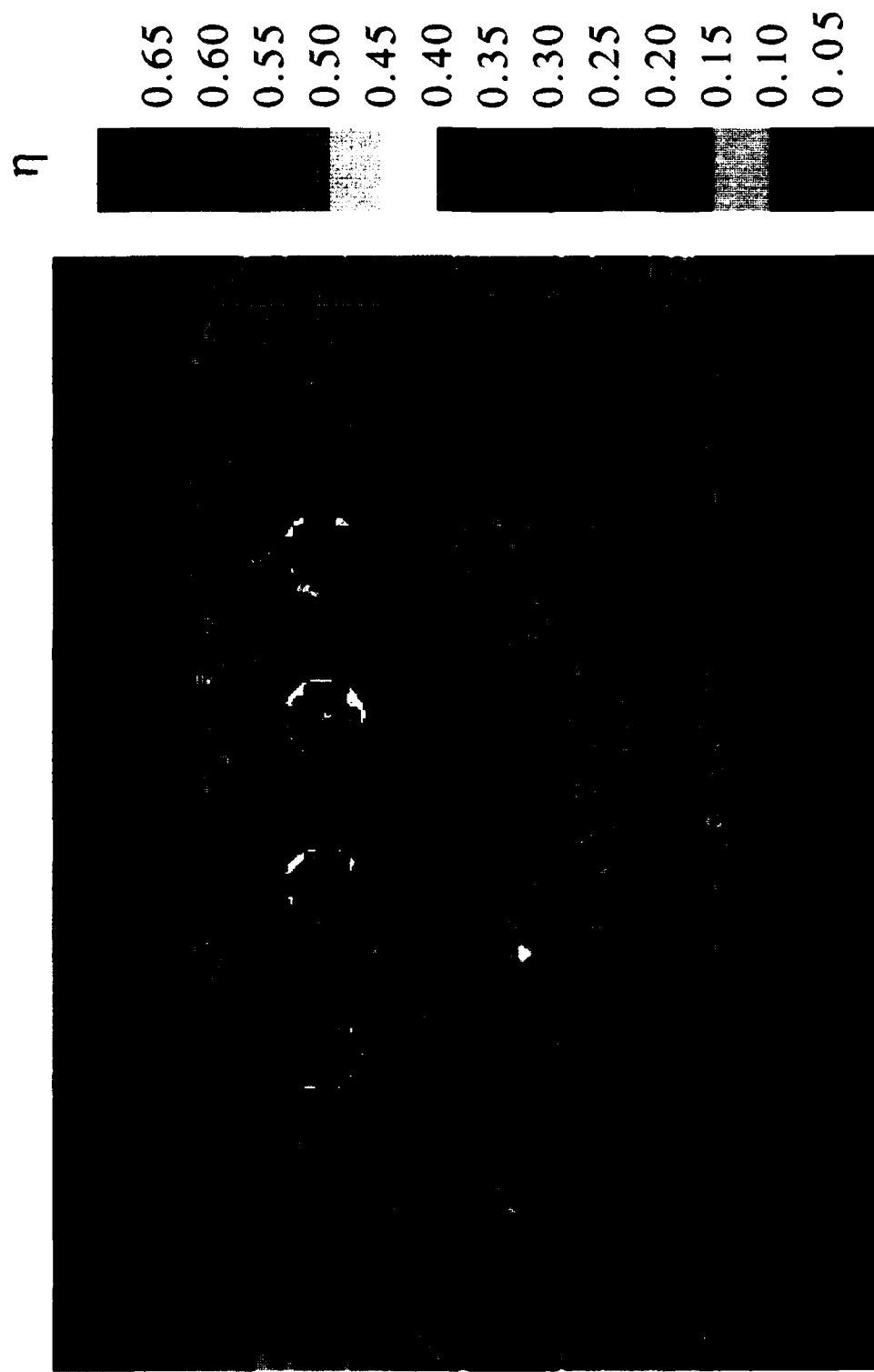


Fig. 64 3/8" cavity, 3/16" clearance gap, suction side injection,  
 $Re = 30,000$ ;  $M = 0.5$

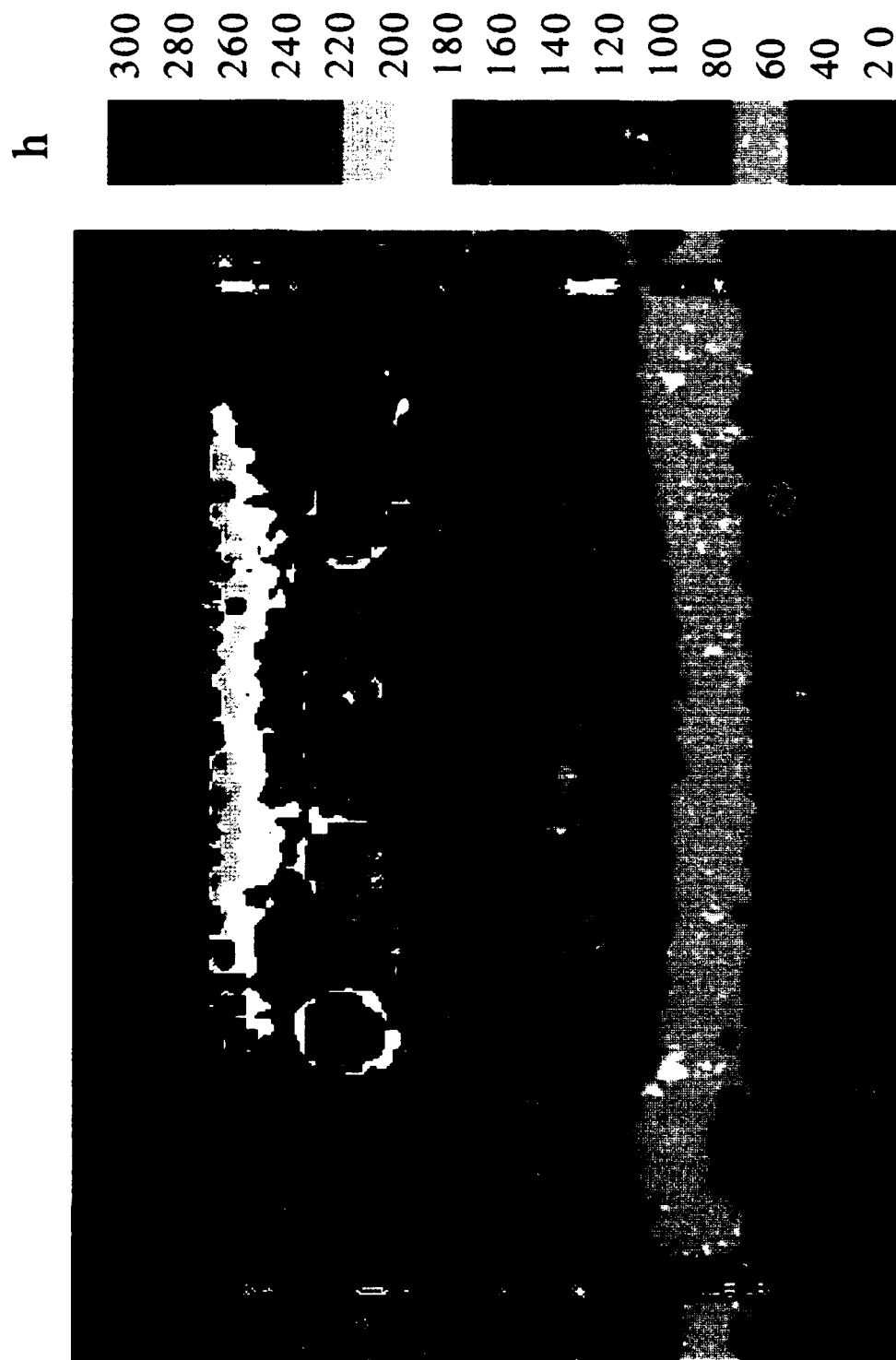


Fig. 65  $3/8$ " cavity,  $5/16$ " clearance gap, suction side injection,  
 $Re = 30,000$ ;  $M = 0.1$



Fig. 66 3/8" cavity, 5/16" clearance gap, suction side injection,  
 $Re = 30,000$ ;  $M = 0.1$

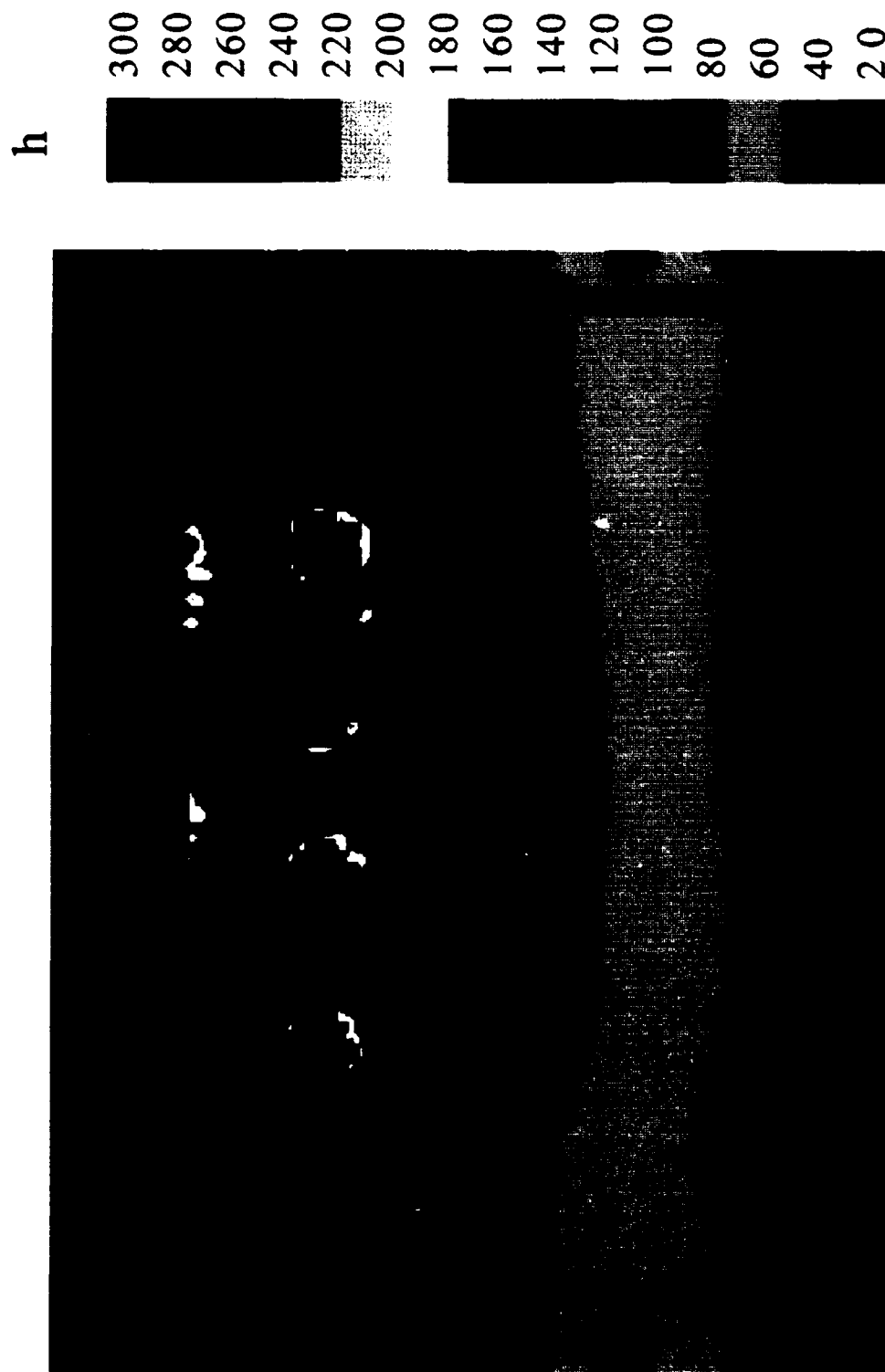


Fig. 67  $3/8$ " cavity,  $5/16$ " clearance gap, suction side injection,  
 $Re = 30,000$ ;  $M = 0.5$

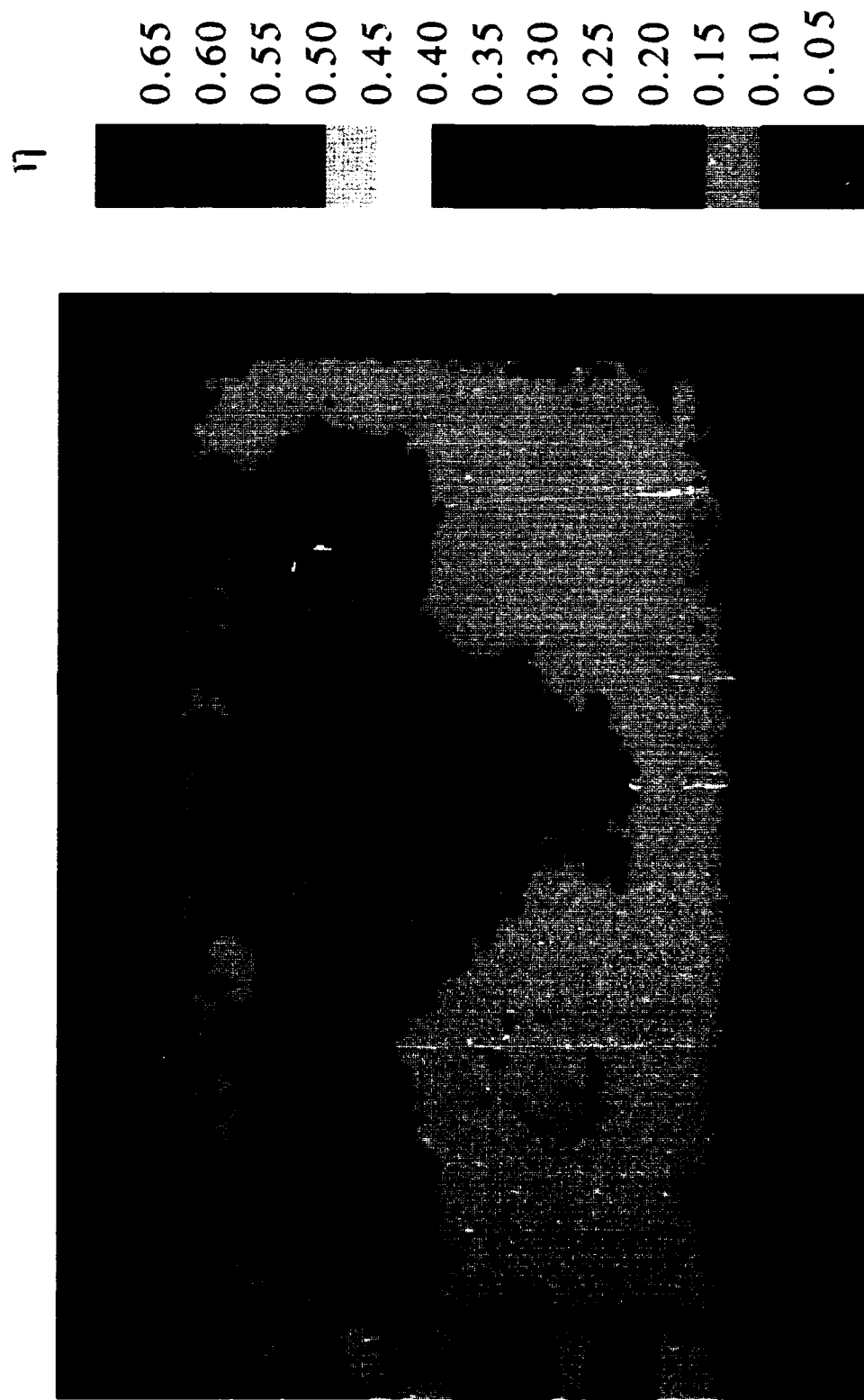


Fig. 68  $3/8$ " cavity,  $5/16$ " clearance gap, suction side injection,  
 $Re = 30,000$ ;  $M = 0.5$

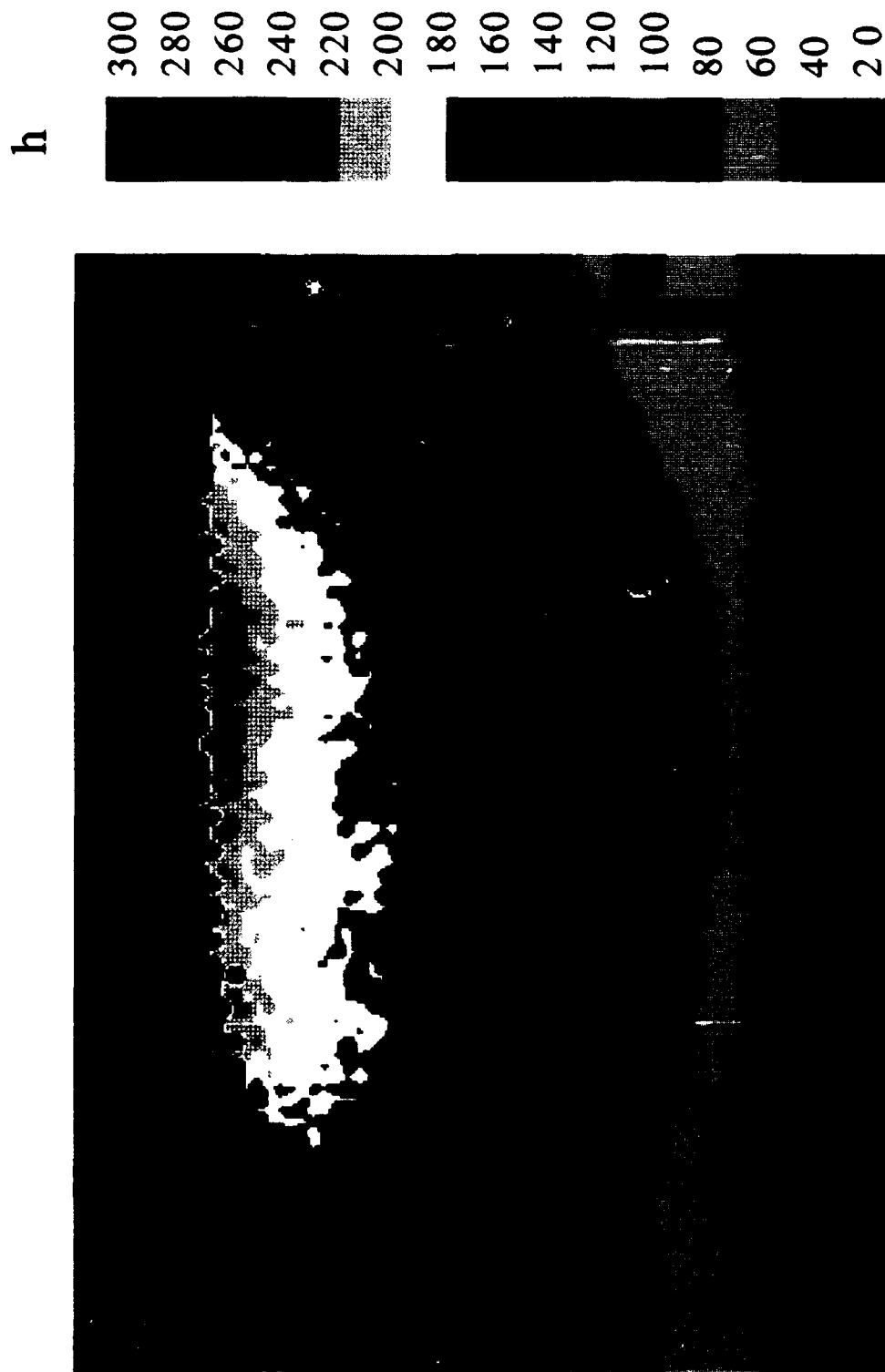


Fig. 69  $3/8$ " cavity,  $3/16$ " clearance gap, pressure side injection,  
 $Re = 30,000$ ;  $M = 0.1$

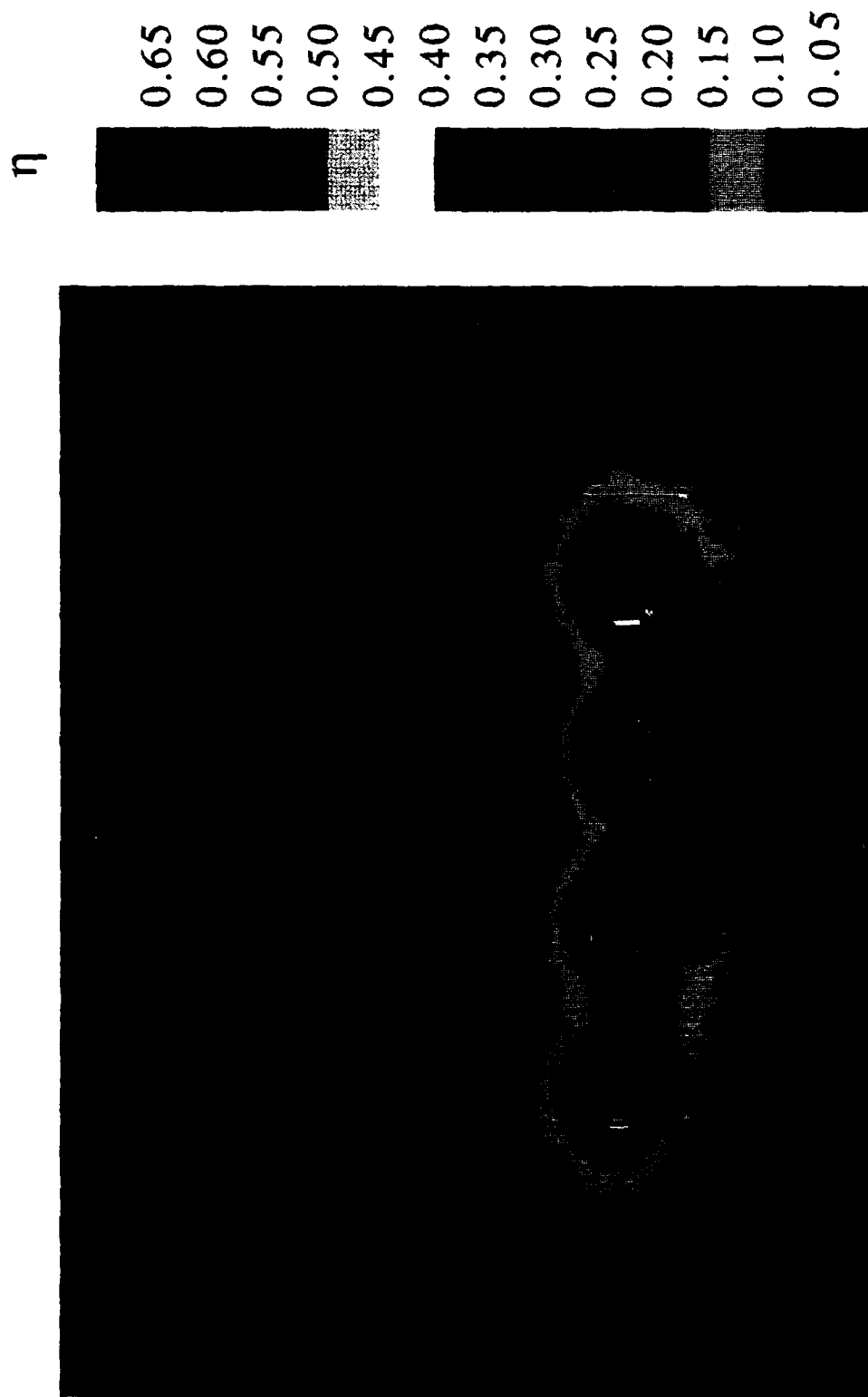


Fig. 70 3/8" cavity, 3/16" clearance gap, pressure side injection,  
 $Re = 30,000$ ;  $M = 0.1$





Fig. 71  $3/8$ " cavity,  $3/16$ " clearance gap, pressure side injection,  
 $Re = 30,000$ ;  $M = 0.5$

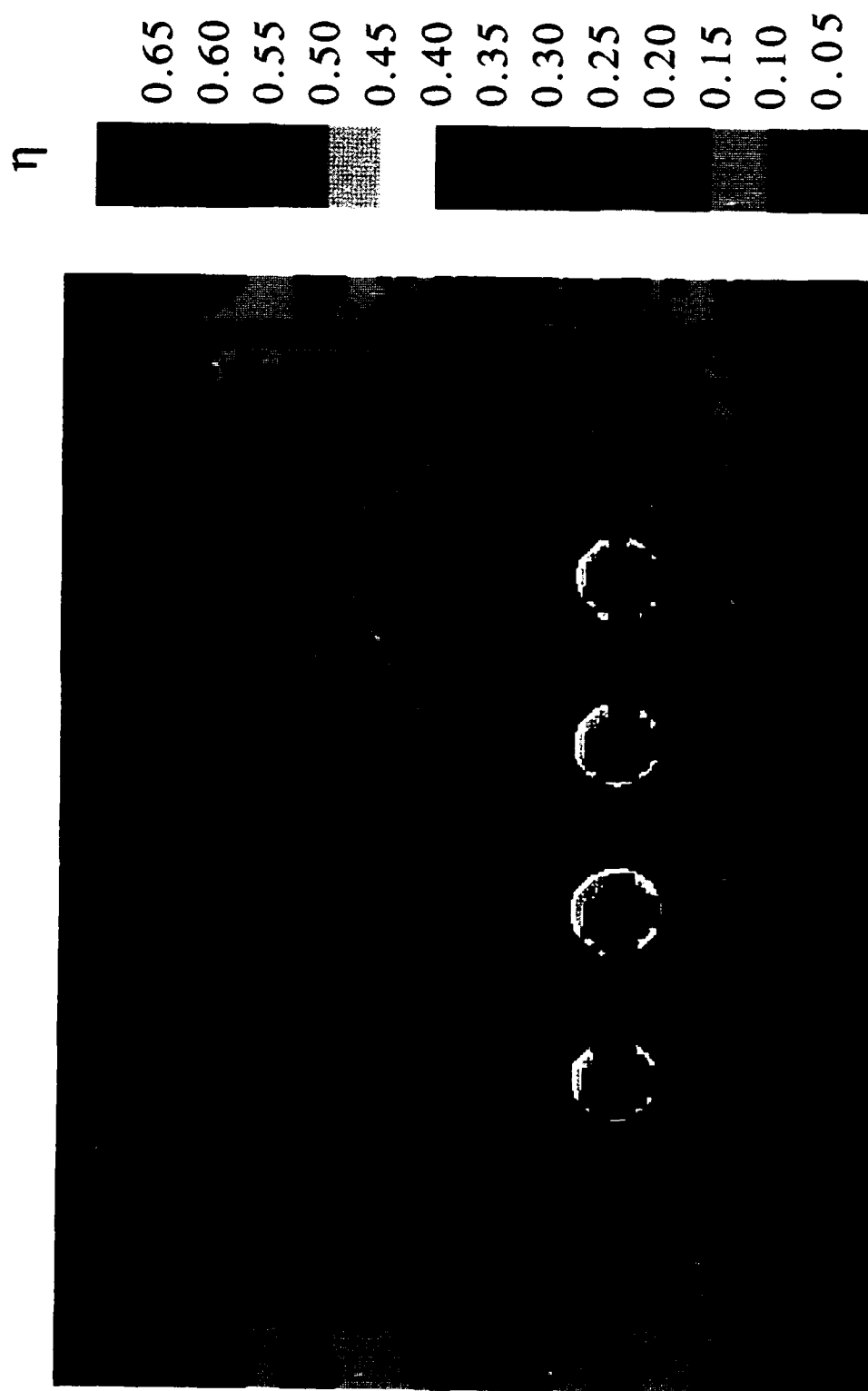


Fig. 72  $3/8$  inch cavity,  $3/16$  inch clearance gap, pressure side injection,  
 $Re = 30,000$ ;  $M = 0.5$

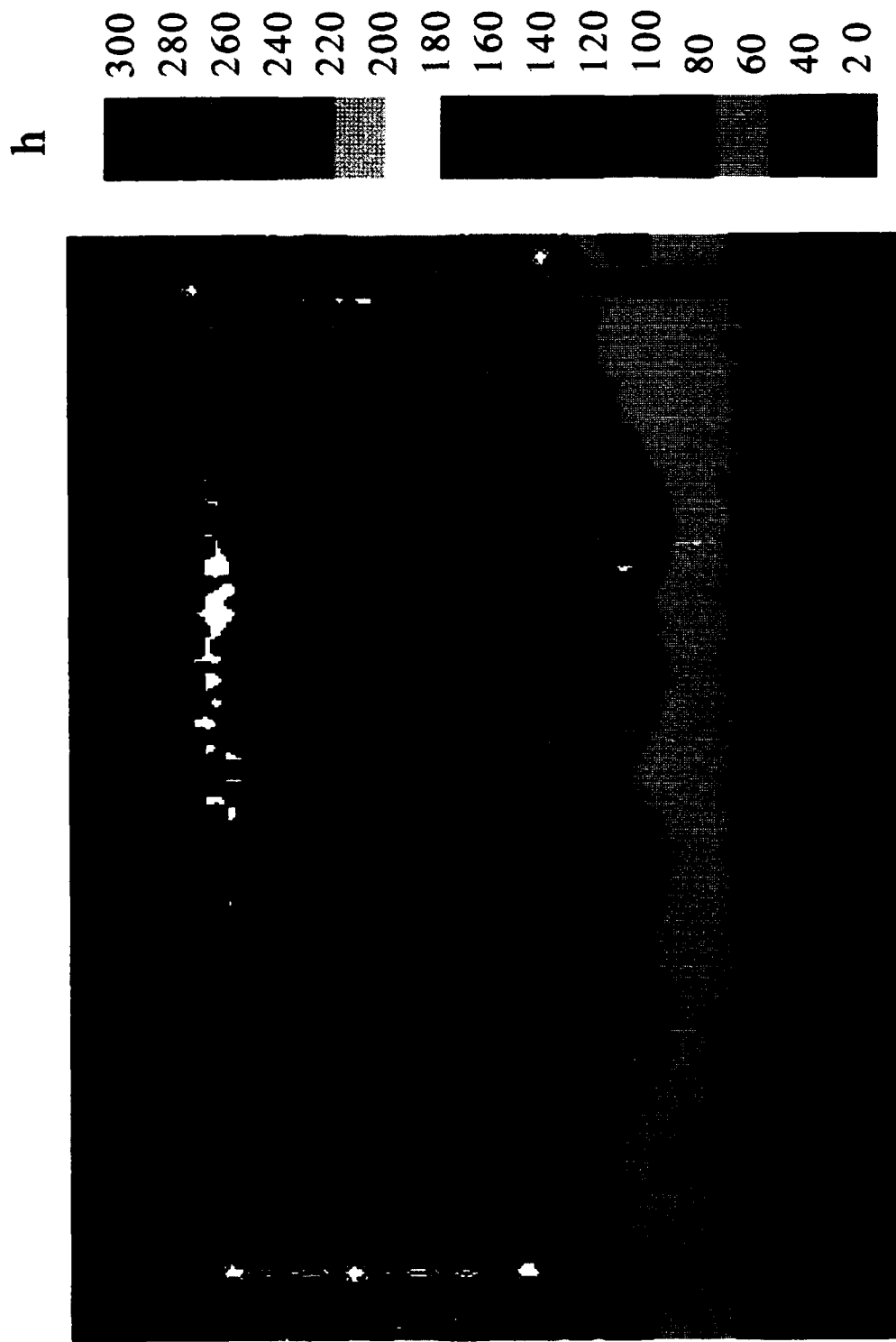


Fig. 73  $3/8$ " cavity,  $5/16$ " clearance gap, pressure side injection,  
 $Re = 30,000$ ;  $M = 0.1$

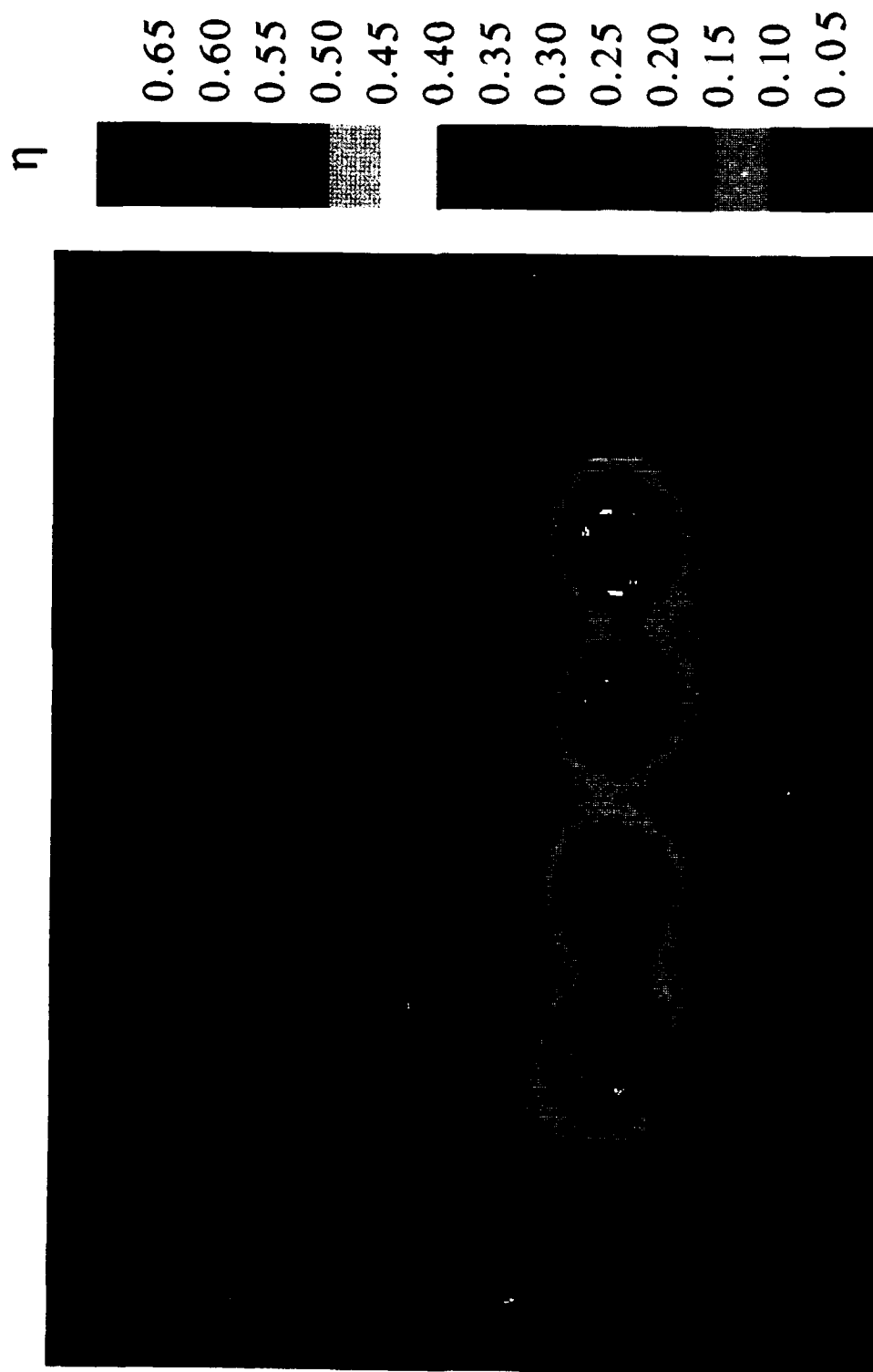


Fig. 74 3/8" cavity, 5/16" clearance gap, pressure side injection,  
 $Re = 30,000$ ;  $M = 0.1$

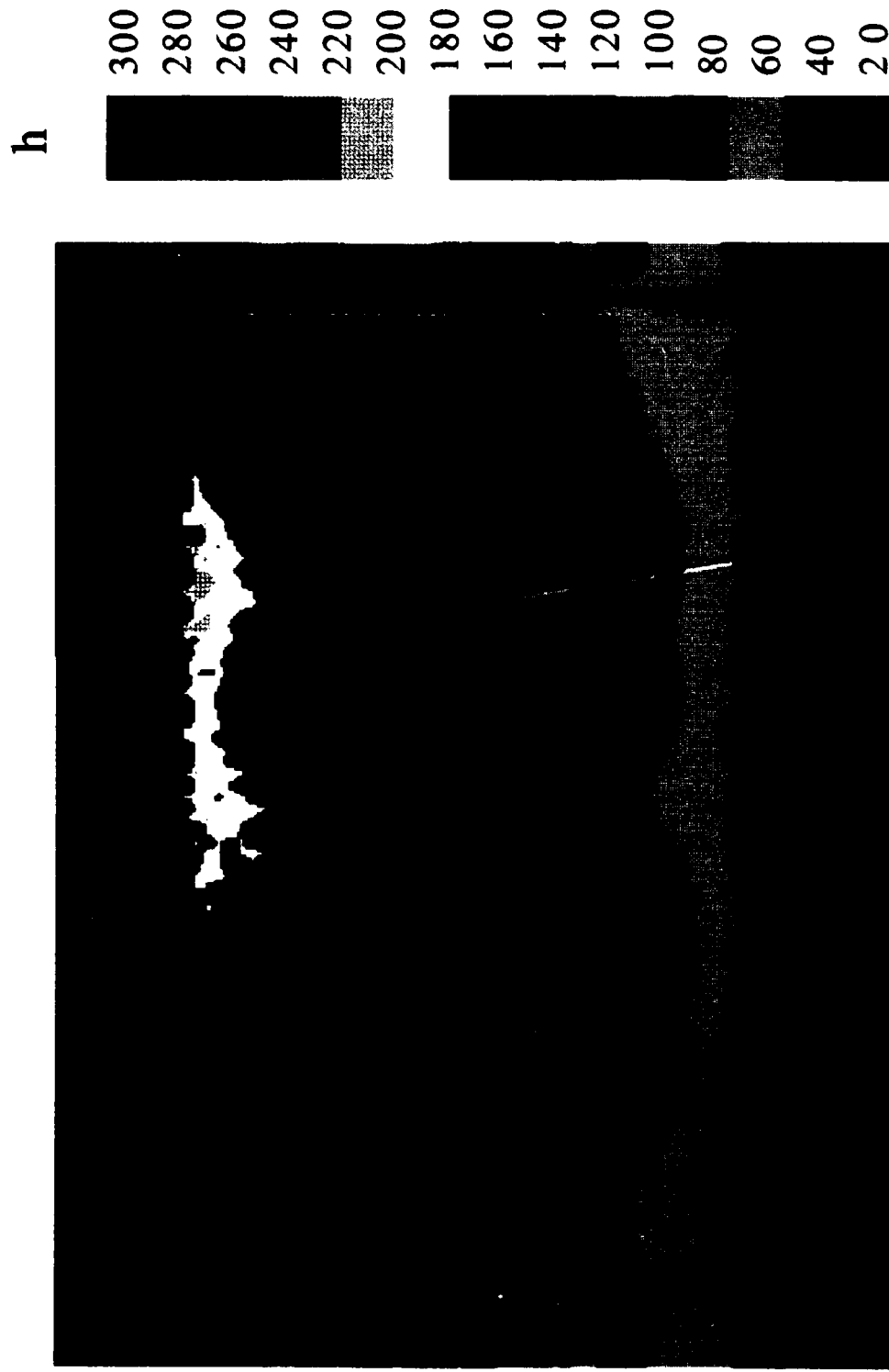


Fig. 75  $3/8$ " cavity,  $5/16$ " clearance gap, pressure side injection,  
 $Re = 30,000$ ;  $M = 0.5$

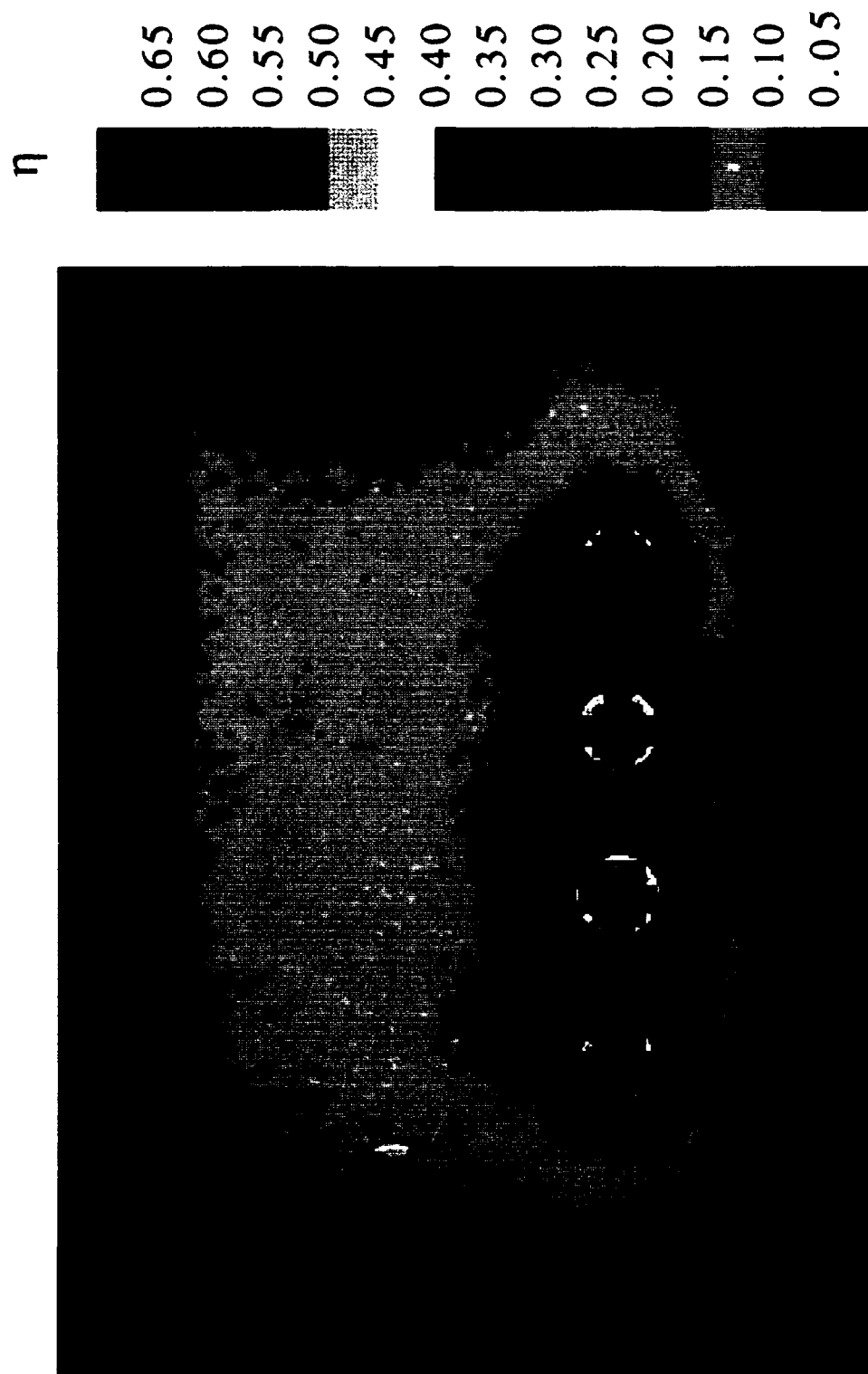


Fig. 76  $3/8$ " cavity,  $5/16$ " clearance gap, pressure side injection,  
 $Re = 30,000$ ;  $M = 0.5$

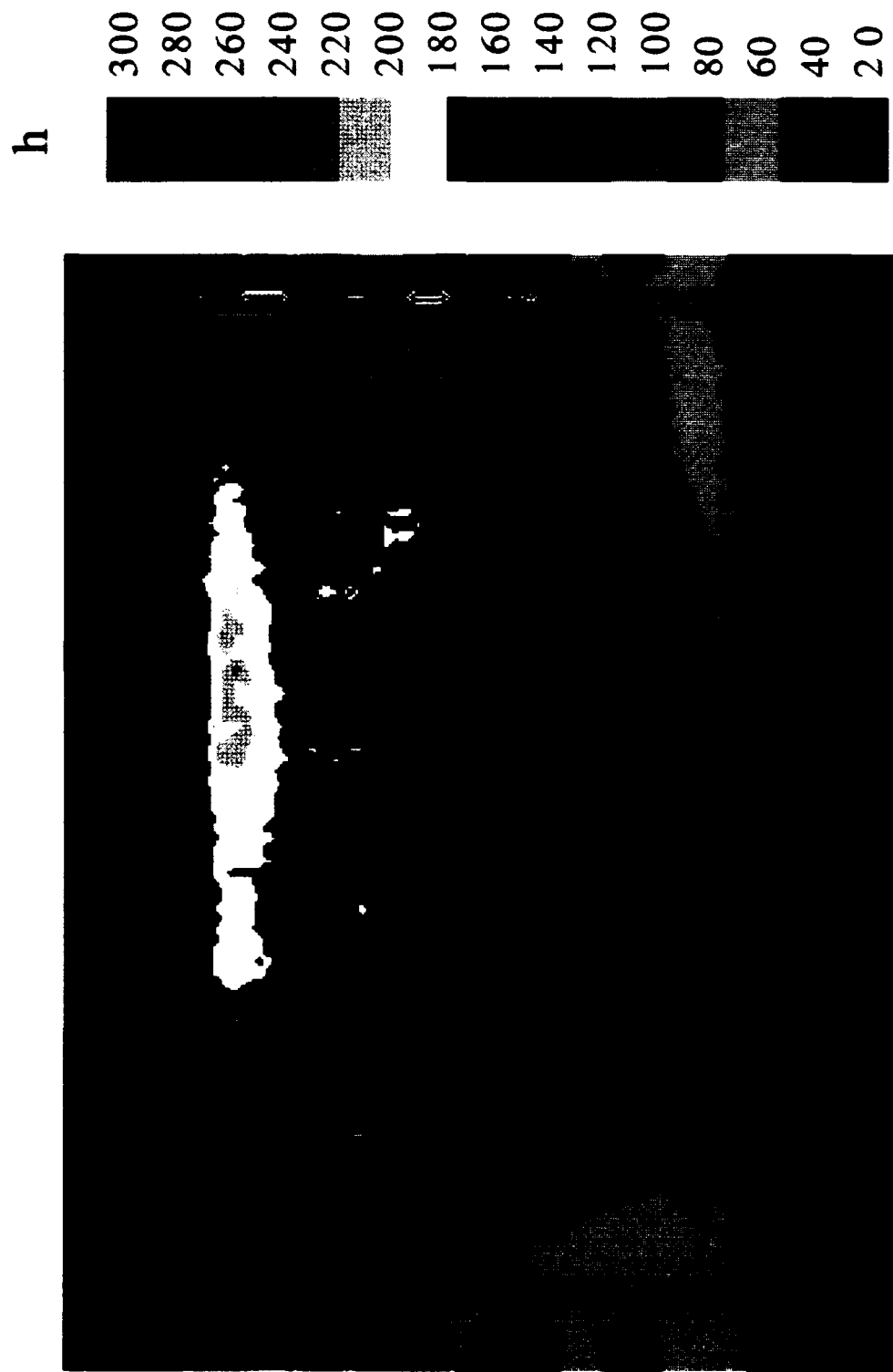


Fig. 77 1.0" cavity,  $3/16$ " clearance gap, suction side injection,  
 $Re = 30,000$ ;  $M = 0.1$

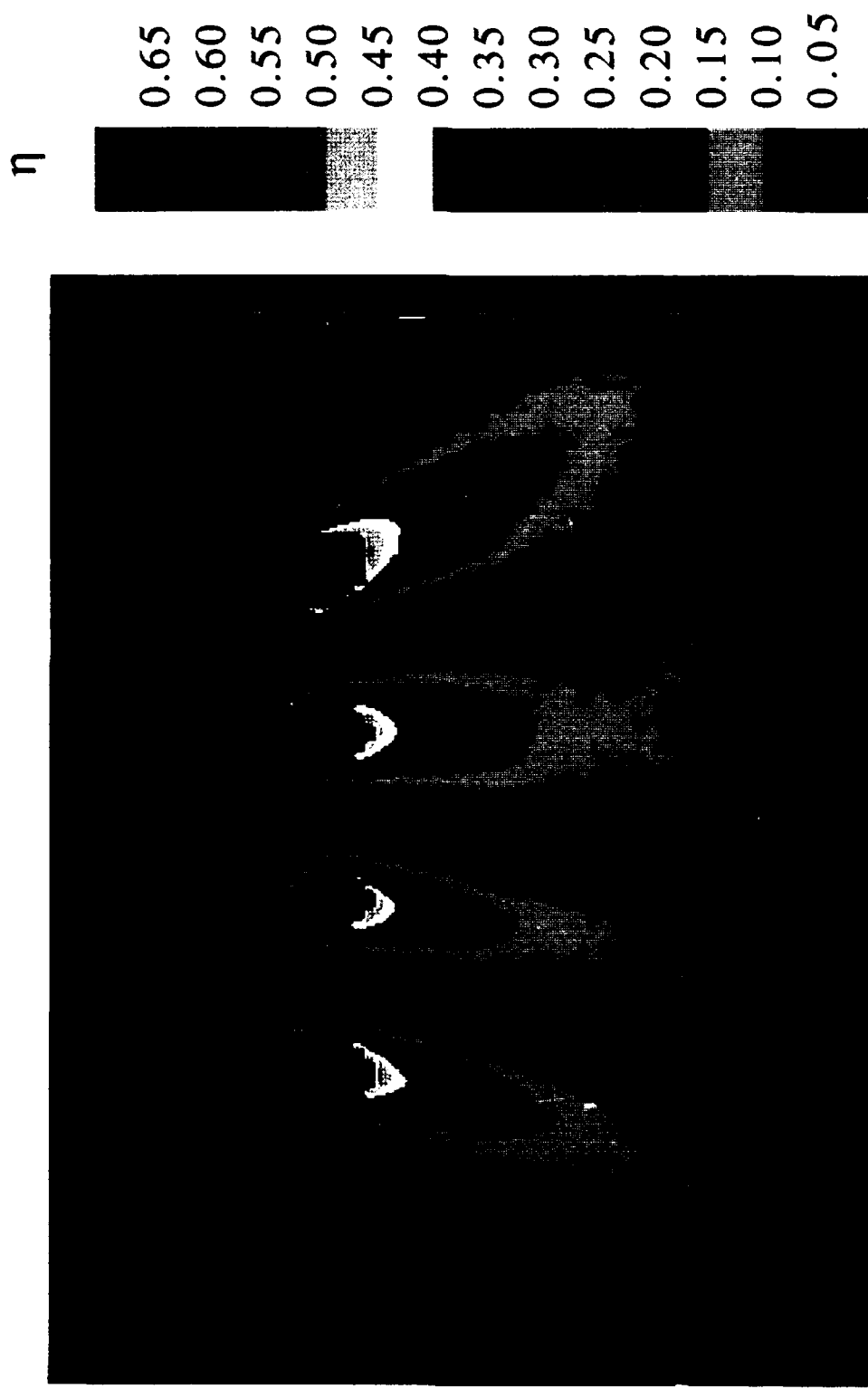


Fig. 78 1.0" cavity,  $3/16$ " clearance gap, suction side injection,  
 $Re \approx 30,000$ ;  $M = 0.1$



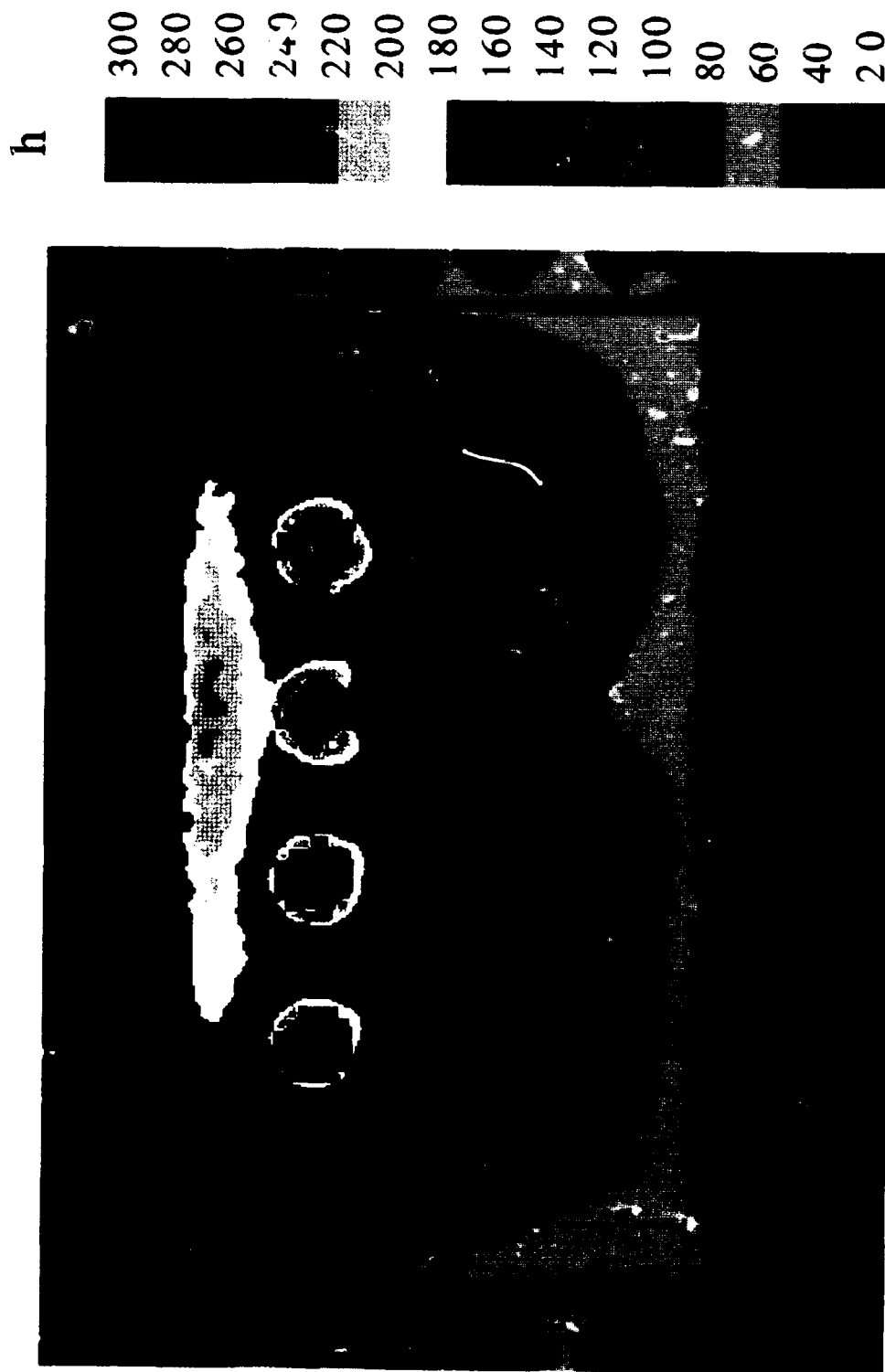


Fig. 79 1.0" cavity,  $3/16$ " clearance gap, suction side injection,  
 $Re = 30,000$ ;  $M = 0.5$

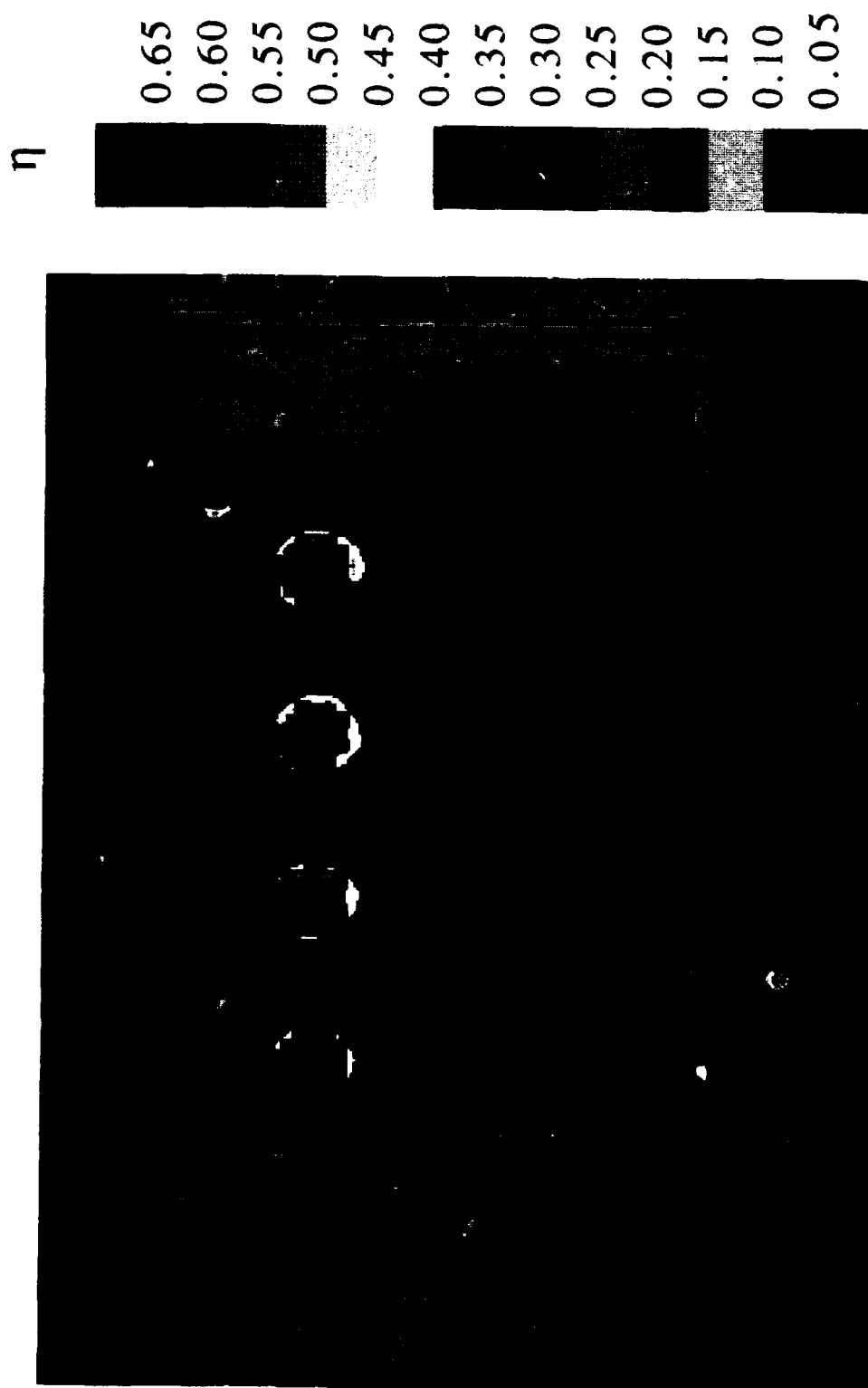


Fig. 80 1.0" cavity,  $\frac{3}{16}$ " clearance gap, suction side injection,  
 $Re = 30,000$ ;  $M = 0.5$

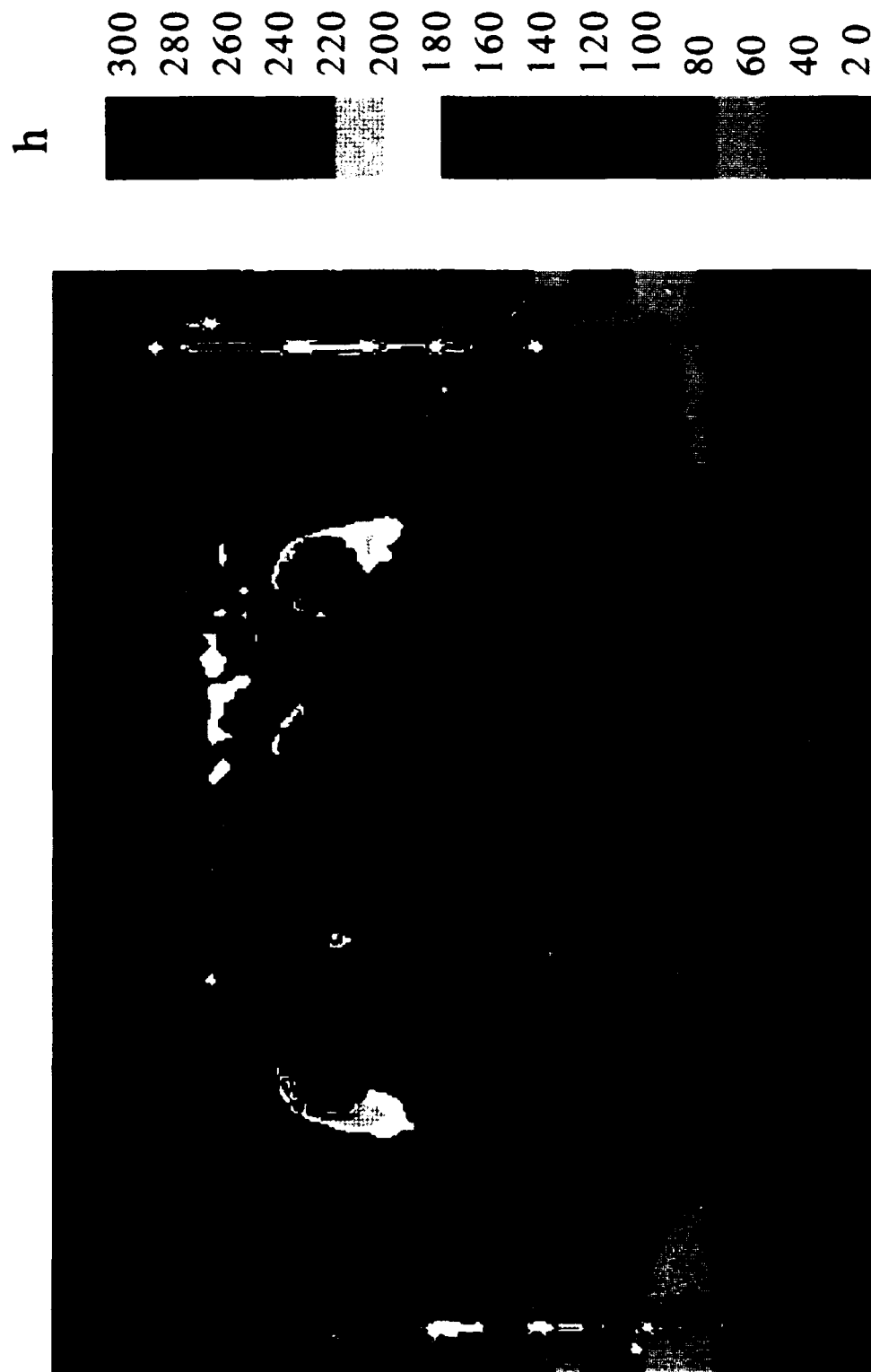


Fig. 81 1.0" cavity,  $\frac{5}{16}$ " clearance gap, suction side injection,  
 $Re = 30,000$ ;  $M = 0.1$

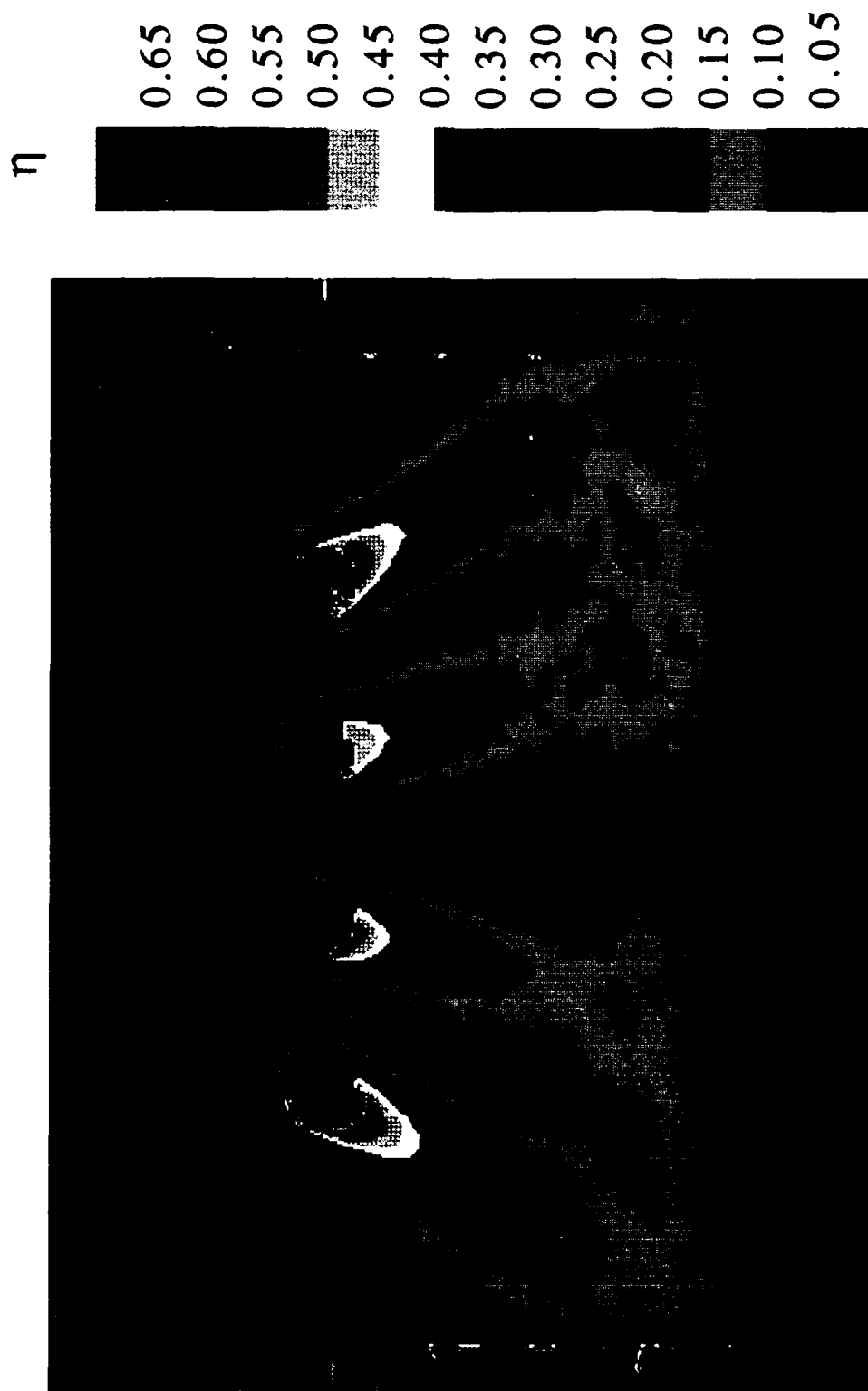


Fig. 82 1.0" cavity, 5/16" clearance gap, suction side injection,  
 $Re = 30,000$ ;  $M = 0.1$

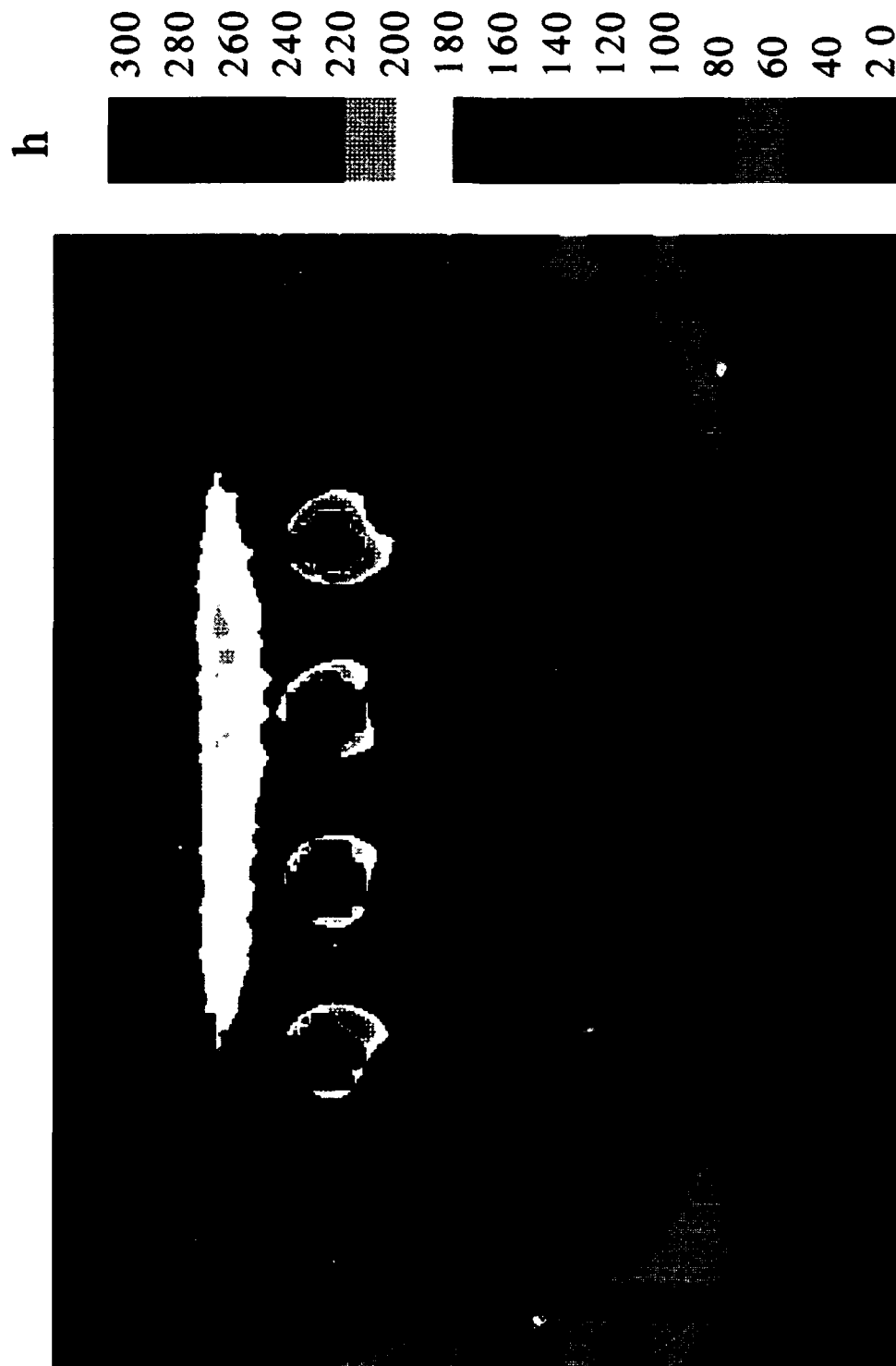


Fig. 83 1.0" cavity,  $5/16$ " clearance gap, suction side injection,  
 $Re = 30,000$ ;  $M = 0.5$

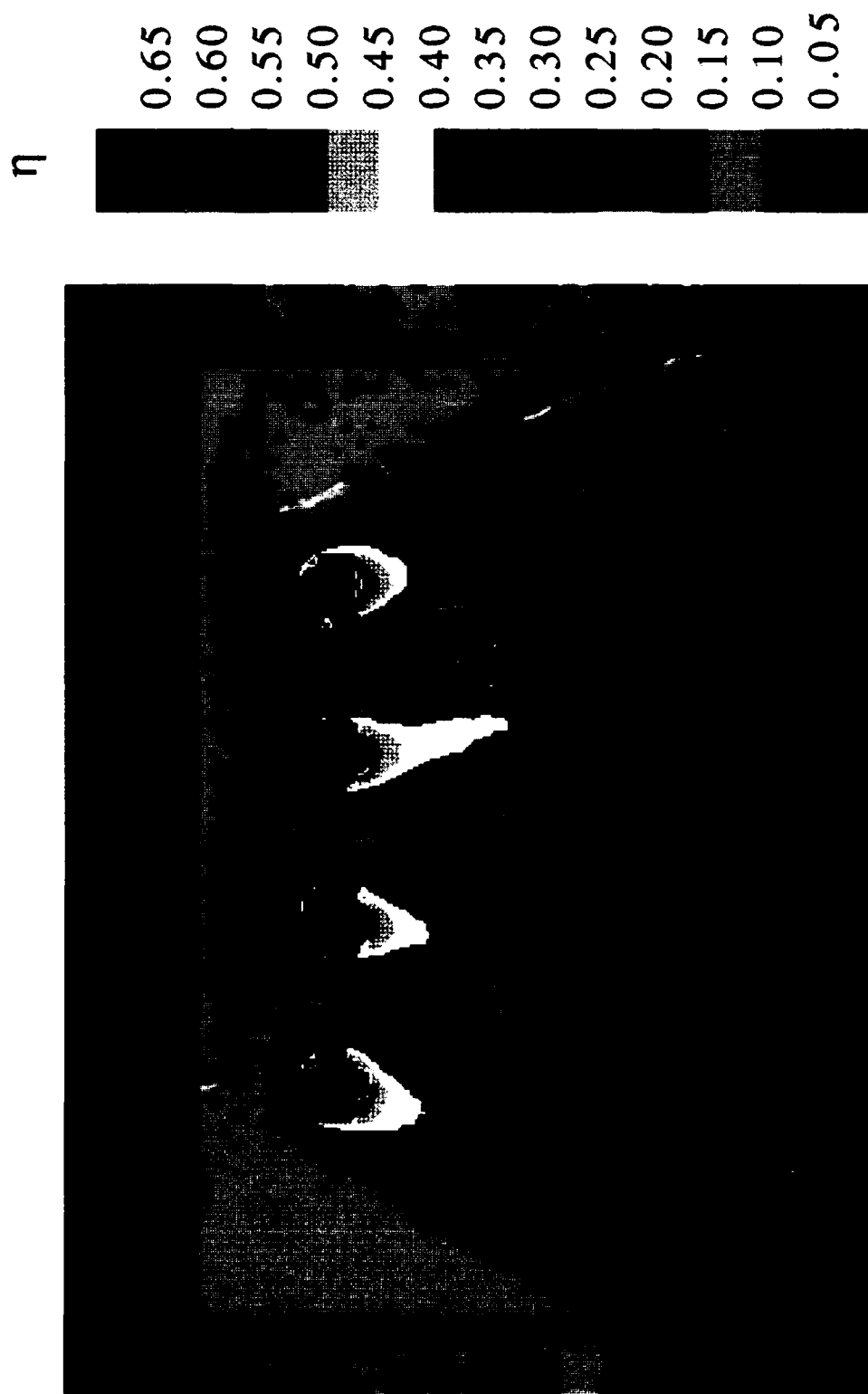


Fig. 84 1.0" cavity,  $5/16$ " clearance gap, suction side injection,  
 $Re = 30,000$ ;  $M = 0.5$

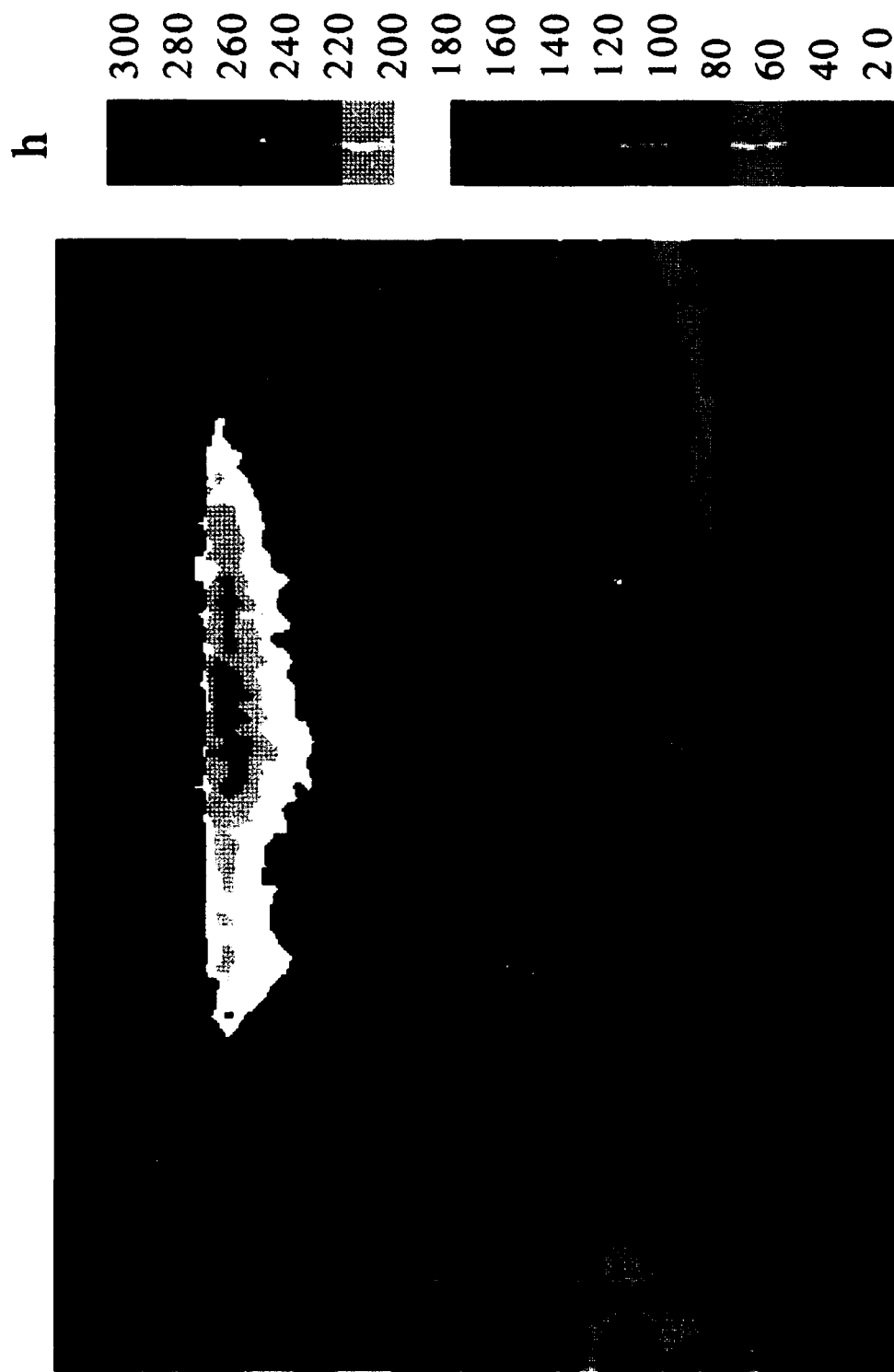


Fig. 85 1.0" cavity,  $3/16$ " clearance gap, pressure side injection,  
 $Re = 30,000$ ;  $M = 0.1$

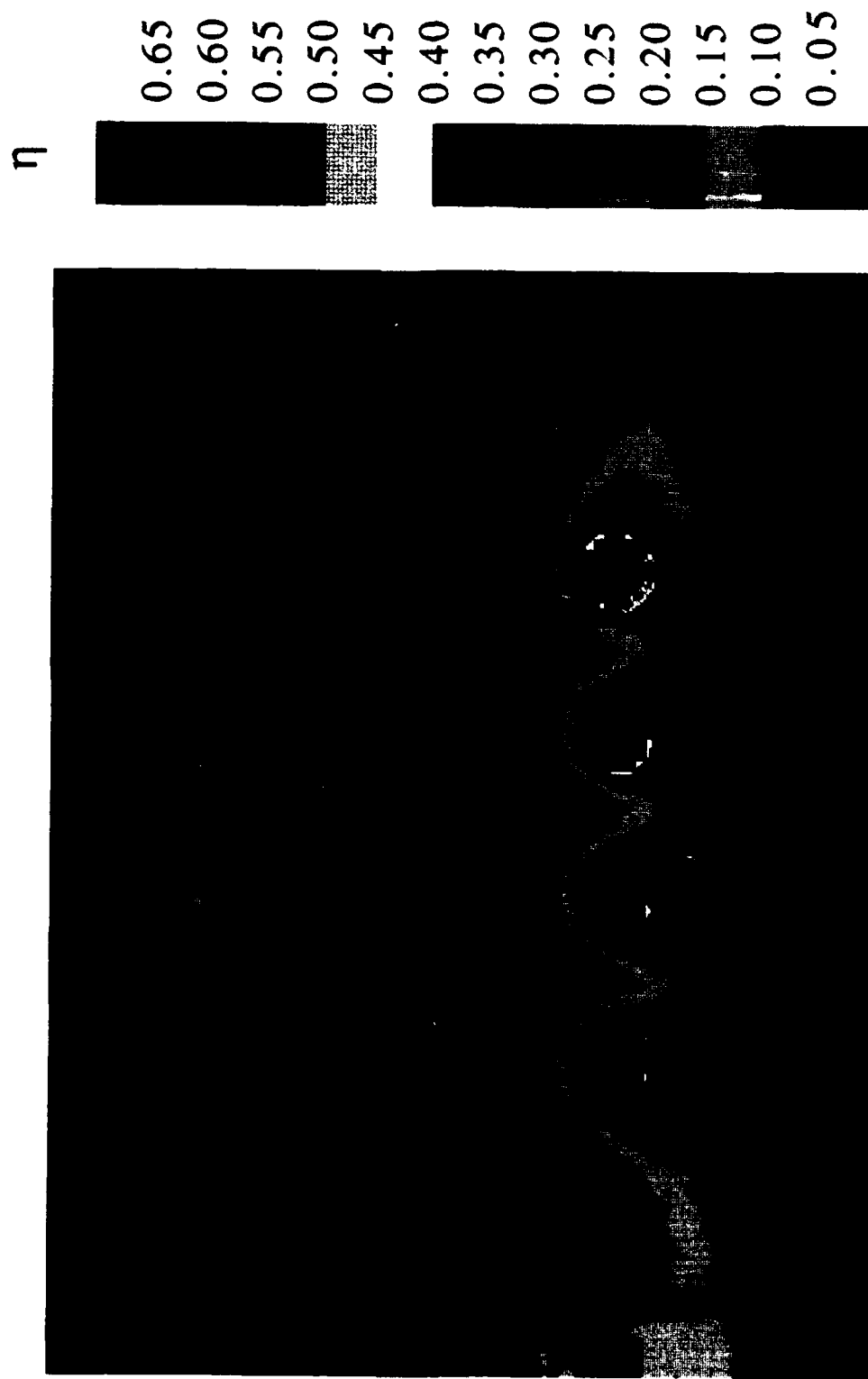


Fig. 86 1.0" cavity,  $3/16$ " clearance gap, pressure side injection,  
Re = 30,000; M = 0.1





Fig. 87 1.0" cavity,  $\frac{3}{16}$ " clearance gap, pressure side injection,  
 $Re = 30,000$ ;  $M = 0.5$

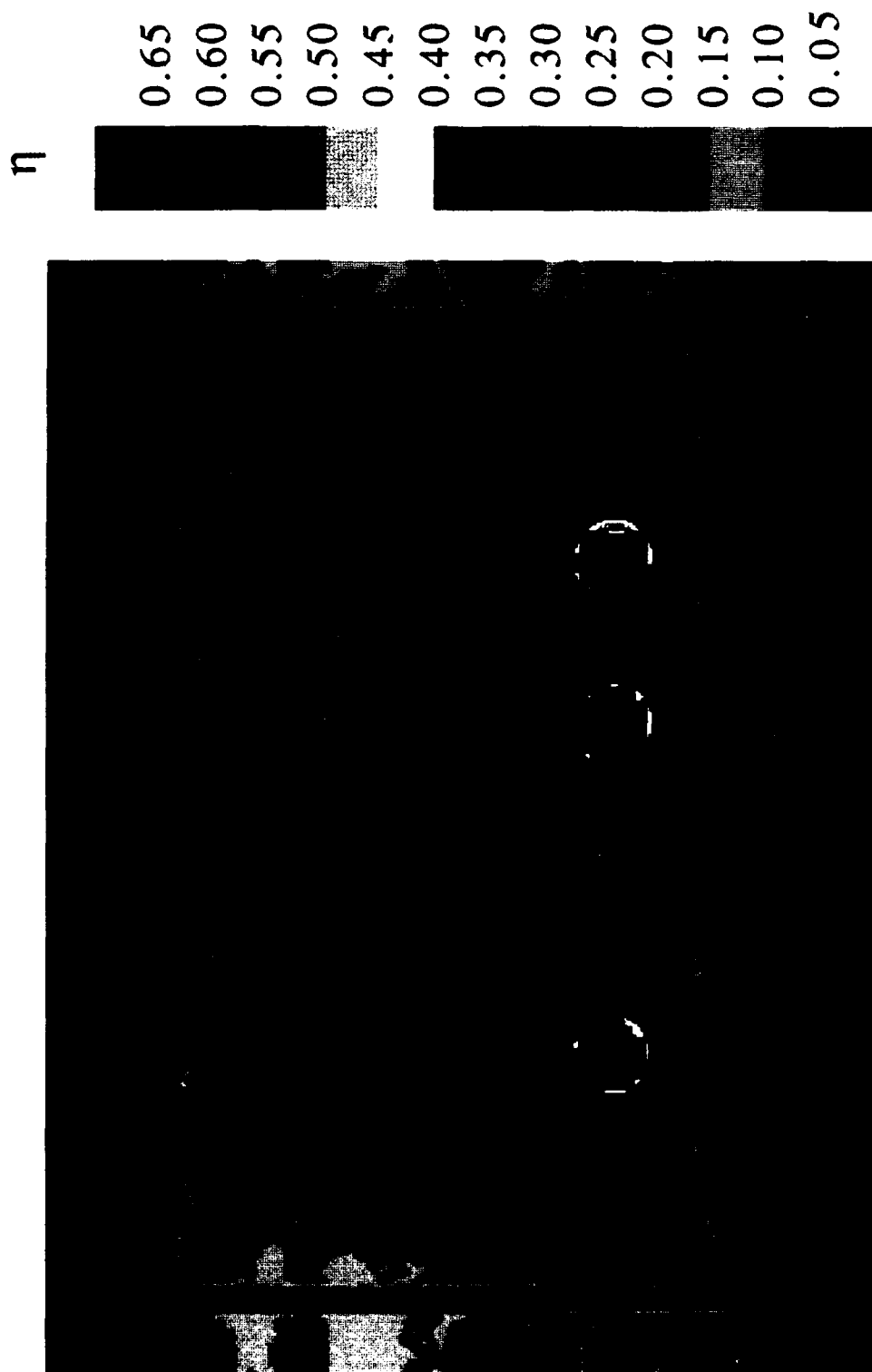


Fig. 88 1.0" cavity,  $3/16$ " clearance gap, pressure side injection,  
 $Re = 30,000$ ;  $M = 0.5$

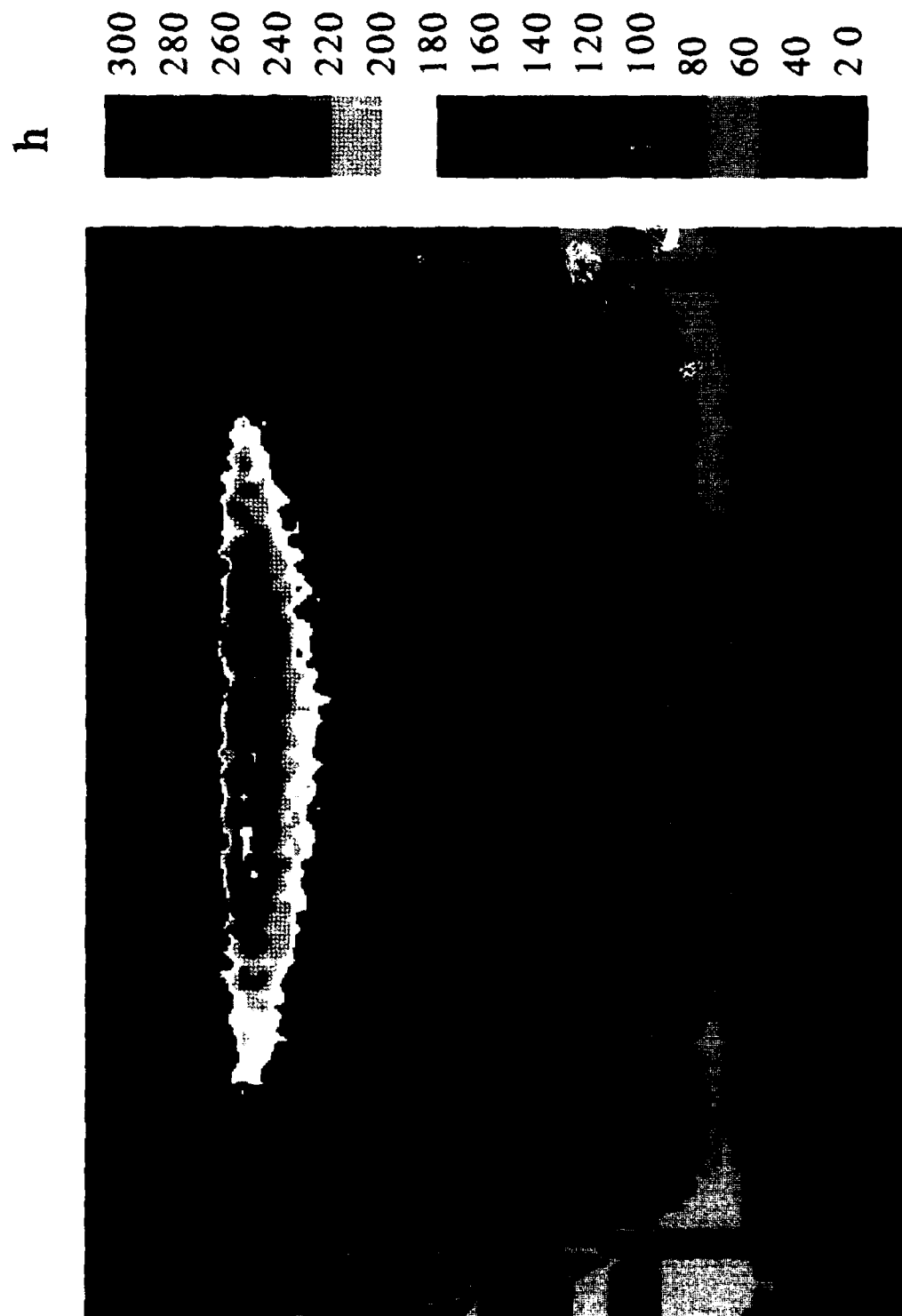


Fig. 89 1.0" cavity,  $S/16$ " clearance gap, pressure side injection,  
 $Re = 30,000$ ;  $M = 0.1$

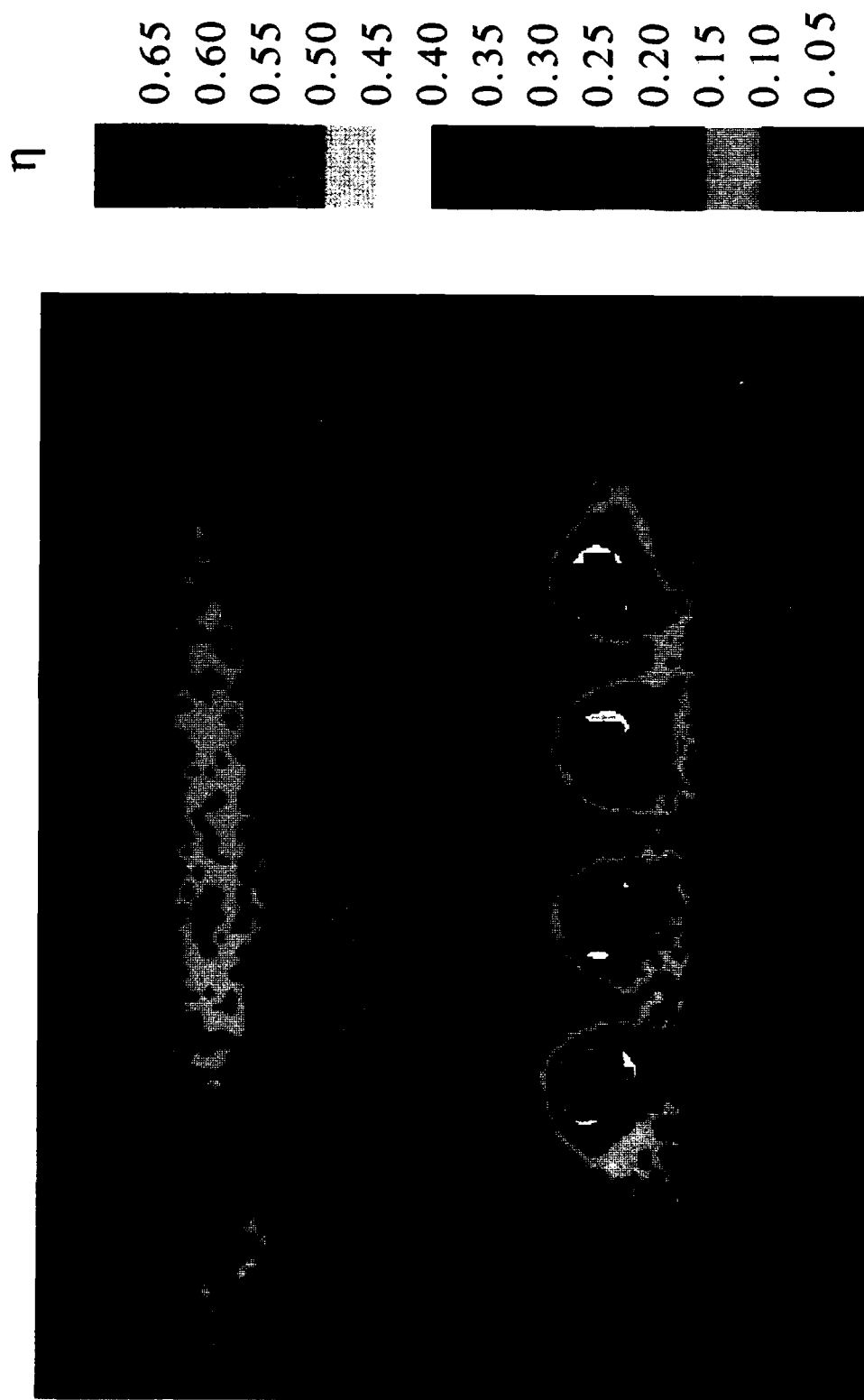


Fig. 90 1.0" cavity,  $5/16$ " clearance gap, pressure side injection,  
 $Re = 30,000$ ;  $M = 0.1$



Fig. 91 1.0" cavity,  $5/16$ " clearance gap, pressure side injection,  
Re = 30,000; M = 0.5

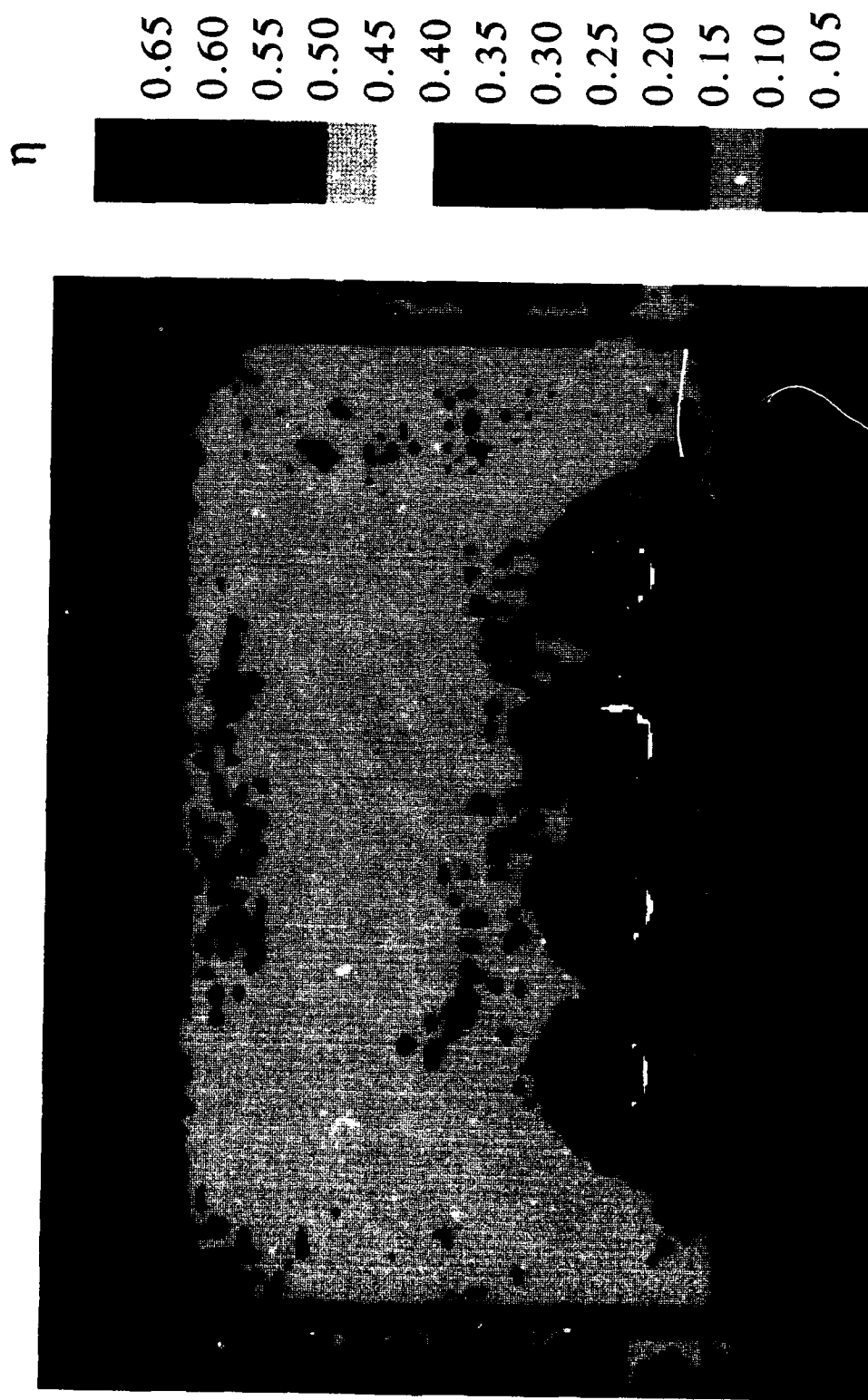


Fig. 92 1.0" cavity,  $5/16$ " clearance gap, pressure side injection,  
 $Re = 30,000$ ;  $M = 0.5$

## CHAPTER 4

### SUMMARY

#### 4.1 Conclusions from Results

The results indicate that the deeper the cavity the lower the overall heat transfer coefficient. The effectiveness is also higher with the deeper cavity, indicating that the film flow adheres to the deeper cavity surface better. This would give the impression that the deeper the cavity the more desirable the heat transfer conditions. The problem is that heat transfer was only calculated for the cavity floor. The cavity depth will also affect the heat transfer on the cavity walls, and warrants further investigation. The injection of film cooling from the pressure side resulted in a more uniform effectiveness, yet the overall average is lower than that for the suction side injection. Modification to the cavity floor might create a more uniform effectiveness with the suction side injection, giving better overall results. Finally, the higher the blowing ratio, the better the cooling. This is a logical conclusion, but engine designers are not at liberty to use as much bleed air from the compressor as they wish. A trade-off must be made between overall engine efficiency, which is dependent on the amount of air bled off of the compressor, and the need for film cooling flow. This study provides useful results on the effects that blade tip geometries and the addition of film cooling have on heat transfer and effectiveness coefficients.

#### 4.2 Recommendations for Future Study

The cavity model has been explored in this presentation. The use of injected film cooling proved to be a valuable addition. Present day designers also inject film cooling on the pressure side of the blade, outside of the clearance gap. Testing is presently being conducted on pressure side injection over a flat surface. A combination of pressure side injection with a cavity tip might also produce some worthwhile results. Under present conditions two similar tests are run, cold and hot. In the future it is hoped that a system can be developed to determine the time of two color changes. The current system uses the color change of green, this would be augmented with the color change of blue which occurs at a higher temperature. The use of TLC in the determination of surface heat transfer is limitless, a variety of surfaces and flow conditions are possible.



## REFERENCES

Dunn, M.G., Rae, W.J., and Holt J.L., 1984a, "Measurement and Analysis of Heat Flux Data in a Turbine Stage: Part I: Description of Experimental Apparatus and Data Analysis," *ASME Journal of Engineering for Gas Turbines and Power*, 106, 229-240.

Dunn, M.G., Rae, W.J., and Holt J.L., 1984b, "Measurement and Analysis of Heat Flux Data in a Turbine Stage: Part II: Discussion of Results and Comparison With Predictions," *ASME Journal of Engineering for Gas Turbines and Power*, 106, 229-240.

Eick, C., 1991, "Modeling and Measurement of Film Cooling Performance for Turbine Tip Shrouds," Masters Thesis, Arizona State University, Tempe Arizona.

Epstein, A.H., Guenette, G.R., Norton, R.J.G., and Yuzhang, C., 1985, "Time Resolved Measurements of a Turbine Rotor Stationary Tip Casing Pressure and Heat Transfer Field," AIAA Paper No. 85-1220.

Hennecke, D.K., 1984, "Heat Transfer Problems in Aero-Engines," *Heat and Mass Transfer in Rotating Machinery*, Hemisphere Publishing Company, Washington DC, pp 353-379.

Ireland, P.T. and Jones, T.V., 1987, "The Response Time of a Surface Thermometer Employing Encapsulated Thermochromic Liquid Crystals," *Journal of Physics E*, 20, pp.1195-1199.

Kim, Y.W., Yu Y., and Metzger, D.E., "Liquid Crystal Image Analysis System Development - Final Report," Technical Report No. ERC-R-91053, Arizona State University, 1991.

Kline, S.J., McKlintock, F.A., 1953, "Describing Uncertainty in Single Sample Experiments," *Mechanical Engineering*, Vol 75, pp 3-8

Mayle, R.E., and Metzger, D.E., 1982, "Heat Transfer at the Tip of an Unshrouded Turbine Blade", *Proceedings, Seventh International Heat Transfer Conference*, 3, pp.87-92.

Metzger, D.E., Dunn, M.G., and Hah, C., 1990, "Turbine Blade Tip and Shroud Heat Transfer," 1990 Int. Gas Turbine and Aeroengine Congress, and to appear, ASME Journal of Turbomachinery.

Metzger, D.E. and Larson, D.E., 1986, "Use of Fusion Point Surface Coatings for Local Convection Heat Transfer Measurements in Rectangular Channel Flows with 90-Degree Turns," *ASME Journal of Heat Transfer*, 108, pp. 48-54.

Metzger, D.E., and Rued, K., 1989, "The Influence of Turbine Clearance Gap Leakage on Flowpath Velocities and Heat Transfer, Part I: Sink Flow Effects on Blade Pressure Sides," *ASME Journal of Turbomachinery*, 111, 284-292

Vedula, R.P., 1989, "Film Cooling Effectiveness and Heat Transfer Measurements Using Thermochromic Liquid Crystals," Ph.D. Dissertation, Arizona State University, Tempe Arizona.

Vedula, R.P. and Metzger, D.E., 1989, "Measurements of Local Film Cooling Performance With Flow over Forward and Backward Facing Steps," AIAA Paper 89-1688.

**APPENDIX A**  
**DATA REDUCTION THEORY**

The test procedures and data reduction theory used in this investigation are essentially identical to those described in Metzger and Larson, 1986 and Metzger and Vedula, 1989, and only a brief overview is presented here. In the technique used, detailed local convection coefficients over the test region of interest are deduced from measurements of local transient surface temperature responses to the driving convective heating load based on well established one-dimensional conduction theory.

The fundamental heat transfer equation is:

$$k \frac{\partial^2 T}{\partial x^2} = \alpha \frac{\partial T}{\partial \theta}$$

with the following boundary conditions:

$$-k \left. \frac{\partial T}{\partial x} \right|_{x=0} = h[T - T_f]_{x=0}$$

$$T_{x=\infty} = T_i$$

With the initial condition:

$$T_{t=0} = T_i$$

The wall temperature response for one-dimensional heat conduction in a semi-infinite solid object to a step change in ambient fluid temperature is described by the following classical solution.

$$(T_s - T_i)/(T_r - T_i) = 1 - \exp(h^2 \alpha \theta / k^2) \cdot \operatorname{erfc}(h \sqrt{\alpha \theta} / k) \quad (1)$$

If material properties are known, the heat transfer coefficient  $h$  can be inversely obtained from Eq. 1 with measurements of transient surface temperature response and fluid temperature  $T_m$ . For a simplified flow situation, the driving fluid temperature  $T_m$  may be considered as the local mixed mean temperature. However, in less restricted cases,  $T_m$  can be substituted by a more readily measurable reference temperature  $T_r$  and  $h$  can be redefined accordingly.

In actual experiments, a true step change in fluid temperature is nearly impossible to achieve and generally the reference temperature will be a function of time. In this case the solution given by Eq. 1 is still valid as a fundamental solution but is used for a series of step changes in  $T_r(q)$  using Duhamel's superposition theorem, ie:

$$T - T_i = \sum_{i=1}^N U(\theta - \tau_i) \Delta T_r \quad (2)$$

where:

$$U(\theta - \tau_i) = 1 - \exp\left[\frac{h^2 \alpha (\theta - \tau_i)}{k^2}\right] \operatorname{erfc}\left[\frac{h \sqrt{\alpha (\theta - \tau_i)}}{k}\right] \quad (3)$$

For the acrylic plastic(Plexiglas) test surface material used, the depth of heating into the surface over the time duration needed to complete the test is less than the surface thickness. In addition, departure from one-dimensionality because of finite lateral conduction in the surface is not expected to have a significant effect on the local surface temperature response for the surface heat transfer gradients anticipated, as shown by Vedula et al, 1989 and Metzger and Larson, 1986.

To minimize experimental uncertainties, the temperature of the supplied flow is chosen so that the color threshold is not reached until sufficient time has elapsed after the start of flow (usually 10 seconds or more) to insure that the elapsed time can be determined accurately. Also, the flow temperature is chosen so that the elapsed time and corresponding penetration of the temperature pulse into the surface are small enough (usually less than 60 seconds) to insure that the test surface can be treated as semi-infinite as assumed in

the data reduction. All of the results presented were obtained with threshold times satisfying these constraints, and the uncertainty in the measured convection coefficients is estimated to be  $\pm 10$  percent by Vedula, 1989; by the methods of Kline and McKlintock, 1953.

**APPENDIX B**  
**SPANWISE VARIATION DATA**



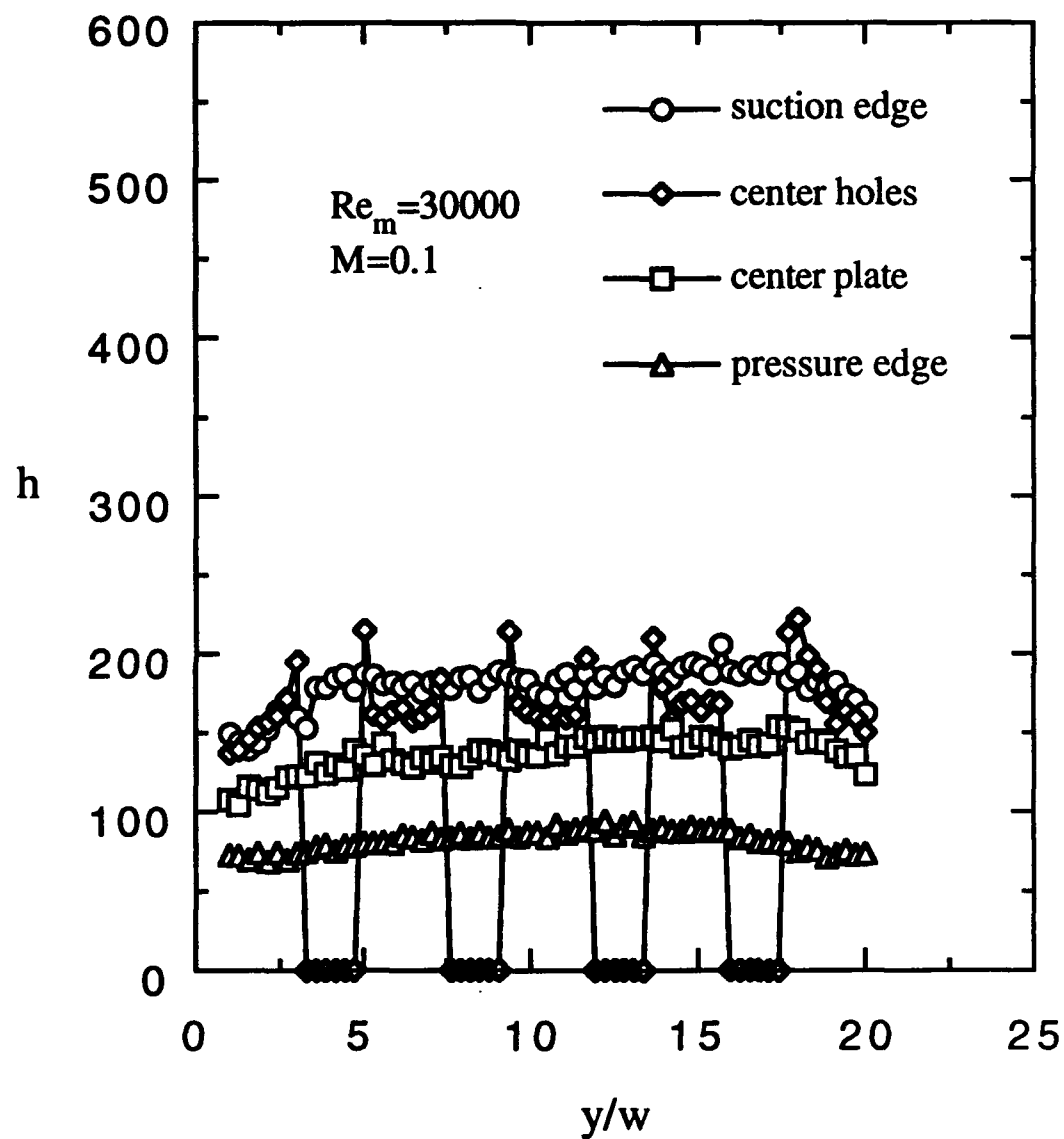


Fig. 93 Heat transfer coeff., spanwise variation, suction side injection,  $3/8$ " cavity,  $3/16$ " clearance gap

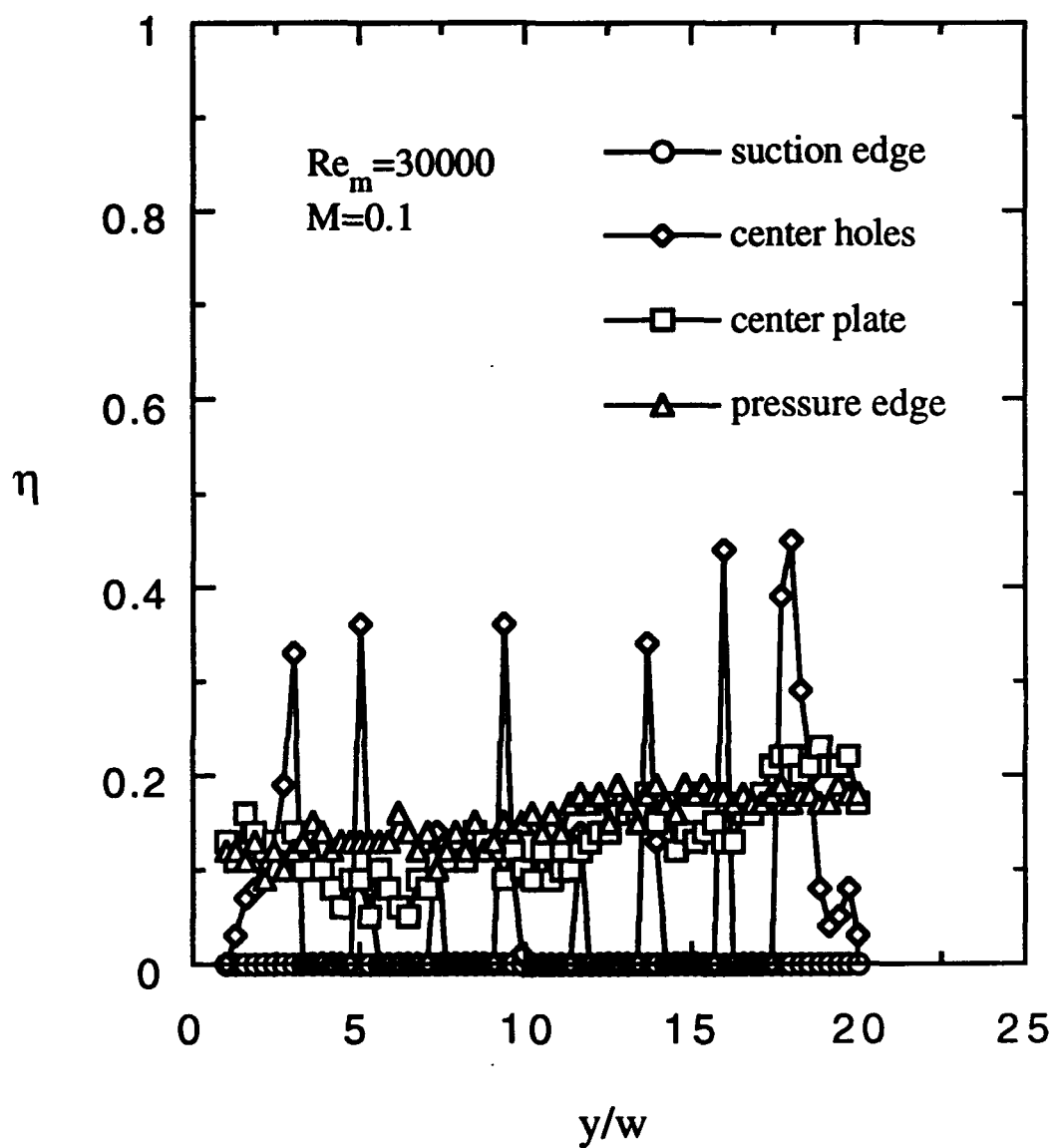


Fig. 94 Effectiveness, spanwise variation, suction side injection,  $3/8$ " cavity,  $3/16$ " clearance gap

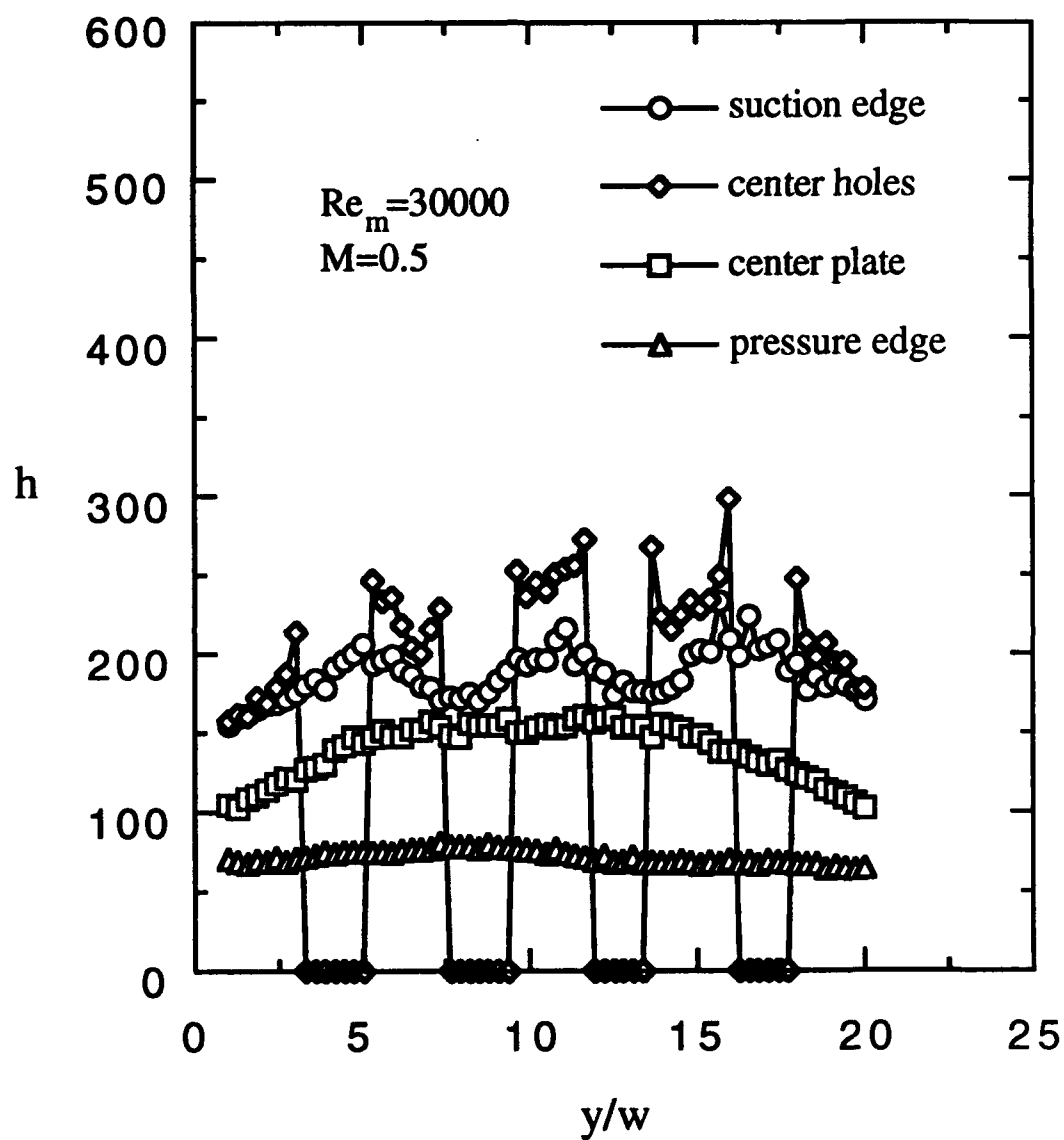


Fig. 95 Heat transfer coeff., spanwise variation, suction side injection,  $3/8$ " cavity,  $3/16$ " clearance gap, #1

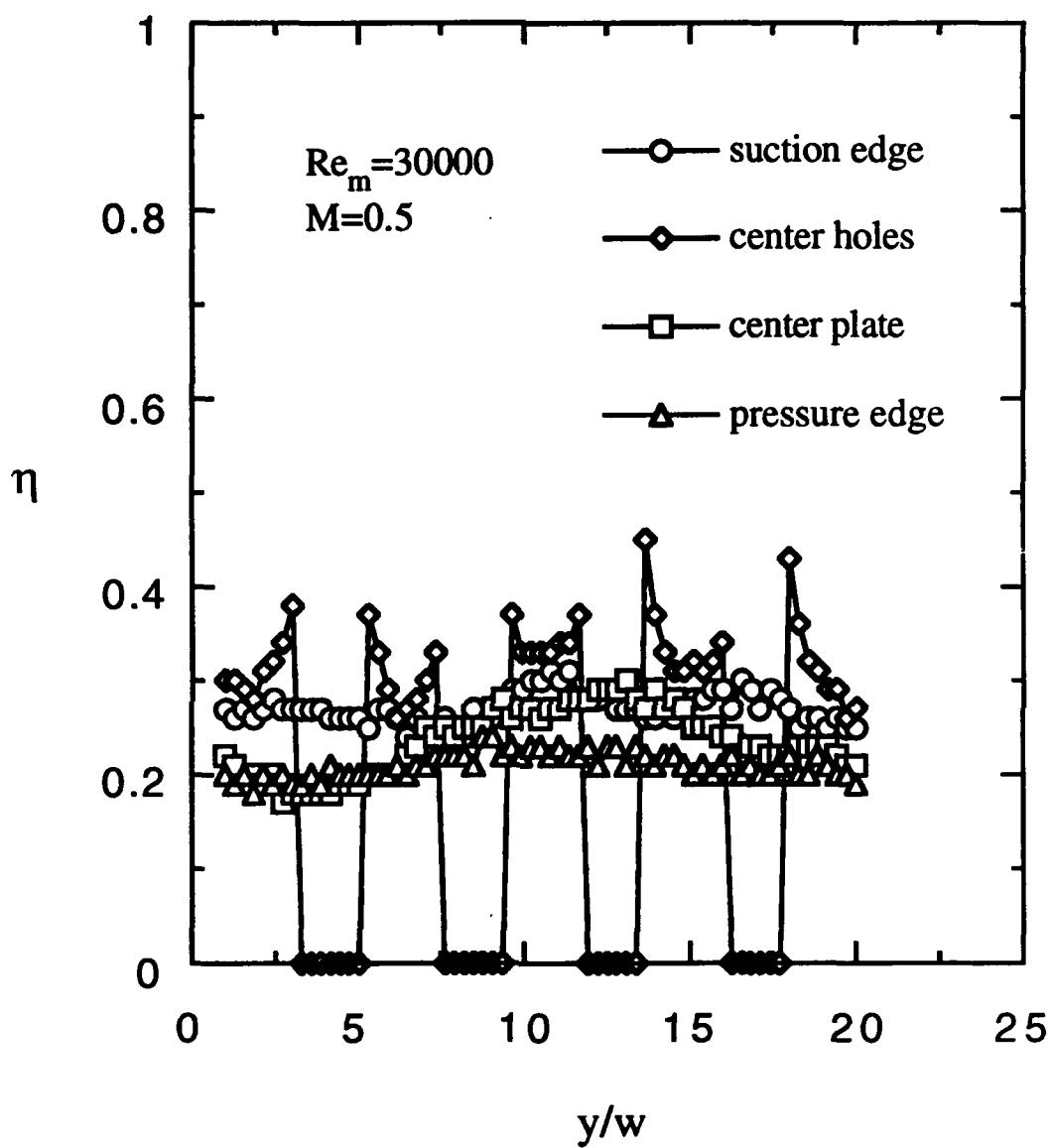


Fig. 96 Effectiveness, spanwise variation, suction side injection,  $3/8$ " cavity,  $3/16$ " clearance gap, #1

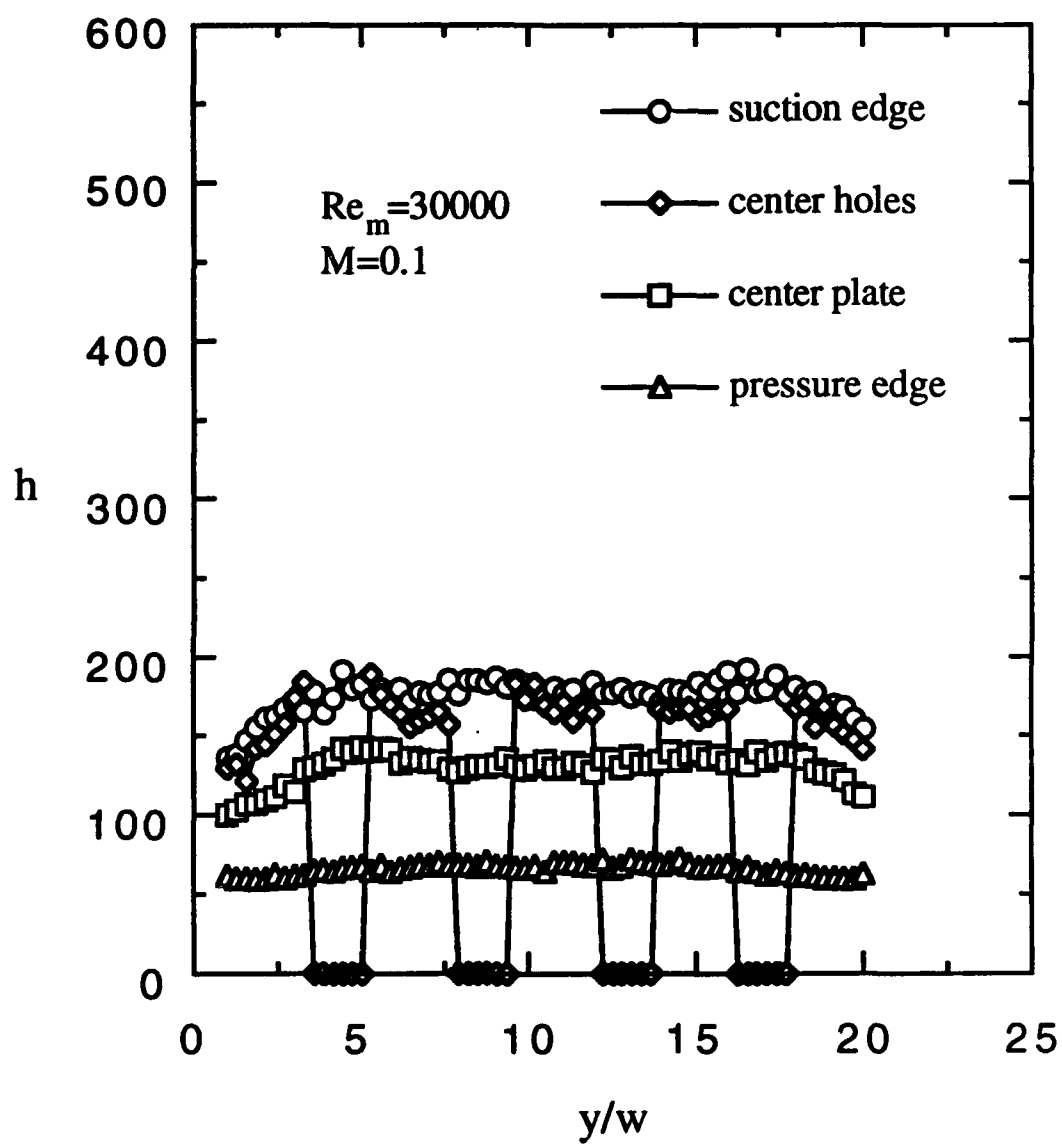


Fig. 97 Heat transfer coeff., spanwise variation, suction side injection,  $3/8$ " cavity,  $5/16$ " clearance gap, #1

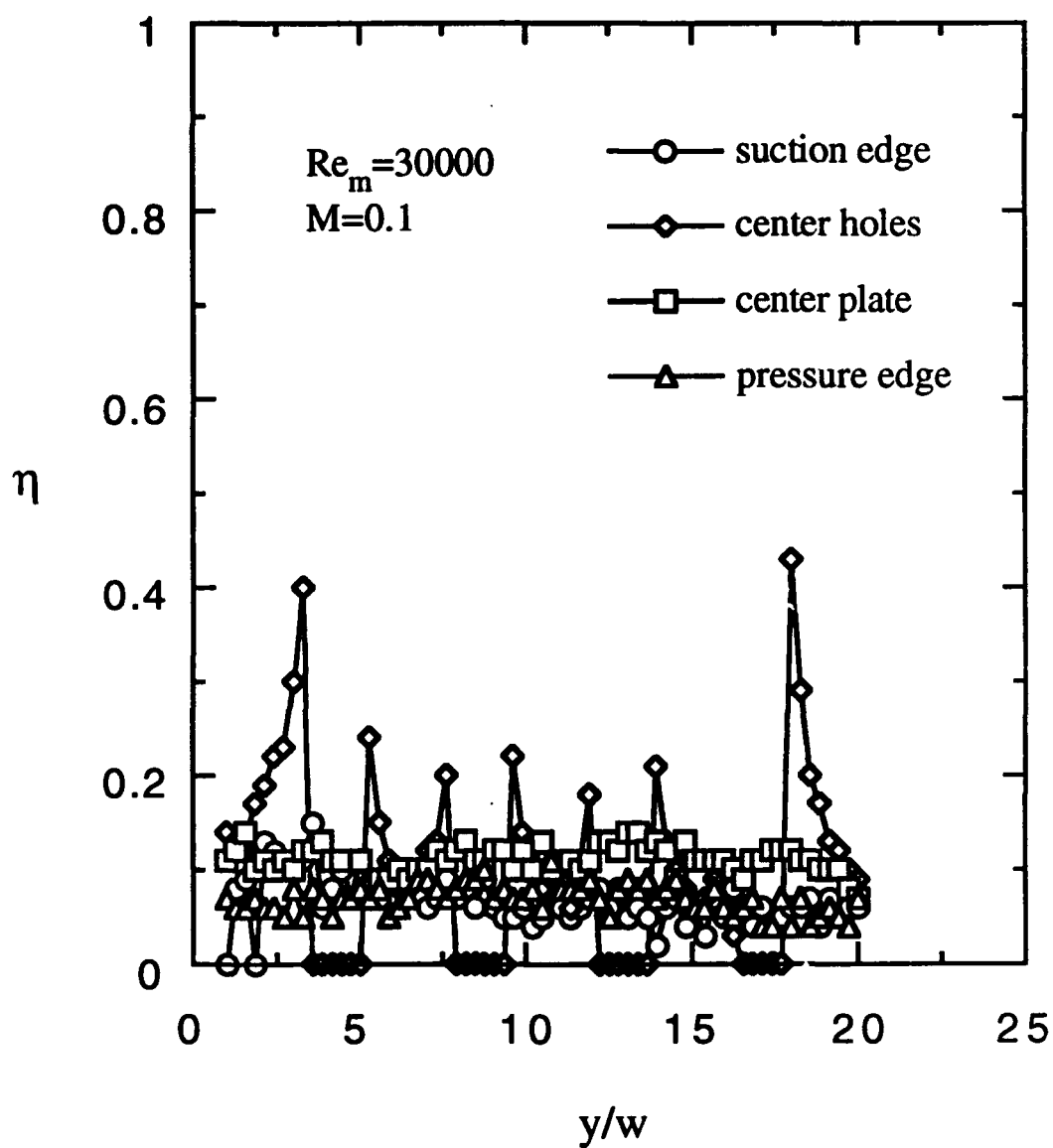


Fig. 98 Effectiveness, spanwise variation, suction side injection,  $3/8$ " cavity,  $5/16$ " clearance gap, #1

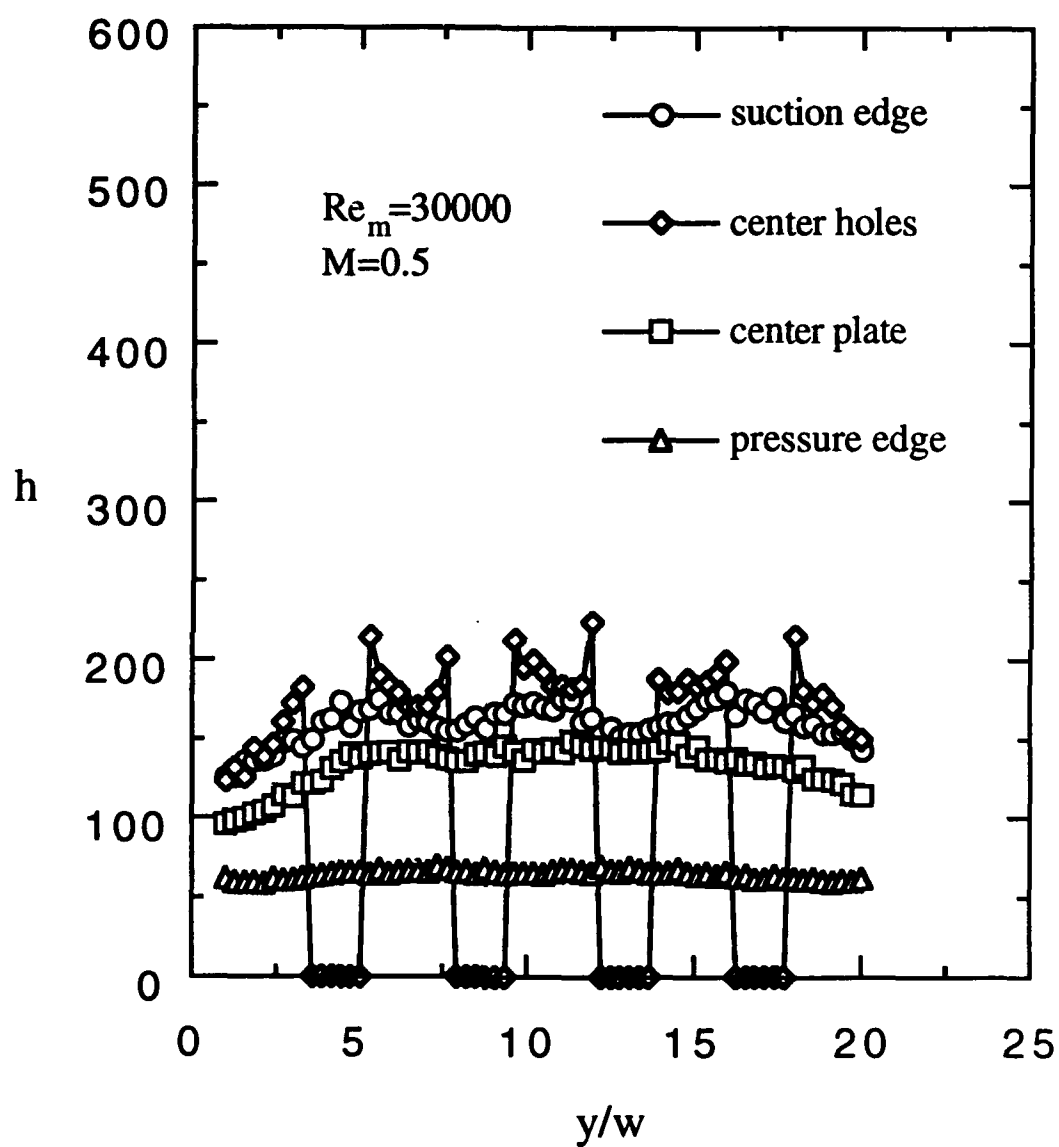


Fig. 99 Heat transfer coeff., spanwise variation, suction side injection,  $3/8$ " cavity,  $5/16$ " clearance gap

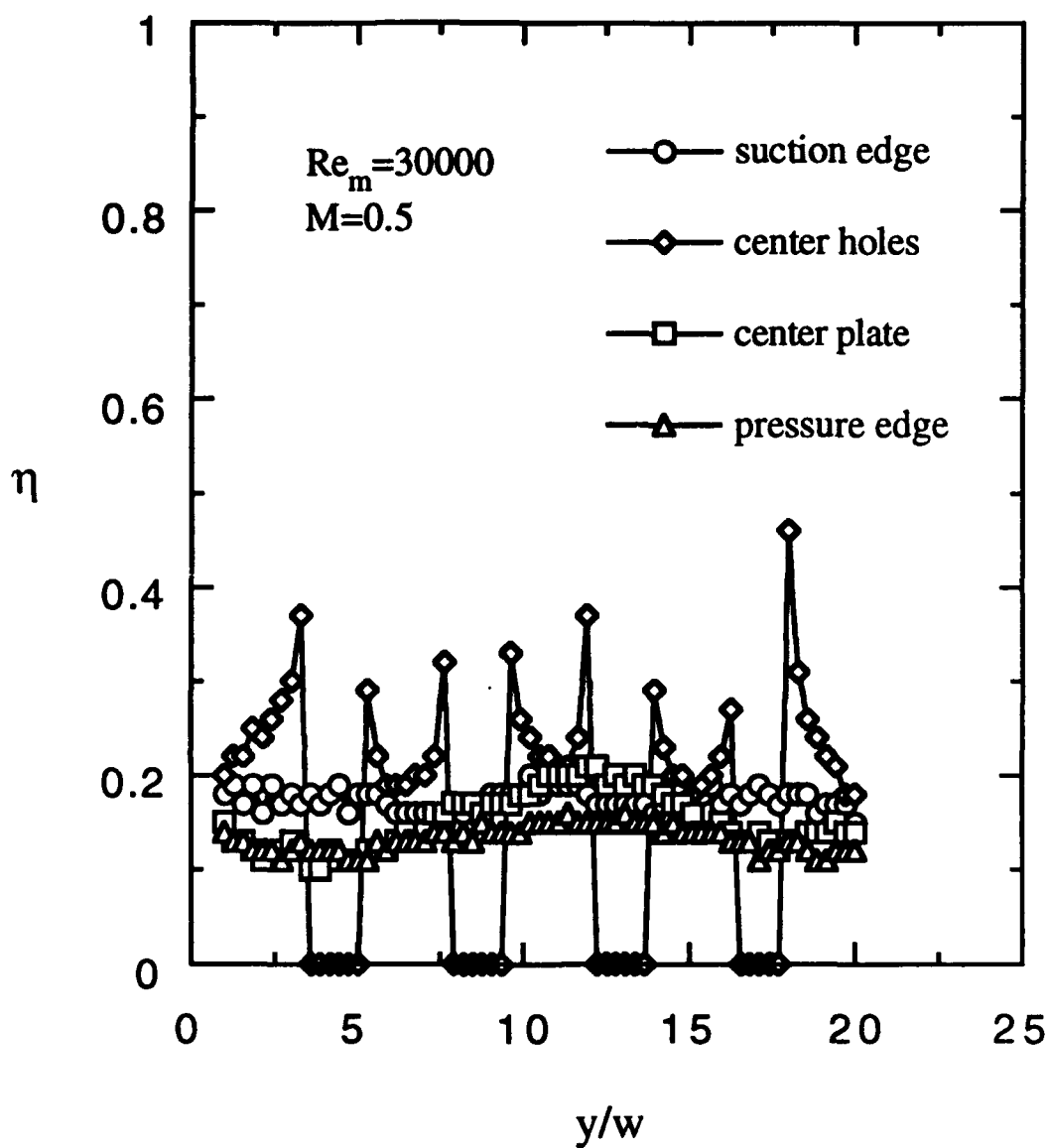


Fig. 100 Effectiveness; spanwise variation, suction side injection,  $3/8$ " cavity,  $5/16$ " clearance gap



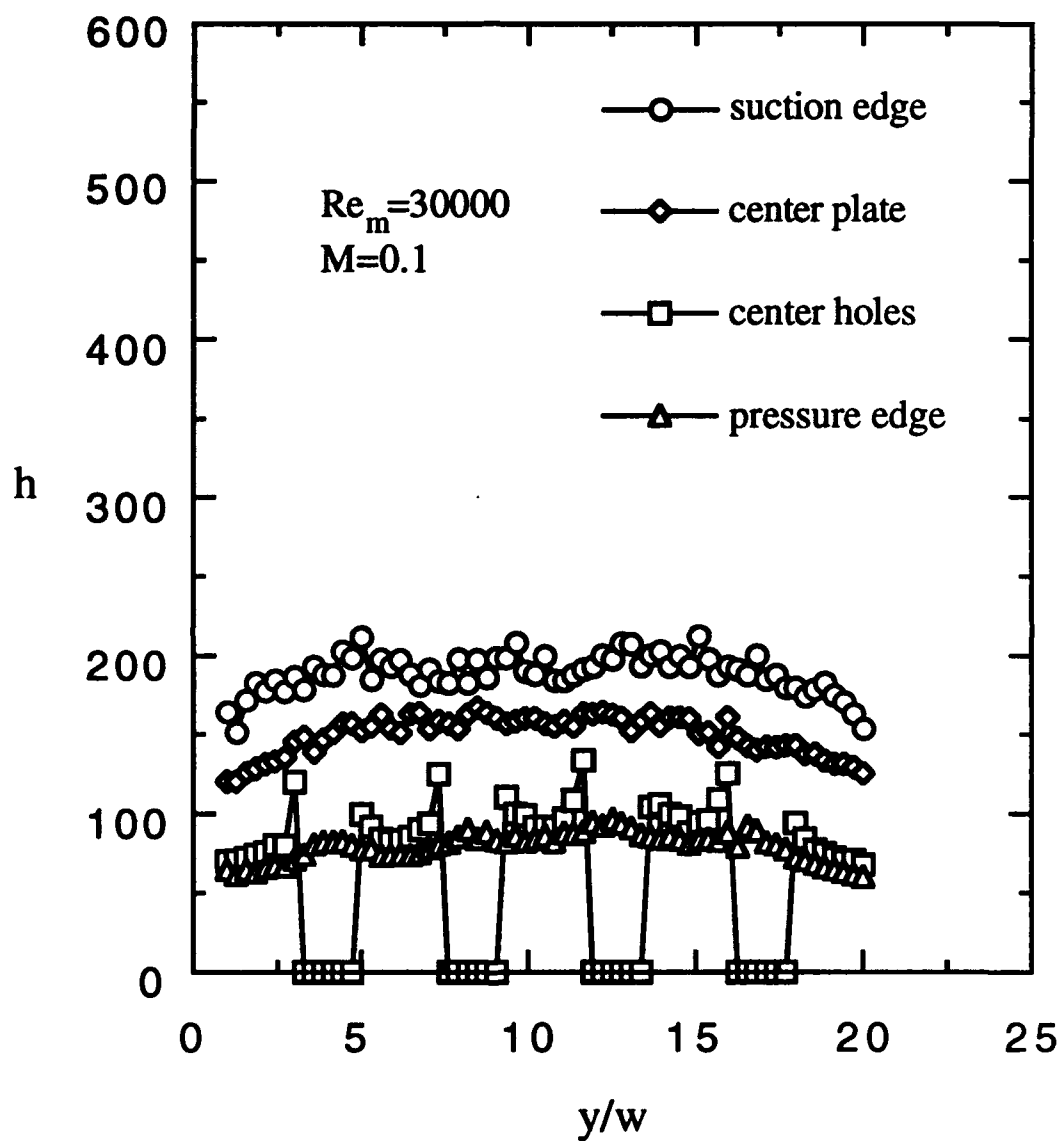


Fig. 101 Heat transfer coeff., spanwise variation, pressure side injection,  $3/8$ " cavity,  $3/16$ " clearance gap, #1

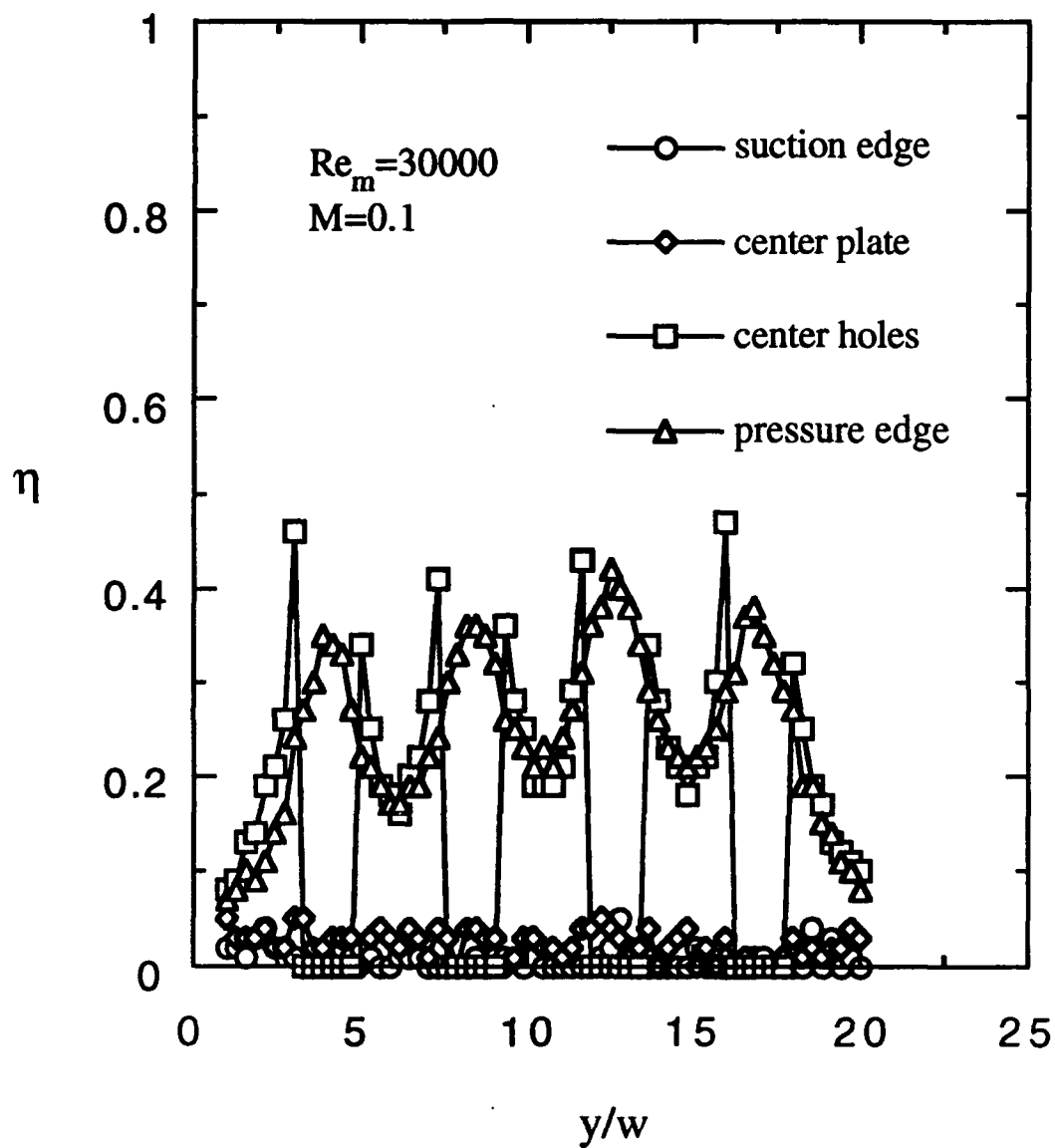


Fig. 102 Effectiveness, spanwise variation, pressure side injection,  $3/8$ " cavity,  $3/16$ " clearance gap, #1

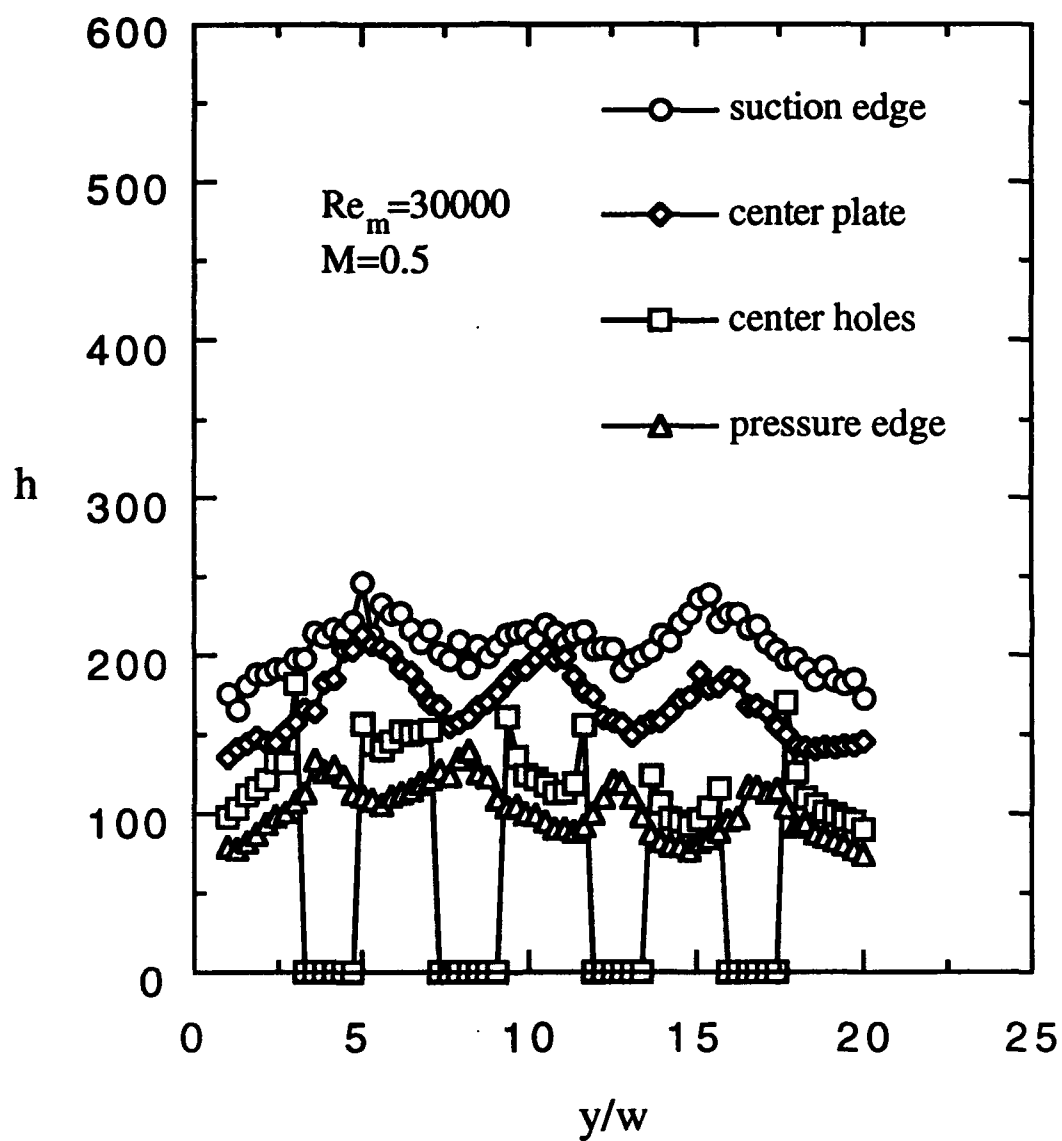


Fig. 103 Heat transfer coeff., spanwise variation, pressure side injection,  $3/8$ " cavity,  $3/16$ " clearance gap

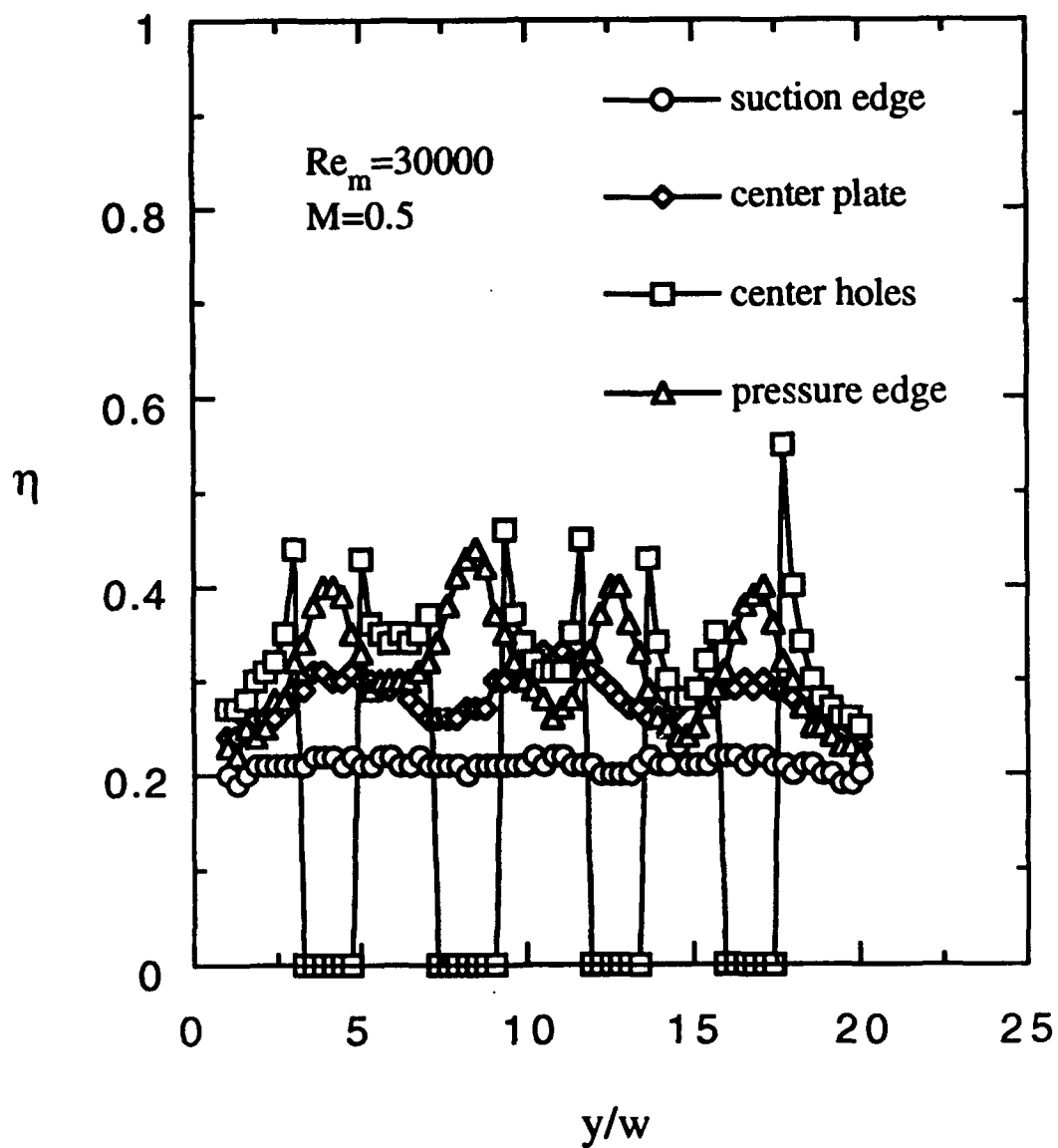


Fig. 104 Effectiveness, spanwise variation, pressure side injection,  $3/8$ " cavity,  $3/16$ " clearance gap, #1

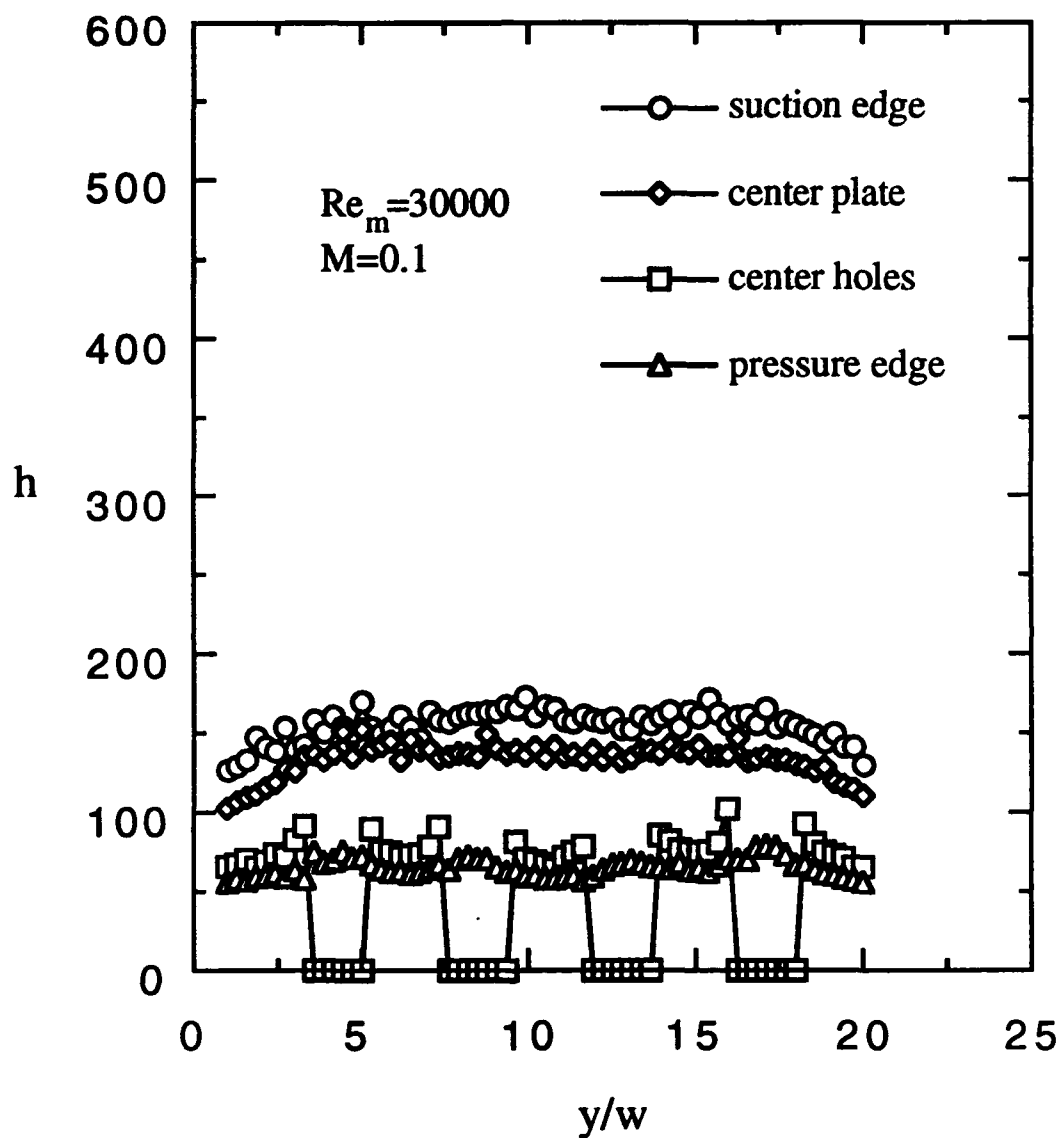


Fig. 105 Heat transfer coeff., spanwise variation, pressure side injection,  $3/8$ " cavity,  $5/16$ " clearance gap

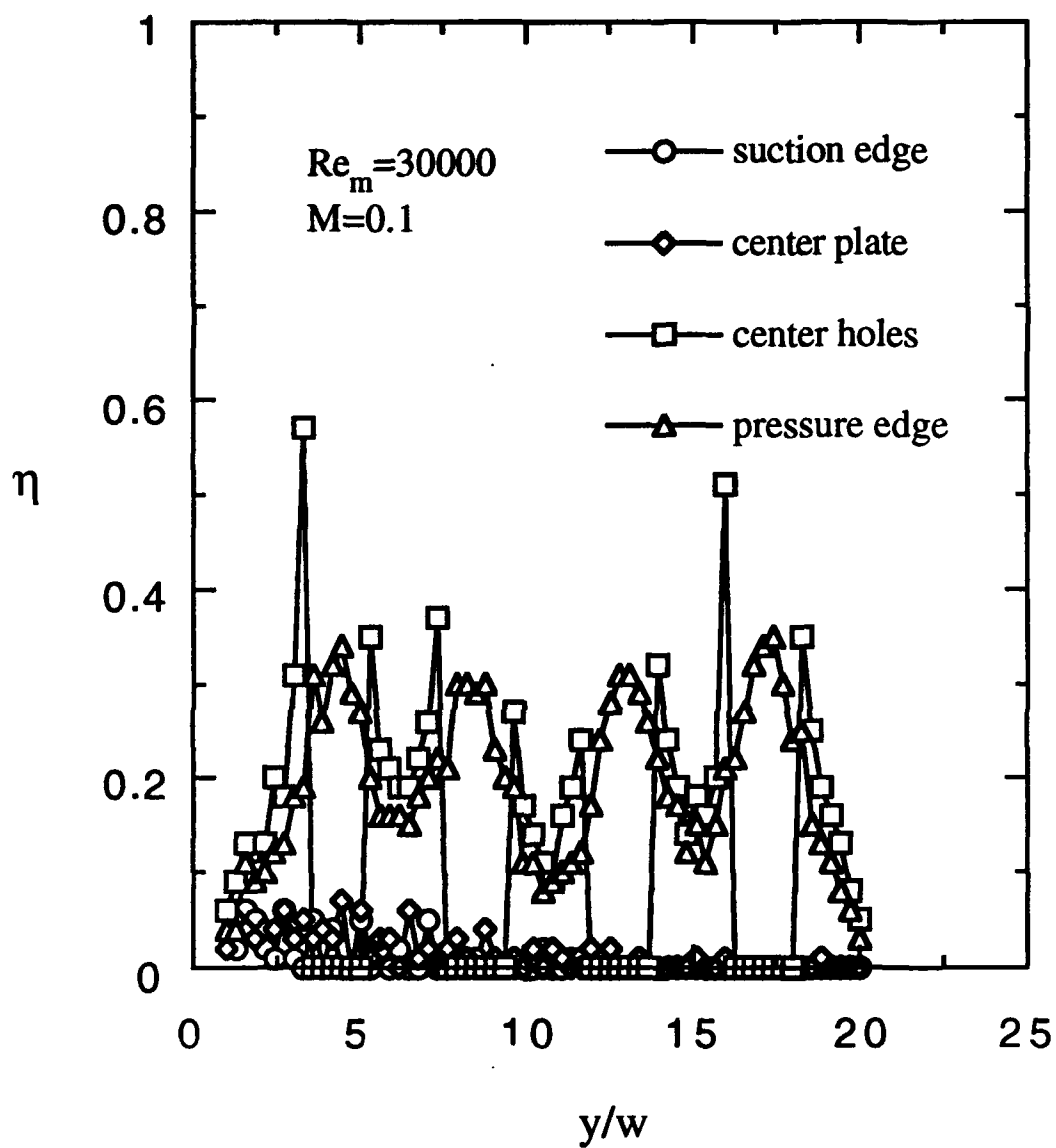


Fig. 106 Effectiveness, spanwise variation, pressure side injection,  $3/8$ " cavity,  $5/16$ " clearance gap

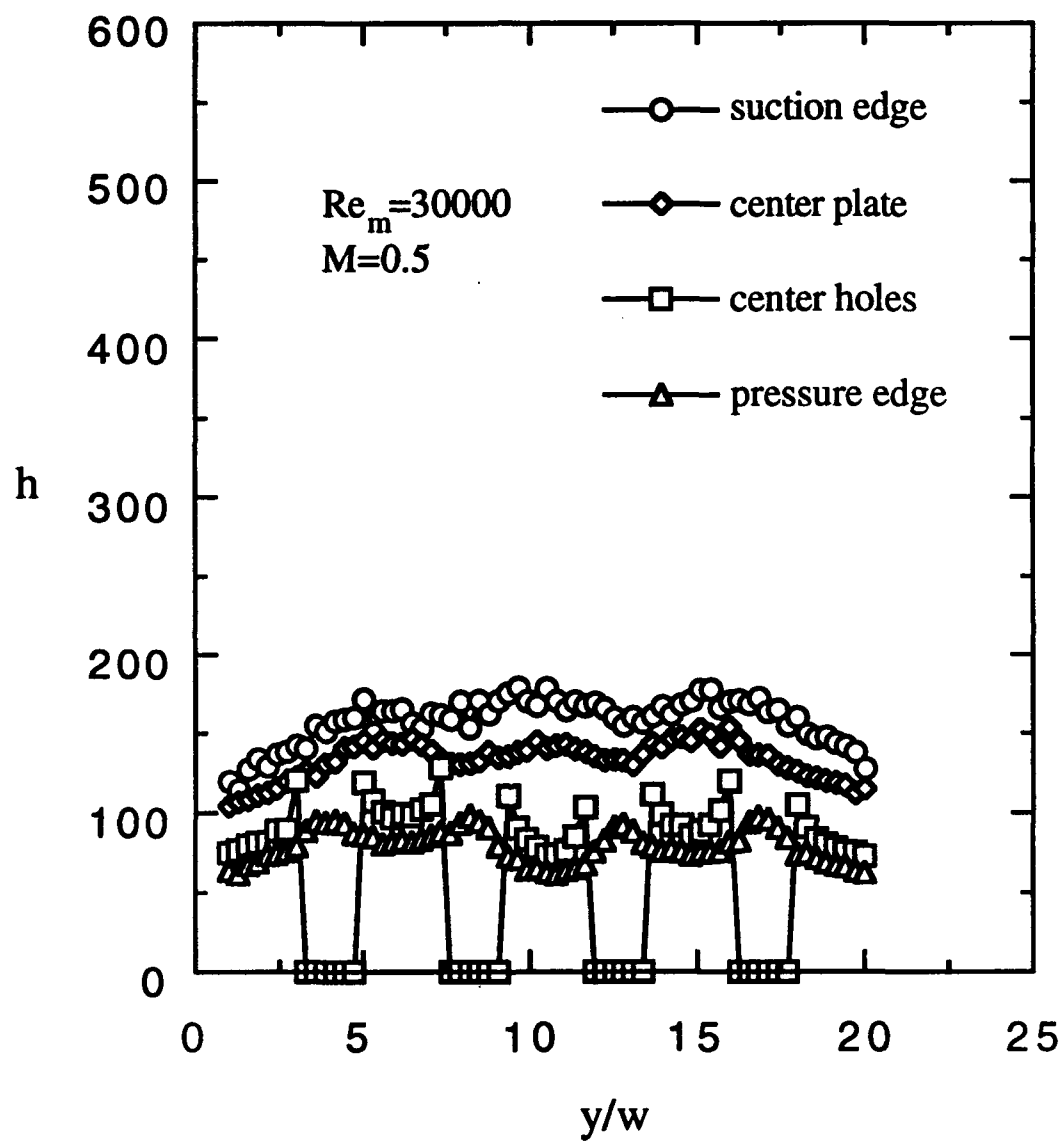


Fig. 107 Heat transfer coeff., spanwise variation, pressure side injection,  $3/8$ " cavity,  $5/16$ " clearance gap, #2

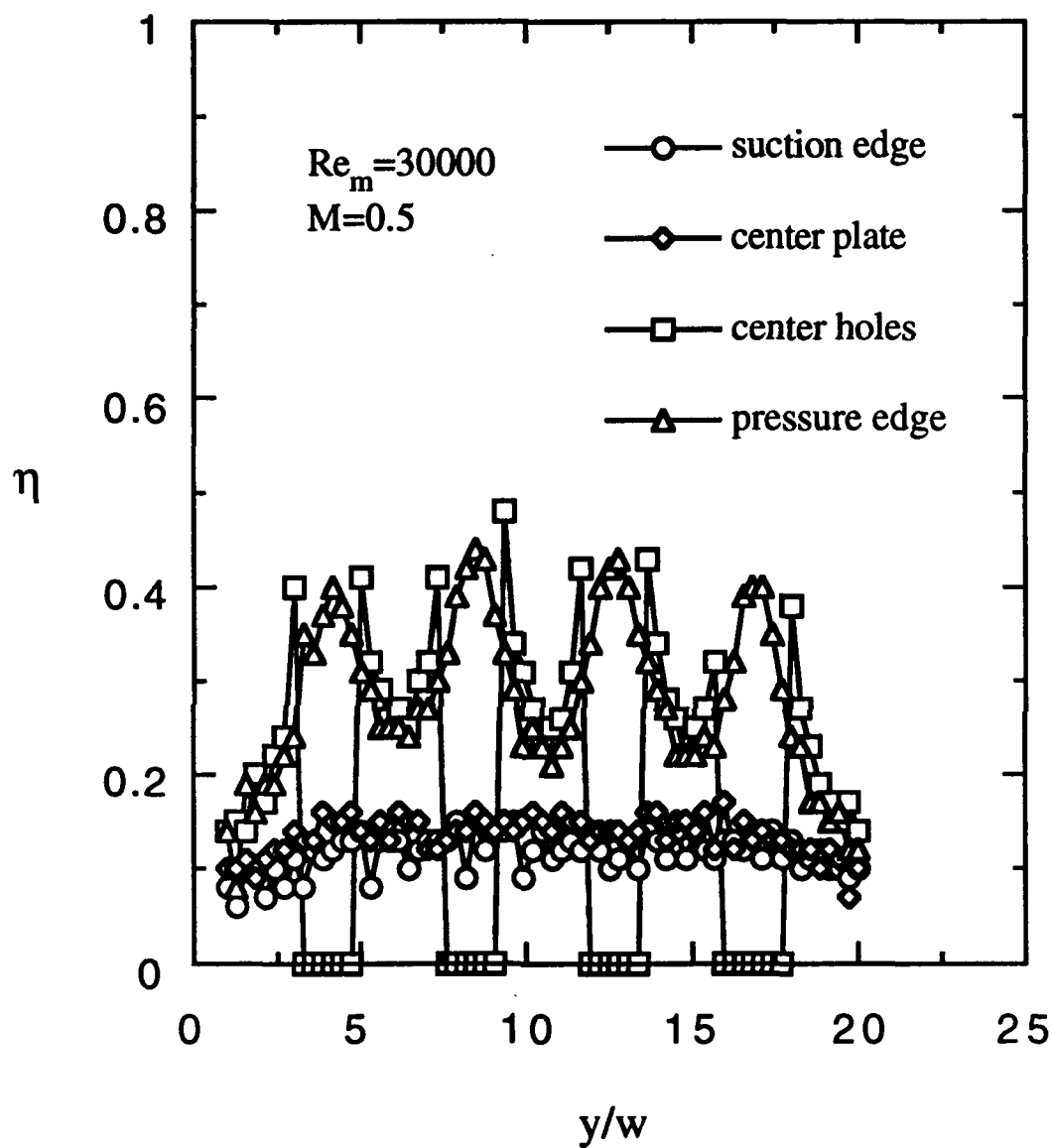


Fig. 108 Effectiveness, spanwise variation, pressure side injection,  $3/8$ " cavity,  $5/16$ " clearance gap, #2



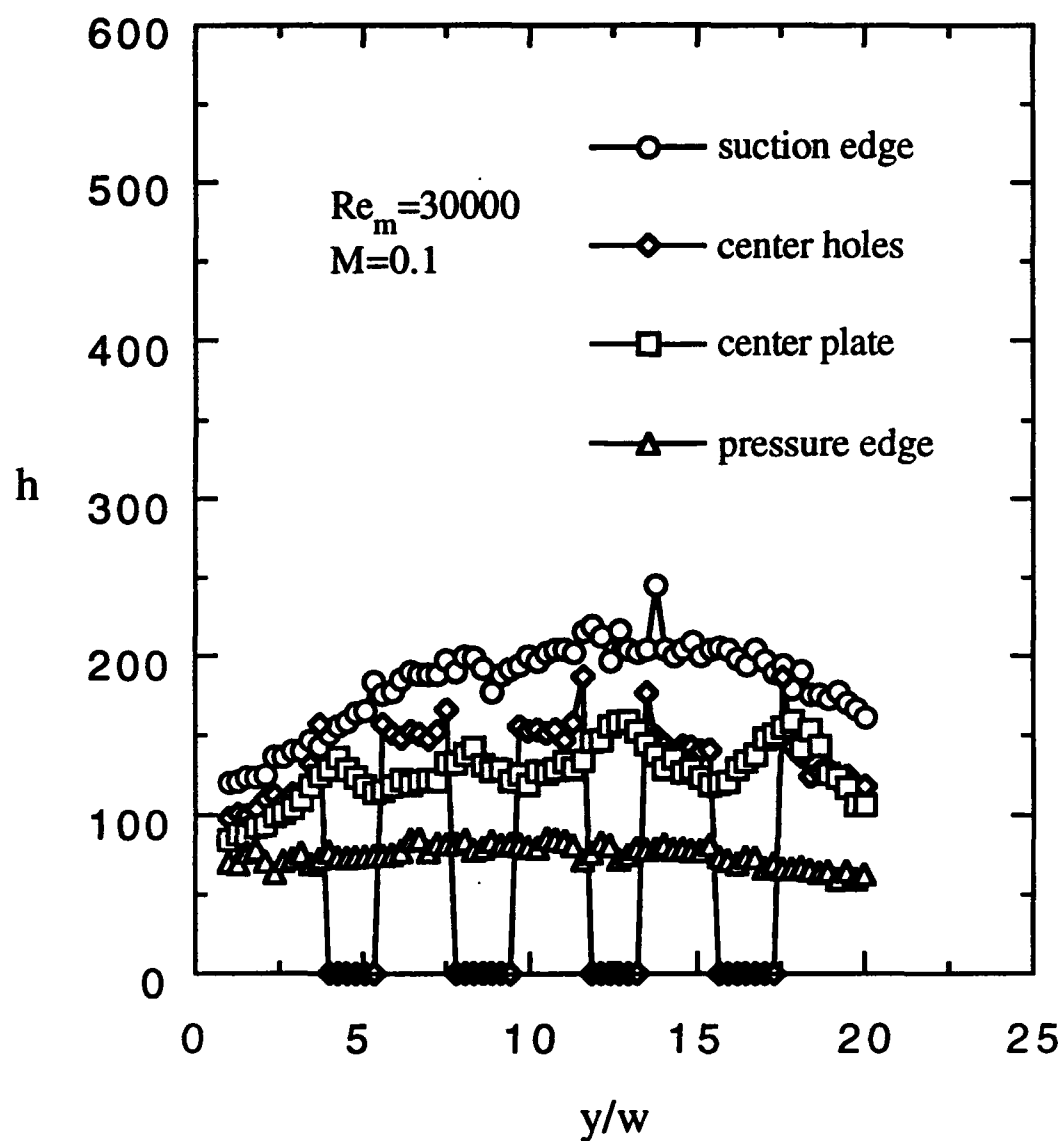


Fig. 109 Heat transfer coeff., spanwise variation, suction side injection, 1.0" cavity,  $3/16$ " clearance gap, #1

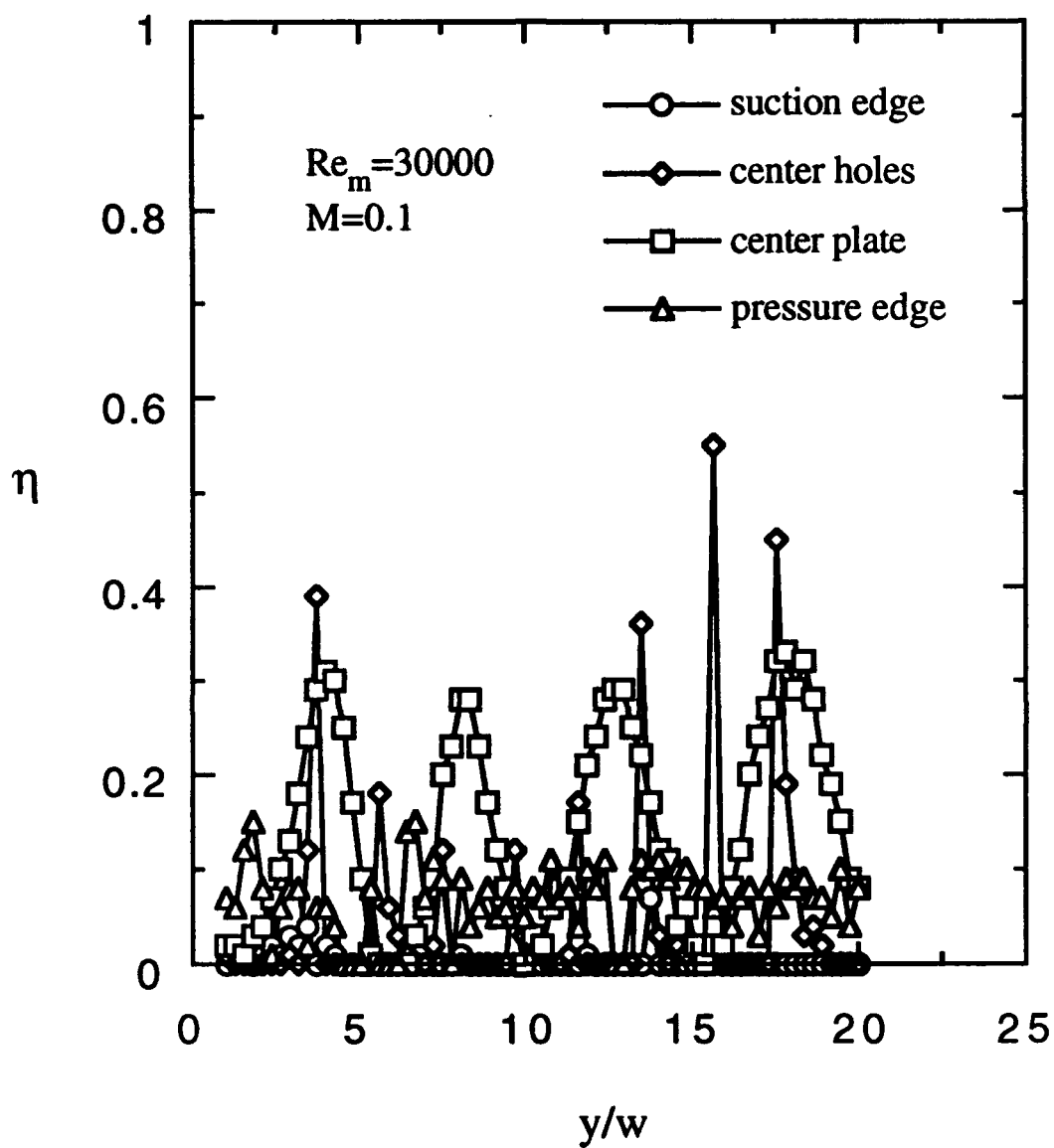


Fig. 110 Effectiveness, spanwise variation, suction side injection, 1.0" cavity,  $\frac{3}{16}$ " clearance gap, #1

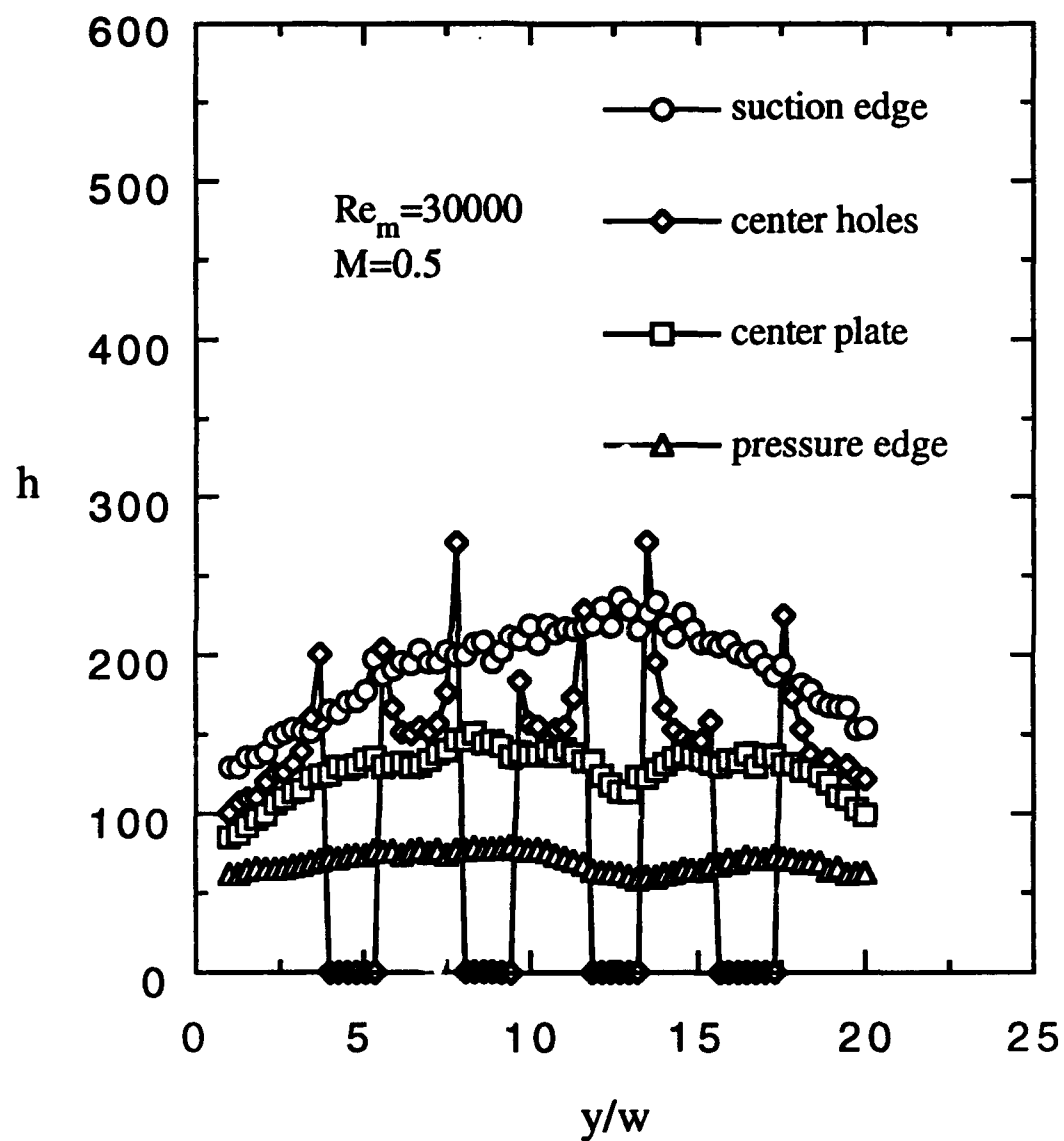


Fig. 111 Heat transfer coeff., spanwise variation, suction side injection, 1.0" cavity,  $3/16$ " clearance gap

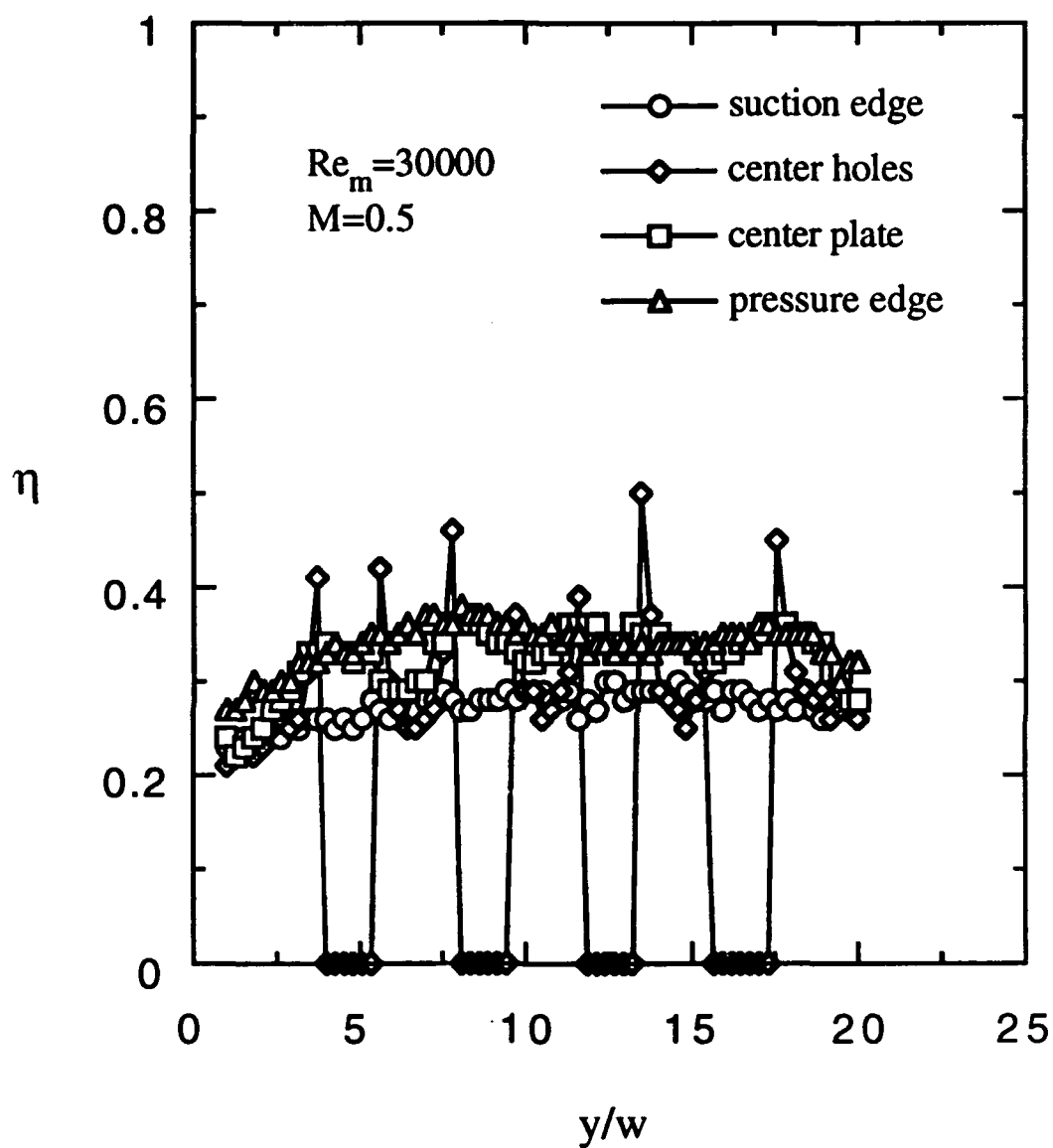


Fig. 112 Effectiveness, spanwise variation, suction side injection, 1.0" cavity,  $3/16$ " clearance gap

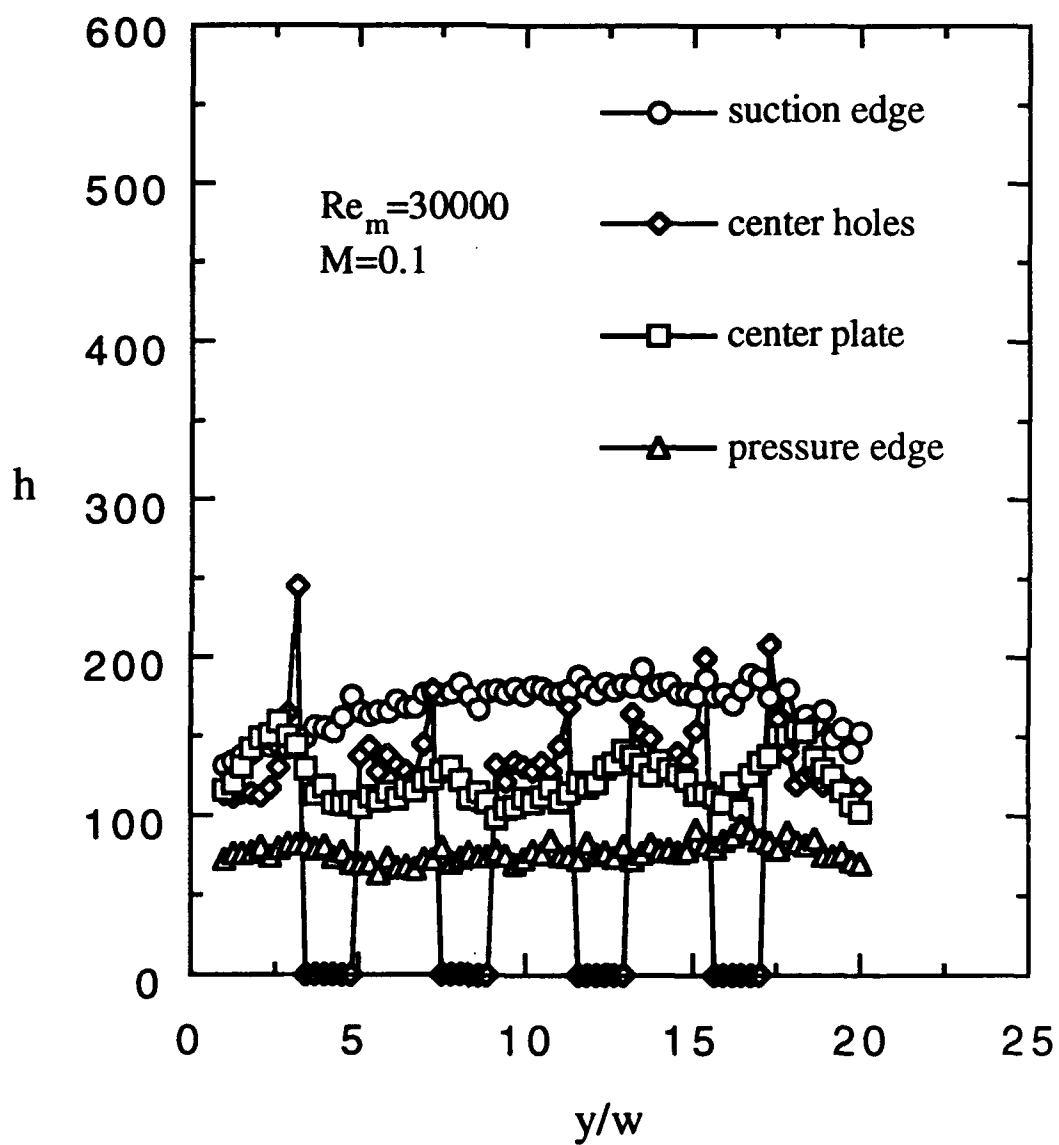


Fig. 113 Heat transfer coeff., spanwise variation, suction side injection, 1.0" cavity,  $5/16$ " clearance gap

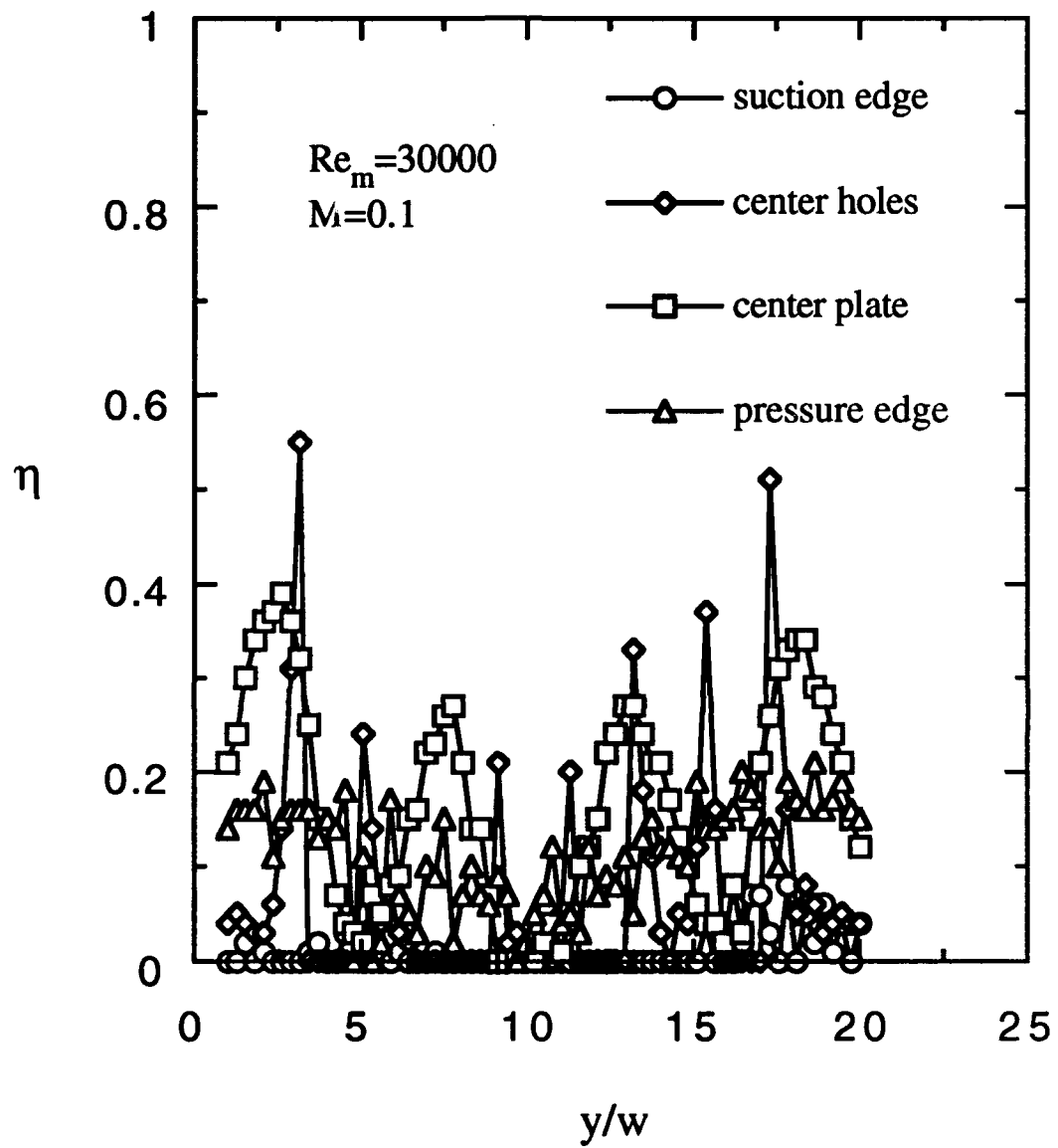


Fig. 114 Effectiveness, spanwise variation, suction side injection, 1.0" cavity,  $5/16$ " clearance gap

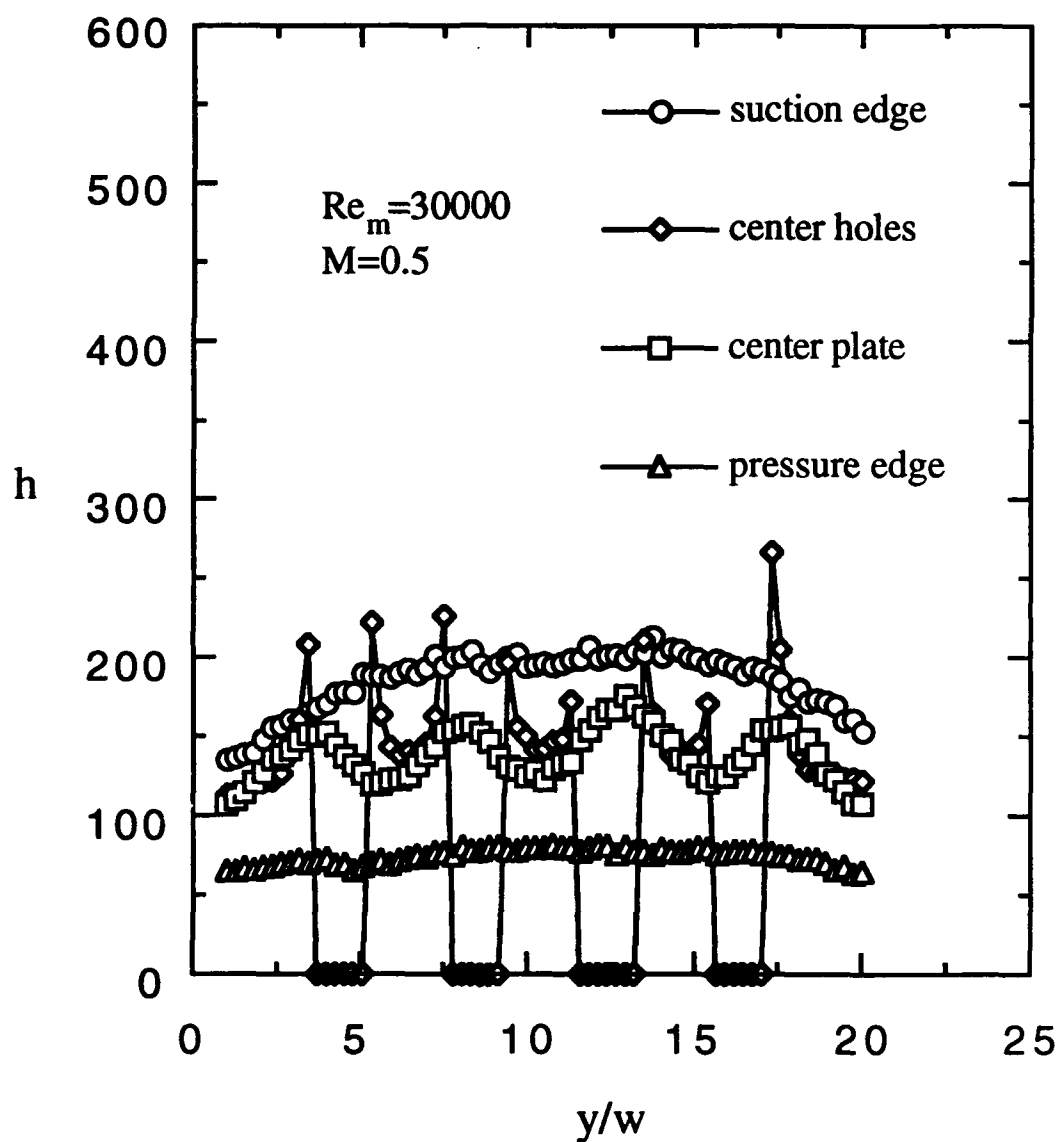


Fig. 115 Heat transfer coeff., spanwise variation, suction side injection, 1.0" cavity,  $5/16$ " clearance gap, #1

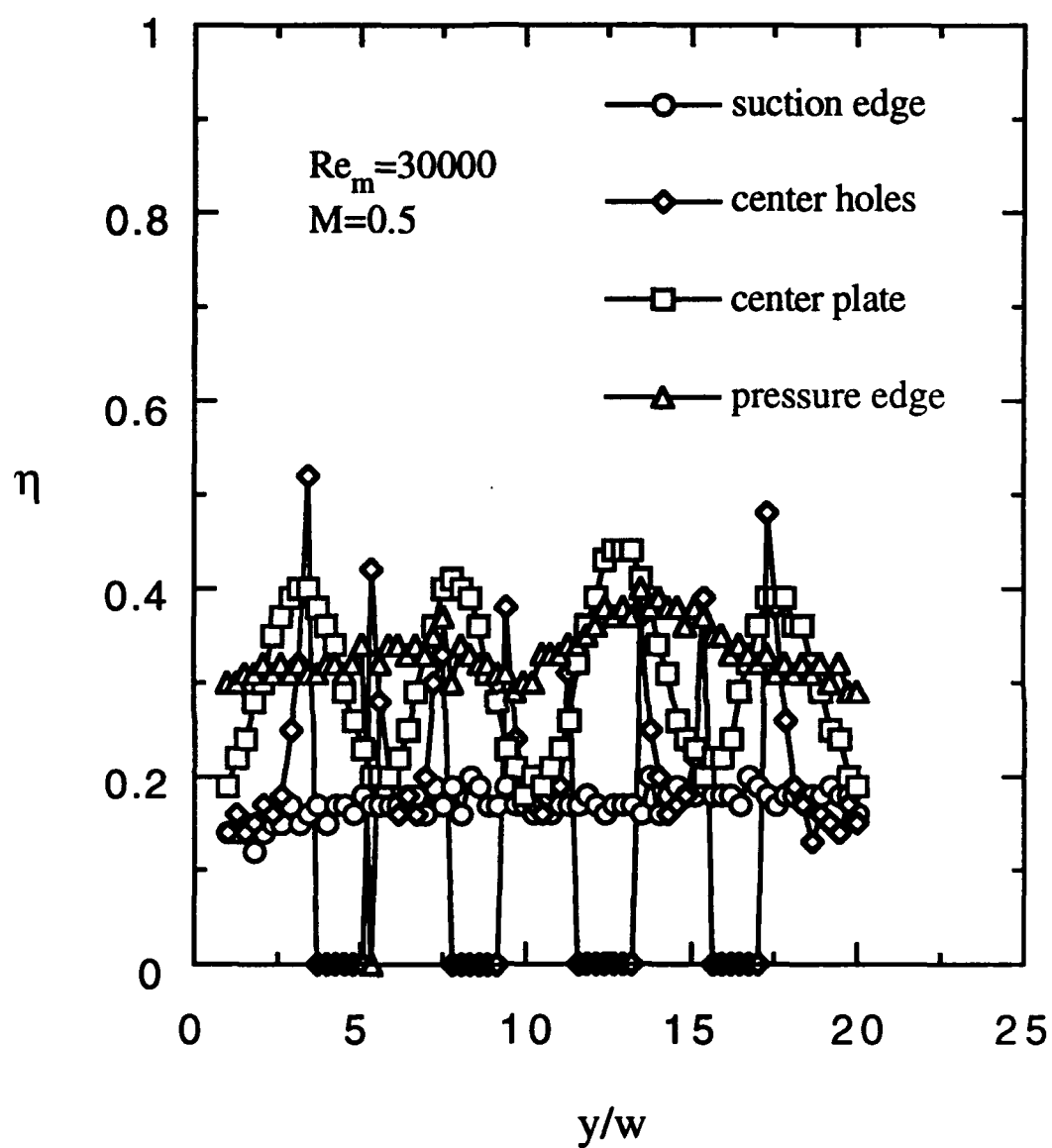


Fig. 116 Effectiveness, spanwise variation, suction side injection, 1.0" cavity,  $5/16$ " clearance gap, #1



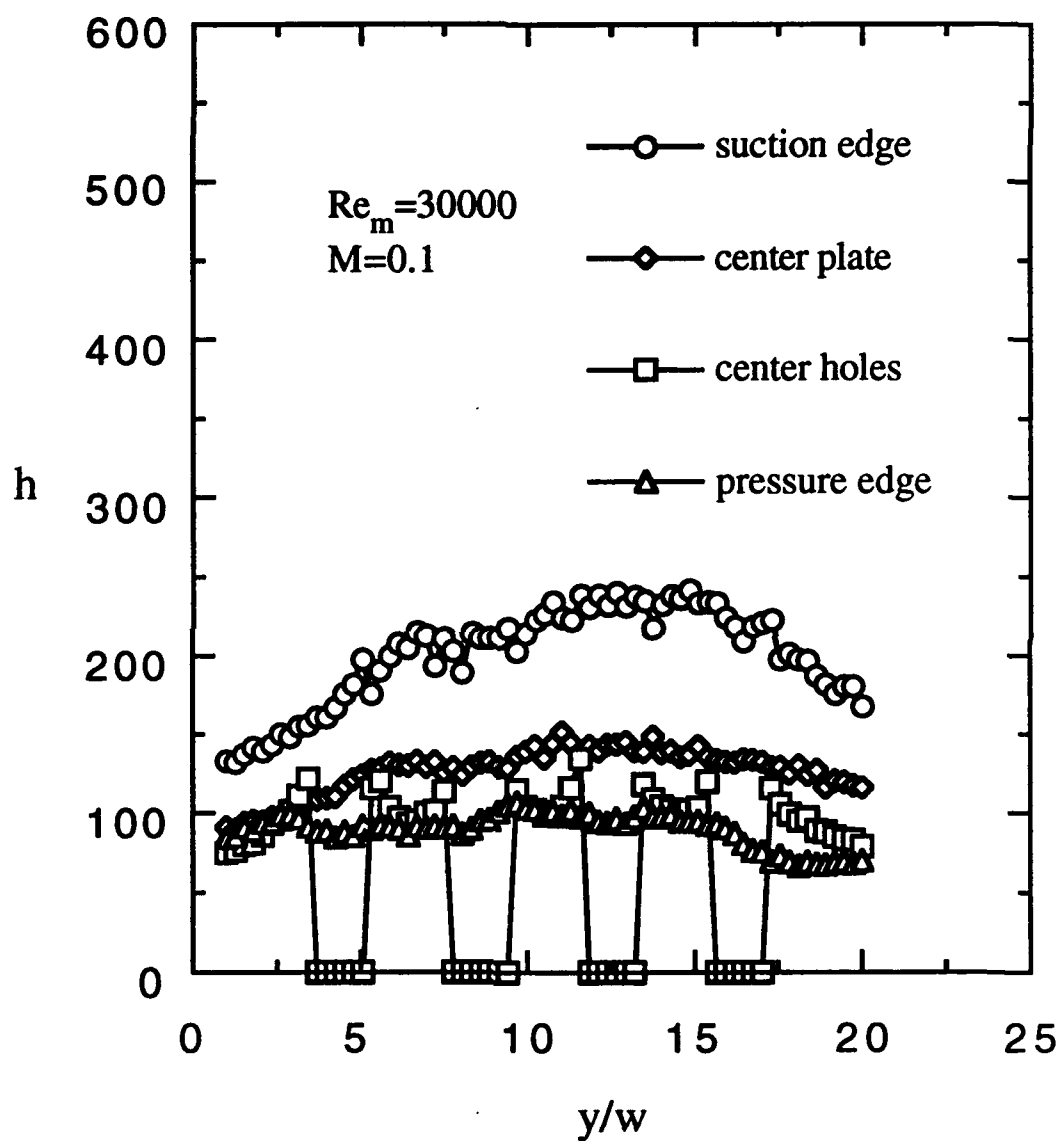


Fig. 117 Heat transfer coeff., spanwise variation, pressure side injection, 1.0" cavity,  $3/16$ " clearance gap

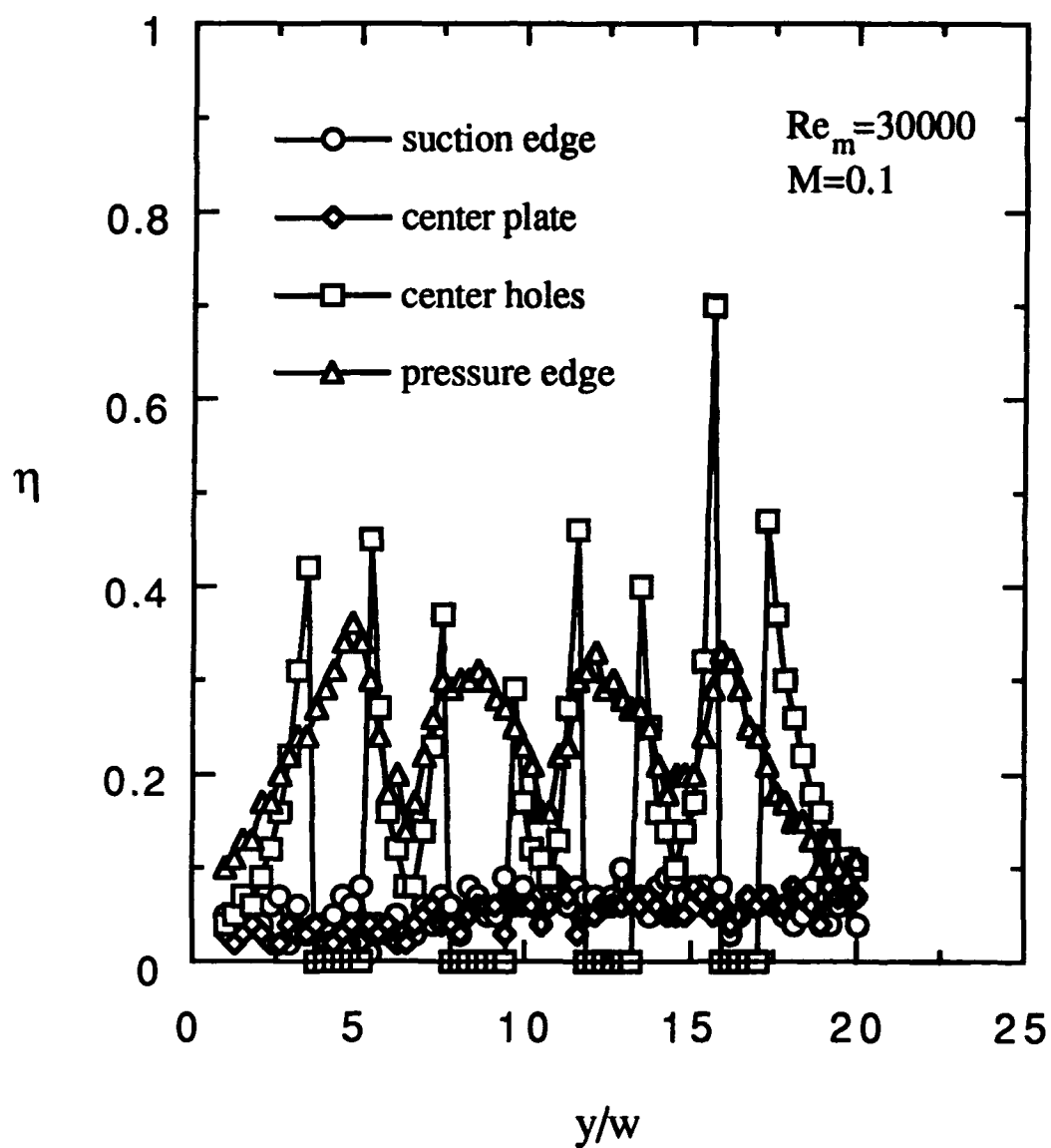


Fig. 118 Effectiveness, spanwise variation, pressure side injection, 1.0" cavity,  $3/16$ " clearance gap

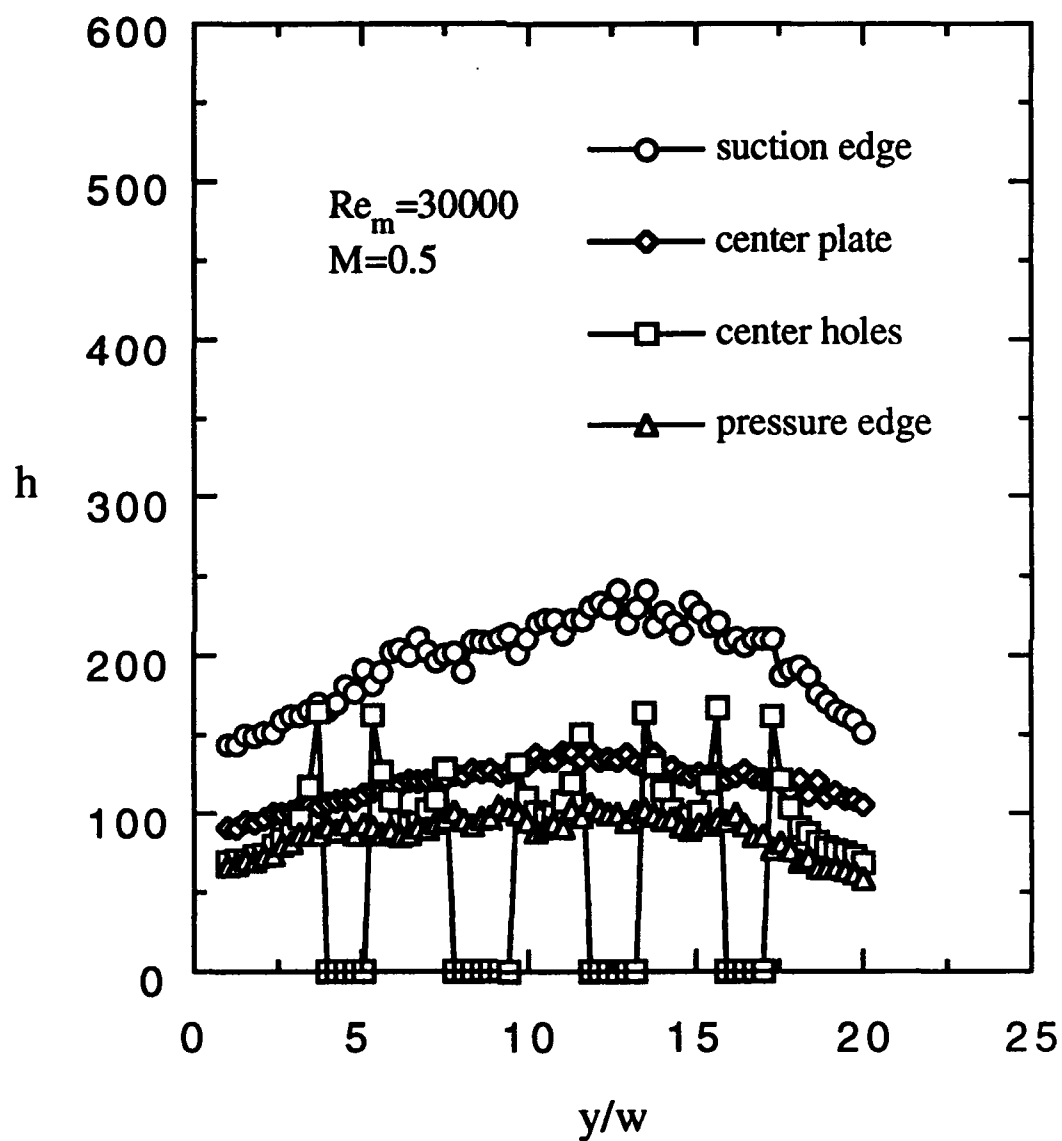


Fig. 119 Heat transfer coeff., spanwise variation, pressure side injection, 1.0" cavity,  $3/16$ " clearance gap, #1

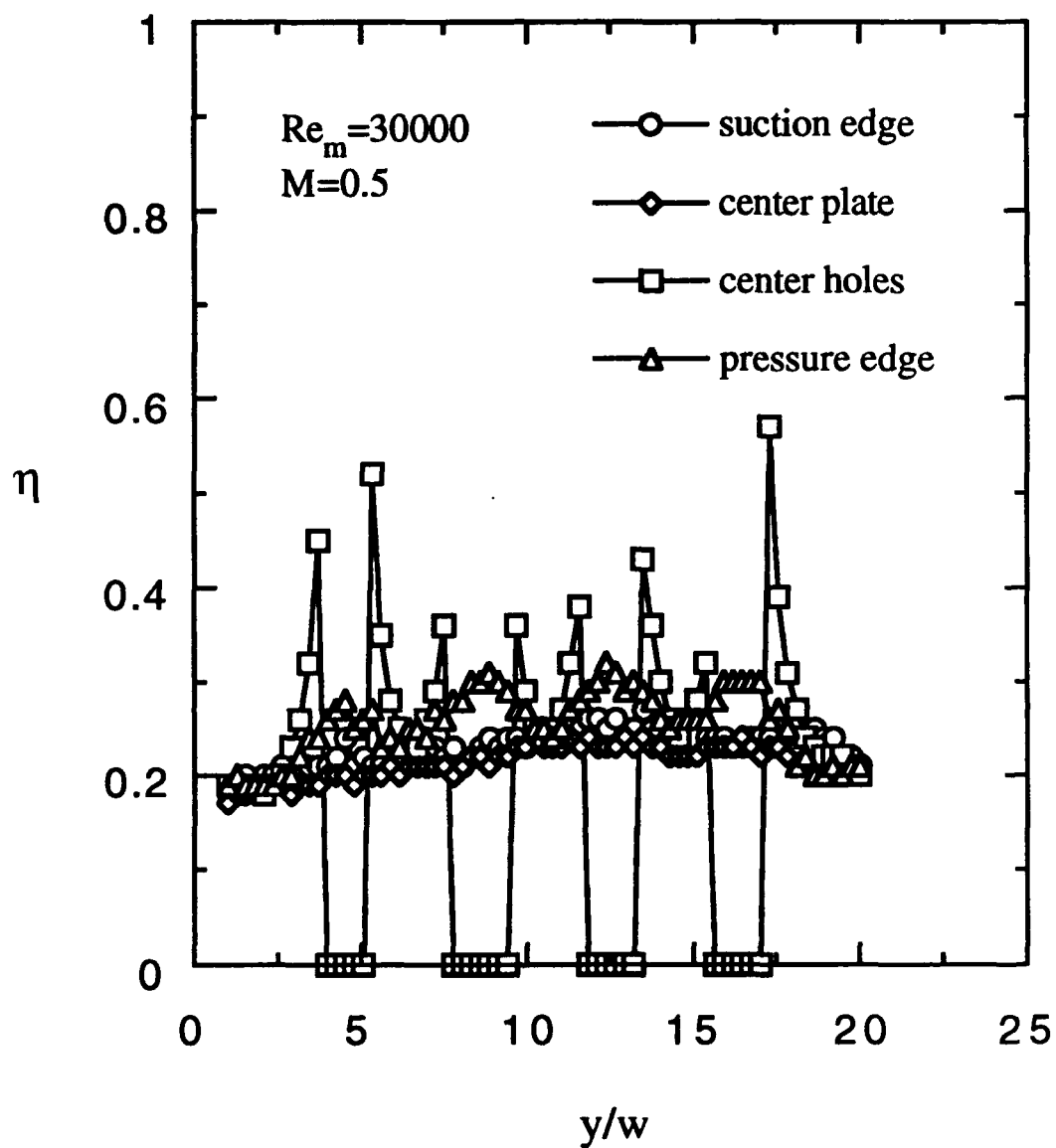


Fig. 120 Effectiveness, spanwise variation, pressure side injection, 1.0" cavity,  $3/16$ " clearance gap, #1

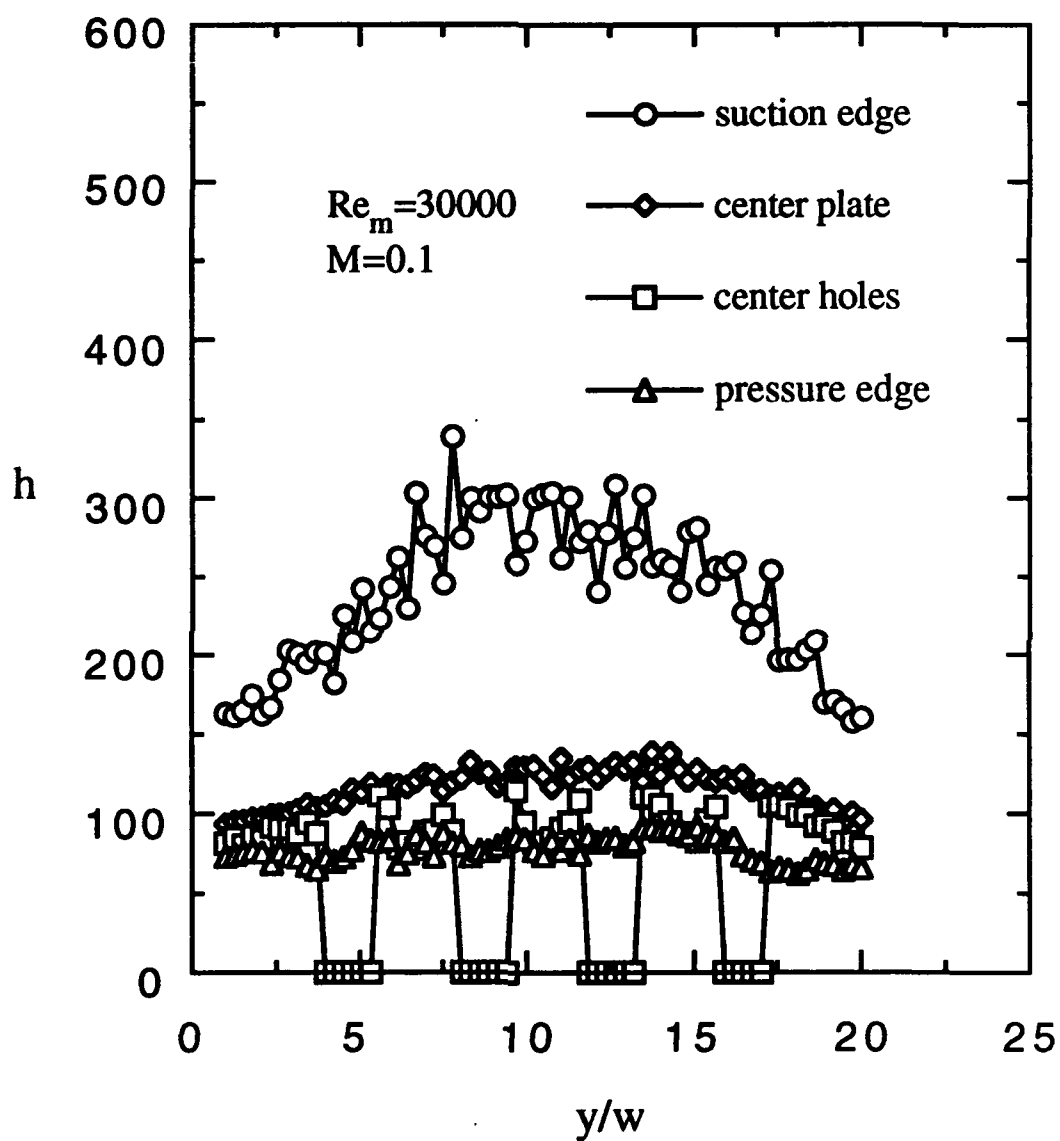


Fig. 121 Heat transfer coeff., spanwise variation, pressure side injection, 1.0" cavity,  $5/16$ " clearance gap

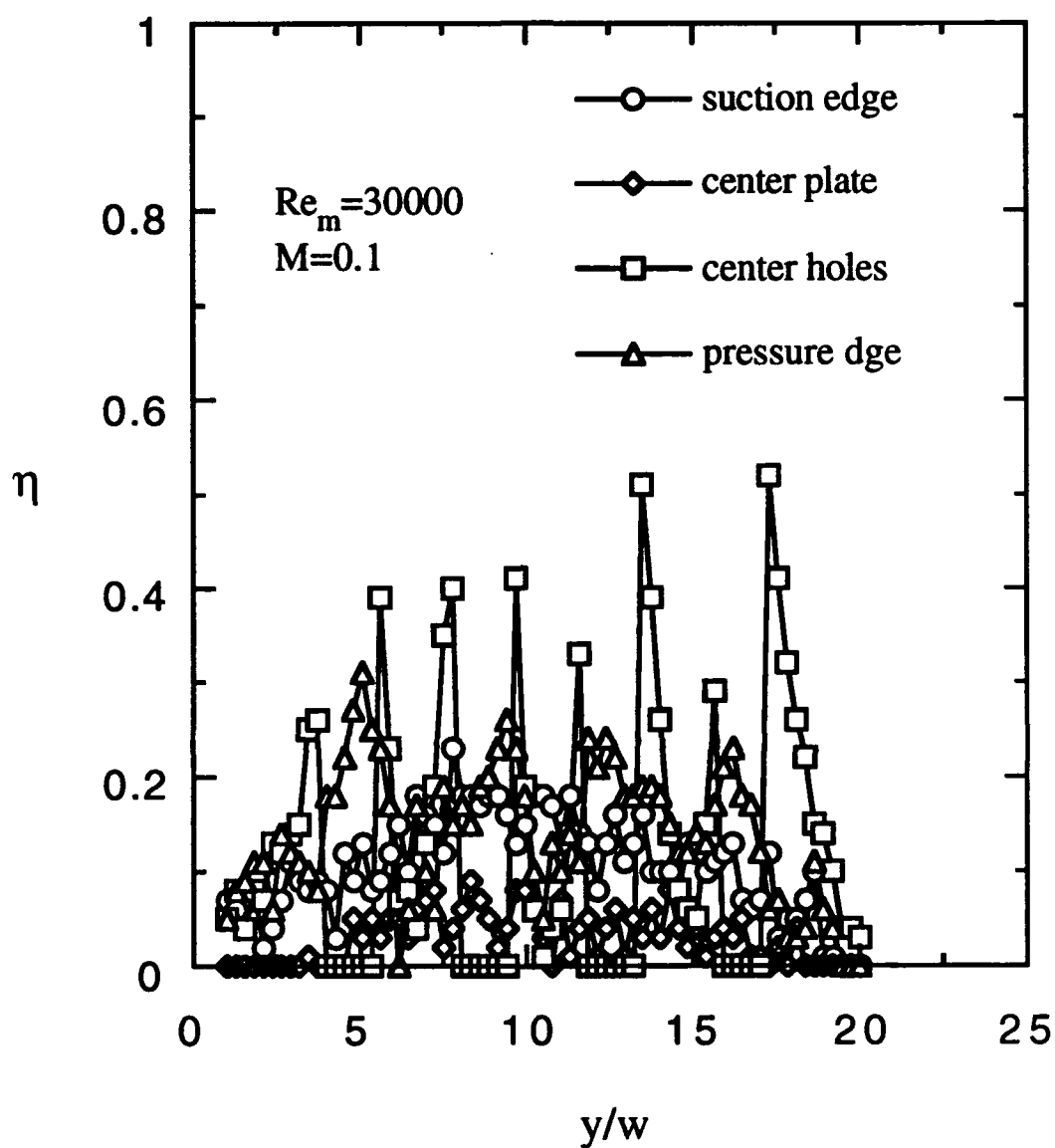


Fig. 122 Effectiveness, spanwise variation, pressure side injection, 1.0" cavity,  $5/16$ " clearance gap

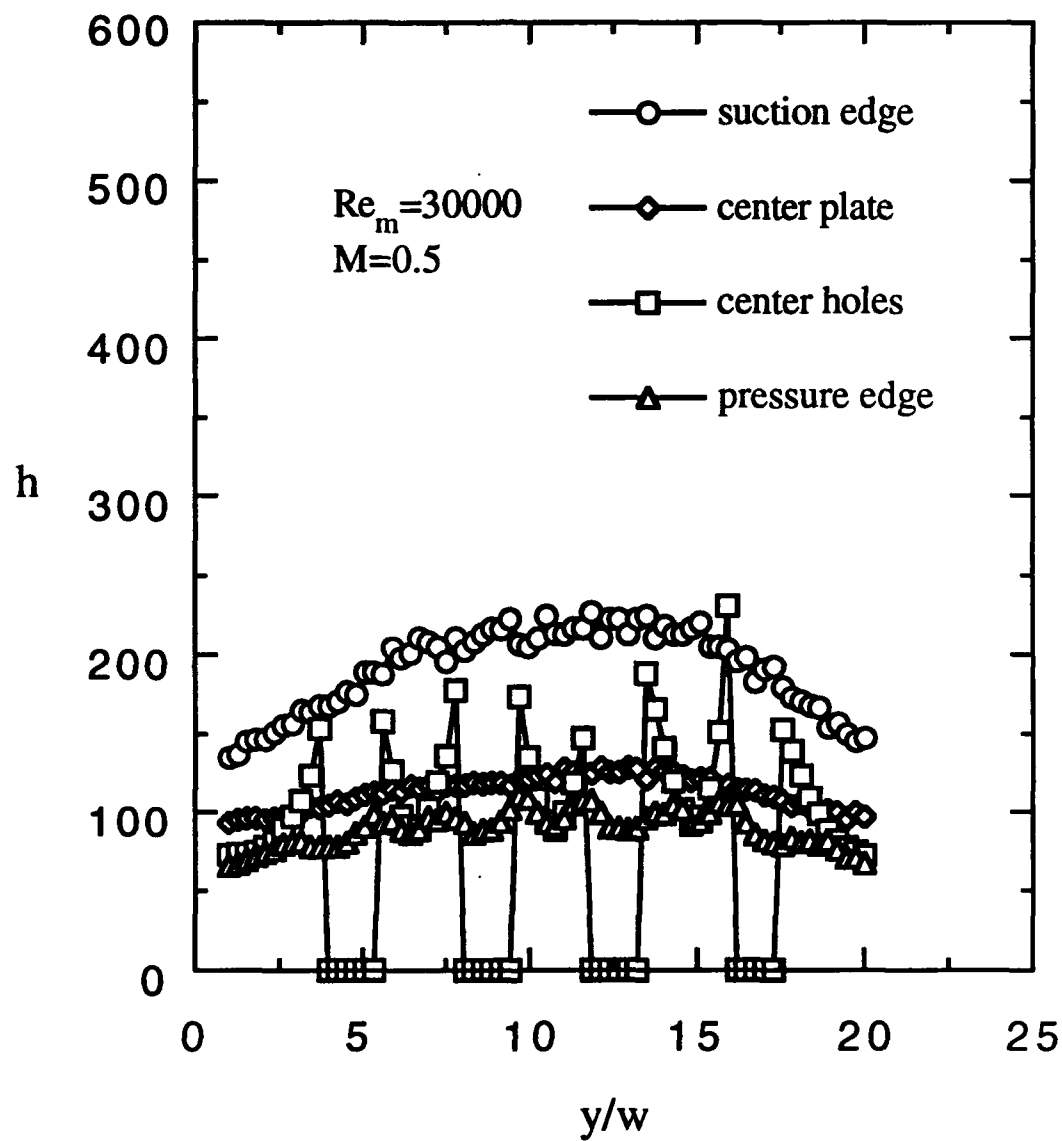


Fig. 123 Heat transfer coeff., spanwise variation, pressure side injection, 1.0" cavity,  $5/16$ " clearance gap

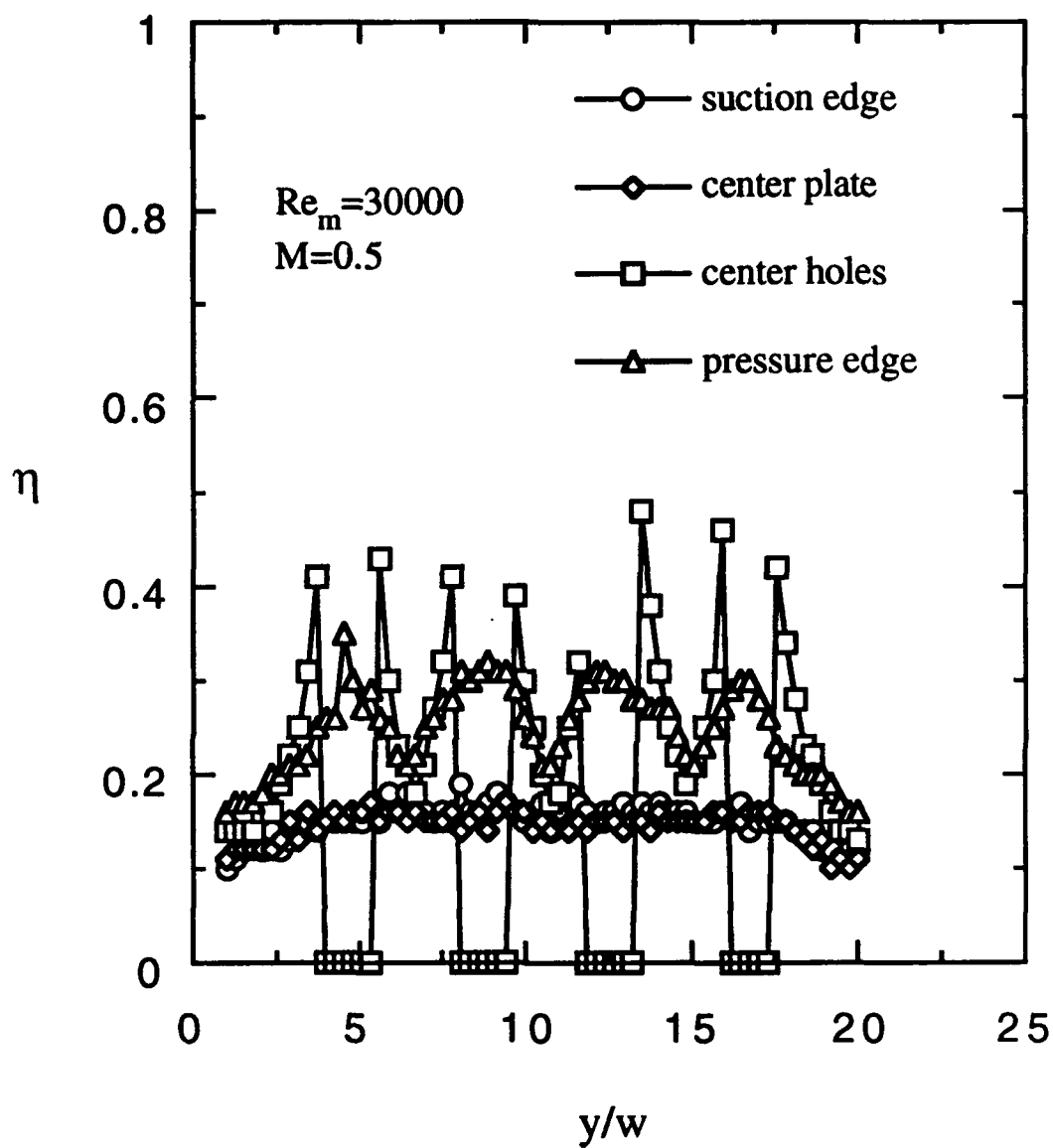


Fig. 124 Effectiveness, spanwise variation, pressure side injection, 1.0" cavity,  $5/16$ " clearance gap



**APPENDIX C**  
**REPEATABILITY DATA**

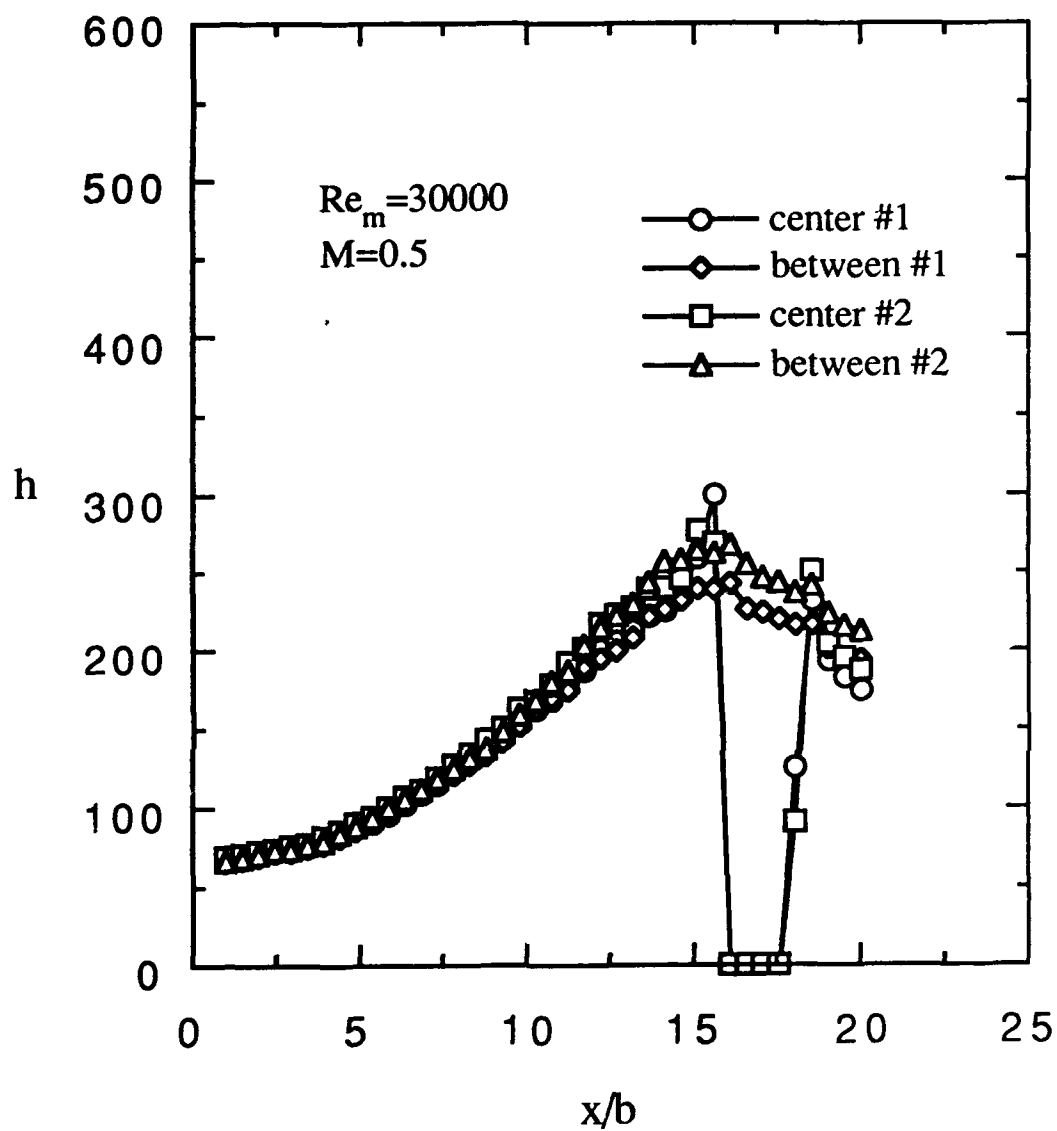


Fig. 125 Heat transfer coeff., streamwise variation,  
 suction side injection,  
 $3/8$ " cavity,  $3/16$ " clearance gap.  
 repeatability

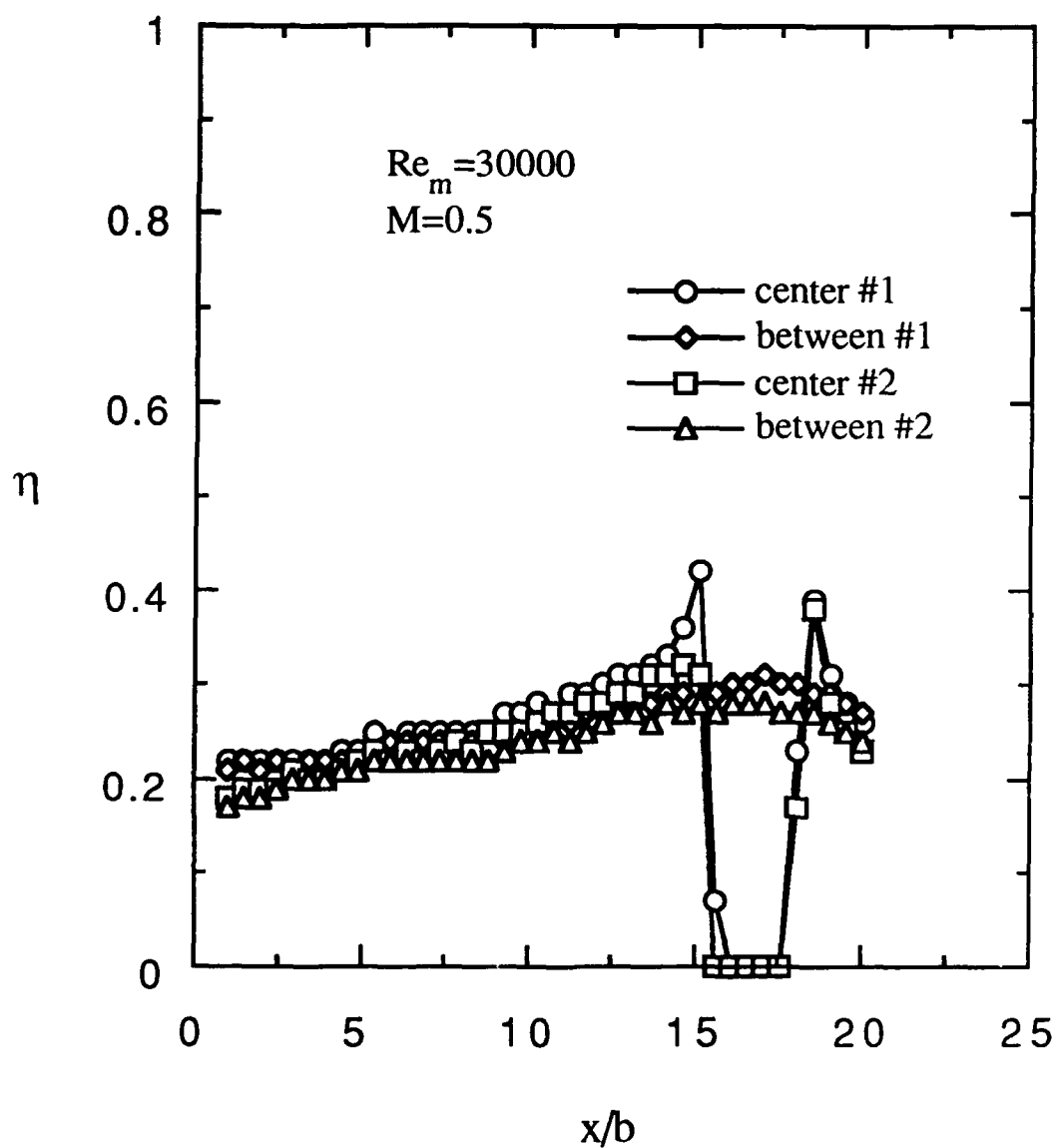


Fig. 126 Effectiveness, streamwise variation, suction side injection,  $3/8$ " cavity,  $3/16$ " clearance gap, repeatability

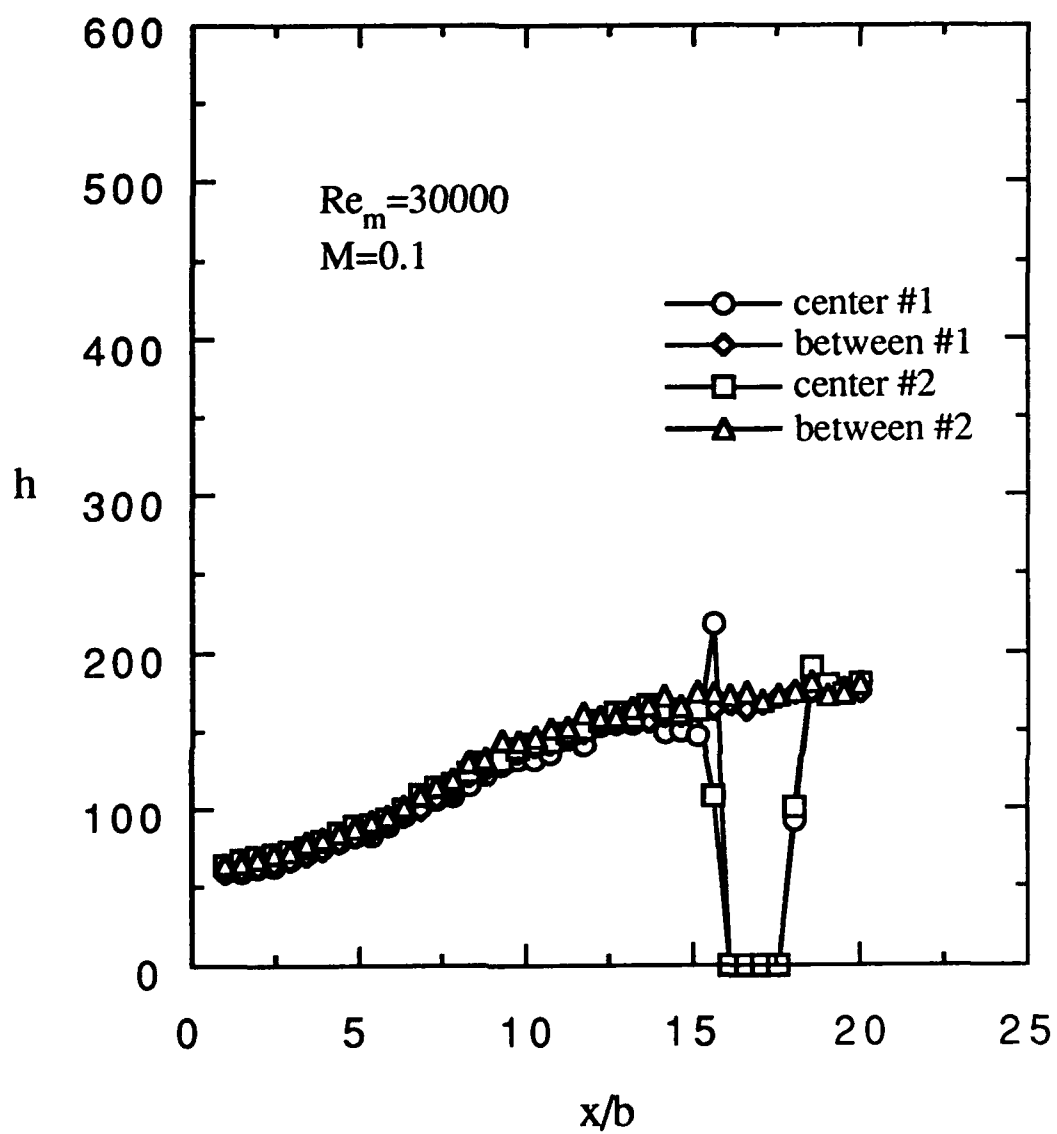


Fig. 127 Heat transfer coeff., streamwise variation,  
 suction side injection,  
 $3/8$ " cavity,  $5/16$ " clearance gap,  
 repeatability

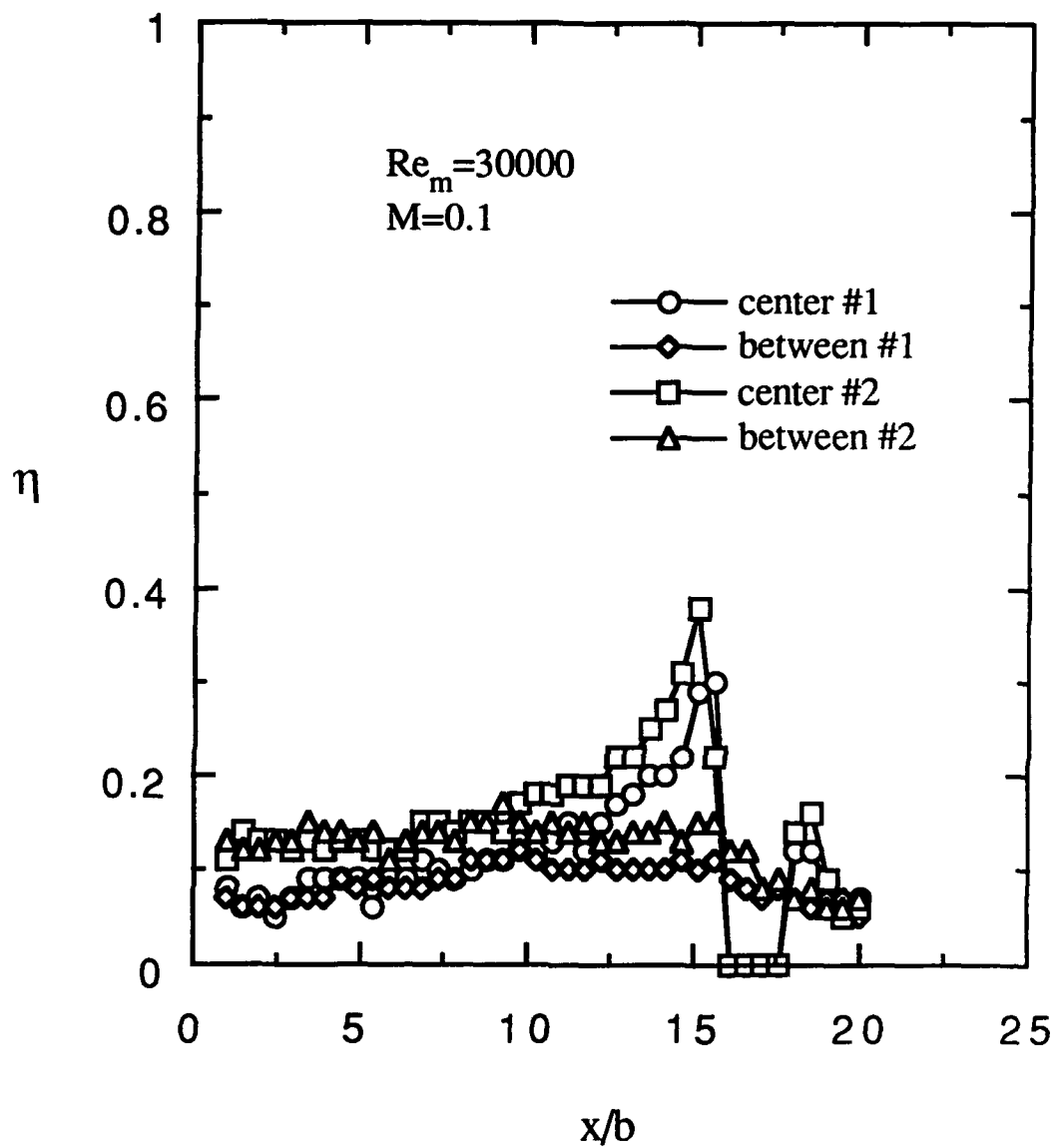


Fig. 128 Effectiveness, streamwise variation, suction side injection,  
 $3/8$ " cavity,  $5/16$ " clearance gap,  
 repeatability

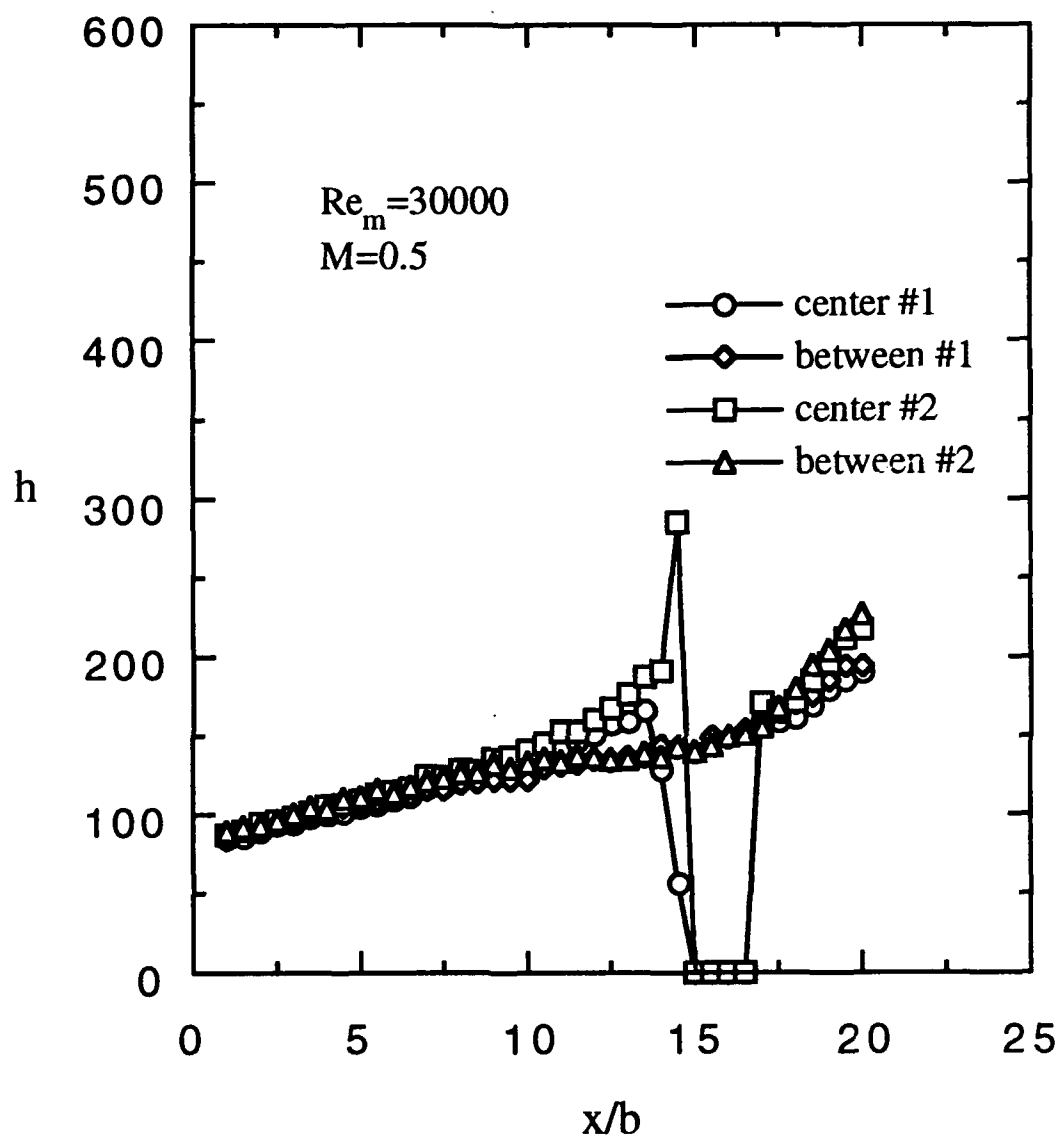


Fig. 129 Heat transfer coeff., streamwise variation,  
 suction side injection,  
 1.0" cavity,  $3/16$ " clearance gap,  
 repeatability

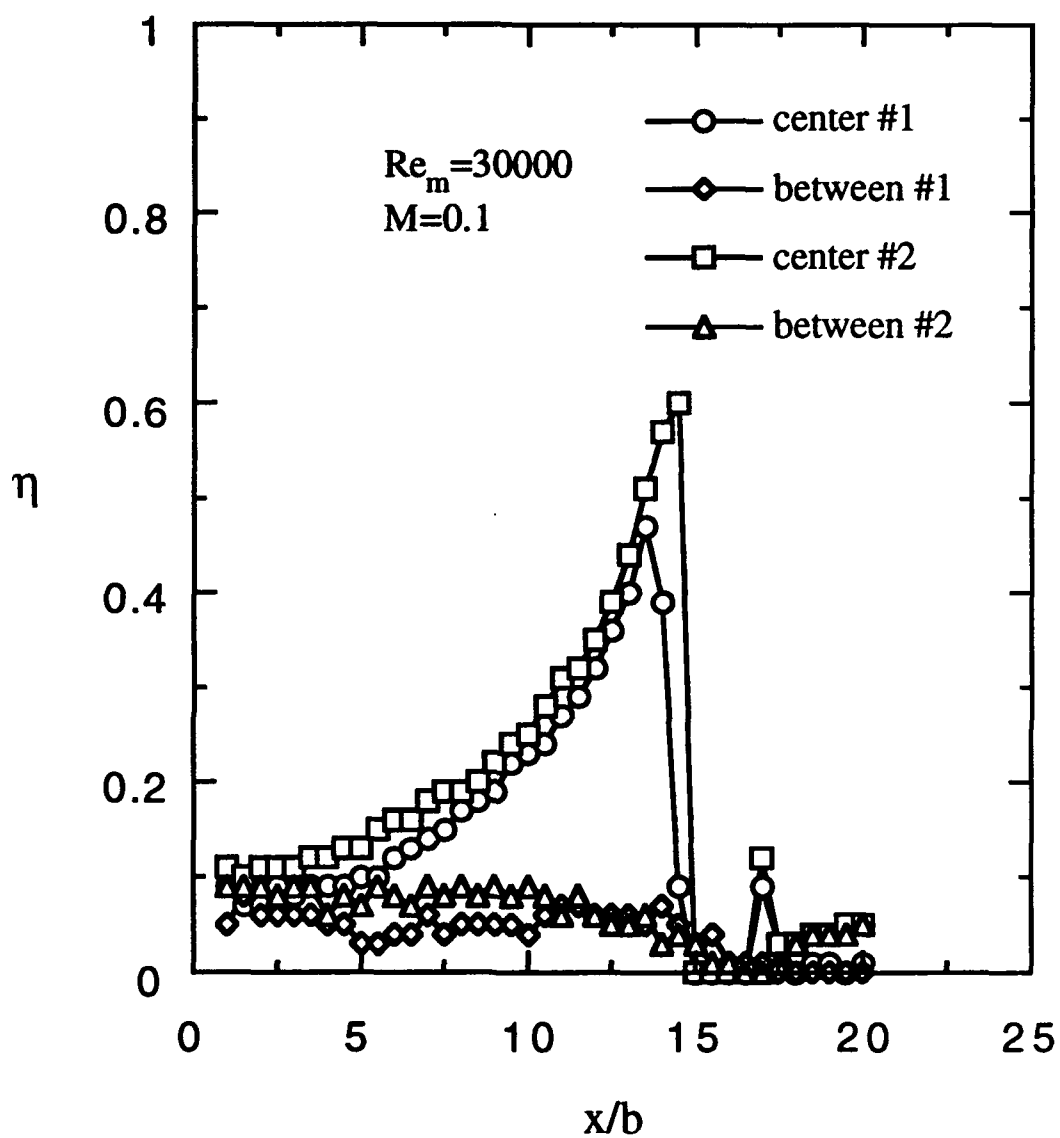


Fig. 130 Effectiveness, streamwise variation, suction side injection, 1.0" cavity,  $3/16$ " clearance gap, repeatability

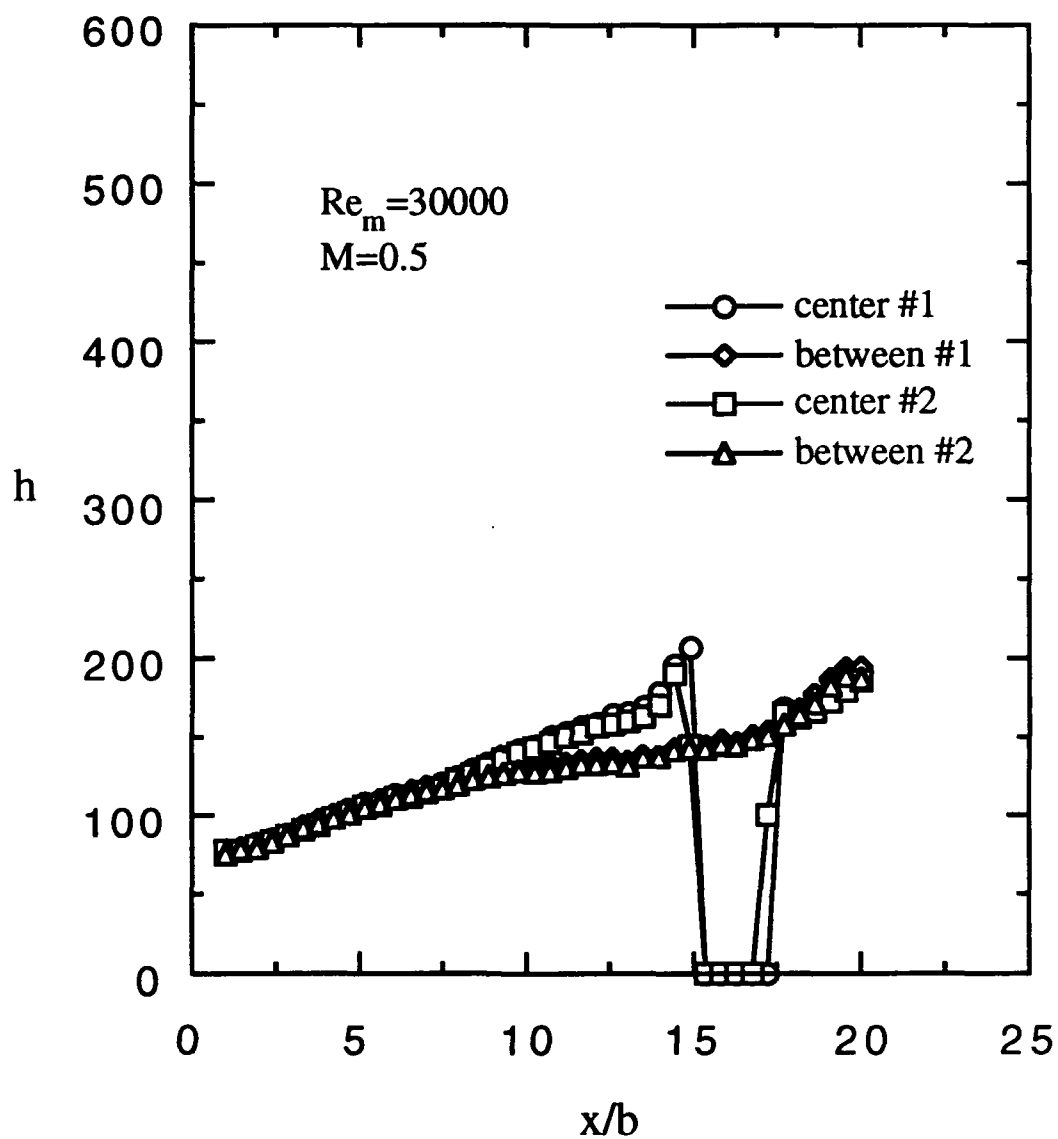


Fig. 131 Heat transfer coeff., streamwise variation,  
suction side injection,  
1.0" cavity,  $5/16$ " clearance gap,  
repeatability



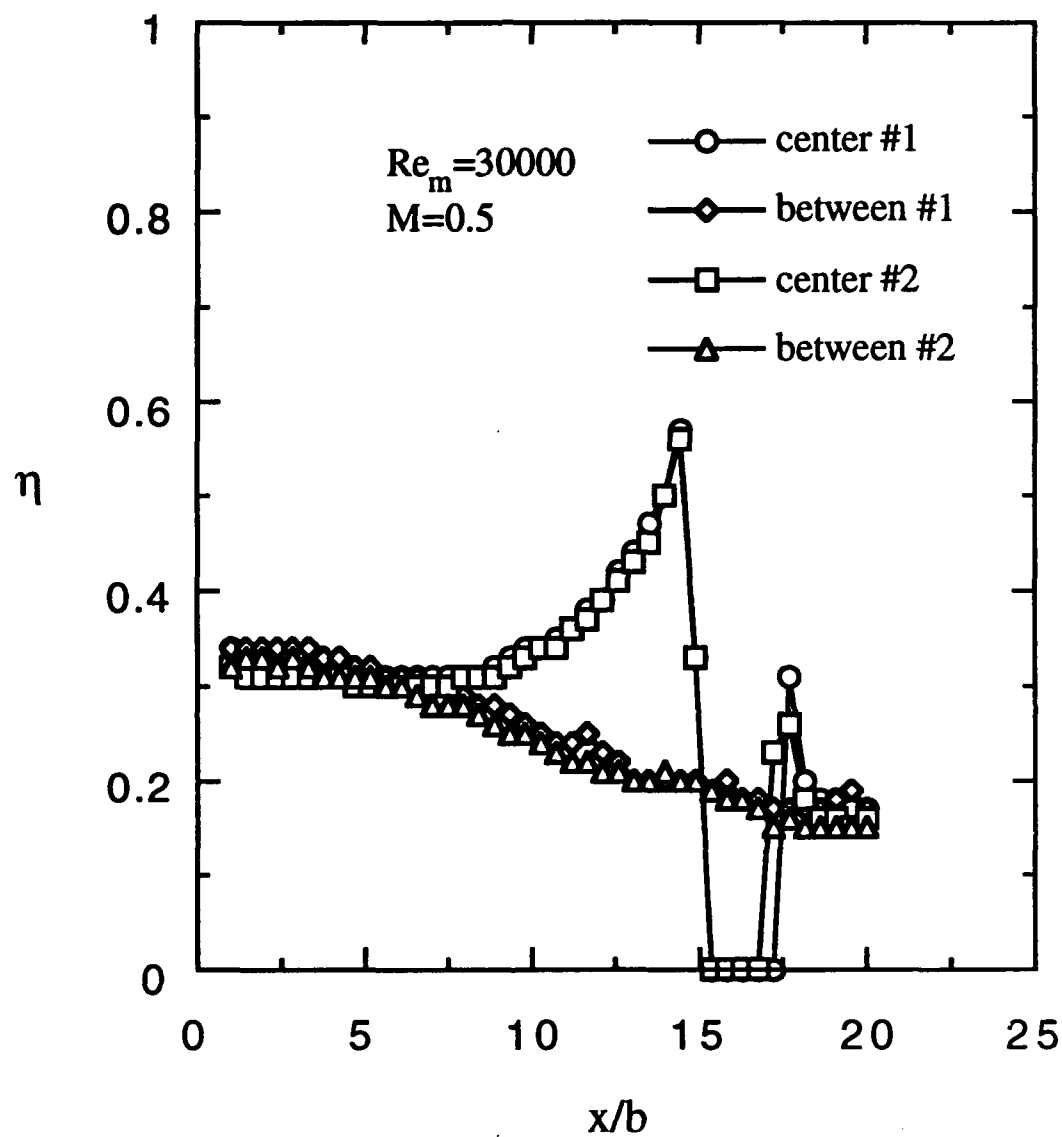


Fig. 132 Effectiveness, streamwise variation, suction side injection,  
1.0" cavity,  $5/16$ " clearance gap,  
repeatability

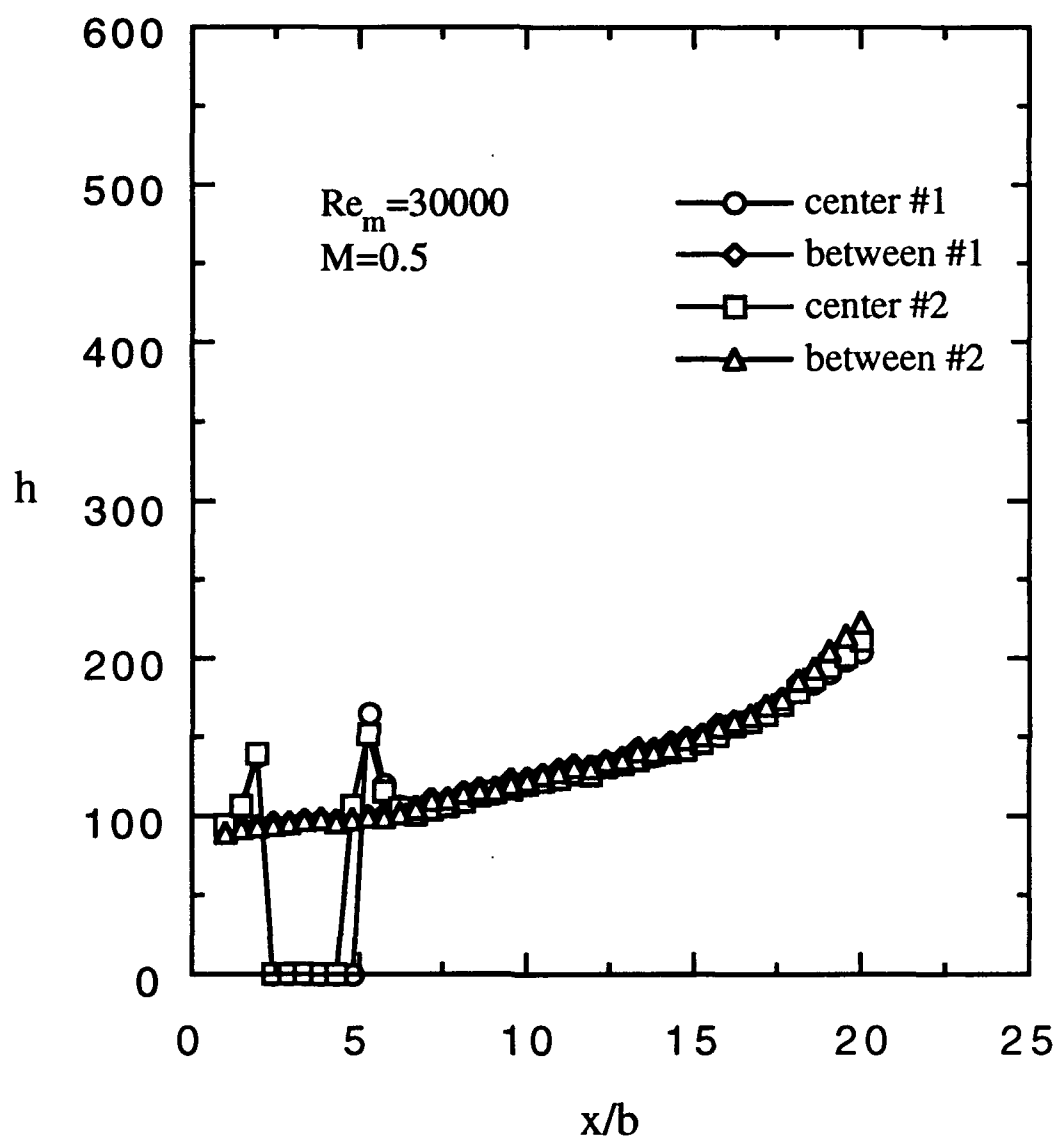


Fig. 133 Heat transfer coeff., streamwise variation,  
pressure side injection,  
1.0" cavity,  $3/16$ " clearance gap,  
repeatability

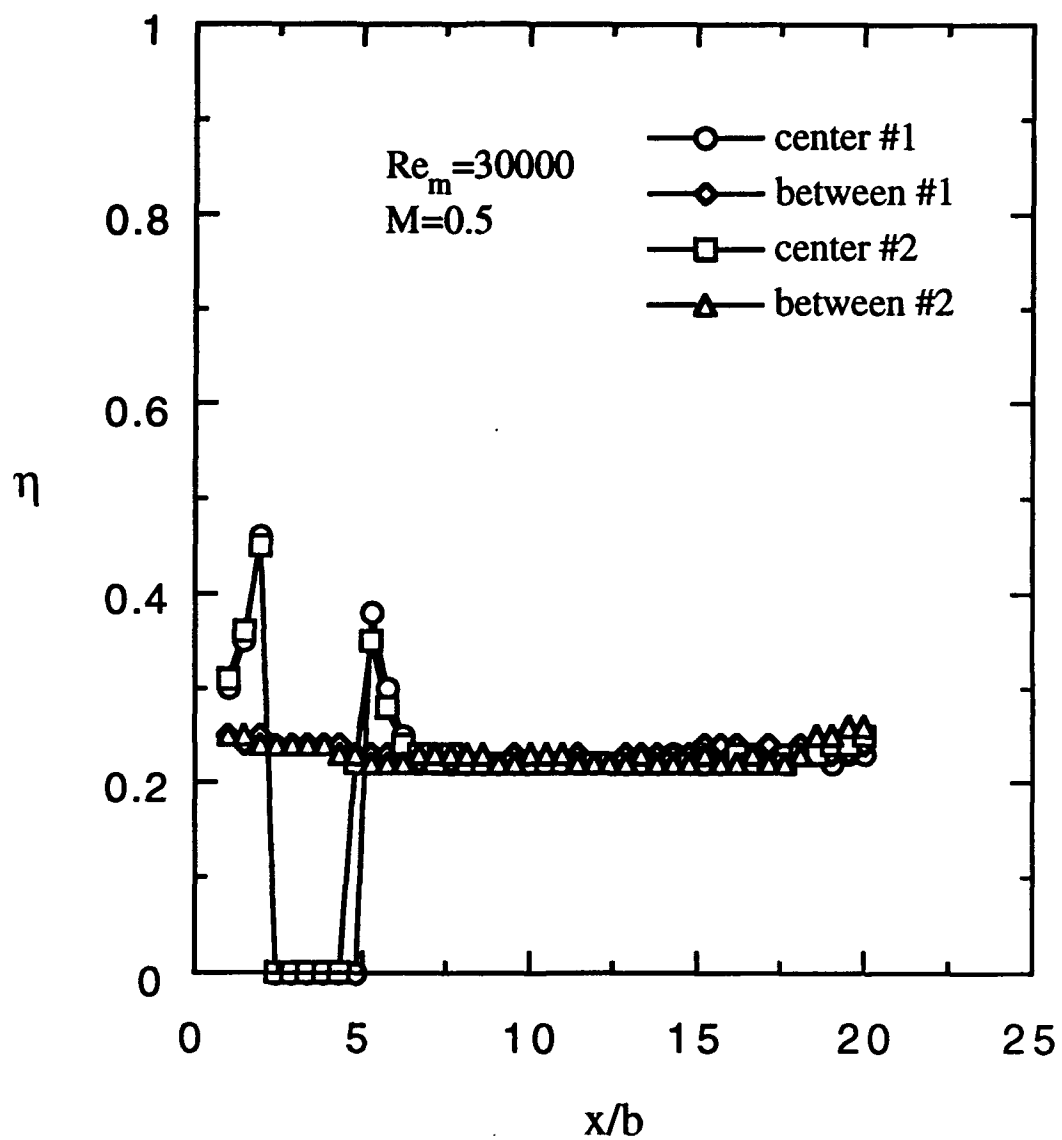


Fig. 134 Effectiveness, streamwise variation, pressure side injection, 1.0" cavity,  $3/16$ " clearance gap, repeatability;

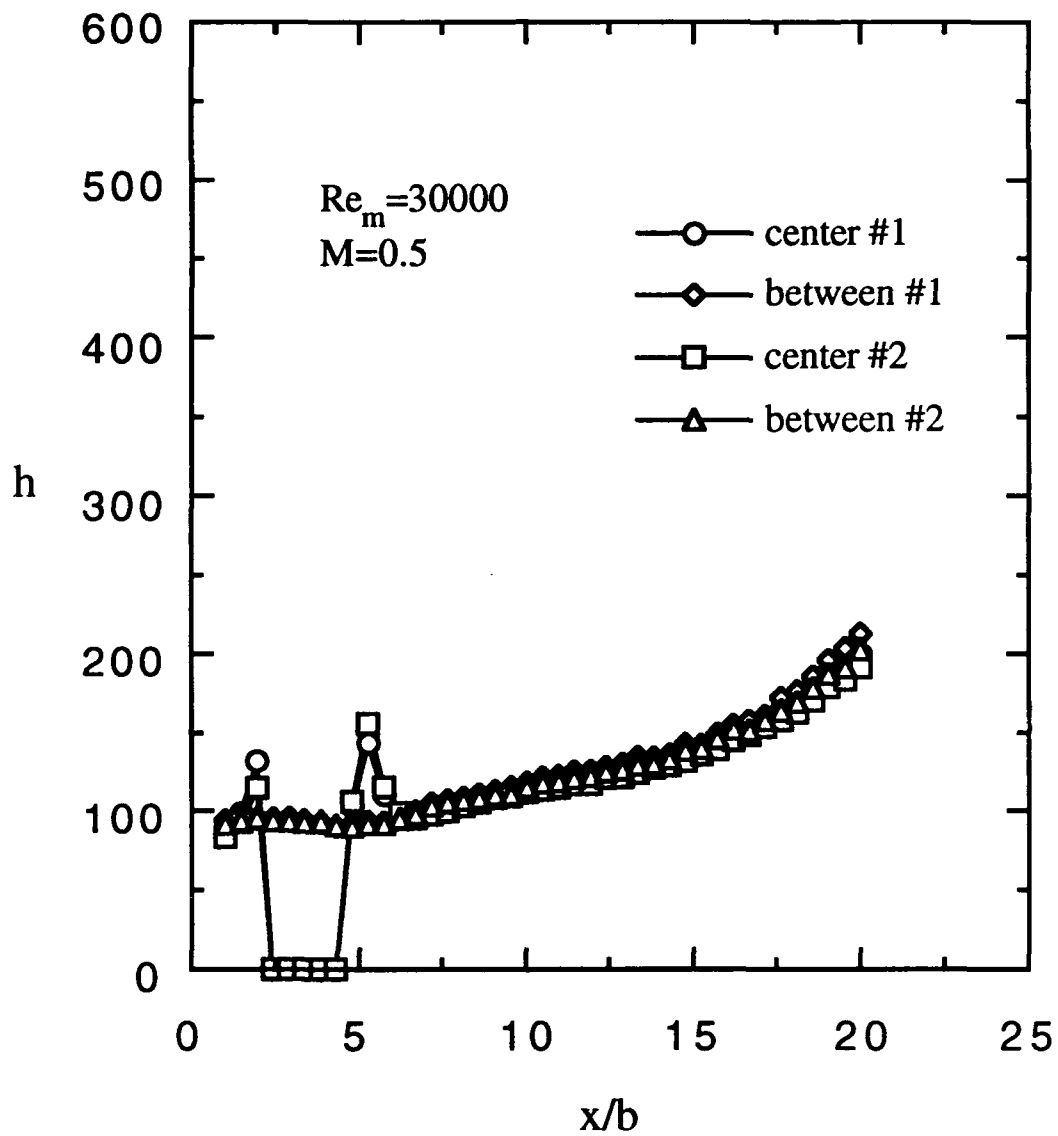


Fig. 135 Heat transfer coeff., streamwise variation,  
pressure side injection,  
1.0" cavity,  $5/16$ " clearance gap,  
repeatability

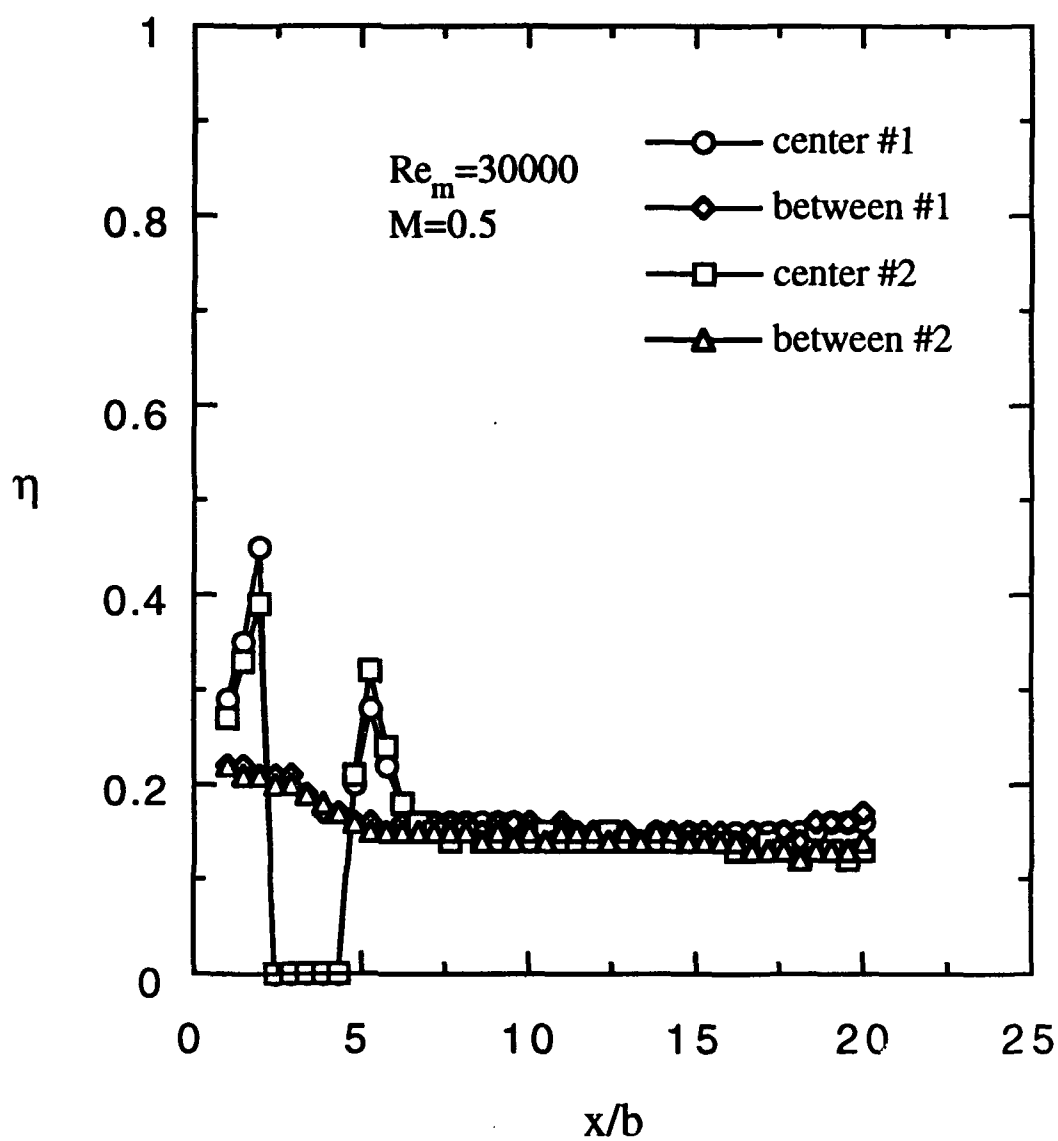


Fig. 136 Effectiveness, streamwise variation, pressure side injection, 1.0" cavity,  $5/16$ " clearance gap, repeatability